Expression, Regulation and Function of Lectin-Like Transcript 1 (LLT1)





Alba Llibre

The Queen's College, University of Oxford

Thesis submitted for the degree of
Doctor of Philosophy in Clinical Medicine
University of Oxford, Michaelmas Term 2016

Supervisors:

Doctor Christian B. Willberg

Professor Paul Klenerman

Professor Rodney E. Phillips

Expression, Regulation and Function of Lectin-Like Transcript 1 (LLT1)

Alba Llibre, The Queen's College

Submitted for DPhil in Clinical Medicine, Michaelmas Term 2015

Abstract

Receptor-ligand pairs of C-type lectin-like proteins have been shown to orchestrate and modulate immune responses within particular immune cell subsets or in distinct body locations. The function of CD161 and Lectin-Like Transcript 1 (LLT1) has not been extensively studied, partially due to the lack of validated anti-LLT1 antibodies. Here, I characterised two novel anti-LLT1 monoclonal antibodies (2H7 and 7G7). Using them for flow cytometric and immunohistological staining, I characterised the expression of LLT1 in different healthy human tissues and found that LLT1 levels were particularly high in immune-privileged sites.

Germinal centres (GC) are microanatomical structures that are critical for the development of high-affinity antibodies and B cell memory. They are organised into two zones, light and dark, with coordinated roles controlled by local signalling. LLT1 protein is known to be expressed on B cells, but its functional role in the GC reaction has not been explored. I found high expression of LLT1 on GC-associated B cells, early plasmablasts and GC-derived lymphomas. LLT1 expression was readily induced via BCR, CD40 and CpG stimulation on B cells. Ubiquitous expression of CD161 on Follicular Dendritic Cells (FDCs) was revealed, as well as on a subset of T follicular cells. Triggering of LLT1 supported B cell activation, CD83 upregulation and Chemokine (C-X-C Motif) Receptor 4 (CXCR4) downregulation, which is consistent with a role in driving transition from a dark to a light zone phenotype. Overall, these data suggest that LLT1-CD161 interactions play a novel and important role in B cell maturation within the GC in humans. A deep understanding of the GC reaction and the process of B cell selection could provide invaluable knowledge into effective vaccine design, generation of auto-antibodies and malignant transformation.

Acknowledgements

Thank you to my main supervisors Chris Willberg and Paul Klenerman, for giving me the opportunity to join the lab and the space to explore and enjoy science. Thank you for your time, for your endless support and for being an inspiration.

I would also like to thank Rodney Phillips for his constant support, as well as Richard Cornall and Chris Norbury, without whom the completion of this DPhil would have not been possible.

Thank you to David Greaves, Adam Ritchie and Constantino Lopez Macias for the encouragement to enjoy science in all its multiple forms, including teaching and writing, as well as for many exciting and useful informal discussions.

Many thanks to Obra Social *La Caixa* and the Nuffield Department of Medicine for my DPhil funding, which has made it possible for me to live and study in Oxford.

Throughout my life, I have shared the joy of learning, discovering and living with many wonderful people. Thank you to David, Ruben, Miquel, Clara, Victoria, Xavi, Joan, Anna and Gina.

A very sweet and sincere thank you to Ruth, Ayako and Jo. The combination of friendship and science is one of the most beautiful feelings I have ever experienced. I am also extremely grateful to various people who have helped, listened, encouraged, cried, laughed, danced and dreamed with me during these years; Phill, Gen, Ghadir, Amy, James, Matt, Leo, Kira, Jacqui, Annette, Maureen, Idalina, Kat, Suzanne, Bodo, Rosie, Carolin, Balaji and Karl. You've made Oxford such a fun and enriching experience.

I wish to thank my cousins, uncles and grandparents for their limitless support, tenderness, visits and supply of hugs and Catalan goods across the British borders.

Thank you Emily for your endless sweetness and understanding, for your support and smiles, for making me realise that French poetry and germinal centres can cohabit in extreme happiness. Thank you for making life the most exciting adventure and for surviving the whole DPhil experience with me.

Last but not least, I want to thank my parents, Montse and Jaume, for their love, support and patience, for awakening my curiosity about the world, for sharing their passion for life and science and for being there all the way through.

Table of Contents

THESIS CONTRIBUTIONS 1

ABBREVIATIONS 2

1 INTRODUCTION 5

1.1 INNATE AND ADAPTIVE IMMUNITY 5
1.2 IMMUNE CELLS AND THEIR RECEPTORS 6
1.3 C-TYPE LECTINS 7
1.3.1 LECTINS AND C-TYPE LECTINS 7
1.3.2 THE NATURAL KILLER GENE COMPLEX (NKC) 11
1.3.3 NKRP1 AND CLEC FAMILIES 12
1.4 LECTIN-LIKE TRANSCRIPT 1 (LLT1) 14
1.4.1 CD161-LLT1 AND THE RODENT HOMOLOGS 14
1.4.2 HUMAN LLT1 16
1.4.3 EXPRESSION PATTERN: MCLR-B VS HLLT1 18
1.4.4 OCIL IN THE CONTEXT OF BONE 22
1.4.5 LLT1 SIGNALLING AND FUNCTION 24
1.4.6 CD161-LLT1/ NKP80-AICL / NKP65-KACL 27
1.5 BASICS OF B CELL BIOLOGY 30
1.5.1 THE DISCOVERY OF B CELLS 30
1.5.2 EARLY UNDERSTANDING OF B CELL BIOLOGY AND NEW QUESTIONS 33
1.5.3 THE LIFE OF A B CELL 35
1.6 GERMINAL CENTRES 38
1.6.1 CELL TYPES 39
1.6.2 THE GERMINAL CENTRE REACTION 43
1.6.3 PLASMABLASTS AND PLASMA CELLS 47
1.6.4 EXPANDING THE CLASSICAL MODEL 49
1.6.5 GERMINAL CENTRES AND TUMORIGENESIS 50
1.7 ANTIBODIES AS IMMUNOLOGICAL TOOLS 52
1.8 AIMS OF THE THESIS 53

2 MATERIALS AND METHODS 54

2.1 CELLS AND TISSUES 54
2.1.1 PBMCS SEPARATION, FREEZING AND THAWING 54
2.1.2 CELL LINES 55
2.1.3 TONSILS 55
2.2 NOVEL ANTI-LLT1 ANTIBODIES 56
2.3 FLOW CYTOMETRY 56
2.3.1 EXTERNAL STAINING 56
2.3.2 INTERNAL STAINING 57
2.3.3 DATA ACQUISITION AND ANALYSIS 57
2.4 DOUBLET FORMATION 57
2.5 REAL-TIME QUANTITATIVE POLYMERASE CHAIN REACTION (QPCR) 58
2.6 IMMUNOHISTOCHEMISTRY 58
2.6.1 IMMUNOPEROXIDASE STAINING 58
2.6.2 IMMUNOFLUORESCENT STAINING 59
2.6.3 DATA ACQUISITION AND ANALYSIS 60
2.7 STATISTICAL ANALYSIS 60
2.8 MEDIA AND BUFFERS 61

3 DEVELOPING AND OPTIMISING THE TOOLS FOR ANALYSIS OF LLT1 64

3.1 INTRODUCTION 64

3.2 AIMS 67
3.3 MATERIALS AND METHODS 67
3.3.1 REAL-TIME QUANTITATIVE POLYMERASE CHAIN REACTION (QPCR) 67
3.3.2 DOUBLET FORMATION 67
3.3.3 TISSUES 68
3.3.4 IMMUNOHISTOCHEMISTRY 68
3.3.5 WESTERN BLOT 68
3.3.6 PNGASE F DIGESTION 69
3.4 RESULTS 69
3.4.1 TESTING OF ANTI-LLT1 ANTIBODIES FOR FACS STAINING 70
3.4.2 INTERACTION BETWEEN LLT1 AND CD161 EXPRESSING CELLS 73
3.4.3 TESTING OF ANTI-LLT1 ANTIBODIES FOR IMMUNOHISTOCHEMICAL STAINING 75
3.4.4 IMMUNOHISTOCHEMISTRY OPTIMISATION 76
3.4.5 GERMINAL CENTRE STAINING WITH THE POLYCLONAL GOAT PAB AND THE 7G7 MAB 82
3.4.6 EFFECTS OF GLYCOSYLATION IN LLT1 ANTIBODY RECOGNITION 87
3.5 DISCUSSION 90
3.6 SUMMARY 94

4 LLT1 IS EXPRESSED IN HEALTHY HUMAN TISSUE 95

4.1 INTRODUCTION 95
4.2 AIMS 98
4.3 MATERIALS AND METHODS 98
4.3.1 CELL LINES 98
4.3.2 TISSUES 99
4.3.3 THP-1 AND HEPATOCYTE-DERIVED CELL LINES STIMULATION 99
4.3.4 NK CELL DEGRANULATION ASSAY 100
4.4 RESULTS 100
4.4.1 LLT1 IS EXPRESSED ON CIRCULATING B CELLS AND MONOCYTES 100
4.4.2 REGULATION OF LLT1 EXPRESSION ON MONOCYTES/MACROPHAGES 103
4.4.3 LLT1 IS EXPRESSED IN IMMUNE-PRIVILEGED SITES 106
4.4.4 LLT1 INHIBITS NK CELL DEGRANULATION 114
4.4.5 LLT1 IS UPREGULATED IN THE LIVER UNDER INFLAMMATORY CONDITIONS 116
4.5 DISCUSSION 119
4.6 SUMMARY 126

5 EXPRESSION AND REGULATION OF LLT1 ON B CELLS 127

5.1 INTRODUCTION 127
5.2 AIMS 129
5.3 MATERIALS AND METHODS 130
5.3.1 CELLS, CELL LINES AND TISSUES 130
5.3.2 IMMUNOHISTOCHEMISTRY 131
5.3.3 B CELL PURIFICATION 132
5.3.4 *IN VITRO* DIFFERENTIATION OF PLASMA CELLS 132
5.3.5 B CELL STIMULATION (REGULATION OF LLT1) 133
5.3.6 PROLIFERATION ASSAY 134
5.4 RESULTS 134
5.4.1 LLT1 IS HIGHLY EXPRESSED ON GERMINAL CENTRE B CELLS 134
5.4.2 LLT1 EXPRESSION IS HIGHER IN THE DZ THAN IN THE LZ 137
5.4.3 LLT1 IS EXPRESSED IN HUMAN B CELL LYMPHOMAS 139
5.4.4 LLT1 IS NOT EXPRESSED ON FDCS OR TBM, AND VERY RARELY ON T CELLS AND NEUTROPHILS 141
5.4.5 LLT1 IS EXPRESSED ON PLASMABLASTS 144
5.4.6 LLT1 IS EXPRESSED ON PLASMABLASTS FROM VACCINATED INDIVIDUALS 148
5.4.7 LLT1 IS NOT EXPRESSED ON PLASMA CELLS 151
5.4.8 REGULATION OF LLT1 EXPRESSION 155

5.4.9 LLT1 EXPRESSION IS LINKED TO B CELL PROLIFERATION 158
5.5 DISCUSSION 160
5.6 SUMMARY 163

6 THE FUNCTION OF LLT1 ON B CELLS 164

6.1 INTRODUCTION 164
6.2 AIMS 166
6.3 MATERIALS AND METHODS 166
6.3.1 TISSUES 166
6.3.2 REAL-TIME QUANTITATIVE POLYMERASE CHAIN REACTION (QPCR) 167
6.3.3 PHOSPHOFLOW EXPERIMENTS 167
6.3.4 DOUBLET FORMATION 168
6.3.5 B CELL ACTIVATION ASSAY 168
6.3.6 BLOCKING EXPERIMENTS 169
6.3.7 CD161+ CELL DEPLETION 170
6.3.8 DATA ACQUISITION AND ANALYSIS 170
6.4 RESULTS 170
6.4.1 CD161 IS EXPRESSED ON FDCS 170
6.4.2 CD161 IS EXPRESSED ON A SUBSET OF TONSILLAR T CELLS 174
6.4.3 LLT1 CROSS-LINKING ON B CELLS DOES NOT INVOLVE ERK SIGNALLING 176
6.4.4 BLOCKING LLT1-CD161 INTERACTION REDUCES B CELL SURVIVAL AND PROLIFERATION 179
6.4.5 LLT1 CROSS-LINKING PROMOTES B CELL ACTIVATION AND DRIVES B CELLS TOWARDS A LZ PHENOTYPE 182
6.5 DISCUSSION 187
6.6 SUMMARY 192

7 DISCUSSION 193

7.1 THE ORIGINAL AIMS OF THE THESIS 193
7.2 TOOLS 195
7.2.1 ANTI-LLT1 ANTIBODIES 195
7.2.2 ANTI-CD161 ANTIBODIES 196
7.2.3 LLT1 ELISA 197
7.3 LLT1 FUNCTION 197
7.3.1 CROSS-TALK 197
7.3.2 ACTIVATION 198
7.3.3 IMMUNE-PRIVILEGE 198
7.3.4 THE GC MODEL 199
7.4 LIMITATIONS AND FUTURE DIRECTIONS 201
7.4.1 LLT1 DISTRIBUTION 201
7.4.2 IMMUNE-PRIVILEGE AND INFLAMMATION 201
7.4.3 SIGNALLING THROUGH LLT1 202
7.4.4 PRE-TFH – PRE-GC B CELL INTERACTION 202
7.4.5 LLT1 FUNCTION WITHIN THE GC 203
7.4.6 CD161 FUNCTION WITHIN THE GC 204
7.4.7 LLT1 IN PLASMABLASTS 205
7.4.8 MOUSE WORK 205
7.5 SUMMARY AND IMPLICATIONS 207

8 REFERENCES 209

9 APPENDIX 230

Thesis Contributions

Experiments and analyses presented in which other than myself contributed are as follows:

Chapter 3

G Freeman – Provided the 300 cell lines and the 2H7 and 7G7 anti-LLT1 monoclonal antibodies

Chapter 4

K Caenzig – performed part of the killing assays

A Patridge – performed some of the tissue array stainings and analyses

C Willberg – performed the LLT1 staining on the hepatocyte-derived cell lines

G Lauer – provided the human inflamed liver sections

Chapter 5

LJ Walker, P Milne, V Bigley, M Collin – Provided the bone marrow samples

T Marafioti – performed the PAX5/CD3/LLT1 triple staining; provided the B cell lymphoma lines

C Willberg – performed the LLT1 staining on the B cell lymphoma cell lines

J Galson and D Kelly – provided the vaccine samples

Chapter 6

H Mehta – performed the qPCR experiments

C Willberg – FACS-sorted and stained Tfh cells

F Rivellesse and ME El Shikh – performed the CD161 immunoflurorescent staining of frozen tonsillar sections

Chapter 7

C de Lara – setting up of the LLT1 ELISA

Thanks to all the healthy and flu-vaccinated volunteers who provided their blood.

Abbreviations

ABC	Activated B cell
AICD	Activation-induced cell death
AICL	Activation-induced C-type lectin
AID	Activation-induced cytidine deaminase
ASC	Antibody-secreting cells
B-NHL	B cell non-Hodgkin lymphoma
BACL	Brain-associated C-type lectin
BAFF	B-cell activating factor
BCL	B cell lymphoma
BCR	B cell receptor
BLIMP-1	B lymphocyte-induced maturation protein 1
CLAX	Lectin-like NK cell receptor
Clec	C-type lectin-like receptors
Clec2D	C-type lectin domain family 2 member D
CLR	C-type lectin receptors
CNS	Central nervous system
CpG	C-phosphate-G
CRD	Carbohydrate recognition domain
CSR	Class-switch recombination
CTLD	C-type lectin-like domains
CTLR	C-type lectin-like receptors
CTV	CellTrace™ Violet
CXCL	Chemokine (C-X-C Motif) Ligand
CXCR	Chemokine (C-X-C Motif) Receptor
D	Diversity
DAMP	Damage-associated molecular pattern
DC	Dendritic cell
DLBCL	Diffuse large B cell lymphoma
DMEM	Dulbecco's modified eagle medium
DMSO	Dimethyl sulfoxide
DZ	Dark zone
E.coli	*Escherichia coli*
EBV	Epstein-Barr virus
ELISA	Enzyme Linked Immuno-Sorbent Assay
ER	Endoplasmatic reticulum
Fab	Fragment antigen-binding
FACS	Fluorescence-activated cell sorting
Fc	Fragment crystallisable
FCS	Fetal Calf Serum

FDC	Follicular dendritic cell
FFPE	Formalin-fixed paraffin-embedded
GC	Germinal centre
GCB	GC B cell
geoMFI	geometric Median Fluorescence Intensity
GI	Gastrointestinal
h	Human
HBV	Hepatitis B Virus
HCMV	Human cytomegalovirus
HIV	Human immunodeficiency virus
HLA	Human leukocyte antigen
HRP	Horseradish peroxidase
HSV	Human herpesvirus
IC	Isotype control
ICOS	Inducible T cell co-stimulator
IFN	Interferon
Ig	Immunoglobulin
IHC	Immunohistochemistry
IL	Interleukin
IRF-4	Interferon regulatory factor 4
ITAM	Immunoreceptor tyrosine-based activation
ITIM	Immunoreceptor tyrosine-based inhibition motif
J	Junction
KACL	Keratinocyte-associated C-type lectin
Kb	Kilobases
Klr	Killer cell lectin-like receptors
LLT1	Lectin-like transcript 1
LP	Lipopeptide
LPS	Lipopolysaccharide
LSEC	Liver sinusoidal endothelial cell
LZ	Light zone
m	Mouse
mAb	Monoclonal antibody
MAIT	Mucosal-associated invariant T
MHC	Major histocompatibility complex
MZ	Marginal zone
NK	Natural Killer
NKC	Natural Killer Gene Complex
Nkrp1	NK cell receptor protein 1
OCIL	Osteoclast inhibitory lectin
pAb	Polyclonal antibody

PAMP	Pathogen associated molecular pattern
PAX-5	Paired box 5
PB	Plasmablasts
PBMCs	Peripheral blood mononuclear cells
PBS	Phosphate buffered saline
PC	Plasma cells
PD-1	Programmed cell-death 1
PGE_2	Prostaglandin E2
PILAR	Proliferation-induced lymphocyte-associated receptor
PMA	Phorbol 12-myristate 13-acetate
Poly(I:C)	Polyinosinic-polycytidylic acid
PRR	Pattern recognition receptors
qPCR	Real-time quantitative polymerase chain reaction
r	Rat
RA	Rheumatoid arthritis
RAG	Recombination-activating gene
RANKL	Receptor activator of NF-κB ligand
rCD161	Recombinant CD161
RCMV	Rat cytomegalovirus
RSV	Respiratory syncytial virus
RT-PCR	Reverse transcription polymerase chain reaction
RT	Room temperature
RTCL	Rat C-type lectin-like protein
SAP	SLAM-associated protein
SHM	Somatic hypermutation
SLAM	Signaling lymphocytic activation molecule
sLLT1	Soluble LLT1
SNP	Single-nucleotide polymorphism
TBM	Tingible body macrophage
TCR	T cell receptor
TD	T cell-dependent
Tfh	T follicular helper cell
TI	T cell-independent
TLR	Toll-like receptor
TNF	Tumor necrosis factor
Treg	T regulatory cell
V	Variable
XBP	X-box binding protein

1 Introduction

1.1 Innate and adaptive immunity

The immune system is a network of biological structures and processes within an organism that protects it against disease-causing pathogens. The efficient detection and control of the invading pathogen needs an orchestrated response of the two main arms of the immune system: the innate and adaptive immune responses.

The innate immune response constitutes the first line of defence. It is ancient, occurs immediately after infection, is non-specific to pathogen and does not trigger immunological memory. It is composed of different cell types such as neutrophils, macrophages and Natural Killer (NK) cells, which express germline-encoded receptors called Pattern Recognition Receptors (PRR). These allow the recognition of conserved pathogen structures called Pathogen Associated Molecular Patterns (PAMP) (Metzhitov 1998), and they trigger innate host defences such as inflammatory responses, phagocytosis, direct cytotoxicity and release of cytokines and chemokines. Innate immunity also plays an essential role in initiating adaptive immune responses, and Dendritic Cells (DCs) are key in such transition. Adaptive immunity is evolutionarily more recent, requires time, is pathogen-specific, induces memory and starts with antigen presentation through Major Histocompatibility Complex (MHC) molecules. B and T lymphocytes constitute the main cell types of the adaptive branch, expressing extremely diverse and somatically-

rearranged receptors. Upon recognition, they clonally expand and become effector cells, capable of antibody production, cytotoxicty and release of cytokines.

1.2 Immune cells and their receptors

Receptors on the cell surface of immune cells play a key role in sensing the environment as well as in interacting with other cell types. Each immune cell subset can be characterised by the particular expression of an array of receptors, which has major functional consequences. From sensing pathogens to altered-self or cytokines, these wide range of receptors can be classified into different categories (Murphy 2011). Fragment crystallisable (Fc) receptors, complement receptors and PRRs are often found in phagocytic cells and are involved not only in the detection of the infectious agent, but also in the process of engulfment and release of inflammatory cytokines. Killer activating and killer inhibitory receptors coat the surfaces of NK cells, and the net balance from their signals will determine NK cell effector function. On the adaptive front, the membranes of B and T cells are covered with a large number of identical copies of different B Cell Receptors (BCRs) and T Cell Receptors (TCRs), respectively, each one having specific binding abilities for a particular antigen. Finally, cytokine and chemokine receptors trigger optimal location, regulation and coordination of different immune cell types, allowing an orchestrated immune response.

Amongst the PRRs, two major subgroups can be distinguished: firstly, Toll-Like Receptors (TLRs) recognise PAMPs on infectious agents, such as

bacterial peptidoglycans or single and double-stranded RNA (Christmas 2010). Secondly, C-type Lectin Receptors (CLRs) comprise a large family of receptors that bind to carbohydrates, generally in a calcium-dependent (Ca^{2+}-dependent) manner (Weis et al. 1998).

1.3 C-type lectins

1.3.1 Lectins and C-type lectins

Lectins are a heterogeneous non-enzymatic group of proteins present in a whole variety of organisms, from viruses, bacteria and yeast to plants and animals (Gupta 2012). The origin of the word 'lectin' is found in the Latin *legere*, which means 'to select'. This phylogenetically ancient class of proteins has a wide variety of functions and possesses a distinctive structural motif. This singular structural signature known as the Carbohydrate Recognition Domain (CRD) is responsible for the shared feature amongst lectins, which is their ability to bind carbohydrates.

The archetypical CRD fold comprises a double loop structure, two antiparallel β-strands and two α-helices (Zelensky & Gready 2005; Weis et al. 1998). The presence of four conserved cysteine residues allows the formation of two disulphide-bonds that contributes to its overall stabilisation. The CRD structure of a subgroup of lectins comprises Ca^{2+} binding sites (Weis et al. 1998). They are located in one of the most evolutionarily flexible regions and some of them are absolutely essential for the binding of carbohydrates. This particular group of lectins are known as C-type (Calcium-dependent) lectins.

They usually present a short cytoplasmic tail, followed by a transmembrane domain, a stalk region and the extracellular CRD (Figure 1-1A). Oligomerisation through the stalk region is common amongst C-type lectins, and they are often found as multimers *in vivo* (Drickamer 1999).

The C-type lectin fold has been found in more than a 1000 proteins. However, despite their structural similarities, some of these proteins have lost their Ca^{2+} binding sites, thus losing its sugar binding restriction. Consequently, C-Type Lectin-like Domains (CTLD) are able not only to recognise carbohydrates, but also proteins, lipids, nucleic acids, inorganic compounds and even ice (Gupta 2012).

Their ligand versatility results in a diverse range of functions, with several receptors being involved in cell adhesion and immune responses to pathogens (Cambi & Figdor 2003; Cambi et al. 2005). Animal lectins are classified into at least 15 distinct structural families (Cummings et al. 2009). Amongst them, group V can be highlighted for its immunological importance and it comprises a wide variety of NK cell receptors. This group is evolutionarily recent, restricted to higher vertebrates, encoded in the Natural Killer gene Complex (NKC) and usually involved in protein recognition (Zelensky & Gready 2005). Although their expression is not limited to NK cells, they are mainly associated with the modulation of NK cell activity. Nonetheless, the precise role of some members of the family remains unknown.

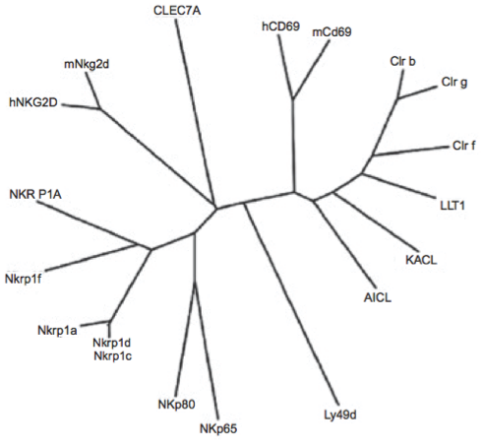
A



B

	Nkrp1	Clr
Mouse	6	8
Rat	4	11
Human	1	1

C



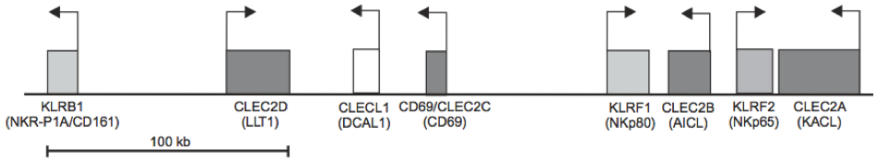
D

Mouse - Clec2d8/Clr-b

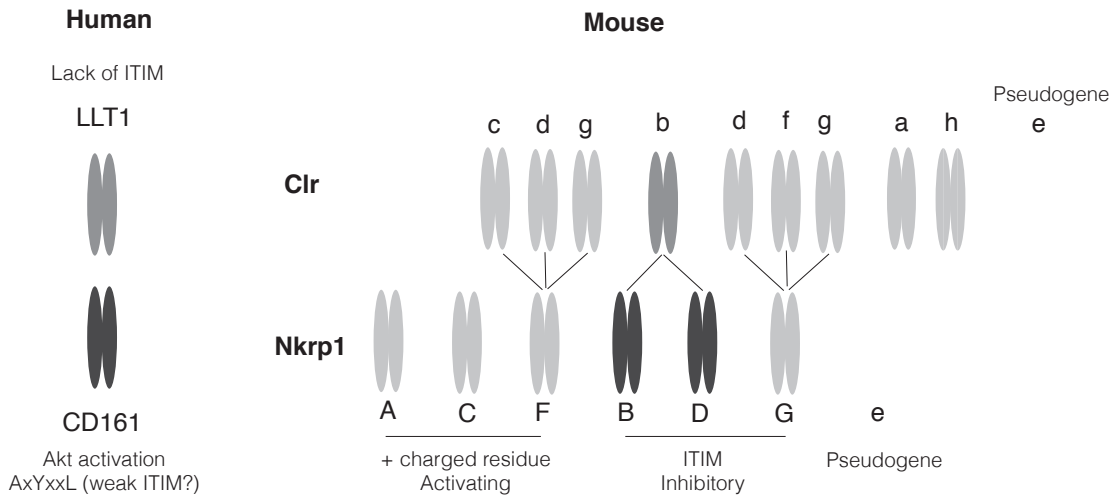
Rat - Clec2d11/Clr11

Human - Clec2d, Ocil, LLT1, CLAX

E



F



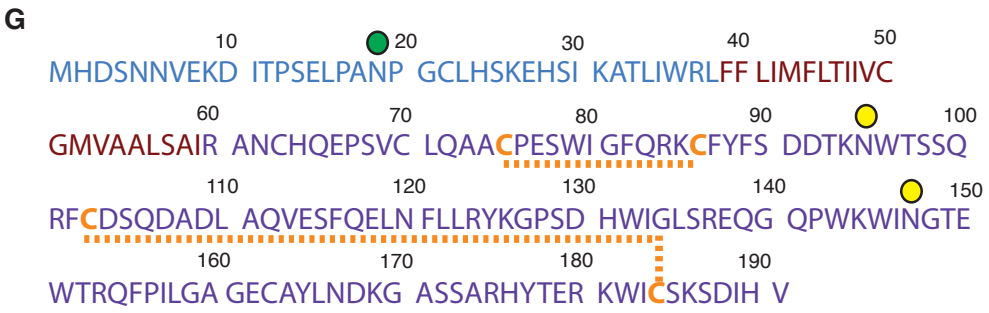


Figure 1-1. LLT1 and its homologs. (A) shows the general structure of a C-type lectin-like protein, with a short cytoplasmic domain (Cyt), a transmembrane region (TM) a stalk region (ST) and the lectin-like shaped domain. (B) shows the numbers of Nkrp1 and Clr genes in mice, rats and humans. (C) shows a phylogenetic analysis of CTL domain of NKRP1 and CLEC2 receptors of man and mouse (Spreu et al. 2010). (D) shows the closest homolog to human LLT1 in both mice and rats, as well as its alternative names. (E) Schematic representation of a region of the human NKC complex. Boxes and arrows represent CLEC2 (dark gray) and NKRP1 genes (light gray) and transcriptional orientation, respectively (Spreu et al. 2010). (F) shows the Nkrp1-Clr binding partners in both man and mouse, as well as their described signalling motifs, orphan receptors and pseudogenes. (G) shows LLT1 aminoacid sequence and its cytoplasmic (blue), transmembrane (red) and extracellular (purple) domains. The disulphide bridges are depicted by orange dashed lines, the N-glycosylation sites with yellow dots and the described Single Nucleotide Polimorphism (SNP) with a green dot.

1.3.2 The Natural Killer Gene Complex (NKC)

The NKC dates from more than 300 million years ago. It was first identified in mice, where the presence of several genes encoding structurally related type II (N-terminal facing the cytosol) C-type lectins was reported (Yokoyama et al. 1990). These C-type lectin-like receptors (CTLRs) are expressed in various cell types but, as previously mentioned, they are most commonly found on NK cells.

There is an interesting paradox in the evolutionarily history of the NKC. Hao *et al*. studied the NKC complex of four major groups of mammals (Hao et al. 2006) and concluded that there is a high degree of heterogeneity in gene content, as well as abundant birth and death of such genes, mainly occurring through duplications and deletions. In fact, there has been a remarkable process of expansion and contraction of rodent NKC genes. However, the genomic structure is extraordinarily conserved, with mice, rats and humans presenting very similar NKCs (Kelley et al. 2005; Yokoyama & Plougastel 2003).

The human NKC accommodates around 30 genes encoding for C-type lectin-like proteins, as well as some poorly characterised orphan genes. A wide variety of immune-related cells, including NK cells, T cells and myeloid cells have been found to express CTLRs.

1.3.3 Nkrp1 and Clec families

CTLRs can be divided into two large groups based on their expression patterns. Killer cell Lectin-like Receptors (Klr) are mainly expressed on NK cells, whereas C-type lectin-like receptors (Clec) are usually expressed in other cell types rather than NK cells. The nomenclature used has been rather complex. It is now accepted that *Klrb1* genes encode Nkrp1 (NK cell receptor protein 1) proteins and *Clec2* genes encode Clr proteins.

The Nkrp1 cluster is comprised within the NKC complex, which is located in chromosome 6 in mice, chromosome 4 in rats and chromosome 12 in humans (Ryan et al. 1991; Ryan & Seaman 1997; Suto et al. 1997; Yokoyama et al. 1991). Since its discovery, evidence suggested high conservation of the Nkrp1 family between rodents and humans (Lanier 1994; Chambers et al. 1989; Giorda et al. 1990). It is a highly stable genomic region, comprising minimal diversity as well as limited and focused allelic polymorphism (Carlyle et al. 2006; Ljutic et al. 2006; Voigt et al. 2007).

In contrast to the polymorphisms within the Nkrp1 family, their Clr cognate ligands are even more conserved, suggesting susceptibility to selection pressure on the former but not on the latter (Carlyle et al. 2008). The need to keep self-integrity could explain the extreme stability of the Clr family.

The *Clr* gene family was first identified by Plougastel and colleagues, who mapped this genetic region also within the NKC complex on mouse chromosome 6 (Plougastel et al. 2001). The ability of Nkrp1 receptors to engage with Clr molecules has been known for a while and described in detail

elsewhere (Iizuka et al. 2003; Carlyle et al. 2004). This grants the NKC complex a striking peculiarity, as the Nkrp1 genes are interspersed with the genes encoding their Clr ligands (Yokoyama et al. 1993). It has been suggested that they could all share a common ancestor that once engaged in homophilic interactions. Moreover, this tight genetic linkage could be a way of ensuring coinheritance, providing a mechanism for biological self-recognition.

Both the products of *Nkrp1* and *Clec* genes are C-type lectin-like proteins. As mentioned in the *1.2.1 Lectins and C-type lectins* section, C-type lectins have evolved to recognise carbohydrates. Carlyle and colleagues (Carlyle et al. 2004) showed that Nkrp1 receptors are also capable of protein recognition. However, there is still the possibility that glycans present in Clr proteins play a prominent role in receptor binding.

The NKC complex is an orthologous region in humans and mice. Whereas it is true that there is a large overlap in genomic organisation and even function, some gene families have evolved in a different way. Despite abundant similarities between Nkrp1 and Clr receptors from man and mouse, there are no obvious homologies, with very few exceptions (e.g. CD69).

Three members of the human Nkrp1 family have been identified: CD161, NKp65 and NKp80. The corresponding ligands that belong to the Clec2 family are LLT1, Keratinocyte-Associated C-type Lectin (KACL) and Activation-Induced C-type Lectin (AICL), respectively. Amongst these, the CD161-LLT1 pair is the one that presents greatest homology with the mouse (Zhang et al. 2012).

1.4 Lectin-Like Transcript 1 (LLT1)

1.4.1 CD161-LLT1 and the rodent homologs

Lectin-like transcript 1 (LLT1) is a C-type lectin-like protein that was first described by Boles *et al*. (Boles et al. 1999). Its characterisation as the ligand for the CD161 receptor (Aldemir et al. 2005; Rosen et al. 2005) depicted another pair of receptor-ligand C-type lectins with a prominent role in the immune system. Both receptors are located within the NKC.

The human (h) gene homologous to mouse (m) *Klrb1* encodes the NK receptor Klrb1/NKR-P1A/CD161 (Takahashi et al. 2005, Lanier et al. 1994). This is in fact the only well-accepted homolog of the rodent Nkrp1 family, as mNkrp1d and hCD161 share a 46% of their aminoacid sequence (Vogler & Steinle 2011). The product of the *Clec2d* gene (Ocil/Clr-b) was identified as the ligand of the Klrb1 receptor (Iizuka et al. 2003; Carlyle et al. 2004).

Therefore, it has been possible to establish homologous C-type lectin-like pairs in mice, rats (r) and humans. In humans, CD161 receptor binds LLT1; in rats Nkrp1A receptor binds Clr11 and in mice, Nkrp1B/D engages with Clr-b. In the latter, *Nkrp1d* has been identified as an allele of the *Nkrp1b* gene (Carlyle et al. 2006). All hLLT1, mClr-b and rClr11 have been shown to inhibit NK cells, as discussed in further sections.

The term ‘LLT1’ will only be used in this work to refer to the human Clec2D, and the term ‘OCIL’ will be used in the context of bone.

The number of genes comprising the Nkrp1 and Clr families is different between mouse, rat and man (Figure 1-1B). Phylogenetic analysis of the CTLD of both families shows a high degree of interspecies homology, although they are still different (Figure 1-1C). The alternative names for LLT1 in humans as well as its rodent homologs are specified in Figure 1-1D. Within the human NKC complex, CD161 and its binding partner LLT1 are only separated by a 100 kilobases (kb) (Figure 1-1E). Thus, the human receptor-ligand pair CD161-LLT1 and their closest homolog in mouse (Nkrp1B/D-Clr-b) share the genetic linkage that allows coinheritance as well as their gene organisation, orientation and copy number. Evidence is less clear when it comes to their expression pattern, particularly regarding hLLT1 and mClr-b (see *1.3.3.Expression pattern: mClr-b vs hLLT1*). The members of the Nkrp1 and Clr families, as well as their binding partners and signalling motifs are detailed in Figure 1-1F. To date, there are still a few orphan receptors such as Nkrp1A/C and some promiscuous ligands (e.g. Clr-d binds both Nkrp1F and G). Currently, the diversity within the mouse system makes it difficult to establish enough similarities to be able to use the mouse as a valid animal model for the study of human CD161-LLT1 interactions.

The unexpected presence of two C-type lectins within the chicken MHC was reported a few years ago (Kaufman et al. 1999; Rogers et al. 2005). This finding led Rogers *et al*. to suggest that the MHC and the NKC regions could share an ancient common origin. They identified B-NK and B-lec, an inhibitory receptor and an early activation antigen, respectively, that highly resemble the

human CD161-LLT1 receptor-ligand pair (Viertlboeck et al. 2008). However, interaction between B-NK and B-led has not been shown.

1.4.2 Human LLT1

LLT1 was first identified as a member of the C-type lectin-like protein family in 1999 (Boles et al. 1999). Alternative names are Clec2D (C-type lectin domain family 2 member D), OCIL (Osteoclast inhibitory lectin) and CLAX (Lectin-like NK cell receptor). Its sequence and domains are specified in Figure 1-1G.

Using an expressed sequence tag database together with human and mouse consensus sequences of C-type lectin receptors, Boles *et al*. described the molecular characterisation and the chromosomal mapping of human LLT1. *LLT1* is located in the NKC within human chromosome 12. AICL and CD69, both also encoded in the NKC, were identified as the structurally closest receptors, sharing 59% and 56% of sequence similarity, respectively.

At a genomic level, southern blot analyses suggested a single gene for LLT1, or a small number of genes. A traditional or inverted TATA sequence is missing in the LLT1 gene. Alternatively, a GAATCA sequence can be found upstream of the transcription start site (Hu et al. 2004). Expression of the rat *Clr11* is regulated by Sp1 transcription-factor binding sites (Quan et al. 2009). At the expression level, northern blot analyses postulated the existence of several spliced variants. This was later confirmed and described in detail by Germain *et al*. (Germain et al. 2010). *LLT1* comprises five exons and four introns, with five alternatively spliced variants as the result of exon skipping, a

part from a nonsense-mediated RNA decay product (isoform 3). Variant 1 or LLT1 was identified as the only surface protein. On the contrary, variants 2 and 4 were found to be retained in the endoplasmatic reticulum (ER), forming homodimers or heterodimers with LLT1. Finally, isoforms 5 and 6 were identified as the soluble versions of LLT1 and variant 4 respectively, lacking the transmembrane domain encoded in exon 2.

The crystal structure of LLT1 was recently solved (Skálová et al. 2015). One monomeric and one hexameric structure, as well as two dimeric structures with different glycosylation patterns were characterised. For the first time, the two α-helices, the two antiparallel β-sheets and the disulphide bonds that help to stabilise the structure could be experimentally observed. Furthermore, a detailed analysis of the dimeric interface suggested the existence of a hydrophobic core responsible for leading the interaction. The study concluded a main role for glycosylation in both structure and flexibility in the interface; plasticity and variability are essential in cellular interactions within the immune system. The LLT1 extracelullar domain, responsible for receptor recognition, was also crystalised by Kita and colleagues, who cast further light on the binding surface and acknowledging the conservation within CTLRs at the structural, binding and signalling levels (Kita et al. 2015).

The homodimeric nature of LLT1 as well as its large polysaccharide content have been described (Rosen et al. 2008; Germain et al. 2010). It is now accepted that the most common presentation of LLT1 is as a highly glycosylated homodimer located on the cell surface.

The C-type lectin-like protein family still comprises abundant orphan receptors. LLT1 left this category in 2005, when two simultaneous studies characterised it as the ligand for the CD161 receptor, another C-type lectin-like protein encoded only 100 kilobases downstream of *LLT1* (Aldemir et al. 2005; Rosen et al. 2005). As previously mentioned, genetic linkage between receptor-ligand pairs of C-type lectin-like proteins is not uncommon. Amongst all the previously described isoforms, LLT1 is the only one able to interact with CD161 (Germain et al. 2010). The molecular basis of CD161 and LLT1 interaction is characterised by low affinity (K_d = 48 μM) and fast kinetics, which is very common within cell-cell recognition receptors (Kamishikiryo et al. 2011). This implies that only small conformational changes may be necessary to allow binding.

1.4.3 Expression pattern: mClr-b vs hLLT1

Despite the existence of CD161-LLT1 homologs in rodents, large differences in expression pattern have been acknowledged between mice and humans, particularly on the Clr-b side. Such singular expression could translate into distinct functionality of these C-type lectins, depending on the host.

Expression of different Clr genes has been shown to be highly variable as well as regulated. Zhang and colleagues studied the expression of different members of the NKrp1 and Clr families in a wide range of mouse tissues, reaching the conclusion that the majority of Clr genes are specifically expressed in certain tissues (Zhang et al. 2012). However, there seemed to

be one exception to the rule, this being Clr-b. More common were the cases of Clr-d, the expression of which is restricted to the eye, or Clr-f, found in kidney, liver and intestine. These restricted expression patterns would imply tissue-specific functions (Zhou et al. 2002).

Clr-b expression was found in nearly all haematopoietic cells, although absent on erythrocytes, and in a wide range of mouse tissues (Zhang et al. 2012). Interestingly, it could not be detected in the brain.

Downregulation of Clr-b in mouse tumor cell lines and a consequent increased susceptibility to NK cell killing has been described (Carlyle et al. 2004). This broad expression pattern combined with a decrease upon malignant transformation resembles the one of MHC class I molecules, although Clr-b expression is β2-microglobulin independent. The expression pattern of Clr-b still presents, however, some controversies. Whereas its broad expression has been reported several times in the literature, some studies suggest a more restricted expression pattern, predominantly on DCs and macrophages (Iizuka et al. 2003).

The ubiquitious expression of Clr-b, its downregulation upon transformation and the presence of its ligand on NK cells suggest that it plays a role in missing-self recognition. This broadens the missing-self hypothesis, which postulates a role for NK cells in the recognition and elimination of cells that fail to express self-MHC class I molecules (Kärre et al. 1986).

The literature about LLT1 is limited, partially due to a lack of extensive and validated tools for its study and characterisation (ie. antibodies). This issue has been previously addressed by several groups, including ours, which have generated their own anti-LLT1 antibodies (Mathew 2004; Germain et al. 2010).

However, there are still many inconsistencies in the published data regarding the distribution of LLT1 in human tissues and cell types (Table 1.1). When LLT1 was first characterised, it was found predominantly expressed on NK cells but also on T and B cells, as well as in thymus, lymph node and spleen (Boles et al. 1999). Some future studies questioned and expanded these results, bringing new insights into the expression pattern of LLT1. Mathew *et al*. reported LLT1 expression in all monocytes, most B cells and a few T and NK cells, as well as in Phorbol 12-Myristate 13-Acetate (PMA) and Interleukin (IL)-2-activated Peripheral Blood Mononuclear Cells (PBMCs) (Mathew et al. 2004). Other groups could not detect LLT1 in resting PBMCs but only after pathogen, Interferon-γ (IFN-γ) (Germain et al. 2011) or PMA stimulation (Eichler et al. 2001), as well as on activated B cells and DCs (Rosen et al. 2005). Enhanced levels of LLT1 could be detected on B cells following TLR9, BCR and CD40 stimulation (Rosen et al. 2008). Viral infection (Epstein-Barr virus (EBV), Human immunodeficiency virus (HIV), influenza, Human herpesvirus (HSV)) has also been identified as a cause for LLT1 upregulation (Rosen et al. 2008; Germain et al. 2011). Recently, increased expression of LLT1 was described in the lung following Respiratory Syncytial Virus (RSV) infection (Satkunanathan et al. 2014). Also, LLT1 was detected in the surface

Reference	Method	Antibodies	Cell type / Tissue	Function
Boles 1999	Northern Blot	-	T, B and NK cells; Lymph node, thymus, spleen, LAK	-
Eichler 2001	RT-PCR	-	PMA-stimulated PBMCs	-
Zhou 2001	Northern blot, IHC, *In situ* hybridization	-	Osteoblasts; Liver, kidney, gut, heart, skeletal muscle	-
Iizuka 2003	RT-PCR	-	DCs, Macrophages (from bone marrow)	-
Carlyle 2004	FACS	mAb 4A6 (rat IgMκ)	Hematopoietic cells (no erythrocytes); Down-regulation in tumour cell lines	Inhibition of NK cytotoxicity
Mathew 2004	FACS	mAb L9.7	All monocytes, most B cells, few T and NK cells; PMA and IL-2 activated PBMCs	Induction of IFN-γ in NK (in LLT1 expressing cells)
Hu 2004	RT-PCR	-	Osteoblasts, Osteoblast cell line (MG63); Upregulated with IL-1α and PGE_2	-
Aldemir 2005	LLT1 Multimer	-	-	Inhibition of NK cytotoxicity via CD161
Rosen 2005	LLT1 containing liposomes	-	-	Inhibition of NK cytotoxicity and IFN-γ; enhancement of CD3-triggered IFN-γ in T cells
Roth 2007	RT-PCR, FACS	mAB 4C7 (Abnova)	Glioma cells (Upregulated with TGF-β)	Immunosupressive
Rosen 2008	FACS, WB, RT-PCR	2F1, 4F68; mAb 402624 and 402659 (R&D); Rabbit anti-LLT1 antisera	Activated B cells and DCs; B cell-derived cell lines(*)	Inhibition of NK cytotoxicity and cytokine production
Bambard 2010	FACS, RT-PCR	402659 (R&D) and 4C7 (Abnova)	NK92 cells	IFN-γ production (in LLT1 expressing cells)
Germain 2010	FACS, RT-PCR, Real Time RT-PCR	2F1, 4F68; mAb 3480 (R&D); 4C7 (Abnova)	T and B cells, NK cells (low); B cell-derived cell lines(**), THP-1 (low)	-
Germain 2011	FACS, WB, Real time RT-PCR	2F1, 4F68; 3480 (R&D), 4C7 (Abnova)	No in resting PBMCs – upregulated with pathogen/IFN-γ stim; Raji	Inhibition of NK cell function; Costimulation of T cells
Satkunanathan 2014	RT-PCR, IHC, Live cell confocal imaging	4C7 (Novus Biologicals)	RSV-infected/TLR and cytokine stimulated respiratory epithelial cells	-
Chalan 2015	FACS, IHC	FACS: 402659 (R&D) IHC: 4C7 (Abnova)	Monocytes and macrophaes from RA joints	-

Table 1-1. Summary of LLT1 expression and function in the published literature.

of monocytes from Rheumatoid Arthritis (RA) synovial fluid, as well as in tissue resident macrophages from RA joints (Chalan et al. 2015). This was also the first study to detect soluble LLT1 (sLLT1) in serum and to describe its increased abundance in this autoinflammatory condition.

Several studies have also reported the expression of LLT1 on B cell and monocyte-derived cell lines (Boles et al. 1999; Rosen et al. 2008; Germain et al. 2010; Germain et al. 2011).

1.4.4 OCIL in the context of bone

Bone homeostasis involves the constant removal of mature bone tissue (bone resorption) as well as the continuous formation of new bone tissue. Osteoclasts, from the Greek *osteo* (bone) and *clasts* (break) are responsible for the former, whereas osteoblasts, *blast* meaning to germinate, lead the formation of new bone cells.

Osteoclasts are derived from the monocyte-macrophage lineage and they are large, multinucleate cells. On the contrary, osteoblasts are terminally differentiated cells derived from mesenchymal stem cells and present a single nucleus.

OCIL expression has been described in osteoblasts and osteoblast-derived cell lines in mice, presenting a very similar expression pattern to that of the Receptor activator of NF-κB ligand (RANKL) (Zhou et al. 2001) which, in contrast to OCIL, promotes the differentiation and formation of osteoclasts. OCIL expression levels are susceptible to hormone treatment, as they are

increased by parathyroid hormone, calcitriol, IL-1α, IL-11 and retinoic acid (Zhou et al. 2001). IL-4 does not seem to play a role in the regulation of OCIL (Mirosavljevic et al. 2003), nor mechanical stimuli (Kreja et al. 2008).

Functional studies have shown that murine and human OCIL inhibits osteoclast formation and function, therefore diminishing bone resorption (Zhou et al. 2001; Hu et al. 2004). In order to analyse the physiological function of OCIL, *ocil*$^{-/-}$ mice were generated (Kartsogiannis et al. 2008). They were healthy and fertile and the abnormalities presented were restricted to the bone environment. They presented reduced bone formation and increased osteoclast formation compared to their wild-type counterparts, which resulted in the animals suffering from osteopenia. Therefore, this study confirmed OCIL as a negative physiological regulator of bone metabolism. There were no obvious immunological defects, although immunological function of these animals was not assessed. In the human *LLT1*, a naturally occurring Single-Nucleotide Polymorphism (SNP) that results in a non-synonymous mutation (Asn19Lys) has been associated with a decrease of bone mineral density in post-menopausal women (Pineda et al. 2008, Figure 1-1G).

Interestingly, the role of OCIL inhibiting osteoblast differentiation has also been reported (Nakamura et al. 2007). In this study, Nakamura *et al*. described not only the reduction in osteoblastic function but also the blocking of adipocytic differentiation. This is a remarkable fact, as it provides the first evidence of the involvement of NK cell receptors in the regulation of mesenchymal cell differentiation and function. Up until that point, none of the aforementioned studies had addressed the question of OCIL ligand in the

context of bone metabolism. Nakamura and colleagues were the first ones to approach it, and they found that OCIL bound to high molecular weight sulfated glycosaminoglycans, as is typical of the C-type lectin family. However, the binding was not Ca^{2+}-dependent. It is important to note that, to my knowledge, there are no studies assessing the presence CD161/Nkrp1A in the bone.

1.4.5 LLT1 signalling and function

C-type lectin-like proteins can bind to a wide variety of ligands. This results in an equally versatile response, including different processes such as endocytsis, pro-inflammatory and anti-inflammatory responses. Such variety of outcomes is a consequence of the multiple signalling pathways that can be involved in CLR signalling, which has been reviewed elsewhere (Sancho & Reis e Sousa 2012). Nonetheless, all these pathways share a prominent role for tyrosine-based motifs.

Up until now, no consensus signalling motifs or charged transmembrane residues have been described in Clr proteins. The published literature regarding LLT1 signalling is very limited. The lack of intracellular Immunoreceptor Tyrosine-based Inhibition Motifs (ITIM) has been described (Boles et al. 1999), which suggests that LLT1 may trigger activating signals. To my knowledge, there is only one study that has addressed the full signalling pathway triggered by LLT1 (Bambard et al. 2010). In this work, LLT1 signalling was investigated on NK92 cells stimulated with a transfectant K562-CD161 cell line. Pharmacological inhibitors were employed to elucidate the LLT1 signalling mechanism; Bambard *et al*. concluded that this particular

C-type lectin uses Src-PTK, p38 and ERK signalling pathways, but not PKC, PI3K or calcineurin.

Several studies have shown changes in LLT1/Clr-b expression levels due to viral infection, malignant transformation or cellular stress. In a study published by Fine *et al*. (Fine et al. 2010), genotoxic stress caused rapid downregulation of Clr-b, enhancing the killing capabilities of Nkrp1B-expressing NK cells. Clr-b surface expression was lost in murine cells upon poxvirus infection resulting in increased susceptibility to NK cell lysis (Williams et al. 2012). In rats, downregulation of Clr-b as a consequence of Rat Cytomegalovirus (RCMV) infection has also been described (Voigt et al. 2007). This drop in Clr-b surface levels makes viral-infected cells a better target for NK killing. Interestingly, RCMV encodes a rat C-type lectin-like protein (RCTL) homologous to Clr ligands that confers protection to infected cells. RCTL interacts with NK cells through Nkrp1B receptor, thus preventing killing. These three examples suggest a role for Clr-b in the negative regulation of NK cells. This hypothesis has been further addressed and confirmed by others. Tran *et al*. (Tran et al. 2010) used a lentiviral transduction system to overexpress Nkrp1B on primary mouse NK cells. This resulted in increased sensitivity to inhibitory signals delivered by Clr-b-expressing target cells. A recent study by Rahim and colleagues supported the idea that the Nkrp1B:Clr-b system plays a role in NK tolerance, tumor surveillance and immune escape in an MHC-I-independent manner (Rahim et al. 2015).

In humans, LLT1 cross-linking through CD161 receptor on NK cells resulted in inhibition of cytotoxicty (Aldemir et al. 2005; Rosen et al. 2005) and cytokine

production (Aldemir et al. 2005; Rosen et al. 2008). Inhibition of NK cells through Clr-b/LLT1 has also been described in tumours, both in mice (Carlyle et al. 2004) and humans (Roth et al. 2007; Mathew et al. 2014). However, there is one study postulating an activating role for rClr11 (Yang et al. 2006).

There is conflicting evidence regarding the consequences of LLT1 binding to CD161 expressing T cells. Several studies have suggested a costimulatory role for CD161, as it increases cytokine production upon TCR engagement (Exley 1998; C. D. Rosen et al. 2005; Fergusson et al. 2014). However, cross-linking CD161 was shown to inhibit Tumor Necrosis Factor α (TNF-α) production in TCR-activated CD8+ T cells (Rosen et al. 2008).

The data available is much more limited when it comes to analysing the consequences of LLT1-CD161 interaction on the LLT1 expressing cells. Resting and IL-2 activated NK cells increased their IFN-γ production upon LLT1 engagement, but their cytotoxic potential remained unchanged (Mathew et al. 2004). The same was true for the NK cell line YT. Ligation of LLT1 in another NK cell line, NK92, also resulted in a higher release of IFN-γ (Bambard et al. 2010). Further investigation is required to elucidate the precise consequences of LLT1-CD161 interaction on both sides.

Table 1.2 summarises the cell types expressing both LLT1 and CD161, together with potential sites for interaction and function, according to the published literature.

	Cell type	Potential sites for interaction	Potential function
CD161 expression	T cells NK cells	Bone Lymph nodes Inflamed tissues	NK cell inhibition T cell inhibition/activation
LLT1 expression	Osteoblast PBMCs (Table 1.1) RSV-infected lung epithelia RA joints		NK IFN-γ production Osteoclast inhibition

Table 1.2. CD161 and LLT1 expression and function. Cell types expressing the C-type lectins CD161 and LLT1 are specified, as well as potential sites for their interaction and functions described in the published literature.

1.4.6 CD161-LLT1/ NKp80-AICL / NKp65-KACL

In humans, there are three well-characterised NKC-encoded receptor-ligand pairs. These are the CD161-LLT1, NKp65-KACL and NKp80-AICL, all of them being akin and unique at the same time. Table 1.2 summarises the distribution described for LLT1 and CD161.

CD161 is expressed in the vast majority of NK cells (Lanier et al. 1994). It has also been found on different innate-like T cell subsets such as NKT cells (Exley et al. 1998), Mucosal-associated invariant T (MAIT) cells (Martin et al. 2009), γδ T cells (Maggi et al. 2010; Rajoriya et al. 2014) and in other T cell subgroups, both in the CD4+ and CD8+ compartments. Recently, CD161 was identified as a defining transcriptional and functional feature across different human T cell lineages (Fergusson et al. 2014).

There is no clear signalling pathway for CD161 receptor, which might be linked to its heterogeneous functionality described so far. However, it has been shown that triggering CD161 stimulates activity of acid sphingomyeliase with consequent ceramide production and Akt activation (Pozo et al. 2013). Also, there is an atypical motif (AxYxxL) comprising a Tyr residue in the CD161 cytoplasmic domain that could function as a weak ITIM (Ryan et al. 1997; Rosen et al. 2005). ERK signalling pathway has been suggested to be involved downstream LLT1 (Bambard et al. 2010).

NKp65 is mainly expressed on NK cells whereas its ligand KACL is restricted to skin (Spreu et al. 2007). Such expression pattern suggests a role for these C-type lectins specific to skin immunobiology. Upon binding, NK cell activation and production of proinflammatory cytokines is induced (Spreu et al. 2010). The bidirectionality of NKp65-KACL interaction has not been explored. The fact that KACL is found as a monomer, as well as the absence of disulphide bridges, distinguish NKp65-KACL binding from the other two pairs. It is a high affinity interaction driven by a largely hydrophobic interface. The existence of a few essential binding residues for all three Nkrp1-Clec2 pairs has been suggested (Li et al. 2013).

KACL is also known as Clec2A1 or Proliferation-Induced Lymphocyte-Associated Receptor (PILAR). Initial studies described it as a ligand for CD161 (Huarte et al. 2008), but future research established PILAR/KACL as the ligand for NKp65 and not CD161 (Spreu et al. 2010).

NKp80 is an activating receptor (Vitale et al. 2001) expressed on nearly all NK cells, absent in rodents but conserved amongst primates (Biassoni et al. 2005; Mavilio et al. 2005). Its ligand AICL was first described in activated PBMCs (Hamann et al. 1997) and further characterised in various myeloid cells, including macrophages, granulocytes and TLR-stimulated monocytes (Le Naour et al. 2001). Upregulation of AICL on NK cells has also been described, proposing an autonomous control of NK cell function under inflammatory conditions (Klimosch et al. 2013). Upon interaction, an increase on NK cell cytotoxicity and proinflammatory cytokine release has been reported (Vitale et al. 2001; Welte et al. 2006; Kuttruff et al. 2009). Interestingly, and in contrast to the NKp65-KACL pair, bidirectional signalling and function has been characterised on NKp80+ NK cells and AICL+ monocytes (Welte et al. 2006). This mutual activation study suggested a role for NKp80-AICL interaction in the start and maintenance of immune responses at the inflammation site.

Interestingly, NKp80 has also been found in a subset of T cells that presents innate-like characteristics, high responsiveness and effector memory phenotype (Kuttruff et al. 2009).

A hemi-Immunoreceptor Tyrosine-based Activation Motif (ITAM), responsible for signal transduction, has been identified in the cytoplasmic domains of both NKp65 and NKp80 (Spreu et al. 2010; Dennehy et al. 2011).

1.5 Basics of B cell biology

Unexpectedly, I found expression of LLT1 on GC B cells. Therefore, a large part of this thesis has focused on exploring the expression, regulation and function of this C-type lectin on GC B cells.

1.5.1 The discovery of B cells

In 1890, Emil von Behring and Shibasaburo Kitasato described the presence of antitoxins targeting diphtheria and tetanus, providing the first hint of B cell existence (von Behring & Kitasato 1890) (Figure 1-2). However, it was not until a few decades later that Paul Ehrlich postulated that such antitoxins were the product of cells bearing pre-formed antibody receptors (Ehrlich 1908). Abundant studies in birds, mammals and immunodeficient patients were required to establish B cells as a functionally distinct branch within the adaptive immune system responsible for humoral immunity (Landsteiner and Chase 1942; Bruton 1952; Good and Varco 1955). Bruce Glick performed one of the breakthrough experiments when he removed the bursa of Fabricus, an intestine-resident lymphoid organ, from chicks and observed their inability to produce antibodies (Glick et al. 1956). Further studies demonstratred that these bursectomised birds resembled individuals with X-linked agammaglobulinemia, which implies an absence of GCs, plasma cells and antibodies, but sustained lymphocyte numbers and cellular immunity almost intact, in contrast to thymectomised animals (Hilschmann & Craig 1966). These studies led to the still accepted broad division of adaptive immunity in B cells (bursa-dependent) and T cells (thymus-dependent) lymphocytes,

accounting for humoral and cellular immunity, respectively (Roitt et al. 1969). Nonetheless, at this point, the question of what constituted the bursa equivalent in mammals was still unresolved. Although the early candidates were the gut-associated lymphoid tissues, Peyer's patches and the appendix, evidence could not be provided for them being the essential source of B cells in mammals. Later research showed that B lymphocytes originate and mature in the bone marrow and the fetal liver (Osmond, D. G. & Nossal 1974; Ryser et al. 2015).

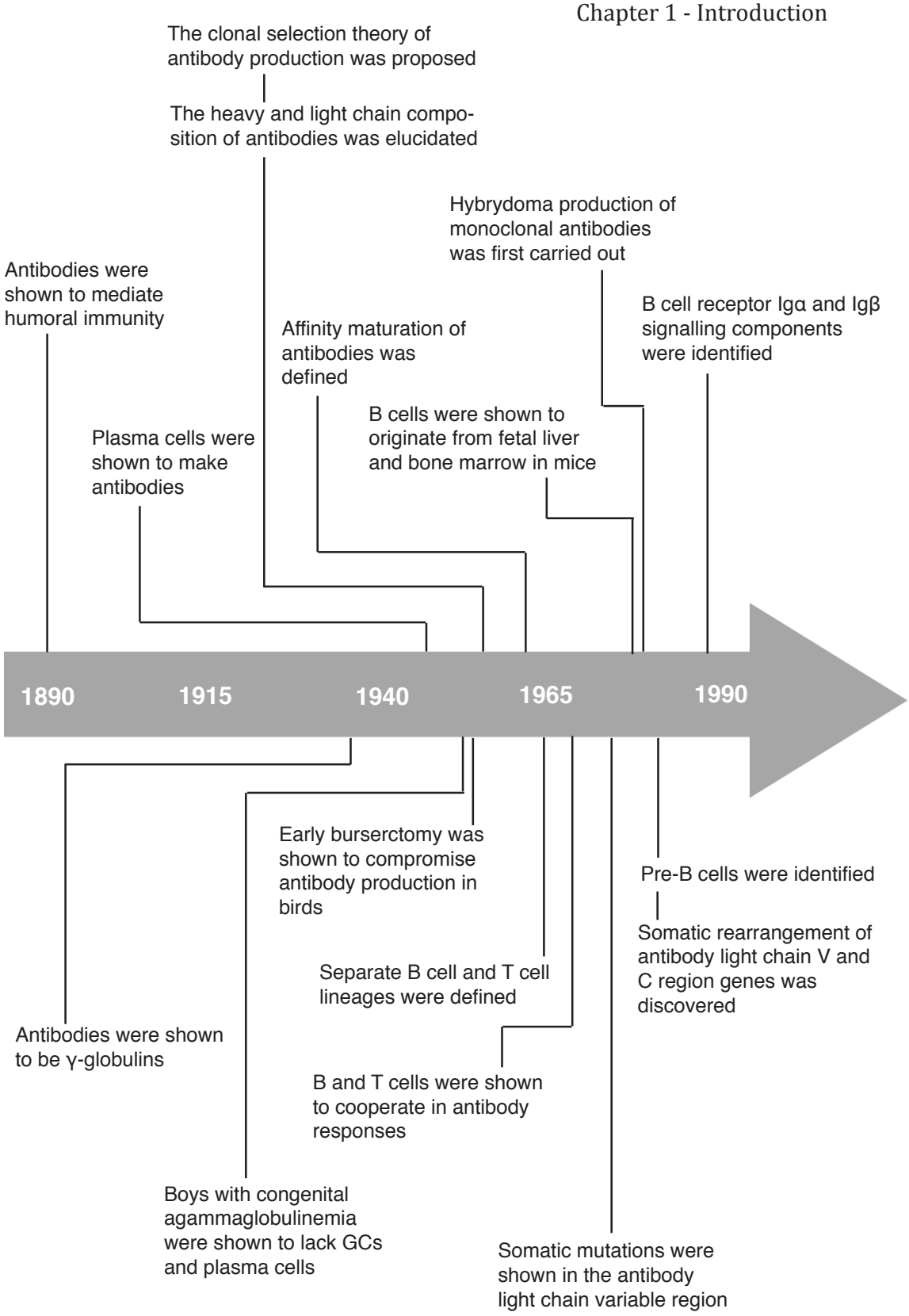


Figure 1-2. **Timeline of the most relevant discoveries in the history of B cells**. Adapted from *The early history of B cells* (Cooper 2015).

1.5.2 Early understanding of B cell biology and new questions

The idea that a wide variety of pre-formed antibody receptors might be stimulated by their cognate antigen and this interaction leads to increased production and secretion of that particular receptor was already present in the very early days of B cell research (Ehrlich 1908). Such hypothesis was fine-tuned later on, when the existence of a clonally diverse repertoire of antibody-producing cells was postulated, together with the idea that interaction with cognate antigen would result in production and release of that same antibody type (Burnet 1959). The main focus of attention became understanding the basis of antibody diversification and selection. In-depth studies that used a diverse range of recently available technologies allowed the field to move forward, bringing some insight, together with abundant new questions.

In the late 1950s, studies on multiple myeloma, a precious source of homogenous antibodies, revealed the basic four-chain structure of an antibody (Edelman 1959; Porter 1956), exposing the existence of heavy and light chains, both with constant Fc and variable Fragment antigen-binding (Fab) regions sustained by disulphide bonds (Figure 1-3).

Further studies elucidated that the variable fragment played a major role in antibody specificity and antigen recognition, while the constant portion was responsible for antibody effector functions. The amino acid sequence technology allowed the elaboration of a combinatorial theory, in which different gene regions could be joined to give rise to a large and diverse antibody repertoire (Hilschmann & Craig 1966).

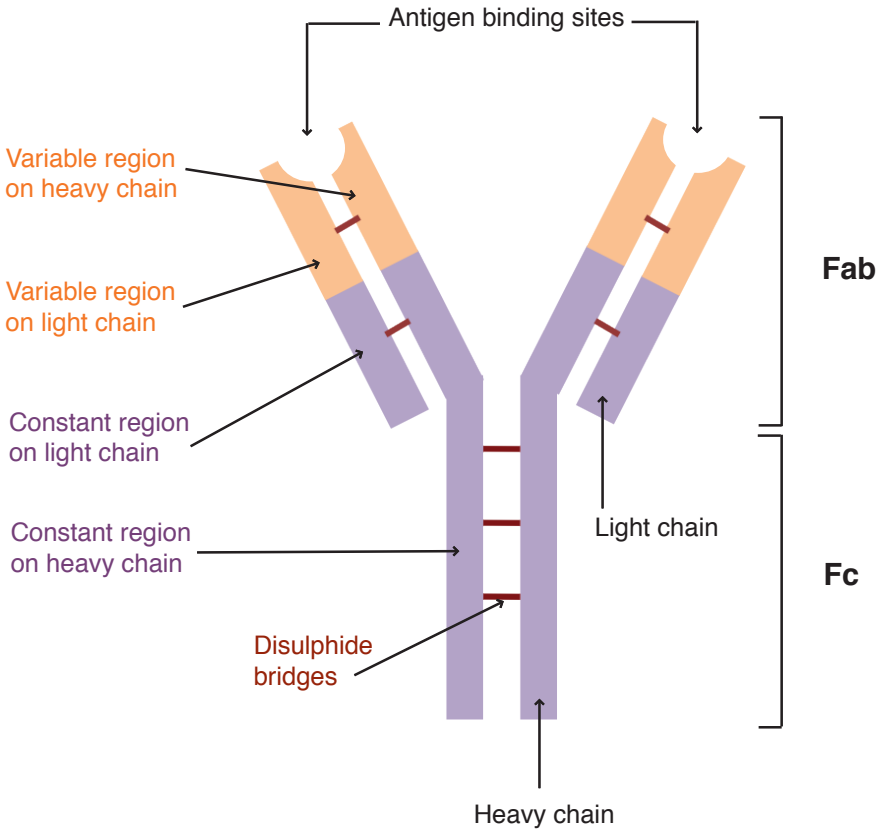


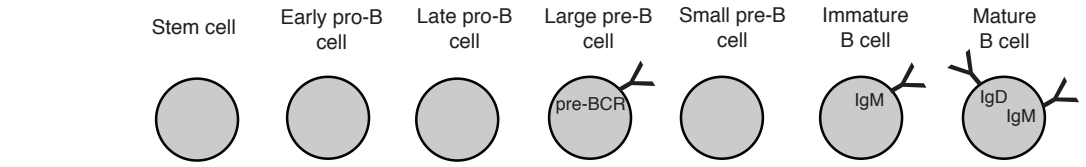
Figure 1-3. **Antibody structure**. Schematic of the structure of an antibody, comprising two identical binding sites, two heavy and light chains both with variable (orange) and constant (purple) regions. The disuplhide bridges (dark red), as well as the Fab and Fc portions are specified.

The discovery of variations in affinities of antibodies in the course of an immune response (Eisen and Siskind 1964), as well as of somatically diversified light chains (Weigert et al. 1970), posed some new challenges on the understanding of B cell biology and antibody generation. The advances in recombinant DNA technology allowed the detailed characterisation of somatic rearrangements in variable and constant regions during B cell differentiation (Hozumi & Tonegawa 1976). Such description prepared the way for an understanding of the V (variable), D (diversity) and J (junction) recombination process (Bernard & Hozumi 1978; Early et al. 1980), based on the idea that immunoglobulin genes are rearranged in antibody-producing cells, potentially allowing a limitless number of combinations. This concept fits with our understanding of our exposure to countless different antigens and our immune system evolving a mechanism to cope with such great diversity.

1.5.3 The life of a B cell

B lymphocytes derive from haematopoietic stem cells in the bone marrow. It is in this central lymphoid organ where BCRs are generated through rearrangement of immunoglobulin genes. After a negative selection process to ensure that the newly generated BCRs do not target self-antigens, mature B cells migrate to peripheral lymphoid organs, where they can bind foreign antigen and be activated, either through soluble antigen or specialised antigen presenting cells such as DCs or subcapsular sinus macrophages (Batista & Harwood 2009; Cyster 2010). Such activation results in the production of antibody-secreting plasma cells and memory B cells.

The development of B-lineage cells occurs according to different stages outlined by the rearrangement and expression of the immunoglobulin genes (Figure 1-4). The paired recombination-activating gene 1 (RAG1) and RAG2 encode enzymes which are crucial for initiating V(D)J recombination (Schatz & Oettinger 1989). The heavy chain locus rearranges first in the pro-B cell stage. Only one gene locus is rearranged at the time, and the process happens in a well-defined sequence. Once the reaction results in a successful VDJ combination and thus, a functional heavy chain, the pre-B cell expresses a pre-BCR, which serves as the signal to move forward to the following step, the light chain rearrangement. At this point, signalling through the pre-BCR also inhibits further rearrangement of the heavy chain locus, a process termed allelic exclusion (Pernis et al. 1965). Pre-B cells rearrange the light chain locus and once it has been productive, they express a cell surface Immunoglobulin M (IgM), becoming immature B cells. It is important to mention that apart from allelic exclusion, light chains also display isotypic exclusion (Wabl & Steinbergt 1982): this is the expression of a single type of light chain (κ or λ) by an individual B cell. At this stage, immature B cells are tested for autoreactivity in a process known as central tolerance (Guilbert & Dighiero 1982; Mcheyzer-williams et al. 1988; Souroujon et al. 1988). If the newly generated B cells react to self-antigens, they will either die through clonal deletion, remain anergic or ignorant or, lastly, they will have a chance to replace their autoreactive BCR through a mechanism known as receptor editing (Gay et al. 1993; Tiegs et al. 1993). Once the B cells have completed their development in the bone marrow, they migrate to peripheral lymphoid



	Stem cell	Early pro-B cell	Late pro-B cell	Large pre-B cell	Small pre-B cell	Immature B cell	Mature B cell
H-chain genes	Germline	D-J rearrangement	V-DJ rearrangement	VDJ rearranged	VDJ rearranged	VDJ rearranged	VDJ rearranged
L-chain genes	Germline	Germline	Germline	Germline	V-J rearranging	VJ rearranged	VJ rearranged
Ig status	None	None	None	μ heavy chain. Surrogate light chain. Pre-BCR on cell surface	μ chain in endoplasmatic reticulum	μ heavy chain. μ or κ light chain. IgM on surface	IgD and IgM on surface

Figure 1-4. **Schematic of the developmental stages of a B cell.** The rearrangement state of heavy (H) and light (L) chains is specified, as well as its immunoglobulin (Ig) status. Adapted from Murphy 2011.

tissues and become fully mature naïve B cells, expressing low levels of IgM and high levels of IgD.

There are three major subsets of mature B cells (Allman & Pillai 2008; Carsetti 2004): follicular B cells, which are the most abundant and reside in the lymphoid follicles of spleen and lymph nodes; marginal zone (MZ) B cells, which are located in the spleen and are specialised in detecting blood-borne pathogens; and B1 cells, which are found primarly in peritoneal and pleural cavities, and express a limited receptor repertoire. Due to their particular location, both MZ B cells and B1 cells have the ability to rapidly respond to T cell-independent (TI) antigens, such as repetitive bacterial structures. In contrast, follicular B cells are more specialised in responding to antigens that require CD4+ T cell help, although they can also elicit TI responses. It is in this particular context of T cell-dependency that GCs arise in secondary lymphoid organs, ultimately leading to the production of B cells expressing high affinity antibodies.

1.6 Germinal centres

Germinal centres (GCs) are histological, transient and highly dynamic compartments that form in secondary lymphoid organs in response to T-cell dependent antigens (MacLennan 1994). They were first described in 1884 as distinct microanatomical structures containing dividing cells (Nieuwenhuis & Opstelten 1984). Two distinct regions, the dark zone (DZ) and the light zone (LZ), can be distinguished, implying phenotypical and functional polarisation of the GCs. Today, we know they are the basis of humoral immunity, the sites

for B cell clonal expansion, somatic hypermutation and affinity-based selection, which results in the generation of high-affinity memory B cells and plasma cells.

1.6.1 Cell types

Although B cells are the most abundant cell type and the main characters of the GC reaction, a few other cell types are essential for the process, the main ones being T follicular helper cells (Tfh), FDCs and Tingible Body Macrophages (TBMs).

1.6.1.1 Germinal centre B cells

Activated B cells constitute the vast majority of cells within the GC. They are much larger and have greater proliferative capacity than their naïve counterparts, as well as having lost surface IgD expression. One of their key features is high expression of the transcriptional repressor of B cell lymphoma 6 (BCL-6) (Onizuka 1995). BCL-6 allows GC B cells to maintain their identity, as well as a proapoptotic state, rapid proliferation, mutation and DNA damage tolerance (Ci et al. 2009; Phan & Dalla-favera 2004; Ranuncolo et al. 2007; Cattoretti et al. 1995).

The frequency of cells undergoing mitosis is higher in the DZ than in the LZ (Nieuwenhuis & Optelten 1884). Due to their reported larger size and high proliferative capacity, DZ B cells are known as centroblasts. In contrast, LZ B cells are termed centrocytes, with a more quiescent and smaller phenotype

(MacLennan 1994). Nonetheless, several studies failed to clearly distinguish both cell types based on such features (Klein et al. 2003; Hogerkorp & Borrebaeck 2006; Nakayama et al. 2006). Recent advances, particularly in intravital microscopy, have allowed a more in-depth understanding of the DZ versus LZ divergence, emphasising their transient nature, the dynamism and fluidity between the two states (Schwickert et al. 2007; Allen et al. 2007; Allen & Okada 2007; Caron et al. 2009). Nonetheless, it has been possible to identify several surface markers that allow accurate distinction between them. Thus, DZ B cells are CXCR4^{high} CD83^{low} CD86^{low}, whereas LZ B cells are CXCR4^{low}, CD83^{high} CD86^{high} (Victora et al. 2010).

1.6.1.2 T follicular helper cells (Tfh)

One of the earliest discovered functions of T cells was their ability to help B cells, hence the term T helper (Th) cell (Claman et al. 1966). Further experiments demonstrated that T cell help was crucial for effective antibody responses (Mitchell & Miller 1968). However, it was only a few years ago that Tfh cells were recognised as a distinct CD4+ T cell lineage, when the defining transcription signature based on BCL-6 expression was described (Johnston et al. 2009; Yu et al. 2009).

B cell help is essentially dependent on contact, which allows for both receptor-ligand interactions and directional cytokine stimulation. An abundant range of molecular pairings occurs at the cell surface level between GC B cells and Tfh cells (Nutt & Tarlinton 2011). Amongst these, a few key ones have been

carefully characterised. The importance of CD40 in B cell proliferation and prevention of apoptosis has been known for more than 25 years (Clark & Ledbettert 1986). Furthermore, other molecules such as Inducible T cell co-stimulator (ICOS), SLAM-associated protein (SAP) and Programmed cell-death 1 (PD-1) have been shown to be required for optimal GC responses (Crotty et al. 2003; Mcadam et al. 2001; Tafuri et al. 2001; Haynes et al. 2007). One of the main features of Tfh cells is their high expression levels of CXCR5, required for T cell entry into the B cell follicle (Rasheed et al. 2006; Ma et al. 2012). Apart from direct cell to cell contact, Tfh cells help B cells through secretion of various cytokines and chemoattractants such as IL-4 (Peschel et al. 1987, Howard & Paul 1982), IL-21 (Parrish-novak et al. 2000) and Chemokine (C-X-C Motif) Ligand 13 (CXCL13), which is involved is the recruitment of CXCR5+ B cells to facilitate colocalisation and further interaction (Ansel et al. 2000).

All the aforementioned interactions are highly relevant, although the most important of them all is antigen presentation from B cells to Tfh cells, the key event for selection and future development of high-affinity memory B cells and plasma cells (Victora et al. 2010). T cell help involves a wide range of functions, with each factor contributing differently (e.g. IL-21 is particularly relevant in plasma cell differentiation). These are proliferation, survival, plasma cell differentiation, somatic hypermutation (SHM), class-switch recombination (CSR), adhesion and attraction (Crotty 2015).

Other minor T-cell resident populations include some CD8+ T cells, Th17 cells and FoxP3+ regulatory T cells (Treg) (Cells et al. 2001; Hsu et al. 2008; Alexander et al. 2011; Linterman et al. 2011).

1.6.1.3 Follicular dendritic cells (FDCs)

FDCs are radioresistant, stromal cells of mesenchymal origin (Nierop & Groot 2002). They reside in follicles of secondary lymphoid tissues in the shape of dense networks. Morphologically, they possess fine, long dendrites, which allow for close interaction with neighbouring cells (Szakal et al. 1988). They play an essential role in antigen presentation to B cells. Interestingly, they are non-mobile antigen-bearing cells that display it in the form of immune complexes or iccosomes, which are multimolecular antibody-antigen complexes (El Shikh et al. 2010). Thus, antigen is not processed and simultaneous engagement of multiple BCRs is possible (El Shikh et al. 2009). Within the GC, they are concentrated in the LZ and they produce CXCL13, the ligand for CXCR5, thus attracting B cells and T cells, contributing to the overall organisation of the lymphoid microarchitecture (Cyster et al. 2000).

Other stromal cell types have been described to help supporting B cell follicles, such as the fibroblastic reticular cells, particularly involved in T zone maintenance (Ngo et al. 1999; Luther et al. 2000). Recently, a novel population of reticular cells was characterised in murine GCs. They are located in the DZ and express CXCL12, the ligand for CXCR4, thus

contributing to the appropriate positioning of different cell types in different stages of the GC reaction (Rodda et al. 2015).

1.6.1.4 Tingible body macrophages (TBMs)

The GC reaction involves high cell proliferation and active apoptosis. TBMs are distributed throughout the GC and are responsible for engulfing and eliminating dying cell debris. Defects in TBM function have been linked to systemic lupus erythematosus (Baumann et al. 2002).

1.6.2 The germinal centre reaction

1.6.2.1 Getting started

In the absence of pathogen, secondary lymphoid organs contain GC-free primary follicles with naïve B cells. T-cell rich areas border these follicles and, in the course of infection, they can be primed by interaction with conventional DCs, thus becoming able to activate naïve B cells through cognate antigen (Batista & Harwood 2009; Figure 1-5). Such interaction results in reciprocal activation. Interestingly, at this stage, both B and T cells will upregulate BCL-6, the master regulator for both the GC B cell and the Tfh cell transcriptional programmes (Kerfoot et al. 2011; Baumjohann et al. 2011). This ensures an orchestrated expression of receptors and ligands that will be essential for optimal interaction of these two cell types in further stages of the GC reaction.

A subset of the recently activated B cells are differentiated into short-lived plasmablasts (Jacob & Kelsoe 1992) or unswitched memory B cells (Taylor et

al. 2012) (Figure 1-5). However, the majority of them migrate to the centre of the follicle and displace the resident follicular B cells, forming an early GC. The GC quickly expands due to the very high rates of GC B cell proliferation, with a division time estimated between 6 and 12h (Liu et al. 1997; Zhang et al. 1988). By day 7, a fully mature GC is established, with clearly distinguishable dark and light zones.

1.6.2.2 Dark and light zones: phenotypical and functional polarisation

The DZ of the GC is densely packed with CXCR4-expressing B cells, together with a recently described reticulum of CXCL12-expressing stromal cells (Rotta et al. 2015). In contrast, the LZ is less populated with B cells expressing higher levels of CXCR5, thus being chemoattracted to CXCL13-expressing FDCs. The LZ also comprises the majority of Tfh cells (Figure 1-5). Such polarisation is conserved across species (Allen et al. 2004) and is essential for optimal GC function.

In the DZ, B cells proliferate at very high rates and mutate their BCRs. This process is known as somatic hypermutation (SHM) and it involves the introduction of point mutations in the heavy or light chain of the variable region gene segments (MacLennan 1994). This results in a wide variety of BCRs with different affinities and specificities for antigen. These B cells are selected according to their affinity for antigen, and this process takes place in the LZ. FDCs act as antigen reservoirs during the GC reaction. B cells expressing high affinity BCRs bind, internalise and process the specific antigen, which

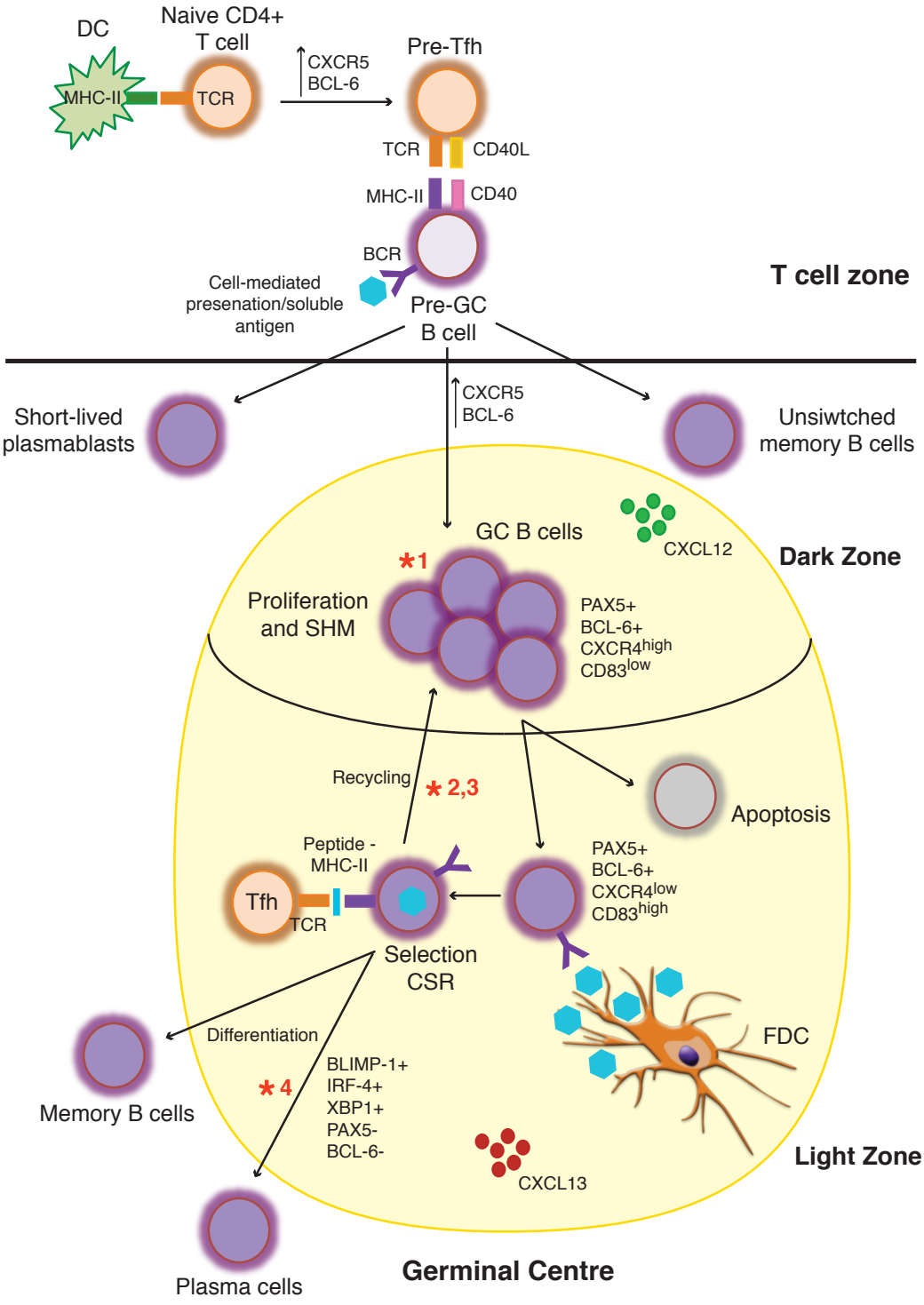


Figure 1-5. Schematic of the GC reaction. The inititation of the GC reaction, as well as the dynamics of B cells and T cells within the GC are illustrated. The most relevant transcription factors, chemokines and surface markers are specified. The different origins of GC-derived lymphomas are marked (red *). Burkitt lymphoma (1), Follicular lymphoma (2), GC B cell-like DLBCL (3) and Activated B cell-like DLBCL (4).

can then be presented through MHC class II molecules to Tfh cells. Tfh cells are the main source of survival signals to B cells, but they are scarce, thus forcing B cells to compete for engagement. This implies that only the B cells that present higher levels of antigen will be able to interact with Tfh and receive the appropriate signals for survival. A correlation between BCR affinity, the amount of antigen internalised and displayed, as well as T-cell contact time has been shown (Victora et al. 2010; Shulman et al. 2014), thus demonstrating that affinity for antigen is the basis for selection. While B cells are in the LZ, they can change their isotype, thereby expressing one of a range of different immunoglobulin heavy chain constant regions (Manis et al. 2002). This process is known as class-switch recombination (CSR) and has consequences for antibody effector functions. Mutations in both SHM and CSR processes are driven by the activation-induced cytidine deaminase (AID) enzyme (Durandy 2003).

1.6.2.3 Selected B cells: three possible fates

As described above, high-affinity B cells are selected for survival, whereas their low-affinity counterparts will die from apoptosis. Positively selected B cell clones can exit the GC as either memory B cells or as plasmablasts, which will further differentiate into antibody-secreting plasma cells. Memory B cells are key in antigen-recall responses, as they can rapidly differentiate into plasma cells and produce antibodies to fight the invading pathogen (Minton 2015).

Alternatively, selected B cells can migrate to the DZ in a process known as cyclic re-entry or recycling (Figure 1-5). They can then undergo successive rounds of proliferation, mutation and selection, leading to increased affinity for antigen in a mechanism known as affinity maturation (Jerne 1951, Eisen & Siskind 1964).

What drives selected B cells to the plasma cell differentiation fate has been well characterised (see. *1.5.3 Plasmablasts and plasma cells*). However, the process of memory commitment as well as recycling are still poorly understood.

1.6.3 Plasmablasts and plasma cells

Plasmablasts are the rapidly produced, dividing and antibody-secreting short-lived effector cells (Nutt et al. 2015). In response to T cell-dependent (TD) antigens, a GC-independent extrafollicular step occurs in which naïve B cells are stimulated by antigen and differentiate into plasmablasts (MacLennan et al. 2003). They are the source of most early protective antibodies. Plasmablasts have migratory potential and they can differentiate into plasma cells, the long-lived mediators of humoral immunity. Plasma cells are quiescent, terminally differentiated antibody-secreting cells that arise as a product of the GC reaction and then locate in the bone-marrow (Shlomchik 2012; Radbruch et al. 2006). Both plasmablasts and plasma cells are included under the term of antibody-secreting cells (ASCs).

The transition from an activated B cell into an ASC can be understood as a lineage switch, thus implicating a distinct transcriptional signature (Nutt & Tarlinton 2011). The transcription factors that characterise B cell and ASC identity drive mutually exclusive gene expression programmes (Figure 1-5). The master regulator of plasma cell differentiation is the B lymphocyte-induced maturation protein 1 (BLIMP-1) (Turner et al. 1994; Kallies et al. 2004), a transcriptional repressor of crucial regulators of the B cell programme such as BCL-6 and Paired box 5 (PAX-5) (Shaffer et al. 2002; Lin et al. 2002). Two other key drivers of ASC differentiation are Interferon regulatory factor 4 (IRF-4) and X-box binding protein 1 (XBP-1) (Klein et al. 2006). IRF4 is involved in different phases of the GC reaction and functions in a dose-dependent manner (Sciammas et al. 2006). Downregulation of PAX-5 results in XBP-1 expression (Reimold et al. 1996), which is also induced under ER stress. Due to the vast production of antibody, ASC are particularly sensitive to ER stress (Iwakoshi et al. 2003).

Plasma cell production of antibodies allows long-lasting immunity and constitutes the basis of most successful vaccination strategies. A deeper understanding of the ASC differentiation process is needed to fight autoimmune pathologies based on the generation of auto-antibodies. Moreover, this process has been exploited to generate specific monoclonal antibodies with diagnostic, therapeutic and research purposes (see *1.6 Antibodies as immunological tools*).

1.6.4 Expanding the classical model

The GC reaction is extremely efficient, as appearance of high-affinity memory B cells and plasma cells occurs 1 week after antigen exposure (Blink et al. 2005). This is possible due to the particularities of the GC microenvironment, which facilitates close interactions and rapid movements of distinct cell types within a limited space (Victora et al. 2012). Originally, the GC was divided into DZ and LZ, each zone comprising a specific type of B cells (MacLennan 1994). However, this classical perspective is being challenged and a view based on rapid flux, temporal states and cell-intrinsic regulatory mechanisms is gaining strength (Bannard et al. 2013).

GCs can be understood as sophisticated microchambers for high-speed evolution, allowing us to keep up the pace with fast changing pathogens (Victora & Nussenzweig 2012). The essential elements and basic functioning of the GC have been outlined above. However, there are abundant extra regulatory mechanisms that deserve to be mentioned. For instance, generation of autoreactive antibodies is a permanent risk, as SHM is a stochastic process. The existence of checkpoints for autoreactive B cells has been depicted, although their clearance is poorly understood (Davidson et al. 1987; Chan et al. 2012). It has also been shown that B cells' own secreted products, antibodies, can limit antigen access on FDCs, thus contributing to GC regulation and increased affinity maturation. This process is known as antibody feedback and it has been shown to accelerate the emergence of B cell clones with highest affinities (Zhang et al. 2013). In addition to antibodies infiltrating neighbouring GCs, Tfh have also been shown to have this capacity

(Shulman et al. 2013). Furthermore, recently activated B cells can invade pre-existing GCs (Schwickert et al. 2009). Overall, this remarkable dynamism demonstrates that coordination between different GCs is possible. This idea may challenge the classical hypothesis based on the oligoclonality of antibody responses. However, both mechanisms might not be entirely exclusive and such level of communication could have great potential when fighting against pathogens with high antigenic variation (De Silva & Klein 2015). Epigenetic (Béguelin et al. 2013; Caganova et al. 2013) and microRNA-based regulatory mechanisms (Xu et al. 2012; Thai et al. 2007) have also been described in the GC context.

There are still abundant questions that remain unanswered regarding the intricacies of the GC reaction. Remarkably, all recent studies in GC function and dynamics have been done in mice, as the study of these microanatomical structures in humans is complicated.

1.6.5 Germinal centres and tumorigenesis

Most human B cell lymphomas originate in GCs (Basso & Dalla-Favera 2015). Recent research on GCs has brought a deeper understanding of the transcription factors and signalling pathways involved in the tight regulation of the GC reaction, which are often hijacked during the process of malignant transformation. The same genetic mechanisms that enable high rates of DNA damage, mutation and proliferation, which are necessary for the development

of high-affinity B cell clones, are deeply involved in the development of B cell lymphomas.

Complex regulatory networks drive the GC reaction by activating and repressing specific transcriptional programmes. These pathways can be altered due to genetic lesions such as amplifications, deletions, non-synonymous point mutations or chromosomal translocations, thus leading to malignant transformation (Lohr et al. 2012; Schmitz et al. 2012). A wide variety of genes can be affected, but factors like MYC (Dalla-favera et al. 1982; Taub 1982), BCL-6 (Pasqualucci et al. 2003; Hatzi & Melnick 2014; Cattoretti et al. 2005) and B cell lymphoma 2 (BCL-2) (Küppers 2005; Sungalee et al. 2014) are often altered in GC-derived malignancies.

There is a wide variety of GC-derived lymphomas, depending on the cell type of origin (Figure 1-5) and the genetic alterations that trigger tumorigensis. B cell non-Hodgkin lymphomas (B-NHLs) comprise a range of distinct malignancies that can be characterised at genetic, phenotypic and clinical levels (Basso & Dalla-Favera 2015). About 80% of B-NHLs are derived from GC B cells (Stevenson et al. 2001), these including Burkitt lymphoma, Follicular lymphoma and Diffuse large B cell lymphoma (DLBCL), the latter being the most common and accounting for 40% of all newly diagnosed cases (Basso & Dalla-Favera 2015). The presence of mutated IgV sequences as well as a particular transcriptional signature revealed that Burkitt lymphoma is an aggressive malignancy derived from DZ GC B cells (Dave et al. 2006; Victora & Nussenzweig 2012). Follicular lymphoma is much less aggressive, it is not curable and it often evolves towards DLBCL with worse clinical outcome

(Kridel et al. 2012; Montoto & Fitzgibbon 2011). Both Follicular lymphoma and GC B cell (GCB)-like subtypes of DLBCLs derive from light zone B cells (Alizadeh et al. 2000). On the contrary, Activated B cell (ABC)-like DLBCLs originate from recently GC-exited plasmablasts (Alizadeh et al. 2000; Figure 1-5).

1.7 Antibodies as immunological tools

A breakthrough in immunology occurred when malignant plasma cells were fused with normal B cells to form hybridomas, an invaluable source of monoclonal antibodies with defined specificity for antigen (Kohler and Milstein 1975). This new technique based on continuous cultures of lymphocyte hybrids and consecutive production of monoclonal antibodies, specific for a certain antigen, underpins many of today's modern immunological assays, together with numerous clinical applications, both within diagnostics and therapeutics (Schroder 1980). One of the most striking examples is Rituximab, a chimeric human mAb against the surface marker CD20 which kills B cells and it is currently being used to treat several types of B cell lymphomas and autoimmune disorders (Maloney et al. 1996).

1.8 Aims of the thesis

The published literature regarding LLT1 is limited and presents inconsistencies. The aims of this thesis are:

1. Identify, characterise and optimise the tools necessary for the study of LLT1
2. Describe the distribution of LLT1 in healthy human tissue and how it may be altered in the context of disease
3. Investigate the regulatory mechanisms that determine the levels of LLT1 expression on B cells
4. Explore the distribution of CD161 in the context of LLT1 and investigate the function of LLT1 in the GC

2 Materials and Methods

The general materials and methods used in this thesis are described below. Specific methods and their development are described in the relevant chapters.

2.1 Cells and tissues

2.1.1 PBMCs separation, freezing and thawing

Peripheral Blood Monocluear cells (PBMCs) were obtained from the National Blood Transfusion Service (NHS Blood and Transplant). Whole blood was diluted with Phosphate Buffered Saline (PBS) and layered on a Lymphoprep gradient (Axis Shield Diagnostics, 2200 rpm with no break for 22min). The PBMC layer was removed with a Pasteur pipette and washed twice at 1500rpm for 5 min with R10. Cells were counted using Trypan Blue exclusion (Sigma Aldrich), aliquoted in FCS + 10% dimethyl sulfoxide (DMSO, Sigma Aldrich) and stored in liquid nitrogen until required. At that point, cryovials were partially thawed in a 37°C water bath, the cells transferred to a 15ml falcon with R10 (see *2.8 Media and buffers*) and centrifuged. A second wash with R10 was performed.

2.1.2 Cell lines

Raji Burkitt lymphoma and THP-1 acute monocytic leukemia cells were maintained in R10 and THP-1 media, kept at 37°C 5% CO_2 and split 1:10 three times a week.

300.19 are an Abelson leukemia virus transformed murine pre-B cell line derived from Swiss Webster mice (H-2^d). They are surface Ig negative and negative for B7-1, B7-2, and CD40. They express B220. They are non-adherent single cells. They were maintained in 300 media.

300-CD161 and 300-LLT1 are an Abelson leukemia virus transformed murine pre-B cell line (300.19) derived from Swiss Webster mice (H-2^d) and transfected with a vector expressing human CD161/LLT1 cDNA and the puromycin resistance gene. They were maintained in 300 media supplemented with puromycin (5 μg/ml, Gibco).

All three 300.19 cell lines were a kind gift from Gordon Freeman (Harvard Medical School, Boston, Massachusetts), were kept at 37°C 5% CO_2 and split 1:10 three times a week.

2.1.3 Tonsils

Tonsil samples were obtained from young patients or adults undergoing tonsillectomy at the ENT Department at the John Radcliffe Hospital, Oxford. Single cells were collected by mechanical disruption of tonsil samples, aliquoted in freezing media and stored in liquid nitrogen until required. At that

point, cryovials were partially thawed in a 37°C water bath, the cells transferred to a 15ml falcon with R10 and centrifuged. A second wash with R10 was performed. Alternatively, the tonsils were fixed with 37% formaldehyde (Sigma Aldrich) overnight prior to paraffin embedding.

2.2 Novel anti-LLT1 antibodies

Two novel mouse anti-LLT1 monoclonal antibodies were generated.

359.**7G7**, mIgG1, kappa; 1.35 mg/ml. Validated by Western blotting of LLT1 transfected cells and some lymphoid cell lines.

359.**2H7**, mIgG2a, kappa, 1.42 mg/ml. Validated by flow cytometric stain of LLT1 transfected cells. It could not be validated by Western blotting.

All purified antibodies are dialysed against PBS, are low in endotoxin (< 2EU/mg), and are filtered sterile.

Both antibodies were a kind gift from Gordon Freeman (Harvard Medical School, Boston, Massachusetts).

2.3 Flow cytometry

2.3.1 External staining

For external staining, cells were incubated in PBS with anti-surface antibodies at room temperature (RT) for 20 minutes. Live/dead staining was performed using LIVE/DEAD® Fixable Near-IR Dead Cell Stain Kit, for 633 or 635 nm

Excitation (1:1000 dilution, Invitrogen). After staining, cells were washed twice with PBS and then resuspended, prior to flow cytometric analysis.

2.3.2 Internal staining

For internal staining, a Live/Dead staining was performed followed by fixation of cells with 2% formaldehyde (Sigma Aldrich) in PBS for 10 minutes and permeabilisation with IX permeabilisation buffer (eBioscience) in water for 15 minutes. Cells were then incubated with antibodies diluted in PBS as described above.

All the antibodies used are specified in Table 2-1.

2.3.3 Data acquisition and analysis

FACS analysis was performed on Miltenyi Biotec MACSQuant cytometer and analyzed with FlowJo Version 9.6.2 software (TreeStar). Graphs were designed using GraphPad Prism Version 6.0a (GraphPad Software, USA) and Adobe Illustrator CS4 14.0.0.

2.4 Doublet formation

3 x 10^5 300-LLT1 cells were incubated in 100μl in a 96-well plate with 3 x 10^5 untransfected 300 cells or 300-CD161 transfected cells and rested for 4 hours at 37°C 5% CO_2. Anti-LLT1, anti-CD161 or no antibody was added to the cell mixture.

2.5 Real-time quantitative polymerase chain reaction (qPCR)

Total RNA was extracted from 1 x 10^6 cells using RNeasy Mini Kit (Qiagen) according to the manufacturer's instructions. 5μg of RNA were used to synthesise cDNA by reverse transcription using SuperScript® III Reverse Transcriptase, random hexamer primers, anchored Oligo(dT) primers and 2'-deoxynucleoside 5'-triphosphates (dNTP) mix, in the presence of dithiothreitol (DTT) and RNaseOUT™ Recombinant Ribonuclease Inhibitor (all from Invitrogen). Amplification was assessed using molecular probes from the Universal ProbeLibrary Set, Human (Roche) on a Light Cycler480 (Roche).

The following GADPH primers were used (Eurofins MWG Operon):

GADPH-Forward 5'- AGCCACATCGCTCAGACAC-3'

GADPH-Reverse 5'- GCCCAATACGACCAAATCC-3'.

2.6 Immunohistochemistry

2.6.1 Immunoperoxidase staining

Tissue deparaffinisation was performed using Histo-Clear (National Diagnostics) and ethanol (Sigma Aldrich; 100%, 90% and 70%). Heat mediated antigen retrieval was achieved using Dako target retrieval solution (Dako). Endogenous peroxidase activity was blocked using 3% H_2O_2 (5 minutes x 2; Alfa Aesar) and 0.1% sodium azide (15 minutes, Sigma Aldrich) in water. Non-specific binding was blocked by incubating the sample for 30

minutes at RT with 0.5% blocking reagent (PerkinElmer) in PBS. Primary antibodies were added and incubated overnight at 4ºC. The sample was then incubated with anti-goat/mouse/rabbit polymer conjugated to horseradish peroxidase (HRP) (Vector Laboratories) for 30 minutes at RT. ImmPACT DAB peroxidase substrate (Vector Laboratories) was added and incubated for 2-10 minutes. The reaction was stopped with running deionised water. The section was then covered with Hematoxylin (Vector Laboratories) for 45 seconds and rinsed with deionised water. Samples were then dehydrated by serial passage through 70%, 90% and 100% ethanol followed by Histo-Clear. Samples were allowed to dry and mounted with VectaMount mounting media (Vector Laboratories).

2.6.2 Immunofluorescent staining

Tissue deparaffinisation, heat mediated antigen retrieval and blocking of endogenous peroxidase activity was performed as specified above.

Primary antibodies were diluted in blocking buffer and incubated for 30 minutes at RT. Anti-goat HRP-conjugated antibody was added followed by a 30 min incubation at RT. Cyanine 5 Amplification Reagent (PerkinElmer) was diluted 1/300 in Tyramide amplification buffer (12ml 500mM Tris, 18ml H_2O, 20 mg Imidazole (Sigma Aldrich), 1µl H_2O_2), added and incubated in the dark for 15 minutes. Residual peroxidase activity was blocked by incubating the slides in 3% H_2O_2 for 5 minutes and then 0.1% sodium azide for 15 minutes in water. Anti-mouse/rabbit HRP-conjugated antibody was added followed by a

30 min incubation at RT. Fluorescein Amplification Reagent (PerkinElmer) was diluted 1/300 in new Tyramide amplification buffer, added and incubated in the dark for 15 minutes. Slides were mounted with ProLong® Gold Antifade Reagent with DAPI (Invitrogen).

All the antibodies used are specified in Table 2-2.

2.6.3 Data acquisition and analysis

For analysis of immunoperoxidase staining, images were acquired on a DSS1 Coolscope Slide Scanner (Nikon).

For immunofluorescent microscopy, images were acquired on an Olympus Fluoview FV1000 microscope (Olympus) and analyzed using Fiji (ImageJ, National Institute of Health, USA).

2.7 Statistical analysis

All graphs and statistical analysis were performed using GraphPad Prism Version 6.0a (GraphPad Software, USA). Data are represented as mean or mean ± standard error of the mean (SEM). Error bars always represent SEM, which estimates accuracy; it quantifies how precisely we know the true mean of the population. It takes into account the sample size as well as the standard deviation (SD), which quantifies scatter. **** $p<0.0001$, *** $p<0.001$, ** $p<0.01$, * $p<0.05$, ns = not significant, by the indicated statistical test as stated in each figure legend. The two statistical tests used are detailed below:

- Unpaired T-test: T-tests are used to compare the means of two groups of data. The unpaired T-test is used when the data is not derived from subjects who have been measured at two time points.
- ANOVA (Analysis of the variance): The multiple comparisons two-way ANOVA test is used to compare the means of three or more unmatched groups.

In certain analyses, due to high variation between different experiments despite following a common trend, a representative experiment with several technical replicates is shown, instead of a single graph with the pooled data.

2.8 Media and buffers

R10: RPMI 1640 (Sigma-Aldrich) supplemented with 10% Fetal Calf Serum (FCS; Gibco), 1% streptomycin/penicillin (Sigma Aldrich), 1% L-glutamine (Sigma Aldrich).

THP-1 Media: R10 supplemented with 0.05% β-mercaptoethanol (Sigma Aldrich).

300 Media: R10 supplemented with 15 μg/ml gentamycin and 50 x 10^{-6} M β-mercaptoethanol.

Freezing mix: 90% heat inactivated FCS (Gibco) 10% DMSO (Sigma Aldrich).

Marker	Fluorochrome	Brand	Clone
CD3	FITC	BioLegend	UCHT1
CD4	PerCP-Cy5.5	BioLegend	RPA-T4
CD10	PE-Cy7	BioLegend	HI10a
CD19	PB	BioLegend	HIB19
CD20	PO	Life Technologies	HI47
CD27	PE-Cy7	BioLegend	M-T271
CD34	FITC	BioLegend	561
CD38	PerCP-Cy5.5	BioLegend	HIT2
CD45-RA	FITC	Miltenyi Biotec	T6D11
CD56	BV-421	BioLegend	HCD56
CD68	APC	BioLegend	Y1/82A
CD69	FITC	BioLegend	FN50
CD83	BV421	BioLegend	HB15e
CD86	PE	Miltenyi Biotec	FM95
CD107a	PE-Cy7	BioLegend	H4A3
CD138	APC	Beckman Coulter	B-A38
CD161	APC	Miltenyi Biotec	191B8
	PE	Miltenyi Biotec	191B8
CD184 (CXCR4)	APC	Miltenyi Biotec	12G5
CD185 (CXCR5)	PB	BioLegend	J252D4
CD278 (ICOS)	APC	BioLegend	C398.4A
BCL-2	BV421	BioLegend	100
BCL-6	AF467	BioLegend	IG191E/A8
BLIMP-1	FITC	Novus Biologicals	3H2-E8
HLA-DR	APC	R&D Systems	L203
Activated Caspase-3	PE	BD Biosciences	CCP32
IgD	FITC	BioLegend	IA6-2
IgM	APC	Miltenyi Biotec	PJ2-22H3
IRF-4	FITC	eBioscience	3E4
Ki67	FITC	Miltenyi Biotec	REA183
IgG2A mouse IC	PE	R&D Systems	20102
Rat anti-mouse IgG2A	PE	R&D Systems	-
Goat IgG Control	Unconjugated	R&D Systems	-
General mouse IgG	Unconjugated	Invitrogen	-

Table 2-1. Antibodies used in flow cytometry.

Marker	Brand	Clone	Dilution
CD3	Leica Biosystems	LN10	1:200
	DAKO	F7.2.38	1:200
CD4	Novus Biologicals	Goat polyclonal	1:500
CD19	DAKO	LE-CD19	1:500
CD20	DAKO	L26	1:1000
CD38	DAKO	At13/5	1:200
CD45	DAKO	2B11+PD7/26	1:1000
CD68	DAKO	PG-M1	1:200
CD79a	DAKO	JCB117	1:200
CD138	DAKO	MI15	1:100
CD161	Miltenyi	191B8	1:100
	Abcam	IMG141F1F1	1:100
	AbD Serotec	B199.2	1:100
	BioLegend	HP-3G10	1:100
Cathepsin G	Leica Biosystems	19C3	1:1000
FDC marker	DAKO	CNA.42	1:100
IgA	Leica Biosystems	N1CLA	1:300
IgD	Leica Biosystems	DRN1C	1:200
IgE	Abcam	Rabbit polyclonal	Prediluted
IgG	DAKO	Rabbit polyclonal	1:1000
IgM	DAKO	Rabbit polyclonal	1:1000
IRF-4	DAKO	Mum1p	1:200
LLT1	R&D Systems	Goat polyclonal	1:100
Ki67	DAKO	MIB-1	1:200

Table 2-2. Antibodies used in immunohistochemistry.

3 Developing and optimising the tools for analysis of LLT1

3.1 Introduction

The main aim of this project is the study of the distribution, regulation and function of LLT1 in the context of human health and disease.

The literature regarding LLT1 is limited, partially due to a lack of validated tools (e.g. antibodies) for its study and characterisation. This issue has been previously addressed by several groups, which have generated their own anti-LLT1 antibodies (Mathew et al. 2004; Germain et al. 2010). However, there are still abundant inconsistencies in the published data regarding the distribution of LLT1 in human tissues and cell types (Table 1-1). For example, Boles and colleagues (Boles et al. 1999) showed LLT1 on NK cells, but these findings could not be reproduced by others (Germain et al. 2011).

There are several reasons which could explain such discrepancies, from the techniques and antibodies used to examine the cells (e.g. Real-time polymerase chain reaction (RT-PCR) versus FACS or different anti-LLT1 antibodies) to the different activation state of the cells. For instance, it has been described that the activation of DC, B, NK and T cells can lead to the expression of LLT1 (Germain et al. 2011).

Differences in antibody binding could be explained by the nature of the target epitope, the recognition of particular isoforms or differences in glycosylation, generating distinct patterns of staining on different cell types.

LLT1 is a C-type lectin-like protein comprising an N-terminal short cytoplasmic tail, a transmembrane region followed by a stalk region and an extracellular lectin-like domain responsible for ligand interaction (see Figure 1-1A). It is expressed on the cell surface as a homodimer (Mathew et al. 2004; Germain et al. 2010). It is important to acknowledge that the current anti-LLT1 antibodies were generated against *Escherichia coli* (*E.coli)*-derived recombinant human LLT1, thus lacking glycosylations. Furthermore, LLT1 has been found to be expressed as a highly glycosylated, sulfide-linked dimer at the cell surface (Mathew et al. 2004; Rosen et al. 2008). This highlights the differences between *E.coli* and human-derived LLT1 and, therefore, suggests that some of the targeted epitopes may not be exposed in their native conformation within the *E.coli* system, potentially eluding antibody binding within human tissues.

Five spliced variants of the *LLT1* gene have been described (Germain et al. 2010). The targeting of epitopes present in certain isoforms but not in others could also account for some of the observed differences.

It is also important to consider that the majority of molecules involved in both innate and adaptive immunity are glycoproteins. Sugars not only contribute to protein stability, but also to specific recognition, such as immunoglobulin binding (Rudd 2001).

Protein glycosylation is a tightly regulated process that not only changes depending on the differentiation, development and physiological state of the cell, but can also have a significant influence on protein location, half-life, function and biological activity (Varki 1993). For example, N-glycosylation is required for human CD2 adhesion function on T cells during antigen presentation and particular changes in cell surface glycosylation guide intestinal epithelial cell differentiation (Recny et al. 1992). One of its main influences, however, is on antigenicity, where the impact of glycosylation is broad (Lisowska 2002; Brooks 2004). The presence of polysaccharides can 'inactivate' or hide the peptidic epitope, as well as being required for specific antibody recognition. Intramolecular carbohydrate-protein interactions have the potential to alter protein conformation, thus being able to expose/hide particular peptidic epitopes. CD44 illustrates this point, as reactivity of anti-CD44 antibodies is disturbed by N- and O-linked glycosylations at specific sites (Matsuki et al. 2003).

Recently, an anti-LLT1 goat polyclonal antibody became commercially available (Table 3-1). Furthermore, two novel anti-LLT1 monoclonal antibodies (2H7 and 7G7) have been generated (see *2.2 Novel anti-LLT1 antibodies*). I wanted to analyse, characterise and compare these new antibodies with some of the existing anti-LLT1 antibodies, with the ultimate aim of identifying and validating effective tools for the study of the expression and function of LLT1.

3.2 Aims

The first aim of this project was to characterise and optimise the tools necessary for the study of LLT1 distribution, regulation and function. The work performed allowed the following questions to be answered:

- Which antibodies are best for FACS staining of LLT1?
- Can anti-LLT1 antibodies block LLT1-CD161 interaction?
- Which antibodies are best for immunohistological staining of LLT1?
- Can different anti-LLT1 antibodies block each other's binding?
- Is LLT1 antibody binding dependent on glycosylation?

3.3 Materials and Methods

Specific materials and methods for this chapter are detailed below. All other methods and reagents are described in Chapter 2.

3.3.1 Real-time quantitative polymerase chain reaction (qPCR)

The following LLT1 primers were used (Eurofins MWG Operon):

LLT1-Forward 5'-TGGTACTGAATGGACAAGACAGTT-3';

LLT1-Reverse 5'-TTGTCATTCAAATAGGCACACTC-3'

3.3.2 Doublet formation

2H7 mAb, 7G7 mAb or no antibody was added to the cell mixture at a concentration of 1/50.

3.3.3 Tissues

A series of normal paraffin-embedded human tissues comprising samples of tonsil, spleen, lymph node and appendix were obtained from Proteogenix.

3.3.4 Immunohistochemistry

Heat mediated antigen retrieval was achieved using buffer A, B, AC (Electron Microscopy Sciences) or Dako target retrieval solution (Dako).

The following primary antibodies were used: anti-LLT1 goat polyclonal antibody (R&D Systems; 1/100), 2H7 mAb (IgG2A), 7G7 mAb (IgG1), 4C7 (Sigma Aldrich and Abnova) or IgG1/IgG2A isotype controls (R&D Systems) (3 μg/ml).

The following secondary antibodies were tested: donkey anti-goat (1/100 in blocking buffer; Jackson ImmunoResearch), anti-goat polymer (Vector Laboratories) or anti-mouse polymer HRP-conjugated (Vector Laboratories) for 30 minutes at RT.

For the blocking experiments, the blocking antibody or isotype control was incubated for 30 min at RT before addition of the staining antibody.

3.3.5 Western blot

Cells were lysed with Pierce RIPA Lysis and extraction buffer (Thermo Scientific) including Complete, Mini Protease Inhibitor Cockatil Tablets (Roche). Lysates were analysed in a NuPAGE® Novex 4–12% Bis-Tris Midi

Gel w/ MOPS (Invitrogen) under reducing and non-reducing conditions. The anti-LLT1 goat polyclonal antibody was used as primary antibody, and the donkey anti-goat HRP-conjugated as a secondary. Western blots were performed according to Amersham ECL western blotting chemiluminiscence detection system instructions (GE Healthcare).

3.3.6 PNGase F digestion

3 x 10^5 Raji cells were incubated in 100μl of media with PNGase F (New England Biolabs, 500,000 units/ml) 1/100 for 24h at 37°C 5% CO_2.

3.4 Results

In order to define where is LLT1 expressed, I first needed to assess the binding capabilities of the available anti-LLT1 antibodies and decide which ones would be used for my future studies. Six different anti-LLT1 antibodies were tested for both FACS and immunohistochemical staining (Table 3-1).

Company	Type	Host	Isotype	Stock Concentration	Used Concentration	Technique
R&D Systems	Polyclonal	Goat	IgG	1 mg/ml	1/80	Histology FACS
Abnova	Monoclonal (4C7)	Mouse	IgG1κ	0.5 mg/ml	1/100	Histology FACS
Novel 2H7	Monoclonal	Mouse	IgG2A	1.42 mg/ml	1/500	Histology FACS
Novel 7G7	Monoclonal	Mouse	IgG1	1.35 mg/ml	1/500	Histology FACS
Sigma Aldrich	Monoclonal (4C7)	Mouse	IgG1κ	1mg/ml	1/200	Histology
R&D Systems	Monoclonal (402659)	Mouse	IgG1	-	1/50	FACS

Table 3-1. **Anti-LLT1 antibodies**. List of anti-LLT1 antibodies tested. Company of origin, monoclonal versus polyclonal type of antibody, host, isotype, stock and used concentrations, as well as techniques in which they were used are specified.

3.4.1 Testing of anti-LLT1 antibodies for FACS staining

LLT1 expression has previously been described in THP-1 acute monocytic leukaemia cells (Germain et al. 2010) and Raji Burkitt lymphoma cells (Rosen et al. 2008; Germain et al. 2010; Germain et al. 2011). These studies were performed using two commercially available anti-LLT1 monoclonal antibodies (mAb): 4C7 (Abnova) and 402659 (R&D Systems).

I wanted to assess the binding of the 4C7 and 40659 anti-LLT1 antibodies and compare it to two novel mouse monoclonal antibodies (2H7 and 7G7, see *2.2 Novel anti-LLT1 antibodies*), as well as to a goat polyclonal anti-LLT1 antibody (R&D Systems).

THP-1, Raji and 300-LLT1 transfected cell lines (see *2.1.2 Cell lines*) were stained with these antibodies, both externally and internally (Figure 3-1).

The 2H7 mAb bound to THP-1 cells in a non-specific manner, as signal was detected when the isotype control was used (Figure 3-1A). LLT1 could also be detected on Raji cells internally with the 4C7 mAb (Figure 3-1B) and on THP-1 cells, both using the 4C7 and the 2H7 mAbs (Figure 3-1B), although to a lesser extent. Within the conditions tested, only the 2H7 clone stained Raji cells externally for LLT1 (Figure 3-1E). Expression of LLT1 on Raji and THP-1 cells was confirmed by qPCR (data not shown).

All the antibodies tested were able to stain externally for LLT1 on the 300-LLT1 transfected cell line (Figure 3-1C). Unexpectedly, when the staining was performed internally, a positive signal could be detected in the untransfected 300 cells, both with the 2H7 and the 4C7 mAbs (Figure 3-1D). This suggests there might be some level of cross-reactivity between the human and the mouse Clec2D proteins (see *3.5 Discussion*).

The project involved phenotyping as well as functional studies on immune cells. I wanted to assess the effect of LLT1 cross-linking when interaction with CD161-expressing cells occurred. In order to do so, the presence of LLT1 in the cell surface is a requirement. Therefore, considering that Raji cells express natural levels of LLT1 and thus better represent *in vivo* conditions in comparison to the 300-LLT1 transfected cells, I decided to use the 2H7 mAb for further FACS stainings.

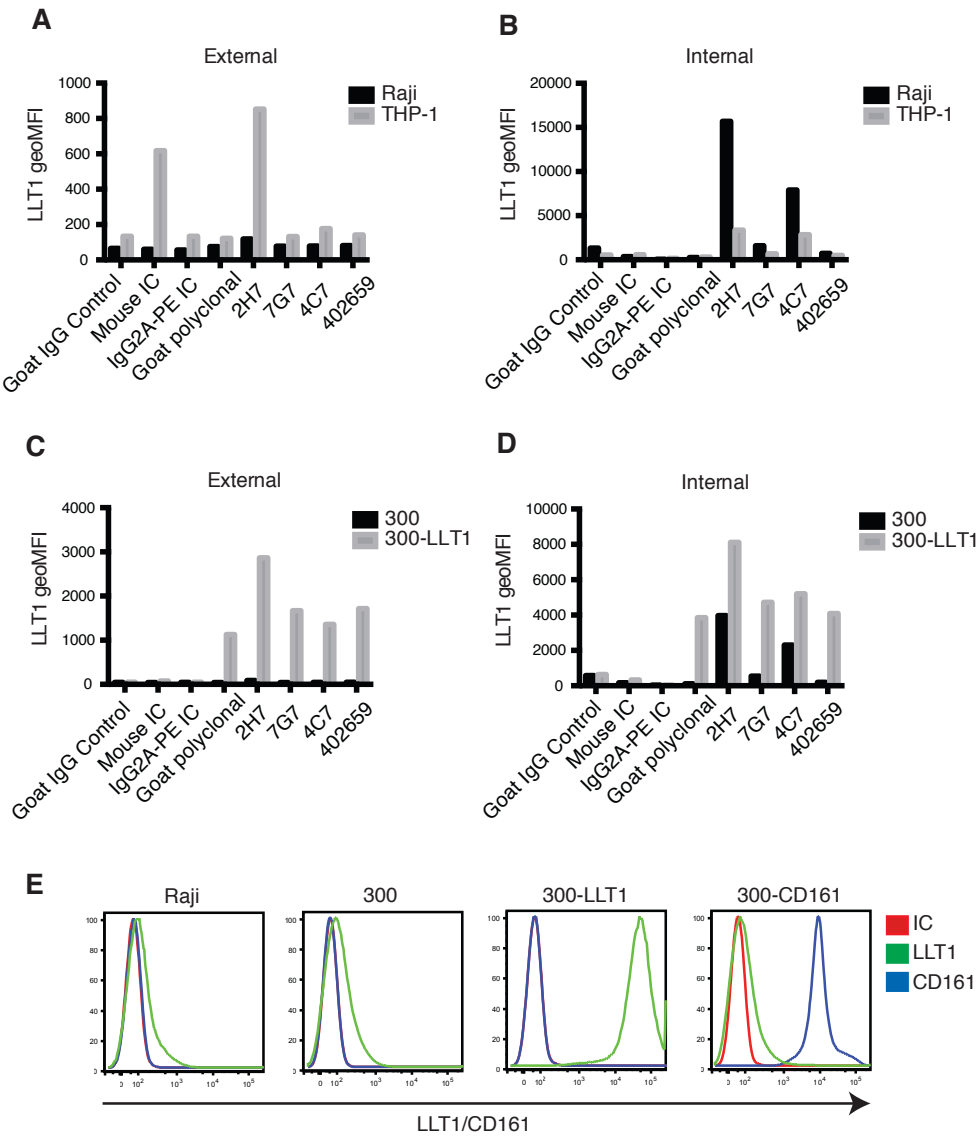


Figure 3-1. LLT1 can be stained by FACS (2H7, 4C7). LLT1 expression was analysed by flow cytometry on Raji and THP-1 cell lines using different anti-LLT1 antibodies, both externally (A) and internally (B). LLT1 expression was also measured on untransfected 300 cells as well as 300-LLT1 transfected ones, both externally (C) and internally (D). A goat polyclonal anti-LLT1 antibody was tested, together with the mouse monoclonals 2H7, 7G7, 4C7 and 402659 (see Table 1). (E) Expression of LLT1 and CD161 on Raji, untransfected 300, 300-LLT1 and 300-CD161 cell lines. Data from different experiments has not been pulled together due to high variation between them, despite following the same trend. Representative of three independent experiments with three technical replicates.

Figure 3-1E shows representative histograms of LLT1 and CD161 stainings on Raji cells, as well as on untransfected 300, 300-LLT1 and 300-CD161 transfected cells. There was no CD161 expression on Raji, untransfected 300 and 300-LLT1 transfected cells. In contrast, CD161 was highly expressed in 300-CD161 transfected cells, as expected. On the contrary, LLT1 could be detected on the four cell lines tested, its levels being much higher in the 300-LLT1 transfected cells, as expected. As previously mentioned, this suggests cross-recognition of the human and mouse form of Clec2D protein product.

3.4.2 Interaction between LLT1 and CD161 expressing cells

One of the essential tools for the development of this project has been the 300 cell line and their CD161 and LLT1 transfectants (see *2.1.2. Cell lines)*. I wanted to determine whether these two cell lines with their respective transfectant proteins could interact with each other, and I quantified the levels of such interaction by measuring the percentage of aggregate formation after coincubation. Aggregates were defined as a population with high SSC and FSC which was almost absent when just a single 300 type of cells was present (data not shown).

300-LLT1 transfected cells were incubated with untransfected 300 cells or 300-CD161 transfected cells for 4 hours in a 1:1 ratio. When the former was added, aggregate formation was almost absent (1.05%, Figure 3-2A). In contrast, addition of 300-CD161 cells resulted in more than 30% of aggregate formation, proving the existence of LLT1-CD161 interaction. Interestingly, the

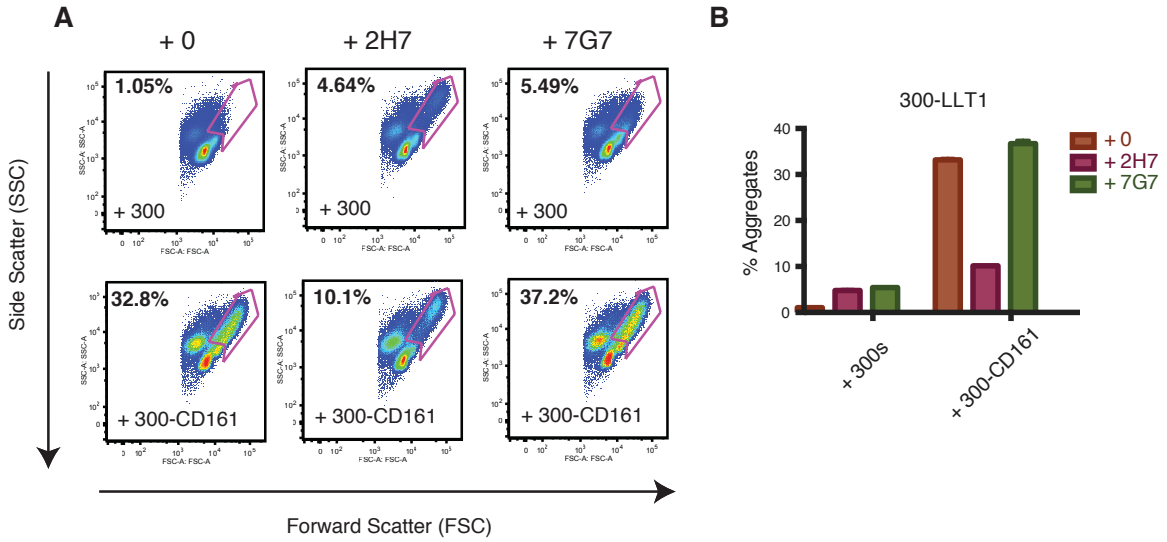


Figure 3-2. 2H7 mAb can block LLT1-CD161 interaction. (A) Aggregate formation of 300-LLT1 cells with untransfected 300/300-CD161 cells after a 4h incubation period. Side and forward scatter are shown in a logarithmic scale. Flow cytometric analysis of the blocking effect of aggregate formation using the anti-LLT1 antibodies 2H7 and 7G7 (A and B). The aggregated cells are gated and the percentage relative to the overall cells specified. Representative of 2 independent experiments (n=3).

aggregate formation could be partially blocked with the 2H7 mAb, but not with the 7G7 mAb (Figure 3-2A and 3-2B). This makes the 2H7 mAb a useful tool for further functional experiments, although its ability to cross-link still needs to be assessed. Such experiments could not be performed at the time because no outcome/function of LLT1 cross-linking had already been described.

3.4.3 Testing of anti-LLT1 antibodies for immunohistochemical staining

Different abilities to recognise LLT1 were also assessed by immunohistochemistry. Having confirmed the expression of LLT1 on Raji cells and considering that, at the time, LLT1 had been described on circulating B cells (Boles et al. 1999; Mathew et al. 2004; Rosen et al. 2008; Germain et al. 2010), I wanted to test whether I could detect LLT1 in tissue B cells. An association between LLT1 and GC B cells had been suggested (Germain et al. 2010) and has been recently confirmed by us and others (Germain et al. 2015). Therefore, I decided to take an immunohistological approach to stain tonsillar tissue testing the five different anti-LLT1 antibodies.

LLT1 expression was detected at very high levels on GC B cells with the goat polyclonal antibody, as well as with the novel 2H7 and 7G7 mAbs (Figure 3-3A). I could not observe any staining with the 4C7 clone, both from Sigma and Abnova, within the conditions tested (see *2.6.1 Immunoperoxidase staining*).

It is important to note that the staining pattern of GC B cells for the 7G7 mAb and the goat polyclonal was almost identical. The vast majority of GC B cells expressed LLT1 and the staining was mainly cytoplasmic. Although LLT1

could also be detected in GC B cells with the 2H7 mAb, the pattern of staining was different (Figure 3-3A). Only half of the GC B cells expressed LLT1 and the staining was stronger at the membrane compared to the cytoplasm. Furthermore, abundant LLT1+ cells could be detected outside the germinal centre. LLT1 expression of GC B cells was confirmed by FACS using the 2H7 mAb (Figure 3-3B). Overall, these data suggest that the 2H7 mAb may be the most sensitive to LLT1 surface staining.

3.4.4 Immunohistochemistry optimisation

At the beginning of the project, the novel 2H7 and 7G7 mAb were not available, and this is why most of the optimisation was done with the goat polyclonal anti-LLT1 antibody.

Five different steps within the immunohistochemical staining procedure were optimised (Table 3-2). As the tonsillar tissue had been formalin-fixed and paraffin-embedded (FFPE), an antigen retrieval step was needed in order to make the antigen binding sites available. Four different antigen retrieval buffers were tested, with DAKO buffer being the one that gave a better LLT1 staining (Figure 3-4A).

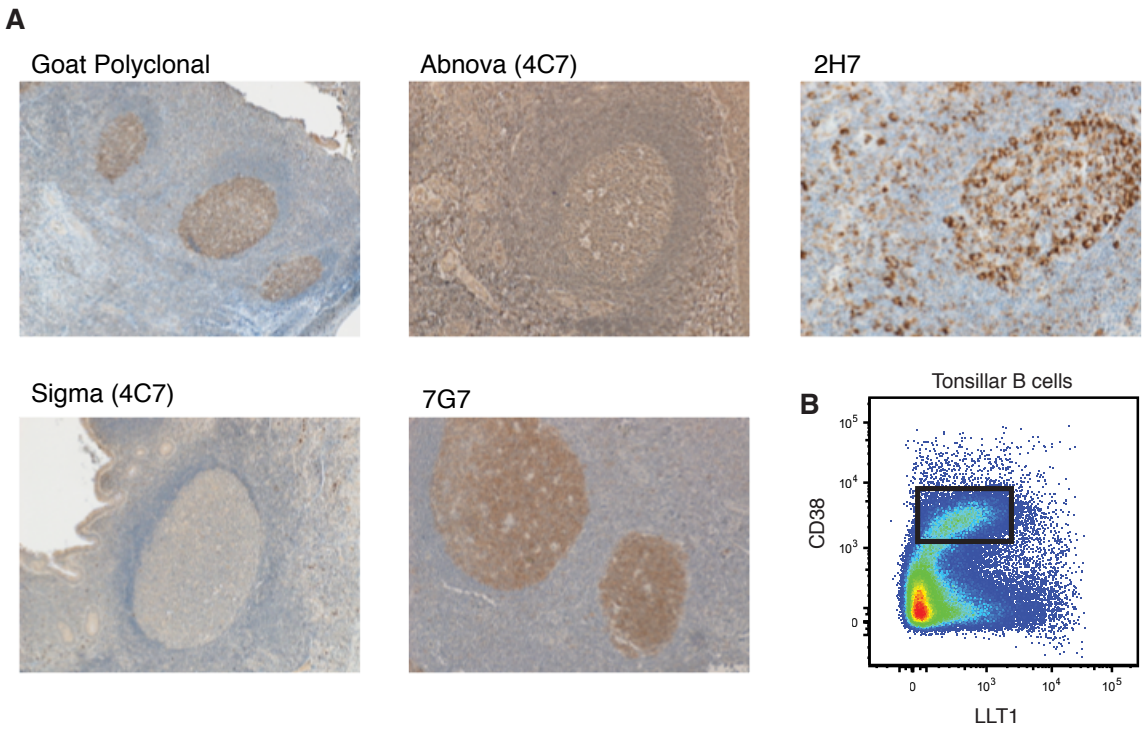
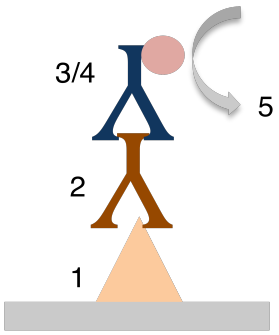


Figure 3-3. LLT1 can be stained immunohistochemically (2H7, 7G7, goat pAb). (A) Representative image of LLT1 staining in human tonsil tissue using five different anti-LLT1 antibodies (see Table 1). Three independent experiments (n=4). (B) LLT1 staining of purified tonsillar B cells with the 2H7 antibody. The GC population is highlighted (rectangle). Representative FACS plot (n=8).

Conditions					Figure
Retrieval buffer (1)	A	B	AC	DAKO	**A**
Goat polyclonal (2) (Secondary: donkey anti-goat)	1/20	1/40	1/80		**B**
Anti-goat secondary (3)	1/100	1/200	1/400	1/800	**C**
Goat polyclonal (4) (Secondary: anti-goat polymer)	Donkey anti-goat	Anti-goat polymer			**D**
DAB enhancing solution (5)	Yes	No			**E**
2H7 / 7G7 (2)	1/200	1/500	1/800		**F**



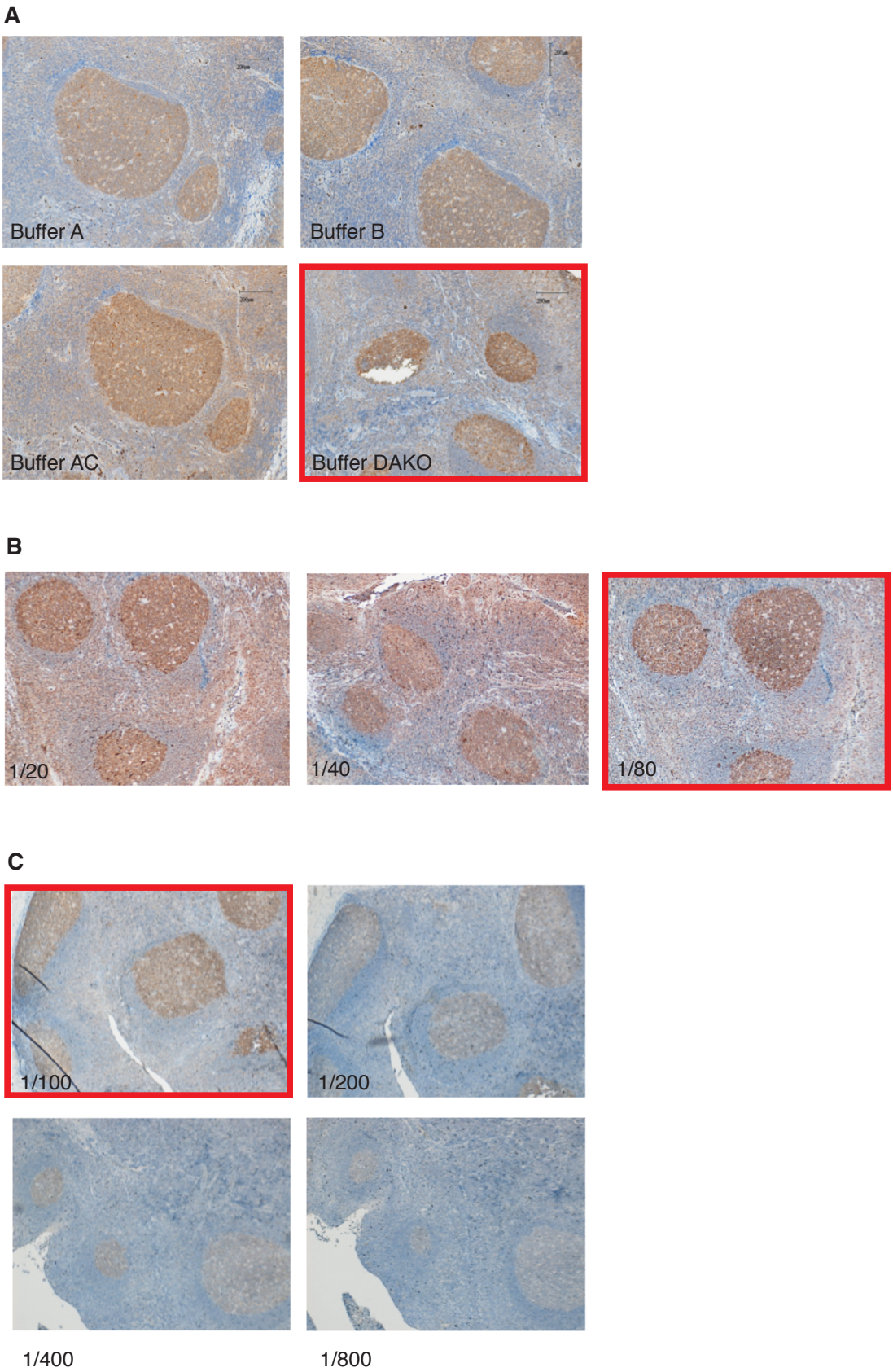
1. Antigen retrieval buffer
2. Primary antibody concentration
3. Secondary antibody type
4. Secondary antibody concentration
5. DAB enhancing solution

Table 3-2. Immunohistochemistry optimisation. Table 3-2 shows the different conditions tested for the optimisation of LLT1 imunohistochemistry, including the antigen retrieval buffer, the concentration for both goat and mouse-derived primary antibodies, type and concentration of secondary antibodies as well as a DAB enhancing step.

Next, different concentrations of the primary goat polyclonal anti-LLT1 antibody were tested. 1/80 was the concentration that gave the strongest staining with lowest background, and therefore the concentration I used for further stainings (Figure 3-4B). The concentration of the donkey anti-goat secondary antibody was also optimised (Figure 3-4C), being 1/100 the optimal concentration. I decided to compare that optimal staining with a secondary anti-goat polymer, concluding that the latter gave a stronger LLT1 staining (Figure 3-4D). In order to further increase the signal, I tested a DAB enhancing solution to intensify the reaction product in stained sections. However, the background was increased in the process, thus making LLT1 staining less clear (Figure 3-4E).

In summary, the optimal staining conditions with the goat polyclonal antibody included the use of the DAKO antigen retrieval buffer, the primary goat polyclonal anti-LLT1 antibody at 1/80, the use of the anti-goat antibody polymer as a secondary and the absence of DAB enhancing solution.

When the 2H7 and 7G7 mAbs became available, they were also tested for optimal staining (Figure 3-4F). 1/500 was the optimal concentration for both of them.


A
Buffer A
Buffer B
Buffer AC
Buffer DAKO
B
1/20
1/40
1/80
C
1/100
1/200
1/400
1/800

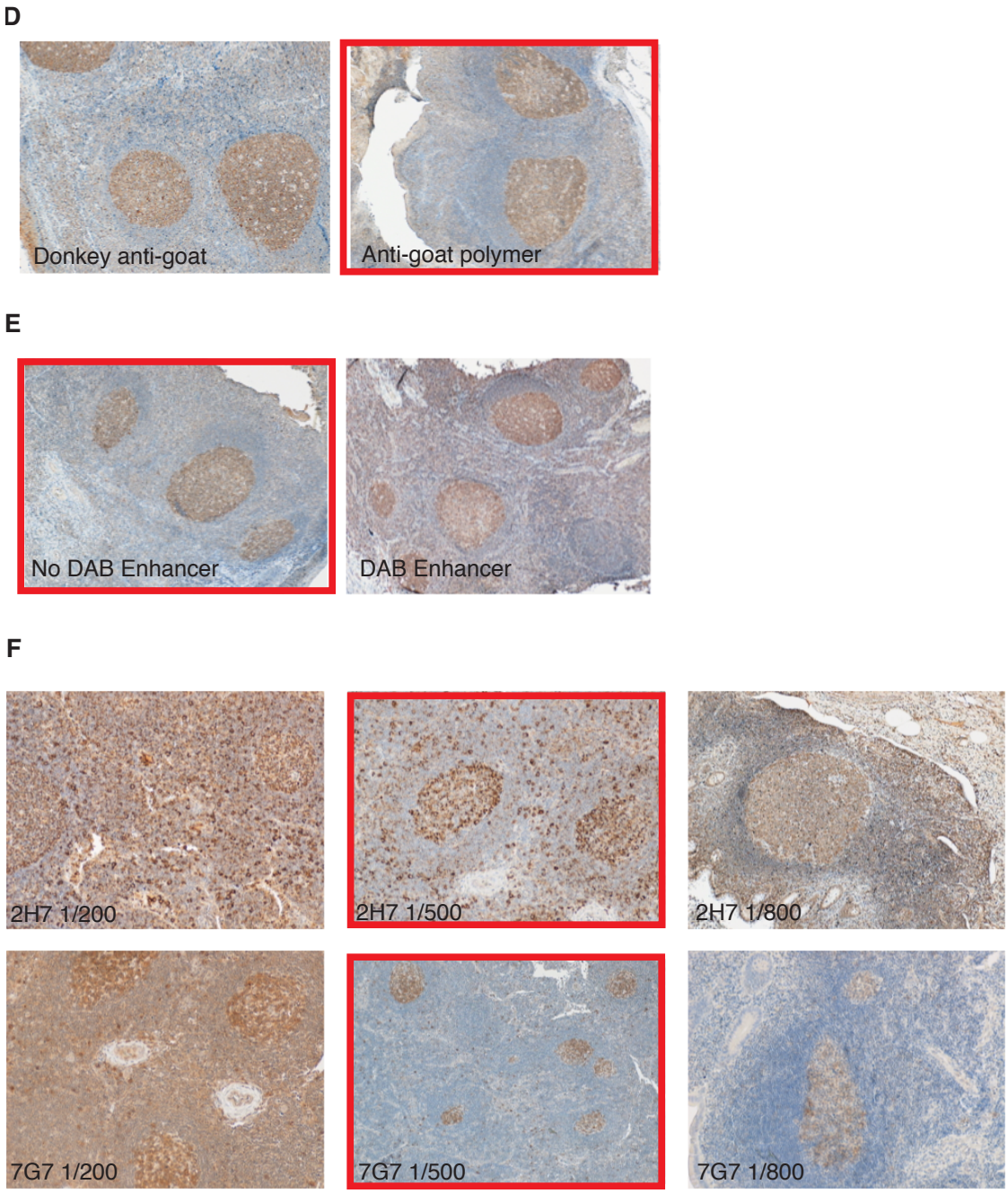


Figure 3-4. Optimisation coniditions for IHC staining of LLT1. Germinal centres in secondary lymphoid organs of human tonsil, appendix and lymph node tissues were stained under different conditions for optimisation. Four different antigen retrieval buffers were assessed (A); the anti-LLT1 goat polyclonal antibody was titrated when the donkey anti-goat secondary antibody was used (B); the anti-LLT1 goat polyclonal antibody was titrated when the anti-goat polymer was used (C); a comparison between the donkey anti-goat secondary antibody and the anti-goat polymer was performed (D); DAB enhancing solution was tried to improve staining (E); anti-LLT1 mouse monoclonal antibodies 2H7 and 7G7 were titrated when the anti-mouse polymer was used (F). Representative of three independent experiments.

3.4.5 Germinal centre staining with the polyclonal goat pAb and the 7G7 mAb

I showed strong expression of LLT1 in GCs from human tonsillar tissue (Figure 3-5A). I decided to explore whether such staining was comparable in GCs from other human tissues such as appendix (Figure 3-5B), spleen (Figure 3-5C), and lymph nodes (Figure 3-5D).

Strong expression of LLT1 could be seen in all GCs tested, independent of the tissue. The presence of LLT1+ cells outside the GCs could be observed (Figure 3-5C).

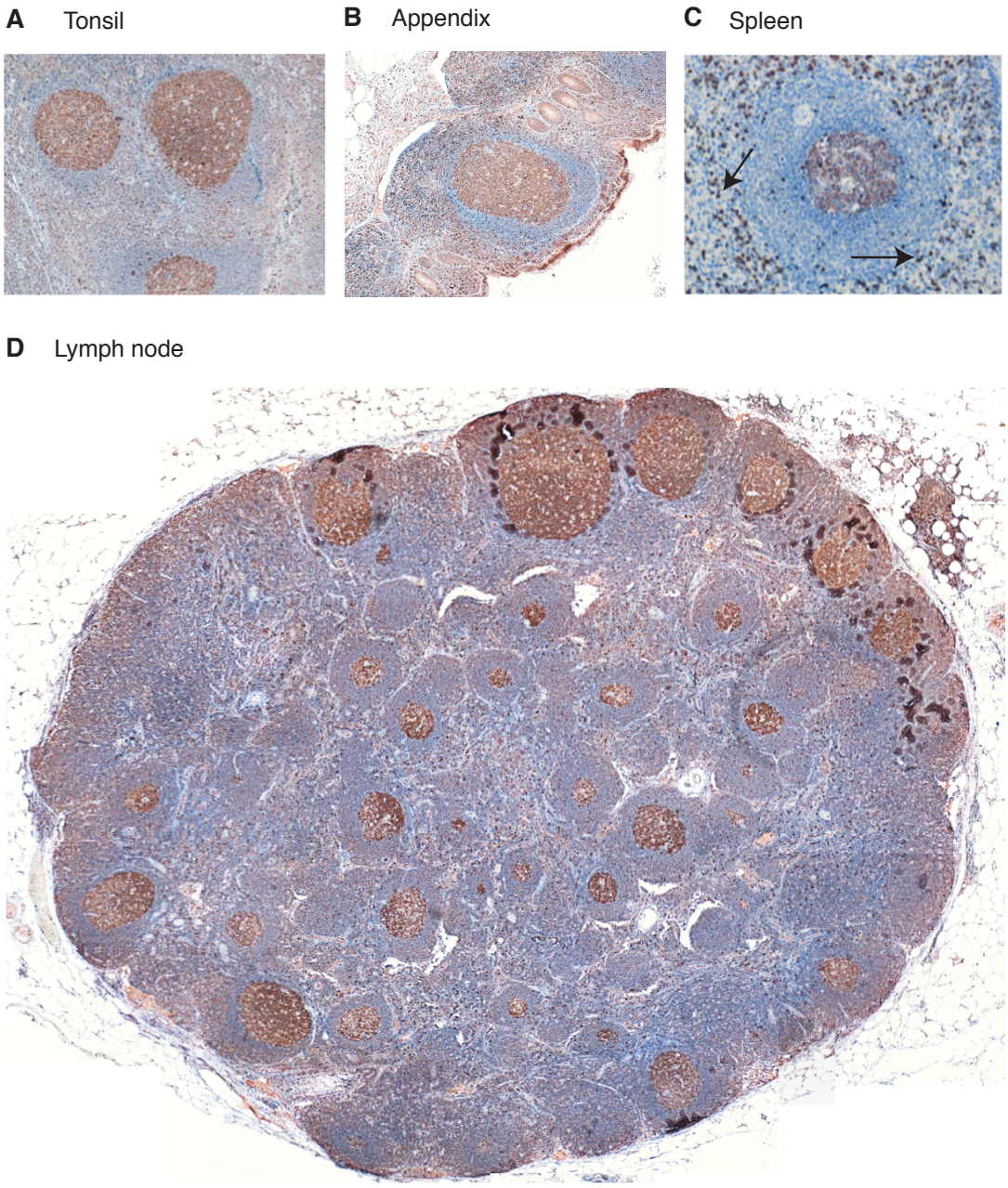


Figure 3-5. Germinal centre staining with the polyclonal goat anti-LLT1 antibody. Germinal centres in secondary lymphoid organs of human tonsil (A), appendix (B), spleen (C) and lymph node (D) were stained for LLT1 using the polyclonal goat anti-LLT1 primary antibody and the donkey anti-goat as secondary antibody. Arrows point LLT1+ cells outside the germinal centre (C). Representative image of three independent experiments.

Next, I studied whether the same staining pattern in GCs from different human tissues could be obtained using the novel 7G7 mAb. Figure 3-6 shows strong staining of LLT1 in GCs from lymph nodes (Figure 3-6A), appendix (Figure 3-6B), spleen (Figure 3-6C) and tonsils (Figure 3-6D) using the 7G7 mAb. LLT1+ cells outside the GC could also be detected (Figure 3-6A). GCs with aberrant shapes were equally positive for LLT1 (Figure 3-6D). Notice that LLT1 did not seem to be homogeneously distributed throughout the GC (Figure 3-6A and 3-6D), but this is a question that will be further assessed (see *5.4.2 LLT1 expression is higher in the DZ than in the LZ*).

In summary, GCs from spleen, appendix, lymph node and tonsillar human tissue were all strikingly positive for LLT1. The pattern of staining was the same for both the goat polyclonal and the 7G7 mAb. Moreover, LLT1 positive cells could be detected in secondary lymphoid organs outside the GC.

I wanted to explore whether the 7G7 mAb and the goat polyclonal antibody could block each other's binding. As it can be observed in (Figure 3-7A), increasing concentrations of the goat polyclonal anti-LLT1 antibody blocked the 7G7 mAb binding. I hypothesised that the 7G7 epitope could also be targeted by the goat pAb. Alternatively, binding of the goat pAb could have a steric shielding effect on the 7G7 epitope. In any case, the blocking was shown to be specific, as there were no differences in 7G7 binding when increasing concentrations of goat isotype control were used (Figure 3-7B). As expected, the 7G7 mAb could not block binding of the goat polyclonal anti-LLT1 antibody (Figure 3-7C), indicating that the goat pAb targets more than one single anti-LLT1 epitope.

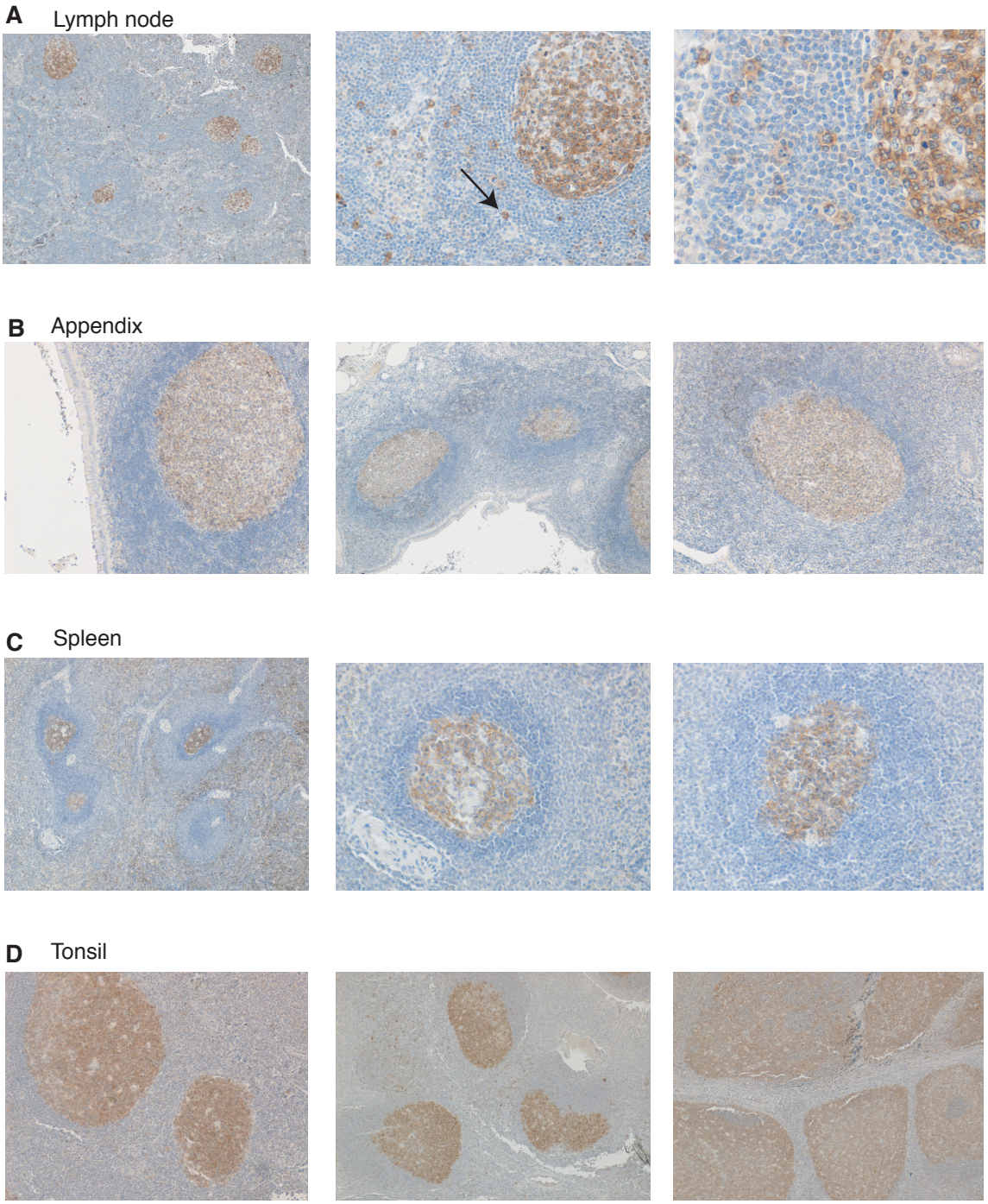


Figure 3-6. Germinal centre staining with the monoclonal 7G7 anti-LLT1 antibody. Germinal centres in secondary lymphoid organs of human lymph node (A), appendix (B), spleen (C) and tonsil (D) were stained for LLT1 using the monoclonal 7G7 anti-LLT1 primary antibody (1/500) and the anti-mouse polymer as secondary antibody. Arrow points LLT1+ cell outside the germinal centre (A). Aberrant germinal centres can be observed in tonsils (D). Representative image of three independent experiments.

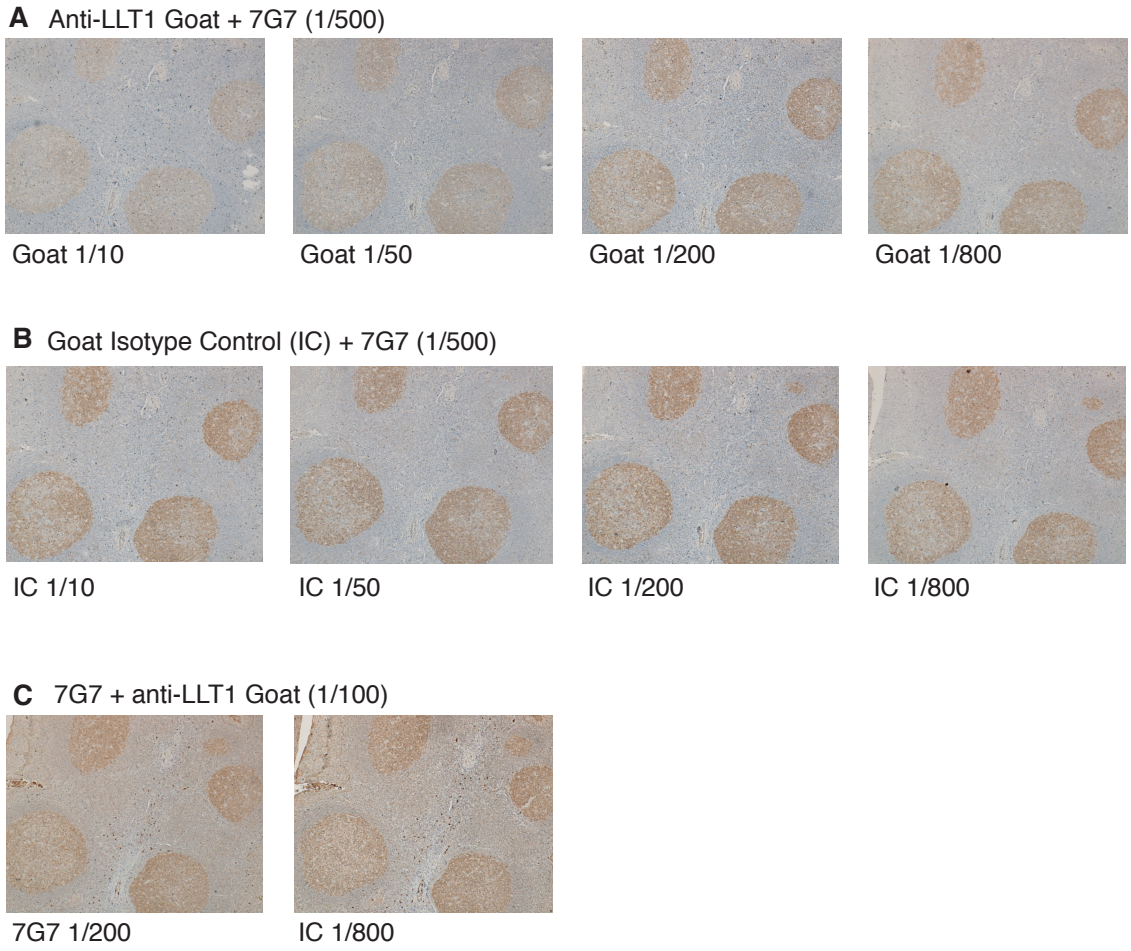


Figure 3-7. Blocking of LLT1 GC staining on human tonsil tissue. (A) shows 7G7 staining after blocking with increasing concentrations of polyclonal goat anti-LLT1 antibody. (B) shows 7G7 staining after blocking with increasing concentrations of goat isotype control antibody. (C) shows goat polyclonal anti-LLT1 staining after blocking with increasing concentrations of monoclonal 7G7 anti-LLT1 antibody. Representative image of three independent experiments.

3.4.6 Effects of glycosylation in LLT1 antibody recognition

While developing and optimising the tools for the study of LLT1, it became obvious that different anti-LLT1 antibodies recognise LLT1 differently. Whether these antibodies were used in FACS or immunohistochemistry also had a big impact on their recognition abilities (Table 3-3).

		Goat pAb	2H7	7G7
IHC		+++	+	+++
External FACS	**Raji**	-	++	-
	300-LLT1	+	+++	+

Table 3-3. Summary of anti-LLT1 antibodies binding abilities. Table 3-3 summarises efficiency of LLT1 staining for the three antibodies tested (goat pAb, 2H7 mAb and 7G7 mAb), both by immunohistochemistry and flow cytometry on Raji and 300-LLT1 cells.

LLT1 has been shown to be expressed on the cell surface as a highly glycosylated homodimer (Figure 3-8A; Mathew et al. 2004) with an average size of 130-140 KDa. Under reducing conditions, the non-glycosylated monomer has a molecular weight of 30 KDa, whereas its glycosylated form doubles the size (65-70 KDa, Figure 3-8B; Mathew et al. 2004). I hypothesised that glycosylation of LLT1 could play a role in differences in antibody binding. In order to test this, I first assessed the level of LLT1 glycosylation on 300-LLT1 cells by Western Blot. As it can be observed in

Figure 3-8C, under non-reducing conditions the vast majority of LLT1 protein lacked glycosylations and was mainly expressed in its dimeric form. When reducing conditions were used, a single band corresponding to the non-glycosylated monomer was observed. The 2H7 mAb was the best at recognising LLT1 on 300-LLT1, but both the goat pAb and the 7G7 also gave good levels of staining (Figure 3-1C). These results imply that all three antibodies are able to recognize the non-glycosylated form of LLT1. It is important to note that LLT1 is extremely abundant in the 300-LLT1 transfected cell line. Therefore, even antibodies with weak binding (ie. Goat polyclonal, 7G7) could give a substantial signal.

To further assess the possible role of glycosylation on antibody binding, Raji cells were treated with PNGase F and antibody binding of the goat polyclonal, the 2H7 mAb and the 7G7 mAb was analysed by flow cytometry. I showed that removal of glycosylations did not alter LLT1 recognition when the goat polyclonal and the 7G7 antibodies were used (Figure 3-8D and 3-8E). However, PNGase F treatment reduced 2H7 antibody binding, suggesting the glycosylation is important for LLT1 recognition in this context.

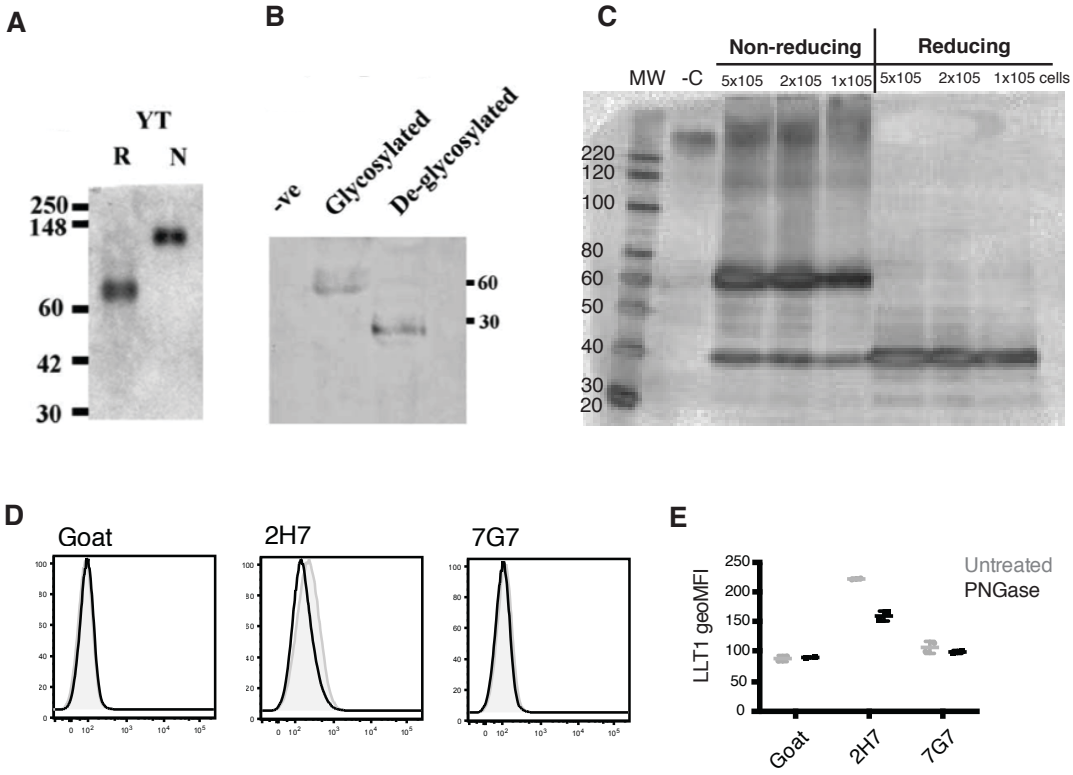


Figure 3-8. Glycosylation affects LLT1 antibody recognition. (A) Western blot analysis of LLT1 in cell lysates of YT cells (Mathew et al. 2004) in reducing (R) and non-reducing (N) conditions. (B) Western blot analysis of YT cell lysate with or without treatment with Endoglycosidase F (Mathew et al. 2004). (C) Western blot analysis of 300-LLT1 cell lysate in reducing and non-reducing conditions. Raji cells were treated with PNGase F for 24h and levels of external LLT1 were measured by FACS. (D) shows the histogram plots for the three antibodies tested (goat polyclonal, 7G7 mAb and 2H7 mAb). (E) shows geoMFI values for LLT1 for the three antibodies tested. Representative plots of two independent experiments (n=2).

3.5 Discussion

The current published research has revealed a number of inconsistent results. For example, early studies showed high levels of LLT1 present on NK cells (Boles et al. 1999). However, they could not be repeated by others later (Germain et al. 2011). Such discrepancies could be explained by the conditions under which the cells were kept (e.g. level of activation) or the variety of anti-LLT1 antibodies used. Here I aim to identify and describe a set of tools that will allow me to further characterise the expression, regulation and function of LLT1.

Differences in LLT1 recognition with the different anti-LLT1 antibodies tested became apparent from the very beginning (Figure 3-1 and Figure 3-4F). It is interesting to note that the effectiveness in antibody binding was opposite in the two techniques tested. While the 2H7 mAb stained very well by FACS, its effectiveness in immunohistochemistry was poor or much more restricted. Conversely, the goat polyclonal and the 7G7 mAb gave a very strong immunohistochemical staining, whereas their binding abilities by FACS were very weak (Figure 3-3 and Table 3-3). This led me to think that such differences in antibody binding were probably due to the nature of the recognised epitope and its glycosylation status, rather than recognition of different Clec2D isoforms (Germain et at. 2010). An example of this is seen with CD44, which also comprises several spliced variants and presents extensive glycosylation. This cell adhesion molecule presents different glycosylation patterns in different circumstances (ie. tumours) and that has been shown to affect antibody recognition (Matsuki et al. 2003).

Although I hypothesised that glycosylation may play a role in these differences, it is important to consider that all three antibodies were raised against *E.coli*-derived recombinant human LLT1, thus lacking glycosylations. As shown in Figure 3-1C, all these three antibodies were capable of recognising the non-glycosylated LLT1 on the 300-LLT1 transfected cells, although the goat polyclonal and the 7G7 mAb to a much lesser extent. In contrast, only the 2H7 antibody effectively stained LLT1 on Raji cells. Interestingly, staining with the 2H7 and the 4C7 allowed for detection of LLT1 in untransfected 300 cells, but only internally (Figure 3-1D). Not only this suggests a certain degree of cross-reactivity between the Clec2D forms of both human and mouse, but also that LLT1 is marginally expressed on the cell surface of 300 cells. It is well described that there are certain requirements for protein trafficking to the cell surface (Ma 2002; Nickel & Seedorf 2008), and one of them is glycosylation (Guan et al. 1985). This can be illustrated by the CD4 receptor, which requires glycosylation for proper folding as well as cell surface expression (Konig et al. 1988; Tiffts et al. 1992). It is tempting to speculate that LLT1 glycosylation might play a role in folding and transport to the cell membrane.

I suggest that the 2H7 antibody is recognising a conformational epitope that is lost during certain treatments of specimens prior to immunohistochemical staining. Formalin fixation is a widely used method to preserve tissue morphology. However, at the same time, it alters the tissue reducing its immunohistochemical reactivity. Formalin induces chemical modifications on the tissue (e.g. Methylene bridges) as well as changes in electrostatic charge,

which can mask antigen sites (Fraenkel-Conrat et al. 1947). Moreover, it may alter the secondary and tertiary structure of the protein, with potential consequences for antibody binding. The heat antigen retrieval process aims to unmask the hidden epitopes by restoring normal protein chemical composition and electrostatic charge, allowing subsequent antibody binding. However, it has been suggested that the antigen retrieval process also leads to irreversible protein unfolding (Fowler et al. 2011). The loss of the protein native structure entails the destruction of conformational epitopes. Therefore, if the 2H7 mAb was recognising a conformational epitope available by FACS staining on the surface of Raji and 300-LLT1 transfected cells, it is plausible that such epitope became non-existing after the formalin treatment and antigen retrieval process. In contrast, this same process would expose epitopes that may be hidden in the protein native structure. I hypothesise that this is the case for the epitopes recognised by the goat polyclonal and the 7G7 antibodies. Both antibodies recognise linear epitopes, which are unmasked after the heat antigen retrieval process. Such linear epitopes could be located outside the extracellular region of the LLT1 protein or hidden upon dimerisation, so antibody binding would be prevented by FACS staining of LLT1 on its native conformation.

Table 3-4 summarises the characteristics of the different LLT1 epitopes targeted by the goat polyclonal anti-LLT1 antibody, as well as the 2H7 and the 7G7 mAbs.

	Goat pAb	2H7	7G7
Epitope	Linear	Conformational	Linear
Influenced by glycosylation	No	Yes	No
IHC	✔	✖	✔
FACS	✖	✔	✖

Table 3-4. LLT1 epitope characteristics and antibody binding efficacy. Table 3-4 shows the nature of the epitope and its glycosylation status for the three antibodies tested (goat pAb, 2H7 mAb and 7G7 mAb). Their binding efficiency by FACS and IHC is specified.

Their recognition by FACS and immunohistological staining is also specified. Notice that removal of glycosylations using PNGase F reduced 2H7 mAb LLT1 binding (Figure 3-8D and 3-8E), suggesting that the presence of polysaccharides play a role in LLT1 recognition in this particular context. However, it is interesting to note that the 2H7 mAb was raised against non-glycosylated *E.coli*-derived LLT1. Due to the high quantities of protein produced or the refolding methods applied, the possibility that mAb were generated against conformational epitopes cannot be ruled out. It is well accepted that glycosylation helps stabilising the secondary and tertiary structures of a protein (Petsko 2009). This could imply that the 2H7 mAb relies on the native structure of LLT1 for optimal recognition.

When characterising the cell lines that will be further used for the study of LLT1, it became noticeable that both the 4C7 and the 2H7 anti-LLT1 mAb

were able to stain the untransfected 300 cells. A high degree of homology has been described for the mouse and human forms of the Clec2D protein (Hu et al. 2004), suggesting that these antibodies could be reacting with both the mouse and human forms of this C-type lectin. The distribution of mClr-b has been widely studied compared to the human one. However, so far, there is no particular mention of the presence of mClr-b in mouse B cells. Considering that the 300 cells derive from murine pre-B cells and that LLT1 is expressed on human B cells, the mouse arises as a potentially useful animal model for the study of LLT1. Nevertheless, this requires further and extensive investigation.

3.6 Summary

- The 2H7 mAb is the best for FACS staining of LLT1
- In contrast to the 7G7 mAb, the 2H7 mAb can block LLT1-CD161 interaction
- Both the goat polyclonal antibody and the 7G7 mAb are very useful for immunohistological staining of LLT1
- The anti-LLT1 goat polyclonal antibody blocks 7G7 binding to LLT1, but not the other way around
- LLT1 recognition by FACS with the 2H7 mAb is affected by removal of glycosylations

4 LLT1 is expressed in healthy human tissue

4.1 Introduction

In Chapter 3, I identified and characterised a good set of tools for the study of LLT1. At this point, and with the final aim of elucidating the function of LLT1, a rigorous and extensive characterisation of its distribution was required. The current published literature presents certain inconsistencies and, to date, there has only been one study assessing the overall distribution of LLT1, as part of a wider project aiming for a tissue-based map of the human proteome, called The Human Protein Atlas (Uhlen et al. 2015). Thus, in this chapter, I wanted to examine the overall distribution of LLT1 using the three anti-LLT1 antibodies that worked efficiently in immunohistological staining (see Chapter 3). These are the commercial goat polyclonal anti-LLT1 antibody (R&D systems) and the two mAbs 2H7 and 7G7.

Apart from studying the distribution of LLT1 in healthy tissues and cell types, I wondered if such expression changed in the context of disease. Particularly, I focused on inflammation and malignant transformation. Situations such as inflammation, infections and transformation alter the range of receptors expressed on the cell surface, and this has a profound impact on our immune responses. Such processes are linked to the release of endogenous damage-associated molecular pattern molecules (DAMPs) (Srikrishna & Freeze 2009), suggesting that immune responses are not only elicited against foreign pathogens, but also activated by the damaged or altered-self (Matzinger

1994). This has been, indeed, one of the big questions of immunology; how to distinguish between self and non-self, and thus how to find the optimal balance between immunity and tolerance. In that respect, the presence of MHC class I molecules fulfil the function of labelling the self, preventing our immune system from attacking our own, healthy cells. They do so mainly by inhibiting NK cells in what is known as the missing-self hypothesis (Kärre et al. 1986). MHC class I molecules also play a key role in peptide presentation, exposing a representative sample of the ongoing protein production within the cell on its surface. This allows T cells to thoroughly examine the state of our cells and react appropriately. This is the reason why MHC class I molecules are often downregulated upon viral infections, illustrating how viral evolution has come up with a clever strategy to evade this effective surveillance mechanism (Hansen & Bouvier 2009). For instance, dowregulation of MHC-I class been shown upon HSV and Human Cytomegalovirus (HCMV) infection (Huard & Früh 2000). Such strategies have also been described in tumours, for example, human melanoma cells (Hicklin et al. 1999; Bubeník 2005; Garrido et al. 2012).

Nonetheless, there are healthy sites within our bodies that present low levels of MHC class I molecules, due to their immune peculiarities (e.g. an excessive immune response in the brain could be fatal). This idea emerged from the study of tissue grafts, which when placed in particular anatomical structures were able to avoid rejection for long periods of time (Barker and Billingham 1977). This observation led to the notion of immune-privilege, believed to be an evolutionary adaptation to protect essential organs from harmful

inflammatory responses. At first, it was thought that certain antigens did not have access to immune-privileged sites, thus avoiding a response. However, more recent evidence suggested that the maintenance of immune-privilege relies on active rather than passive mechanisms (Ferguson et al. 1997). Some examples include the lack of lymphatic drainage, low expression of MHC class I molecules, enhanced expression of inhibitory surface molecules and local production of immunosuppressive cytokines (Hong and Van Kaer 1999). Immunologically privileged sites include the brain, the eyes, the placenta, the fetus and the testes. Although there has been abundant research regarding the mechanisms behind effective suppression of inflammatory responses in immune-privileged structures, further studies are required to fully elucidate and understand them.

Receptor-ligand pairs of C-type lectins have been shown to be involved in the cross-talk between lymphocytes and to play a role in inflammation (Welte et al. 2006), as well as to participate in immune responses in particular body locations (ie. NKp65-KACL in the skin) (Spreu et al. 2010). I wanted to explore whether the LLT1-CD161 pair could be involved in similar processes. However, in order to do so, extensive characterisation of both LLT1 and CD161 expression is required.

4.2 Aims

One of the main aims of this project was to broadly characterise LLT1 distribution in the human body. The work performed in this section allowed the following questions to be answered:

- Where is LLT1 expressed?
- Does LLT1 expression changes in the context of disease?
- What is the function of LLT1?

4.3 Materials and Methods

Specific materials and methods for this chapter are detailed below. All other methods and reagents are described in Chapter 2.

4.3.1 Cell lines

Human leukocyte antigen (HLA) class I –deficient 721.221 (221) cells were maintained in R10.

Placental choriocarcinoma BeWo cells were kept in DMEM/F12 (Dulbecco's modified eagle medium, Sigma Aldrich), supplemented with 10% FCS (PAA Laboratories), 100ug/ml streptomycin (Sigma Aldrich), 100 IU/ml penicillin (Sigma Aldrich), 2mM L-glutamine (Sigma Aldrich).

HHL12, Huh7 and HepG2 cells were kept in DMEM (Life Technologies) with 10% FCS, PAA Laboratories), 1% streptomycin/penicillin (Sigma Aldrich), 1% L-glutamine (Sigma Aldrich) and 1% non-essential aminoacids (Life Technologies).

4.3.2 Tissues

A series of healthy FFPE human tissues comprising samples of healthy liver and lung were obtained from Proteogenix. FFPE human inflamed liver sections (Figure 4-7) were a kind gift from Dr. Lauer (Harvard Medical School, Boston, Massachusetts).

FFPE healthy and tumour tissue arrays were obtained from AMS Biotechnology.

4.3.3 THP-1 and hepatocyte-derived cell lines stimulation

THP-1 cells were stimulated with the following cytokines at 50 ng/ml: IL-2 (R&D Systems), IL-4 (PreproTech), IL-6, (Miltenyi Biotec), IL-7 (R&D Systems), IL-10 (Miltenyi Biotec), IL-15 (Miltenyi Biotec), IL-18 (MBL International) and IL-23 (R&D Systems) and kept overnight at 37°C 5% CO_2. They were also stimulated with Lipopolysaccharide (LPS) *E. coli* K12 (1 µg/ml, Invivogen), PMA (50 ng/ml, Sigma Aldrich) and the Human TLR1-9 Agonist Kit (Invivogen).

Hepatocyte-derived cells from Huh7, HHL12 and HepG2 cell lines were stimulated for 48h at 37°C 5% CO_2 with the Human TLR1-9 Agonist Kit (Invivogen) or with increasing concentrations of Polyionisinic-polycytidylic acid (Poly(I:C)) High molecular weight (HMW) (Invivogen), following manufacturer's instructions.

4.3.4 NK cell degranulation assay

2 x 10^5 PBMCs were seeded per well in 100 µl R10 with IL-15 (1 ng/ml, PeproTech) and IL-2 (1 ng/ml, PeproTech) and incubated overnight at 37ºC 5% CO_2. 4 x 10^4 221, 300 or 300-LLT1 cells were added, together with the CD107a-PE-Cy7 (1/1000, BioLegend) and incubated for 1 h at 37ºC . Monensin (1/1000, BioLegend) was added and the cells were incubated for another 4-5 hours before the cells were stained for flow cytometry.

4.4 Results

4.4.1 LLT1 is expressed on circulating B cells and monocytes

Once I had identified the 2H7 mAb as an effective antibody for LLT1 recognition using flow cytometry (see Chapter 3), I next assessed the presence of this C-type lectin on PMBCs. I analysed different cell subsets (Figure 4-1A) and detected abundant expression of LLT1 on monocytes (60-80%) and B cells (15-30%), but not on NK cells, T cells or CD3+ CD56+ cells (Figure 4-1B and 1C). These results partially fit with the published literature (Boles et al. 1999; Mathew et al. 2004), although they also differ from some studies (Germain et al. 2011). As mentioned in the introduction, there are abundant inconsistencies regarding LLT1 expression on PBMCs (see Table 1-1), and this issue will be further addressed in the *4.5 Discussion* section.

Interestingly, the receptor ligand pair LLT1-CD161 was expressed on PBMCs in an exclusive manner (Figure 4-1C). While monocytes and B cells expressed LLT1, their levels of CD161 expression were null. On the contrary,

all the other subsets tested expressed CD161 to a certain extent, though they did not express its ligand, LLT1.

The fact that LLT1 is expressed on monocytes and B cells matches with the previously characterised expression of this C-type lectin in B-cell derived Raji cells and monocyte-derived THP-1s (Figure 3-1).

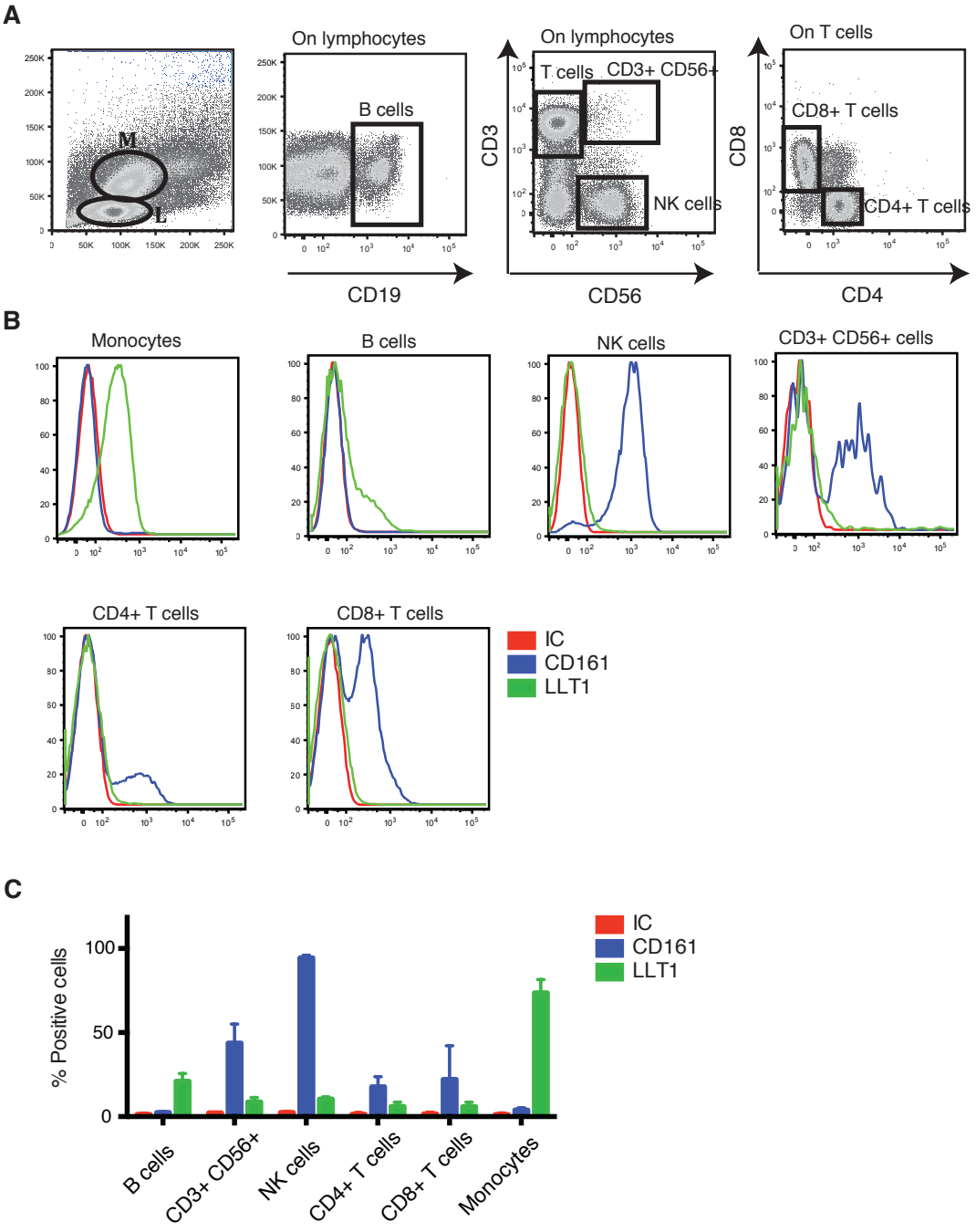


Figure 4-1. LLT1 is expressed on circulating B cells and monocytes. LLT1 (stained using the 2H7 mAb) and CD161 levels were measured by flow cytometry in monocytes (M) and lymphocytes (L). (A) shows the gating strategy. Monocytes and B cells expressed LLT1, whereas most NK cells and a subgroup of CD3+ CD56+, CD4+ and CD8+ T expressed CD161 (B and C). (n=4).

4.4.2 Regulation of LLT1 expression on monocytes/macrophages

LLT1 is expressed on THP-1 cells (Figure 4-2A), as it has been described before (Boles et al. 1999; Rosen et al. 2008; Germain et al. 2010; Germain et al. 2011). Monocytes can be activated by different stimuli, including cytokines, TLR agonists and PMA (Krutzik et al. 2005; Daigneault et al. 2010). I assessed the changes of LLT1 surface levels on THP-1 cells when they were incubated overnight with different stimuli (Figure 4-2B). The cytokines tested, as well as the TLR4 agonist lipopolysaccharide (LPS), had a minor effect on LLT1 expression, with the exception of IL-4 that slightly increased levels of this C-type lectin. However, LLT1 expression decreased when THP-1 cells were stimulated with PMA, which is known to drive their differentiation into macrophages (Daigneault et al. 2010; Park et al. 2007). The results were measured both in terms of percentage of LLT1-expressing cells (Figure 4-2B) and fold-change in LLT1 geoMFI (Figure 4-2C). I also wanted to investigate the effect of different TLR agonists on the levels of LLT1 expression, as TLR stimulation has been described to trigger monocyte differentiation into macrophages and DCs (Krutzik et al. 2005). After 48h stimulation, only the TLR8 agonist ssRNA40 had a large effect on LLT1 levels, enhancing them greatly (Figure 4-2D). Such stimulation also impacted cell viability, reducing the percentage of alive THP-1 cells to 80% (Figure 4-2E). Both the TLR1/2 agonist Pam3CSK4, a synthetic lipopeptide (LP) that mimics bacterial LP, and the TLR9 agonist C-phosphate-G (CpG) oligonucleotide caused LLT1 downregulation on the surface of THP-1 cells. These results suggest that

distinct activation pathways may impact LLT1 expression differently. The fact that PMA strongly decreased levels of LLT1 suggested that expression of this C-type lectin might decrease as monocytes differentiate into macrophages. To further explore this possibility, I performed immunofluorescent staining of tissue resident macrophages from lung (alveolar macrophages) and liver (Kupffer cells). Costainings of LLT1 with the macrophage marker CD68 showed no overlap within these tissues, thus suggesting that terminally differentiated macrophages do not express LLT1 (Figure 4-2F).

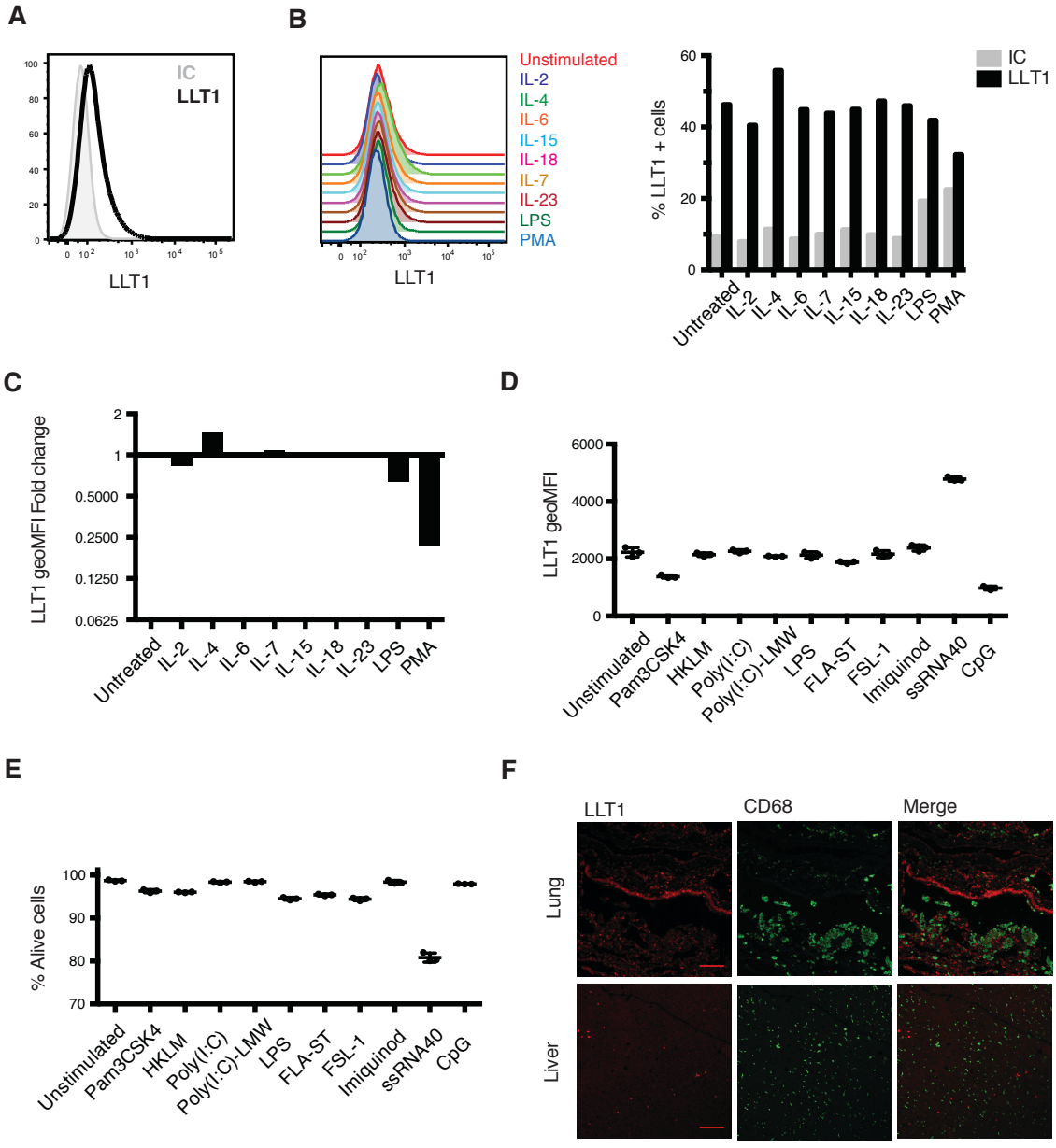


Figure 4-2. Regulation of LLT1 on THP-1 cells. (A) LLT1 could be detected on THP-1 cells with the 402659 anti-LLT1 (R&D). (B) Overnight stimulation of THP-1s with various cytokines only caused small variations in LLT1 levels with the exception of PMA, seen both as percentage of LLT1 expressing cells (B) and fold-change in LLT1 geoMFI (C). Representative plots of three independent experiments (A, B, C). Data from different experiments has not been pulled together due to high variation between them, despite following the same trend. (D) THP-1 cells were stimulated with various human TLR agonists for 48h and levels of LLT1 measured by flow cytometry (D), as well as the percentage of alive cells (E). Two independent experiments (n=3). (F) Immunofluorescent costaining of LLT1 (red) and CD68 (green) in lung and liver sections (scale bar = 100 µm). Representative of two independent experiments.

4.4.3 LLT1 is expressed in immune-privileged sites

There have been limited attempts to broadly characterise the distribution of LLT1 within human tissues (ie. Human Protein Atlas[1]), partially due to the lack of effective antibodies. Here, I screened a wide variety of human healthy tissues using the three antibodies that effectively stain for LLT1 immunohistologically (see Chapter 3), these being the goat polyclonal (R&D Systems) and the 2H7 and 7G7 mAbs. The results are summarised in Figure 4-3 and Table 4-1. Although LLT1 could be detected in a wide variety of tissues such as the lung, the gastrointestinal tract (GI) and the kidneys, its expression was strikingly high in immune-privileged sites like the testes (cells in the seminiferous ducts), the brain (neurons and particularly Purkinje cells) or the placenta (trophoblastic cells) (Figure 4-3 and Figure 4-4A, 4B and 4C)[2].

I next examined the placental choriocarcinoma derived BeWo cell line but could only detect a very marginal portion of LLT1 positive cells (Figure 4-4D).

We also compared the expression pattern of LLT1 in healthy and cancerous human tissues (Figure 4-5 and Table 4-2). Although LLT1 upregulation has been shown in glioblastoma (Roth et al. 2007), my results did not support the idea of upregulation being a common trend in all cancerous tissues. More likely, changes in LLT1 expression upon malignant transformation might be tissue-dependent, as it is illustrated in Figure 4-5.

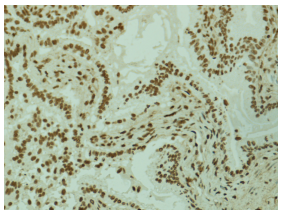
---

[1] A rabbit polyclonal antibody was used (Sigma Aldrich, HPA017649)

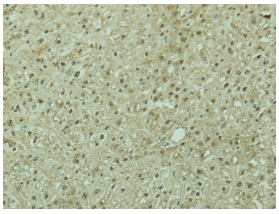
[2] Notice that all the samples tested from the tissue array were negative when the 7G7 mAb was used. However, positivity in germinal centres from spleen and tonsil has been previously shown with this particular antibody (Figure 3-6).

Liver and pancreas

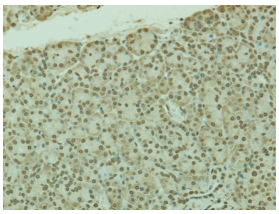
Gallbladder



Liver

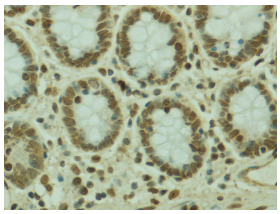


Pancreas

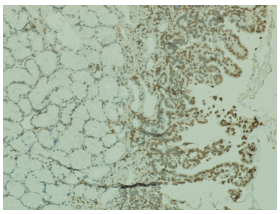


Digestive tract

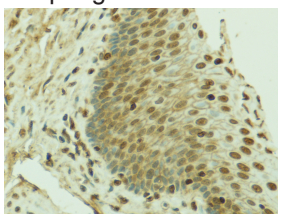
Colon



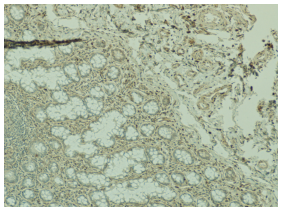
Duodenum



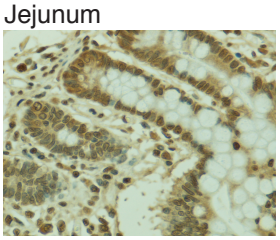
Esophagus



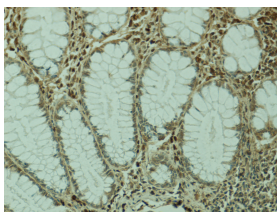
Ileum



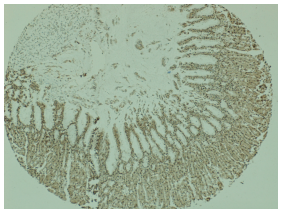
Jejunum



Rectum

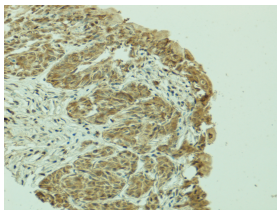


Stomach

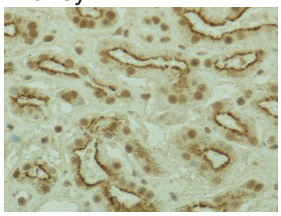


Urinary tract

Bladder

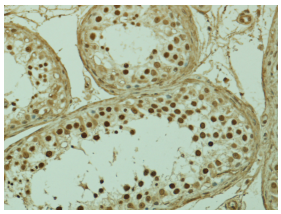


Kidney

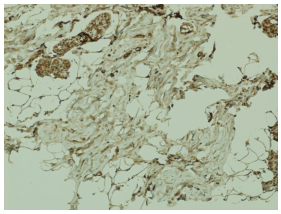


Reproductive system

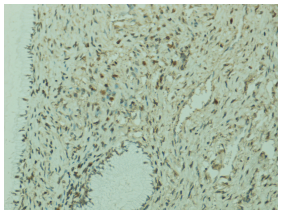
Male - Testis



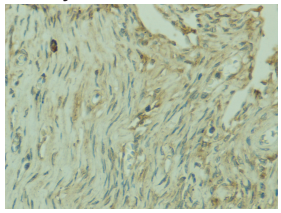
Female - Breast



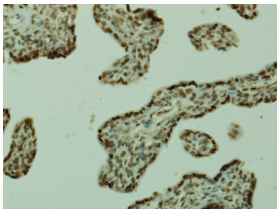
Cervix



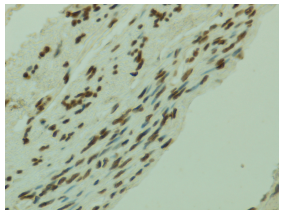
Ovary



Placenta



Uterus



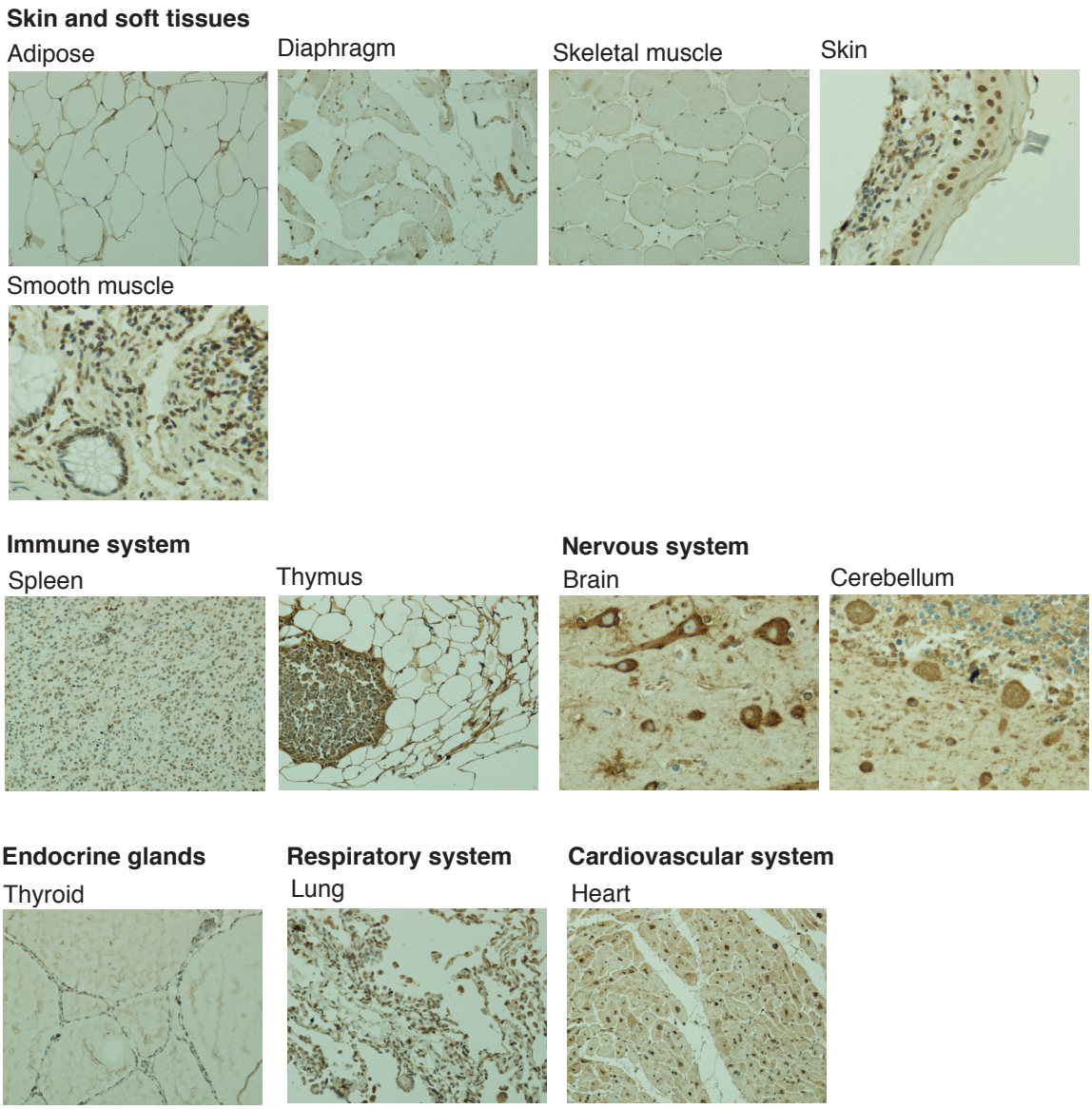


Figure 4-3. Expression of LLT1 in healthy immune tissue. Staining of human healthy tissue with the 2H7 anti-LLT1 antibody at 1/500. Representative image of three independent experiments.

Tissue type	Goat Polyclonal	7G7	2H7	Human Protein Atlas	Cell type
Liver and pancreas					
Gallbladder	+	-	++	++	Glandular cells
Liver	+	-	+	+	Hepatocytes
Pancreas	++	-	++	++	Exocrine glandular cells
Digestive tract					
Colon	++	-	++	+++	Glandular cells
Duodenum	+	-	++	+++	Glandular cells
Esophagus	++	-	++	+	Squamous epithelial cells
Ileum	++	-	++	+++	Glandular cells
Jejunum	++	-	++	+++	Glandular cells
Rectum	+	-	++	+++	Glandular cells
Stomach	+++	-	++	+++	Glandular cells
Urinary tract					
Bladder	++	-	++	++	Urothelium
Kidney	++	-	++	++	Cells in tubules
Reproductive system					
Male - Testis	+++	-	+++	++	Cells in seminiferous ducts
Female - Breast	+	-	++	++	Glandular cells
Cervix	++	-	+	++	Glandular cells
Ovary	+	-	+	-	Stromal cells
Placenta	+	-	+++	+++	Trophoblastic cells
Uterus	+	-	+	++	Glandular cells
Skin and soft tissues					
Adipose	-	-	-	-	-
Diaphragm	+	-	+		Myocytes
Skeletal Muscle	+	-	+	++	Myocytes
Skin	+	-	+	++	Keratinocytes
Smooth Muscle	+	-	++	++	Smooth muscle cells
Immune system					

Spleen	+	-	+	+	Germinal center
Thymus	-	-	+		Thymocytes
Nervous system					
Brain	++	-	+++	++	Neurons
Cerebellum	++	-	+++	+++	Purkinje cells
Endocrine glands					
Thyroid	+	-	+	++	Glandular cells
Respiratory system					
Lung	+++	-	++	++	Pneumocytes
Cardiovascular system					
Heart	+	-	+	++	Myocytes

Table 4-1. Comparison of LLT1 staining using different antibodies. Comparison of LLT1 staining of human healthy tissue with three different antibodies (goat pAb, 7G7, 2H7) and The Protein Atlas. * Positive staining with the 7G7 could be observed (Figure 3-5 and 5-6), although not in the tissue array samples. Negative staining (-), low staining (+), moderate staining (++), strong staining (+++).

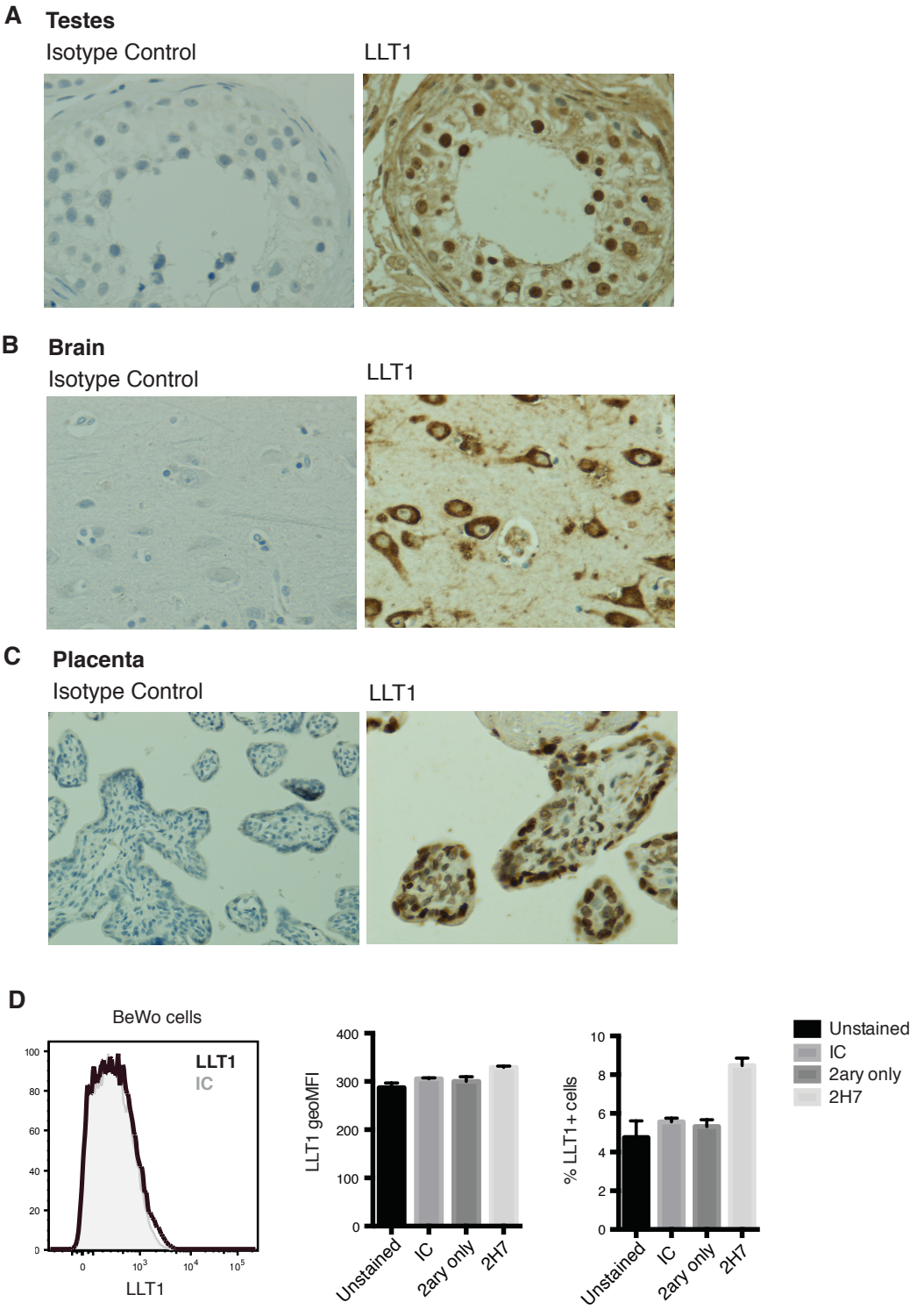


Figure 4-4. LLT1 is highly expressed in immune-privileged sites. LLT1 and isotype control stainings of testes (A), brain (B) and placenta (C) using the anti-LLT1 2H7 mAb (1/500). Representative image of 3 independent experiments. (D) The placental-derived BeWo cells presented negligible levels of LLT1, measured by FACS staining (2H7) both in terms of geoMFI and percentage of positive cells. Isotype control (IC), anti-mouse IgG-PE without primary antibody (2ary only). Two technical replicates.

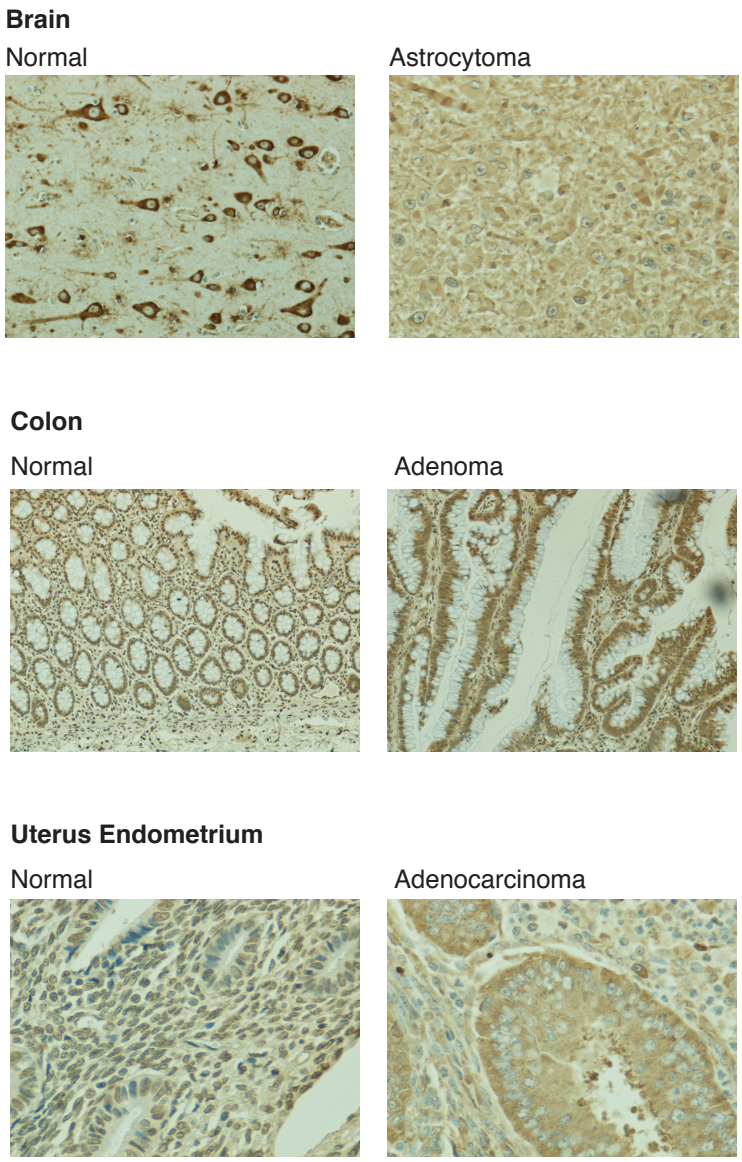


Figure 4-5. LLT1 staining of human tumor tissues with the 2H7 anti-LLT1 antibody. Changes in LLT1 expression were tissue dependent. Examples of brain, colon and uterus tissue are shown. Representative image of three independent experiments. Stainings performed using the 2H7 antibody 1/500.

Tissue type	Normal	Cancer
Adrenal Gland	++	+
Bladder	++	++
Bone		++
Brain	+++	++
Breast	++	++
Cerebellum	+++	++
Colon	++	++
Esophagus	++	+
Kidney	++	++
Liver	+	++
Lung	++	+
Lymph node	+	+/++
Oronasopharynx		++
Ovary	+	+
Pancreas	++	++
Prostate	++	++
Rectum	++	++
Salivary Gland	++	+
Skin	+	+
Small intestine	++	+
Stomach	+	+
Testis	++	+
Thyroid	+	++
Uterus Cervix	+	+
Uterus Endometrium	+	++

Table 4-2. LLT1 staining of human cancerous tissue. Comparison of LLT1 staining of human healthy and tumour tissue with the anti-LLT1 2H7 antibody (1/500). Negative staining (-), low staining (+), moderate staining (++), strong staining (+++).

4.4.4 LLT1 inhibits NK cell degranulation

A key feature of immune-privilege is low expression of MHC class I molecules, which protects certain tissues from excessive and damaging inflammatory immune responses (Hong and Van Kaer 1999). However, this downregulation of MHC class I molecules results in increased susceptibility to NK cell killing. A role for LLT1 in suppression of NK cell function has been described (Aldemir et al. 2005; Rosen et al. 2005; Roth et al. 2007; Rosen et al. 2008). Here, I confirmed that the presence of LLT1 diminishes NK cell degranulation, measured by levels of CD107a using 300 and 300-LLT1 cells as targets (Figure 4-6). In summary, my data suggests a plausible role for LLT1 in immune-regulation and, particularly, in negative modulation of immune responses in immune-privileged sites.

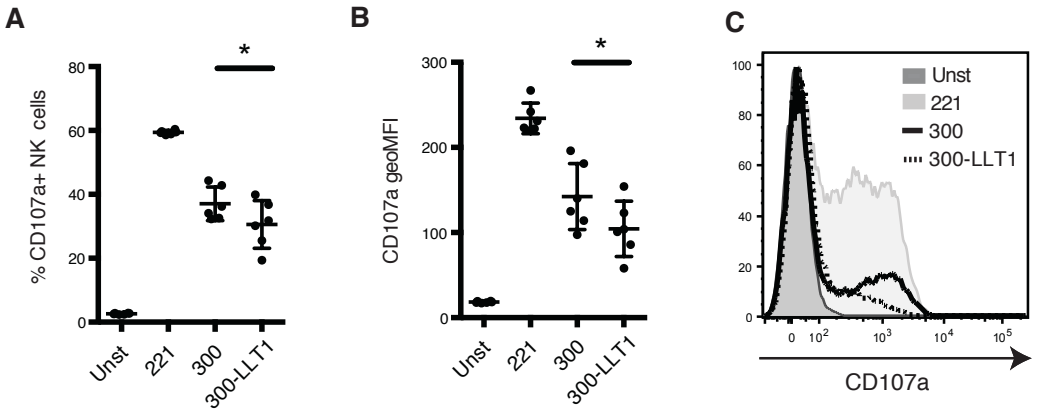


Figure 4-6. LLT1 inhibits NK cell degranulation. The percentage of CD107a expressing NK cells, gated on alive, CD3- CD56+. (A) as well as CD107a geoMFI values (B) were lower when 300-LLT1 were used as targets compared to the unstransfected 300 (*<0.05, non-parametric unpaired T-test). Representative FACS plot of NK cell degranulation (C) (n=6). MHC-class I-deficient 221 cells were used as a positive control for NK cell degranulation.

4.4.5 LLT1 is upregulated in the liver under inflammatory conditions

Although the liver is not generally regarded as an immune-privileged site, it is widely accepted that the hepatic environment is unique when it comes to balancing immune responses and tolerance. The permanent presence of harmless food and microbial antigens, together with potential pathogens, constitutes a big challenge for this essential metabolic organ. I detected expression of LLT1 in the liver (Figure 4-3 and Table 4-1). Interestingly, this organ contains abundant NK and MAIT cells, both expressing high levels of CD161 receptor, the ligand for LLT1 (Lanier et al. 1994, Martin et al. 2009, Fergusson et al. 2014). I wanted to investigate changes on LLT1 expression under hepatic inflammatory conditions. In order to do so, I stimulated HepG2 and Huh7 hepatocyte-derived cell lines with a variety of TLR agonists. The TLR3 agonist Poly(I:C), a synthetic analog of double-stranded RNA commonly associated with viral infection, as well as the TLR7 agonist imiquinod, a guanosine analog with strong antiviral activity, were the two stimuli that had a higher impact on LLT1 upregulation (Figure 4-7A). I next titrated Poly(I:C) on three different hepatocyte-derived cell lines (Huh7, HHL12 and HepG2) and measured LLT1 expression. I observed a striking increase on expression of LLT1 on Huh7 and HHL12 cells, which was dose-dependent, these effects being more modest in HepG2 cells (Figure 4-7B). The HHL12 cell line is the only one which is not derived from hepatocellular carcinoma, thus being more 'hepatocyte-like' (Clayton et al. 2005). Overall, this data suggests that LLT1 is

upregulated in hepatocytes upon inflammatory conditions and, potentially, in the context of viral infection.

I next assessed levels of LLT1 expression by IHC, both in healthy and inflamed liver. Increased expression of this C-type lectin in hepatocytes could be observed in all the different inflammatory conditions tested, thus suggesting that LLT1 expression is enhanced in hepatocytes upon inflammation, but that might not be particularly linked to viral infection (Figure 4-7C). Notice the presence of LLT1 expressing lymphocytes in the Hepatitis C infected liver sections, although they require further characterisation. Overall, my data suggests that LLT1 is upregulated in the liver during inflammation.

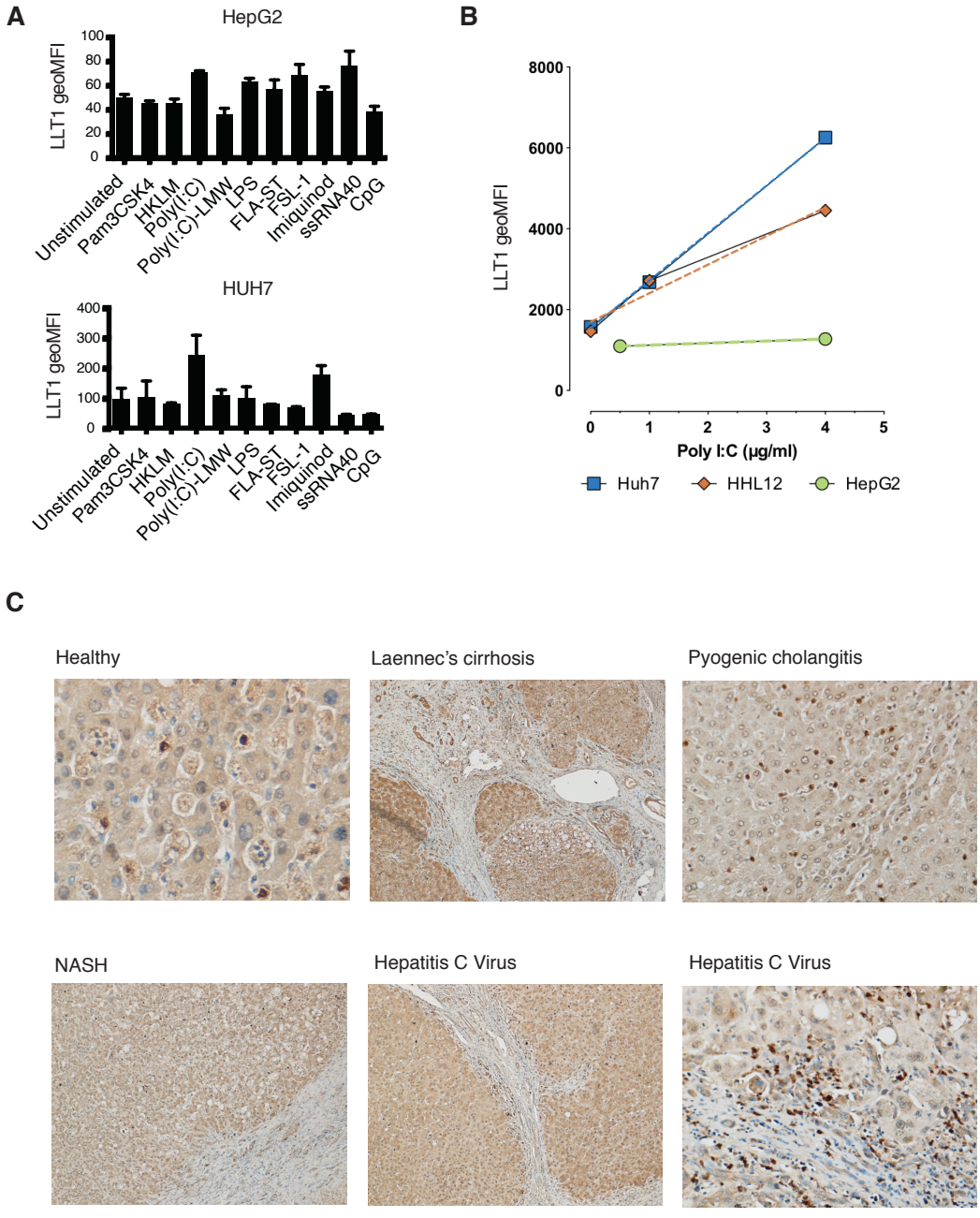


Figure 4-7. LLT1 is upregulated in the liver under inflammatory conditions. (A) shows changes in LLT1 geoMFI in HepG2 and HUH7 cell lines with TLR agonist stimulation (n=2). The 2H7 mAb was used. (B) shows a titration of poly(I:C) induced expression of LLT1 in hepatocyte-derived cell lines. (n=2). The goat polyclonal antibody was used together with a secondary QDot605-conjugated (Invitrogen). (C) shows LLT1 stainings using the 2H7 anti-LLT1 antibody on human liver from different inflammatory conditions (n=3). Nonalcoholic steatohepatitis (NASH).

4.5 Discussion

LLT1 was first described on NK, T and B cells (Boles et al. 1999), although some subsequent studies showed different results. I showed LLT1 expression on circulating B cells and monocytes (Figure 4-1), confirming the results obtained in previous research (Mathew et al. 2004). It is important to notice that the current literature still presents inconsistencies regarding LLT1 distribution on PBMCs (see Table 1-1), which could be due to the use of different antibodies as well as the diverse activation state of the cells tested (Mathew et al. 2004; Rosen et al. 2008; Germain et al. 2011). The fact that LLT1 and CD161 are expressed in distinct cell subsets gives this pair of C-type lectins a potential role in cross-talk between different type of lymphocytes and between lymphocytes and monocytes. This is indeed the case for another well-described C-type lectin receptor-ligand pair (ie. NKp80-AICL). NKp80 and AICL are expressed on NK cells and monocytes, respectively, and their interaction causes mutual activation (Welte et al. 2006). It would be interesting to see whether CD161 and LLT1 also modulate this same interaction, as they are also expressed on NK cells and monocytes respectively, and to explore potential new ones (e.g. B cells – MAIT cells).

Treatment of THP-1 cells with a wide range of TLR agonists and cytokines had different effects on LLT1 surface levels, suggesting that its regulation might be stimuli-specific, rather than a general activation marker (Figure 4-2). PMA-stimulated THP-1 cells downregulated LLT1, suggesting that expression of this C-type lectin decreases during macrophage differentiation. This hypothesis was supported by the absence of LLT1 in tissue-resident

macrophages of lung and liver tissues. However, LLT1 has been shown in joint-resident macrophages of RA patients (Chalan et al. 2015). These results could be explained by the state of activation of such macrophages, suggesting an increase of LLT1 expression under inflammatory conditions, as I showed in the context of the liver (Figure 4-7).

I screened a whole variety of human healthy tissues for LLT1 and found it present in various sites such as the bladder, the lung epithelia and the digestive tract (Table 4-1 and Figure 4-4). However, its expression was particularly high in immune-privileged sites such as the placenta, the brain and the testes.

This wide screening was performed using commercial tissue arrays (see *4.3.2 Tissues*) and this approach presents some limitations. Firstly, the particular tissue sample available for staining is small and may not offer an accurate representation of the overall tissue. The spleen sample clearly illustrates this point, as very little LLT1 could be detected (there were no GCs on the sample; see Appendix 1). Furthermore, it is not possible to do a tissue-dependent optimisation, producing a compromise that might be far from ideal for some tissues. The overall process gets further complicated by the fact that assessing of immunohistochemical stainings is qualitative rather than quantitative (See *7.4.1 LLT1 distribution*, within *7.4 Limitations and future directions*).

Within the tissue array samples, the 2H7 mAb was the antibody that gave the best staining, giving a similar pattern to the goat polyclonal. In contrast, LLT1

could not be detected in any of the tissues using the 7G7 clone. These results do no fit with my initial immunohistochemical optimisation (see Chapter 3). As discussed in Chapter 3, the processing of the tissue sample, particularly the fixation and the antigen retrieval processes, can profoundly impact the nature of the epitopes and, consequently, antibody recognition (Appendix 1). It is tempting to speculate that the fixation method used for the tissue arrays was different from the one used to fix the tonsils in which I performed the optimisation process (overnight with 37% formaldehyde at RT). Overall, I observed that the origin of the sample has major implications for the detection of a particular protein, both because of its processing procedure as well as the particular section available for staining (Appendix 1).

A comparison of my results with these in the Human Protein Atlas led me to conclude that, although there was a common general trend, there were some meaningful differences. A good example is that of GC B cells, which I identified as strongly positive for LLT1, while the Human Protein Atlas attributes them a medium level of LLT1 expression (The Human Protein atlas, 2008). Once again, processing of samples and use of different antibodies (an anti-LLT1 rabbit polyclonal) could explain such differences.

LLT1 staining was particularly strong in immune-privileged sites. Privilege is synonymous of advantage, a form of exemption. Immune-privilege refers to the attenuation or prevention of normal immune responses that could damage vital organs. The definition of immune-privilege has evolved since it was first described. Today, it is perceived as a phenomenon that shares various features with peripheral tolerance (Forrester et al. 2008). However, while the

former is a tissue-specific mechanism designed to allow certain degree of immune response to occur while preventing collateral damage, the latter is based on self versus non-self discrimination, together with absence of reactivity to self-antigens.

Peter Medawar postulated the concept of a blood-tissue barrier as the main mechanism responsible for immune-privilege (Medawar 1961; Medawar 1948). For decades, however, this concept has been challenged, revised and updated. Different studies have shown that peripheral immune cells can penetrate the Central nervous system (CNS) (Weller et al. 1996; Flugel et al. 2001) as well as the blood-retinal barrier (Xu et al. 2003; Xu et al. 2005). More recently, the structure and function of a brain lymphatic drainage system has been characterised (Louveau et al. 2015). Thus, the presence of effector immune cells in the brain is today largely accepted, and particular roles for certain immune cell types have been described, such as the one of CNS-resident NK cells in suppressing Th17 responses and CNS autoimmune pathology (Hao et al. 2010).

The notion of immune-privilege has progressively become more flexible and extensive. Studies in animal models showed that privilege, or at least an altered immune response (immune deviation) was transferable to different sites in an antigen-specific manner, after inoculation of the antigen into a privileged site (e.g. eye or brain; (Galea et al. 2007; Wenkel et al. 2000). Therefore, the quality of immune-privilege can be generated in non-privileged sites and it is a property of the tissue itself.

Together with the eye and the brain, the feto-maternal interface of the placenta is another striking example of immune-privilege, as the body must be able to avoid immune rejection of the fetus, a non-self entity. Both T and NK cells have been described to be involved in interacting with the trophoblast (Kanellopolos-Langerin et al. 2003). Another well-described immune-privileged site is the testes, which host the process of spermatogenesis. Here, abundant and novel autoantigens are generated and immune responses must be tightly regulated (Hedger 2012). The presence of different leukocyte populations has been shown in rodent (Hedger 1997) and human testes, including macrophages and T cells (Pollanen & Niemy 1987; Frungieri et al. 2002).

The mechanisms underlying immune-privilege have been the focus of numerous studies. From physical barriers with strict permeability (Matter & Balda 2003) to antigen sequestration, aberrant lymphatics, limited immune cell access or the presence of particular molecules such as FasL or TRAIL have been described (Ferguson et al. 1997). It is now believed that even the most immunoreactive tissues can be turned into relatively unresponsive ones, a process in which Treg cells would play a prominent role (Yates et al. 2007). However, most of these mechanisms have only been partially characterised. LLT1 arises as a potential molecule involved in immune regulation. Its particular high expression in immune-privileged sites such as brain, placenta and testes (Figure 4-3 and Table 4-1) makes it a good candidate for attenuating both T and NK cell responses, the CD161 expressing lymphocyte populations.

LLT1 expression levels in the GI tract were moderate (Figure 4-3 and Table 4-1). The digestive tract is often included as a tissue with the ability to express immune-privilege due to its need to avoid inappropriate immune responses to the gut flora and dietary antigens (Forrester et al. 2008). Along these lines, Zhou and colleagues showed that the C-type lectin SIGNR-1 expressed on DCs helps promoting oral tolerance (Zhou et al. 2010).

Recently, immune-privilege is starting to be understood as a flexible and even inducible quality. According to this novel notion, what happens in the liver under inflammatory conditions could serve as a good example, although its normal immune status is already unique. Hepatocytes express low levels of MHC class I and are normally hidden behind liver sinusoidal endothelial cells (LSECs). However, during infection, lymphocytes infiltrate into the hepatocyte areas. Upregulation of LLT1 in these particular circumstances (Figure 4-7) could help attenuating NK cells responses, thus exerting a protective function, dampening immune responses and conferring a privileged status.

Overall, the concept of immune-privilege has become relative, context-dependent and tissue-specific. LLT1 could play a role in facilitating this singular immune status.

Amongst the different immune-privileged sites, the brain arises as a particularly interesting one when considered in the context of LLT1. I described strong expression of this C-type lectin in neurons (Figure 4-3 and Table 4-1). However, not only Clr-b is absent in mouse brain, but also there is a general lack of *Clr/Nkrp1* transcript expression in this organ (Zhou et al.

2001; Carlyle et al. 2004; Zhang et al. 2012). This is a remarkable fact, considering the ubiquitous expression of Clr-b in the mouse, which contrast with other tissue-specific Clrs, such as Clr-d in the eye or Clr-f in liver, kidney and intestine (Zhou et al. 2002; Zhang et al. 2012).

Interestingly, a novel brain-associated C-type lectin (BACL) has been recently described (Lysenko et al. 2013). It is an orphan receptor and its expression is restricted to brain tissue, conserved amongst mammals and located outside the NKC, in human chromosome 7 and mouse chromosome 6. Expression in neurons and particularly pronounced expression by Purkinje cells has been characterised. Such pattern matches the one I observed when staining for LLT1 in the CNS (Figure 4-3 and Table 4-1). It would be important to test possible cross-reactivity between the anti-LLT1 antibodies used and BACL-expressing cells to ensure that our antibodies specifically recognise LLT1.

There are obvious differences between the mouse and human systems regarding C-type lectin expression patterns. However, in all of them, this big group of animal lectins plays an important role in immune regulation, tolerance and immune-privilege. Elucidating the intricacies of each receptor-ligand pair on each particular host will majorly contribute to our overall understanding of immune responses, as well as providing a platform for intervention and treatment of conditions such as allergies and autoimmunity.

I have shown that LLT1 is upregulated in the liver in the context of inflammation (Figure 4-7). The enhanced expression of this C-type lectin has been shown in the joints of RA patients, in the context of viral infection and in

hepatocellular carcinomas (Rosen et al. 2008; Germain et al. 2011; Satkunanathan et al. 2014). My data suggest an important role for LLT1 in the context of hepatic inflammation, which becomes particularly relevant when considering the abundance of CD161 expressing cells NK and MAIT cells (Billerbeck et al. 2010; Ussher et al. 2014) within the liver. While the inhibitory effects of LLT1 on NK cell function have been widely described, its effects on CD161+ T cells still remains unclear, with conflicting evidence suggesting both activation (Exley et al. 1998; Aldemir et al. 2005; Fergusson et al. 2014) and inhibition (Rosen et al. 2008) available. Nonetheless, the fact that LLT1 is upregulated under inflammatory conditions in the liver and the broad presence of its ligand CD161 suggests a key role for these C-type lectin-like pair in modulating hepatic immune responses.

4.6 Summary

- LLT1 is expressed on circulating B cells and monocytes, but not in tissue-resident macrophages from lung and liver
- LLT1 is expressed on various healthy human tissues
- LLT1 is strongly expressed in human immune-privileged sites
- LLT1 expression is increased in the liver under inflammatory conditions and might change under malignant transformation, depending on tissue
- LLT1 inhibits NK cell degranulation

5 Expression and regulation of LLT1 on B cells

5.1 Introduction

The GC reaction is critical for long-lasting protection against pathogens. GCs are the anatomical sites within secondary lymphoid organs where B cells proliferate and mutate their BCRs to be selected according to their affinity for antigen. Two distinct areas with different functions can be identified within the GC; these are the DZ where B cells are characterised by being $CD83^{low}$ $CXCR4^{high}$, and the LZ where B cells are $CD83^{high}$ $CXCR4^{low}$ (Victora et al. 2010). In the former, B cells proliferate and hypermutate their BCRs to generate antibody variation. The quality of these BCRs is then assessed in the latter, ultimately leading to selection of high affinity B cell clones (Nieuwenhuis & Opstelten 1984; Victora et al. 2012). FDCs as well as Tfh play an essential role in this selection process based on the affinity of B cells for antigen. In this extremely competitive environment, B cells must fight for survival and selected clones will exit the GC expressing high affinity antibodies and long-lived memory. Thus, this process is exploited by current vaccine design. At the same time, however, as a site of mutation and proliferation, aberrant reactions can lead to the development of many B cell lymphomas and autoimmunity. Understanding the mechanisms that drive this process will have far reaching implications in human health care.

It is estimated that about 95% of human lymphomas are of B-cell origin and the vast majority of these are GC-derived (Küppers 2005; Basso & Dalla-

Favera 2015). During the last few decades, the diagnosis of different B cell lymphomas has notably changed, mainly due to the emergence of novel immune-phenotypical markers and molecular subtype classification schemes. Accurate diagnosis is important to provide the most suitable treatment for a particular lymphoma type. The heterogeneity within B cell lymphomas is high and, despite recent advances, there is still the need for new biomarkers, useful for diagnostic, prognostic and therapeutic considerations.

It has recently been acknowledged that survival and proliferation of certain B cell lymphomas is dependent on their interaction with surrounding cells, as well as BCR expression and antigen activation levels (Küppers 2005). Thus, a detailed understanding of the orchestrated response within the GC could provide invaluable insight into B cell lymphomas. The GC is a unique immunological site, small and highly dynamic, which enables a wide range of interactions between different cell types as well as their movement, within a confined space (Victora et al. 2012). B cells, T cells, FDCs and TBMs are the main constituents of this microenvironment. Close and abundant interactions occur amongst them, both at a surface cellular level and in terms of soluble mediators. For instance, stromal cells are responsible for secretion of CXCL12 and CXCL13 in the dark and light zones, respectively (Gunn 1998; Rodda et al. 2015). This is essential for the functional segregation of the GC, which is mediated by expression of the chemokine receptors CXCR4 and CXCR5 (Allen et al. 2004), the ligands for CXCL12 and CXCL13, respectively. Overall, cellular interactions and soluble factors impact the locasilation and function of GC-resident cells, ensuring a successful reaction, with ultimate

production of high affinity B cell clones which provide the best potential for protection.

One of the main outcomes of the GC reaction is the generation of antibody-producing plasmablasts and plasma cells, which confer long-lasting immunity. This mechanism has been exploited for vaccine design but its intricacies still present some unresolved questions. Whereas BLIMP-1 has been characterised as the master regulator of plasma cell differentiation (Turner et al. 1994, Kallies et al. 2004), the multiple paths in which plasmablasts can develop and their full differentiation process is not yet fully understood.

5.2 Aims

At this point, I had broadly characterised the distribution of LLT1 in healthy human tissues. When optimising the tools for the study of LLT1, I described the expression of this C-type lectin in GCs. Therefore, my next aim was to study the phenotype of LLT1+ cells and its regulation in the particular context of the GC. The work performed in this chapter allowed the following questions to be addressed:

- Where is LLT1 expressed in the GC context?
- Which are the B cell subsets expressing the highest levels of LLT1?
- How is LLT1 regulated?

5.3 Materials and Methods

Specific materials and methods for this chapter are detailed below. All other methods and reagents are described in Chapter 2.

5.3.1 Cells, cell lines and tissues

5.3.1.1 Lymphoma samples

The lymphoma samples analysed were in the form of 0.6-1 mm core tissue-arrays and were obtained from the files of the Department of Cellular Pathology (University College London Hospital, UK). They included representative tumour cell-rich areas of lymphoma entities or whole tissue sections. The diagnosis of all haematological neoplasms was based on the criteria of the World Health Organisation (WHO) classification. Approval for this study was obtained from the National Research Ethics Service, Research Ethics Committee 4 (REC Reference number 09/H0715/64). The lymphoma cell lines were a kind gift from Dr. Teresa Marafioti (University College London Hospital, UK): FL18 (from follicular lymphoma, carrying a 14:18 translocation), KHM2 (from EBV-derived Hodgkin lymphoma), LH21 (from B-NHL), Namalwa (from Burkitt's lymphoma) and SUDH26 (from follicular B cell lymphoma).

5.3.1.2 Vaccine samples

Vaccine samples from clinical trials were obtained through the Oxford Vaccine Group (Churchill Hospital, Oxford, United Kingdom). Flu samples were obtained from lab members one week post-vaccination during the flu season.

Whole blood stainings from healthy and vaccinated individuals were performed. 400 μl of blood were incubated with Red Blood Cell Lysis Buffer (10x) (BioLegend) for 10 min at RT. Cells were washed twice with PBS and surface stained.

5.3.1.3 Bone marrow

Bone marrow samples were obtained from hip joint. Samples were filtered (40 μm), washed with PBS and homogenised with a sterile 10ml syringe plunger. They were then centrifuged for 10 min at 1500 rpm, isolated on a Lymphoprep gradient (Axis Shield Diagnostics), washed with PBS, aliquoted in FCS + 10% DMSO (Sigma Aldrich) and stored in liquid nitrogen until required. Alternatively, they were fixed with formaldehyde overnight prior to paraffin embedding.

5.3.2 Immunohistochemistry

For the triple staining in Figure 5-1B, the goat polyclonal anti-LLT1 antibody (AF3480, R&D Systems) was used for immunohistological staining, as well as CD3 (clone LN10, Leica Microsystems) and PAX-5 (clone 24, BD Biosciences).

For the FDC, CD3 and CD161 immunofluorescent costainings in Figure 11 and Figure 12, frozen tonsils were used. Four different anti-CD161 antibody clones were used, as well as the CD3, FDC markers and the fluorescein labelled anti-Peanut agglutinin (PNA, Vector Laboratories).

5.3.3 B cell purification

B cells were purified, either from PBMCs or tonsils, using the EasySep™ Human B Cell Enrichment Kit (StemCell Technologies). Cell suspensions were prepared at a concentration of 5 x 10^7 cell/ml in R10 in a 5ml tube. 50 μl/ml of the EasySep™ Human B Cell Enrichment Cocktail was added, mixed and incubated at RT for 10 min. The EasySep™ D Magnetic Particles were vortexed and added at 75 μl/ml, mixed and incubated at RT for 5 min. The cell suspension was brought to a total volume of 2.5 ml and placed in the Purple EasySep™ Magnet, where it was kept for 5 min. In one continuous motion, the magnet was inverted pouring the desired fraction containing the B cells in a new tube.

5.3.4 *In vitro* differentiation of plasma cells

Memory B cells were differentiated *in vitro* into plasmablasts and plasma cells, following the protocol described in Jourdan *et al.* (Jourdan et al. 2009).

CD27+ B cells were purified from PBMCs using the EasyStep™ Human Memory B cell Isolation Kit (StemCell Technologies), following manufacturer's instructions (see *5.3.3 B cell purification* as specified above followed by a positive CD27 selection). They were plated at 1.5 x 10^5 cells/ml and cultured for 4 days with CpG oligodeoxynucleotide 2006 (10 μg/ml; Invivogen), histidine tagged soluble recombinant human CD40L (50 ng/ml) and anti-poly-histidine mAb (5 μg/ml) (R&D Systems), IL-2 (20 U/ml; R&D Systems), IL-10 (50 ng/ml; Miltenyi Biotec) and IL-15 (10 ng/ml; Miltenyi Biotec).

At day 4 of culture, the cells were washed and cultured at 2.5 x 10^5 cells/ml with IL-2 (20 U/ml), IL-10 (50 ng/ml), IL-15 (10 ng/ml) and IL-6 (50ng/ml; Miltenyi Biotec).

At day 7 of culture, cells were washed and seeded with IL-6 (50 ng/ml), IL-15 (10 ng/ml) and IFN-α (500 U/ml; R&D Systems) for 3 days.

5.3.5 B cell stimulation (Regulation of LLT1)

B cells were isolated from PBMCs through negative magnetic selection using the EasySep™ Human B cell Enrichment Kit (StemCell Technologies). They were stimulated with CpG oligodeoxynucleotide 2006 (Human TLR9 ligand, Invivogen) at 37°C 5% CO_2, following manufacturer's instructions. For TLR signalling inhibition studies, the MyD88 inhibitory peptide Pepinh-MYD was added (Invivogen). Brefeldin A solution was used at 1/1000 (eBioscience). Purified B cells were stimulated for 48h at 37°C 5% CO_2 with the Human TLR1-9 Agonist Kit (Invivogen), following manufacturer's instructions. The following cytokines and small molecules were used at 50 ng/ml: IL-4 (PreproTech), IL-10, IL-15, IL-21, B-cell activating factor (BAFF) (Miltenyi Biotec) and Prostaglandin E2 (PGE_2). For BCR stimulation, goat anti-human IgM/G/A $F(ab')_2$ (Jackson ImmunoResearch) fragments were used (1 μg/ml). B cells were stimulated with human anti-CD40 (clone S2C6, Macbeth) at 5 μg/ml.

5.3.6 Proliferation assay

Proliferation assays were performed using CellTrace™ Violet (CTV) Cell Proliferation Kit (Life Technologies). Purified B cells were stained with 2.5 µM CTV for 10min at RT, following manufacturer's instructions. Cold R10 was then added to quench the reaction and cells were kept on ice for 5min, following which they were washed three times with R10, transferring them into new tubes at each wash. Before the last wash, the cells were kept at 37°C 5% CO_2 for 5min. Cells were then counted and 2 x 10^5 B cells were plated per well in a U-bottom 96-well plate with CpG (0.5 µg/ml) for 5 days. At the end of the assay, cells were washed and FACS stained.

5.4 Results

5.4.1 LLT1 is highly expressed on germinal centre B cells

LLT1 expression on B cells has previously been shown (Boles et al. 1999; Mathew et al. 2004; Rosen et al. 2005; Rosen et al. 2008; Germain et al. 2011; Germain et al. 2015). When optimising the tools for the study of LLT1, I analysed LLT1 expression of resident B cells in human tonsil tissue by immunohistological staining using a commercial goat polyclonal anti-LLT1 antibody and a novel (7G7) anti-LLT1 antibody (see Chapter 3). I observed that LLT1 was highly expressed on GCs (Figure 3-3). This finding could be reproduced in GCs from human spleen, lymph nodes and Peyer's patches, using both the goat polyclonal anti-LLT1 antibody (Figure 3-5) and the 7G7 mAb (Figure 3-6). I wanted to further characterise LLT1 expressing cells in the

GC (Figure 5-1A). In order to do so, double and triple immunostaining were performed to confirm that LLT1 positive GC cells were B cells as they co-expressed PAX-5 (Figure 5-1B), a fundamental transcription factor for B cell identity and function. We also observed that CD3-positive intra-GC T-cells appeared to be LLT1 negative.

CD20+ B cells constitute the main cell type within GCs, but they are also highly abundant in other areas of secondary lymphoid organs, as could be appreciated in Figure 5-1C. There was an extensive overlap between LLT1 and CD20 staining within the GC structure, confirming that LLT1 is strongly expressed in GC B cells. In concordance with previous stains (Figure 3-6A), the presence of LLT1-expressing cells outside the GC was observed. It is important to note that all the LLT1+ cells were negative for CD20.

As GC B cells, particularly the ones within the DZ, are characterised by being highly proliferative, I examined the expression of nuclear antigen Ki67 in the context of LLT1. Figure 5-3D shows how most Ki67-expressing cells within the GC present LLT1 on their surface.

Contrary to murine B cells (Vences-Catalán & Santos-Argumedo 2011), both human GC B cells and plasmablasts/plasma cells express high levels of CD38 (Lin et al. 2004). As can be observed in Figure 5-1E, not only was there an overlap between CD38 and LLT1 in the GCs, but also most LLT1+ cells outside them were positive for CD38; however, not all CD38 expressing cells stained for LLT1. Expression of LLT1 on GC tonsillar B cells was further confirmed by flow cytometry using a second novel anti-LLT1 antibody (clone

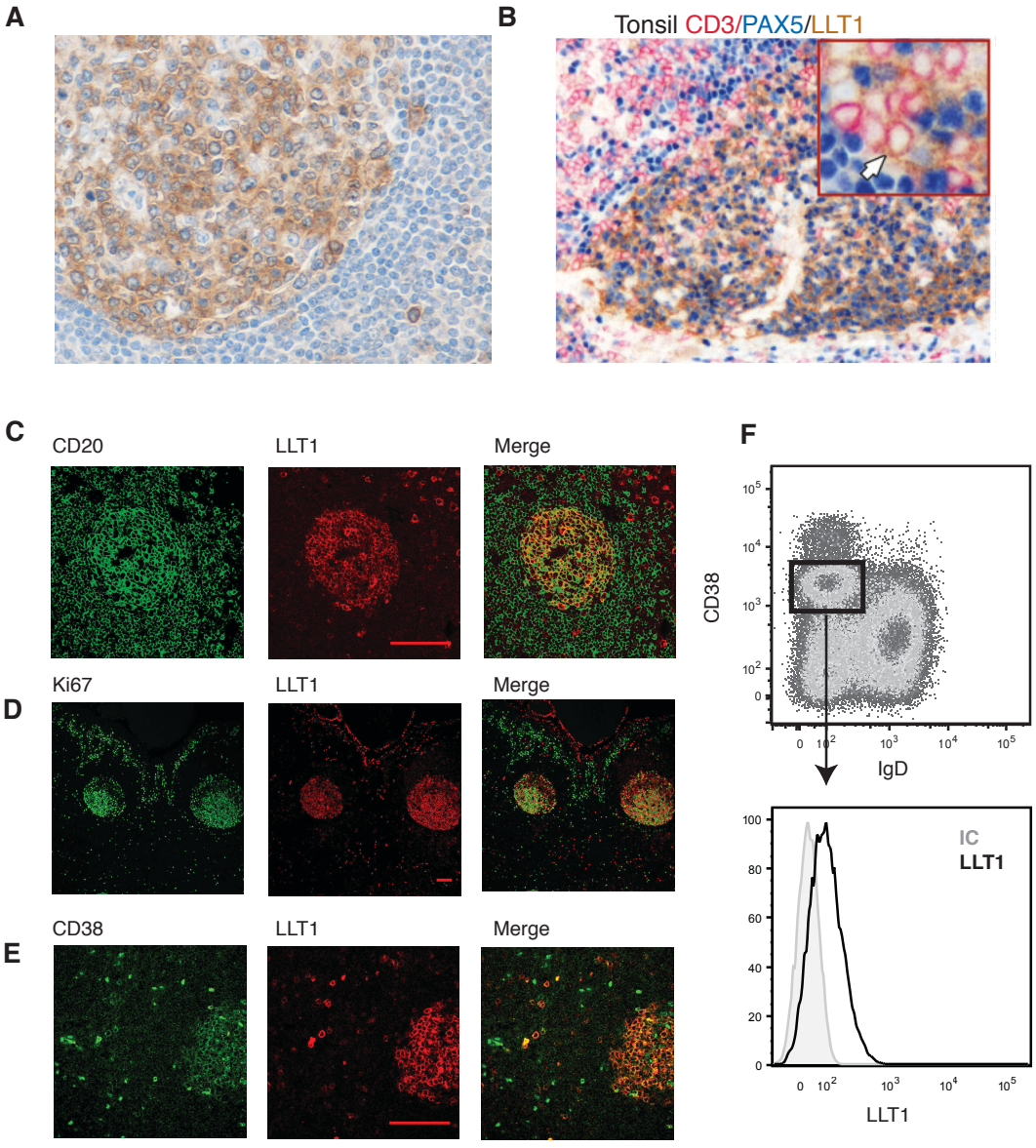


Figure 5-1. LLT1 is expressed on germinal centre B cells. (A) Expression of LLT1 (brown) was assessed (7G7 clone) in formalin-fixed paraffin-embedded (FFPE) human tonsillar tissue sections (x40) (n=5). (B) Triple staining for LLT1 (membrane and cytosol brown; polyclonal antibody AF3480), CD3 (membrane pink) and PAX-5 (nuclear blue) showed LLT1 (brown, polyclonal antibody) strongly associated with PAX-5 and only rarely with CD3 (arrow insert) (x20, insert x60). Immunohistological costaining of LLT1 with CD20 (C), Ki67 (D) and CD38 (E) (Scale bar = 100 µm) revealed LLT1 expression in proliferating tonsillar GC B cells (n=3). (F) FACS analysis (2H7 clone) confirmed LLT1 expression on germinal centre B cells, gated on live CD19+ IgD- CD38+ cells (representative plot of five independent experiments).

2H7, Figure 5-1F). GC B cells were identified by being $IgD^{-}CD38^{mid}$ (Pascual et al. 1994; Frazer et al. 1997; Liu & Banchereau 1997). Overall, the data suggest that GC B cells are positive for LLT1.

5.4.2 LLT1 expression is higher in the DZ than in the LZ

Within GCs, two distinct anatomical areas can be distinguished; these are the dark and light zones. I wanted to explore whether LLT1 expression levels differed on B cells from these two zones. Histological staining of LLT1 showed a non-homogenous distribution of LLT1 throughout the GC (Figure 5-2A). The pattern of staining resembled the one of dark and light zones, identifiable through markers such as Ki67 (Figure 5-1D) and CD3 (Figure 5-2B). Notice that in both cases, LLT1 expression seemed to be higher in the DZ than in the LZ, that is, weaker in the areas where CD3+ cells are more prevalent, and stronger where Ki67 is predominantly expressed. Crosssectional analysis through the light and dark zones showed increased LLT1 levels within the DZ compared to that seen within the LZ (Figure 5-2B).

Therefore, histologically, the results suggested that there was greater expression of LLT1 in the DZ than in the LZ. To confirm this, as well as to exclude the possibility of this observation being due to differences in cell density, I performed flow cytometric analysis of tonsillar-derived GC B cells. GC B cells were gated from purified tonsillar B cells (Appendix 2). DZ B cells can be identified as $CXCR4^{high}$ $CD83^{low}$, whereas their LZ counterparts are $CXCR4^{low}$ $CD83^{high}$. Gating on these two different populations and assessing

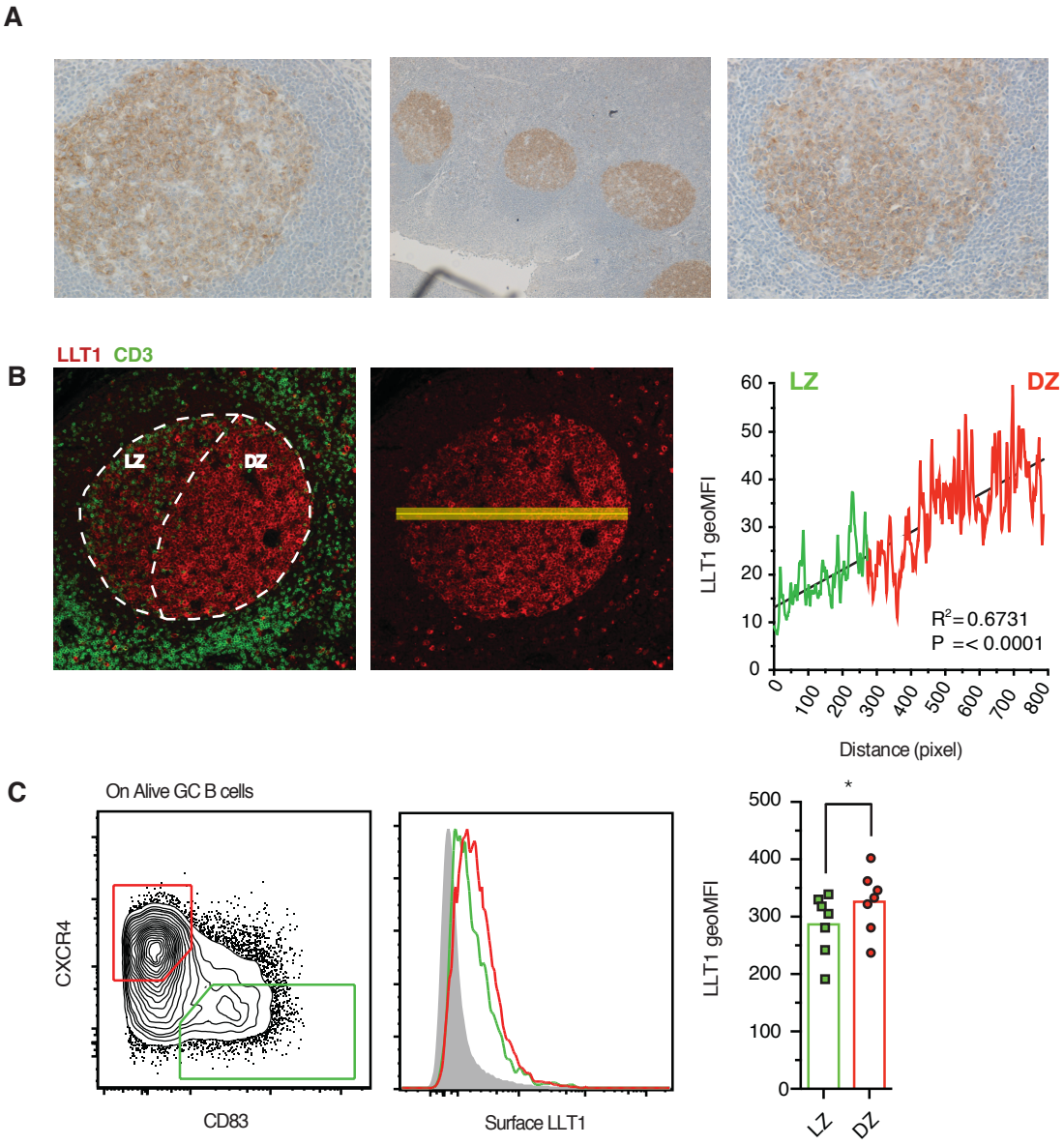


Figure 5-2. LLT1 expression is higher in the DZ than in the LZ. (A) Expression of LLT1 (brown) was assessed by immunohistochemistry (7G7 clone) in formalin-fixed paraffin-embedded (FFPE) human tonsillar tissue sections (x20, x10, x20) (n=10). (B) Cross-sectional analysis through a region (yellow band) of a representative germinal centre (n=3). Mean fluorescent intensity of LLT1 expression within the defined region is plotted against pixel count; the LZ (green) and DZ (red) regions are highlighted. (C) Flow cytometric analysis of LLT1 expression confirmed higher levels of LLT1 in the DZ (2H7 clone) compared to the LZ (Non-parametric unpaired T-test). Purified B cells gated on Alive IgD- CD38mid, then divided into LZ or DZ by CXCR4 and CD83 expression (n=7).

levels of LLT1, I concluded that expression of LLT1 was significantly higher in DZ B cells than in LZ B cells (Figure 5-2C).

5.4.3 LLT1 is expressed in human B cell lymphomas

As a site of mutation and proliferation, many B cell lymphomas are derived from the GC. Therefore, having established LLT1 expression on GC B cells *in vivo* under normal conditions, we next examined whether such linked expression was maintained in the context of neoplasia. We assessed LLT1 expression in five B cell lymphoma cell lines. FL18, KHM2, L421 and SUDHL6 were positive for LLT1, whereas Burkitt's lymphoma-derived Namalwa cells were negative (Figure 5-3A). Using a commercially available LLT1 antibody (goat polyclonal) LLT1 expression was evaluated in a series of lymphomas (Figure 5-3B, 3C and 3D). LLT1 was absent on non-GC derived lymphomas, such as plasma cell neoplasms. In contrast, LLT1 expression was seen on most Burkitt lymphomas (14/19; 73.68%), Follicular lymphomas (48/95; 51%) and also Hodgkin lymphomas (7/16; 44%). Subdivision of the follicular lymphomas revealed the highest association of LLT1 on atypical phenotypes that have been previously described: BCL-2 negative (59%) and BCL-2 and CD10 negative (62%) (Figure 5-3D lower left panel). Interestingly, LLT1 expression was mainly seen on lymphocyte predominant Hodgkin's lymphomas (LPHL) and on a small proportion of classical Hodgkin's lymphomas (cHL) (Figure 5-3D lower right panel). Our data suggests that

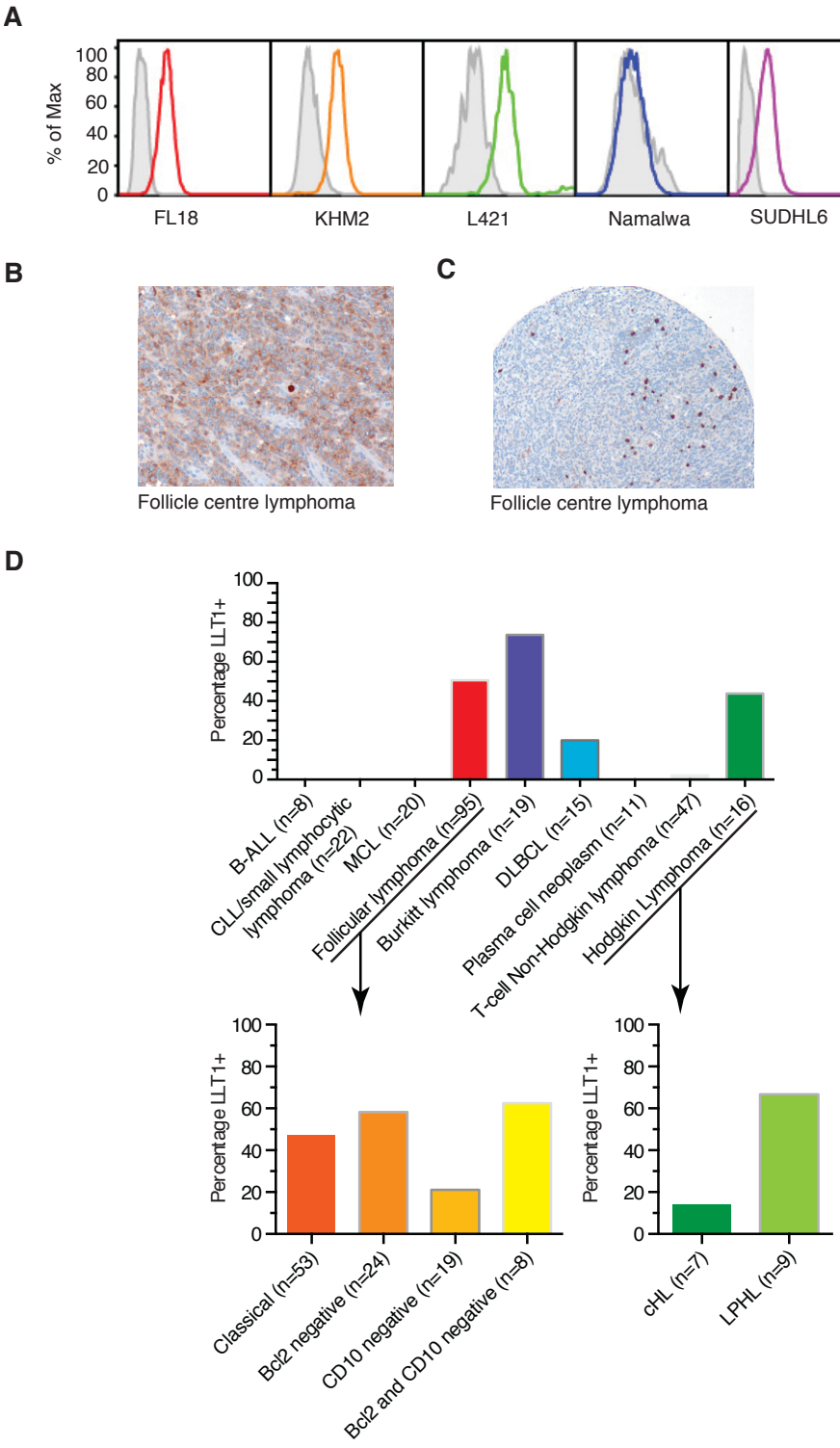


Figure 5-3. LLT1 is expressed in human B cell lymphomas. (A) Different B cell-derived lymphoma lines were positive for internal LLT1 expression (polyclonal antibody AF3480). (B and C) Representative staining of LLT1 (membrane and cytosol, brown) as assessed (polyclonal antibody AF3480) in FFPE tissue sections of follicular lymphoma samples. Two representative stainings out of 95 are shown (B x40 and C x10). (D) The percentage of LLT1+ lymphomas was assessed by immunohistochemistry using the goat polyclonal AF3480 antibody in different B cell Non-Hodgkin lymphomas, T-cell Non-Hodgkin lymphomas and Hodgkin lymphomas.

LLT1 is maintained during malignant transformation in most GC-derived lymphomas and may be a useful additional diagnostic marker.

5.4.4 LLT1 is not expressed on FDCs or TBM, and very rarely on T cells and neutrophils

Immunohistochemical stainings of human secondary lymphoid organs showed expression of LLT1 in GC B cells, but LLT1+ cells outside of these microanatomical structures could also be detected (Figure 5-1). In an attempt to identify them, I started by performing LLT1 costainings with markers of the main cell types present in these immunological sites, other than B cells. These are T cells, TBMs and FDCs.

T cell help to B cells is an essential event in adaptive immune responses. Different types of T cells can be found in distinct anatomical areas of secondary lymphoid organs, where they perform particular functions such as interaction with DCs for priming or selection of hypermutated B cells that display high affinity antibodies (Ma et al. 2012). The distribution of T cells in the GC environment can be appreciated in Figure 5-4. Staining of CD3 allowed a clear distinction of the T cell zone, together with a subset of T cells located inside the GC and mainly confined to its LZ. As could be observed, most T cells in this context were negative for LLT1, with only sporadic presence of double positive cells.

The role of FDCs as sources of antigen for B cells and their involvement in selection of high affinity BCRs is widely accepted (Park & Choi 2005; Wang et

al. 2011). The FDC network within human GCs could be nicely visualised in tonsillar tissue (Figure 5-4). There was no overlapping of LLT1 with FDC staining, thus suggesting that FDCs do not express LLT1.

TBMs are responsible for the uptake of apoptotic cells within GCs (Smith et al. 1998) and they can be detected through CD68 staining. Figure 5-4 showed their abundance and distribution throughout the GC. No double positive cells could be detected, indicating that TBMs are negative for LLT1.

Although neutrophils are not highly present in secondary lymphoid organs, their potential role in GC responses has been addressed (Harwood et al. 2012; Maletto et al. 2006). Costaining of LLT1 with cathepsin G showed the presence of a limited number of neutrophils in human secondary lymphoid organs, the majority of which were negative for LLT1 (Figure 5-4). However, some occasional double positives could be observed.

Therefore, GC B cells were the dominant cell type positive for LLT1 within tonsillar tissue, although occasional presence of T cells and neutrophils positive for this C-type lectin was also detectable. All macrophages and FDCs were negative for LLT1 staining.

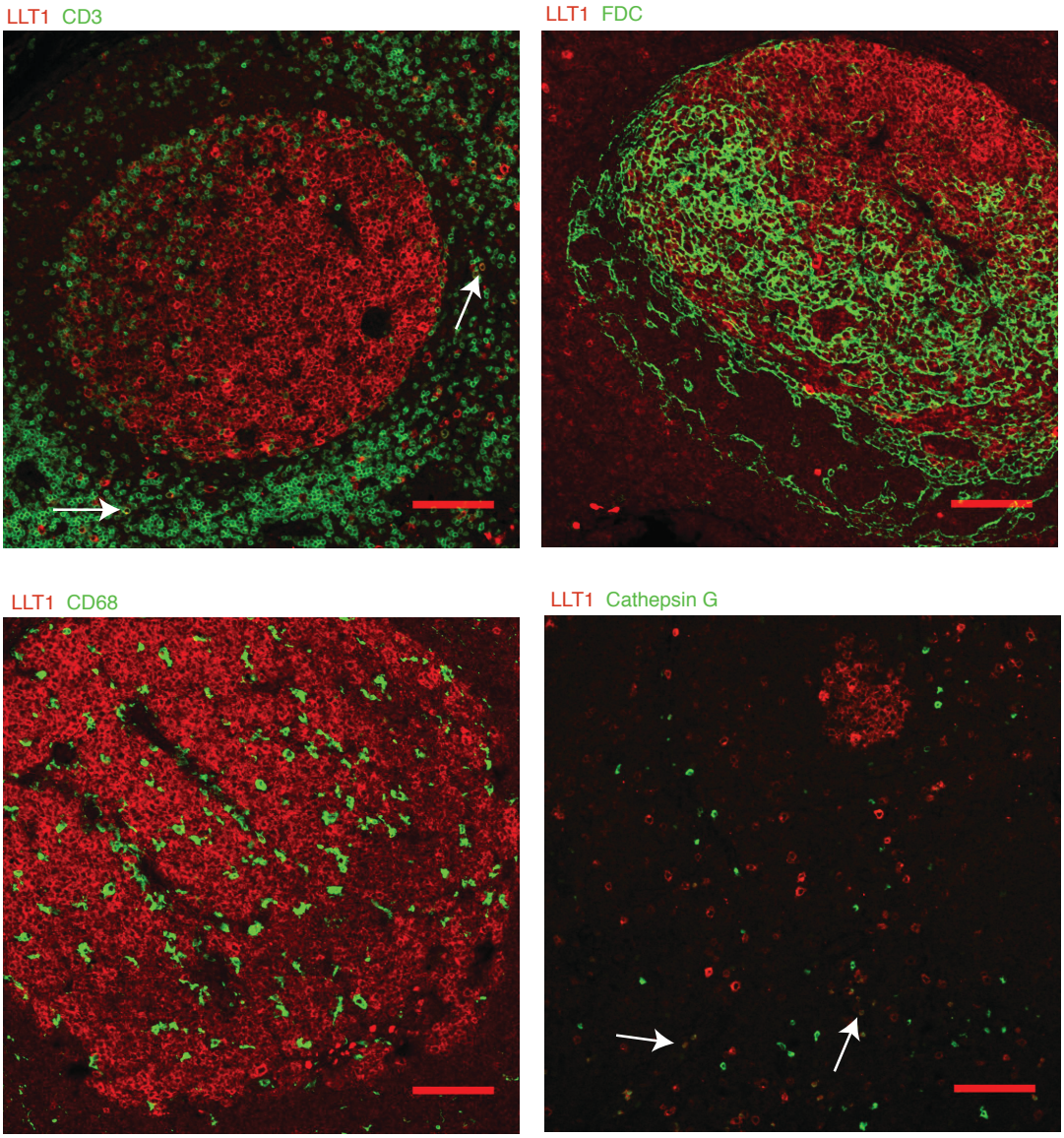


Figure 5-4. LLT1 is not expressed on most T cells, neutrophils, TBMs or FDCs. Expression of LLT1 (red; goat polyclonal antibody AF3480) in FFPE tonsillar tissue sections did not overlap with CD68 (10x) or FDC markers (10x) (green) at all. However, there were occasional overlaps between LLT1 and CD3 and LLT1 and Cathepsin G. Representative images of one experiment out of three are shown. White arrows pointing to double positives. Scale bar = 100 µm.

5.4.5 LLT1 is expressed on plasmablasts

In a further attempt to identify and characterise the LLT1-expressing cells outside the GC, I costained sections of human tonsils for LLT1 with CD19, CD20, CD38, CD45, CD79α, CD138, IRF-4/MUM-1 and immunoglobulins (Figure 5-5A, Appendix 3).

The presence of LLT1+ CD20- cells could be detected outside the GC (Figure 5-5A). As has been described in the literature, GC B cells are both positive for CD19 and CD45. In that context, both markers nicely overlapped with LLT1. However, positive cells for LLT1 located outside GCs presented low levels of both CD19 and CD45 expression.

Interestingly, CD79α expression was predominantly exclusive from that of LLT1 (Figure 5-5A, Appendix 3). These markers negatively correlated, indicating that B cells expressing high levels of CD79α expressed low levels of LLT1, and vice versa. This was true for both B cells inside and outside the GC. CD79α is highly expressed in the terminal stage of plasma cells, as it is CD38 (Tanaka et al. 2009; Harada et al. 2015). As shown previously in Figure 5-1E, and in contrast with CD79α, there was abundant overlapping between CD38 and LLT1 markers outside the GC.

Terminally differentiated plasma cells express transmembrane proteoglycan CD138 (Wijdenes et al. 1996). When costained with LLT1, double positive cells could not be detected (Figure 5-5A). These results suggest that plasmablasts express LLT1 and lose it as they further differentiate into plasma cells.

I next decided to explore whether there was a correlation between LLT1 expression and the different immunoglobulin types (Figure 5-5A, Appendix 3). IgD positive B cells were found only outside the GC, indicating the presence of naïve B cells in this area, within the mantle zone. This was further confirmed by IgM staining. However, in this case, IgM+ cells could also be detected inside the GC. Similarly, IgG positive cells were detected inside the GCs, but not outside. The same results were obtained when costainigs with IgA and IgE were performed, although their presence was much more limited.

LLT1 costaining with the different Igs (G,A,E) revealed strong co-expression on cells outside of the GC, but not on cells within it (Figure 5-5A).

I next examined the expression of Ki67 and IRF-4 in the context of LLT1. Figure 5-5A shows how most Ki67 expressing cells within the GC were also positive for LLT1. However, single cell staining for either marker could also be detected. Interestingly, there were numerous double positives outside the GC, thus indicating LLT1 expression in proliferating cells.

The transcription factor IRF-4 or MUM-1 is commonly expressed in a subset of GC B cells from the LZ, as well as in plasmablasts and plasma cells and activated T cells. Here, I showed abundant coexpression of IRF-4 with LLT1, both inside and outside the GC (Figure 5-5A). Notice that, once again, both markers were also found expressed independently.

Analysis of LLT1 expressing cells outside the GC suggested a phenotype typical of plasmablasts ($CD20^-$, $CD19^{low}$, $CD45^{low}$, $CD38^{high}$, $CD138^-$ Ig^+,

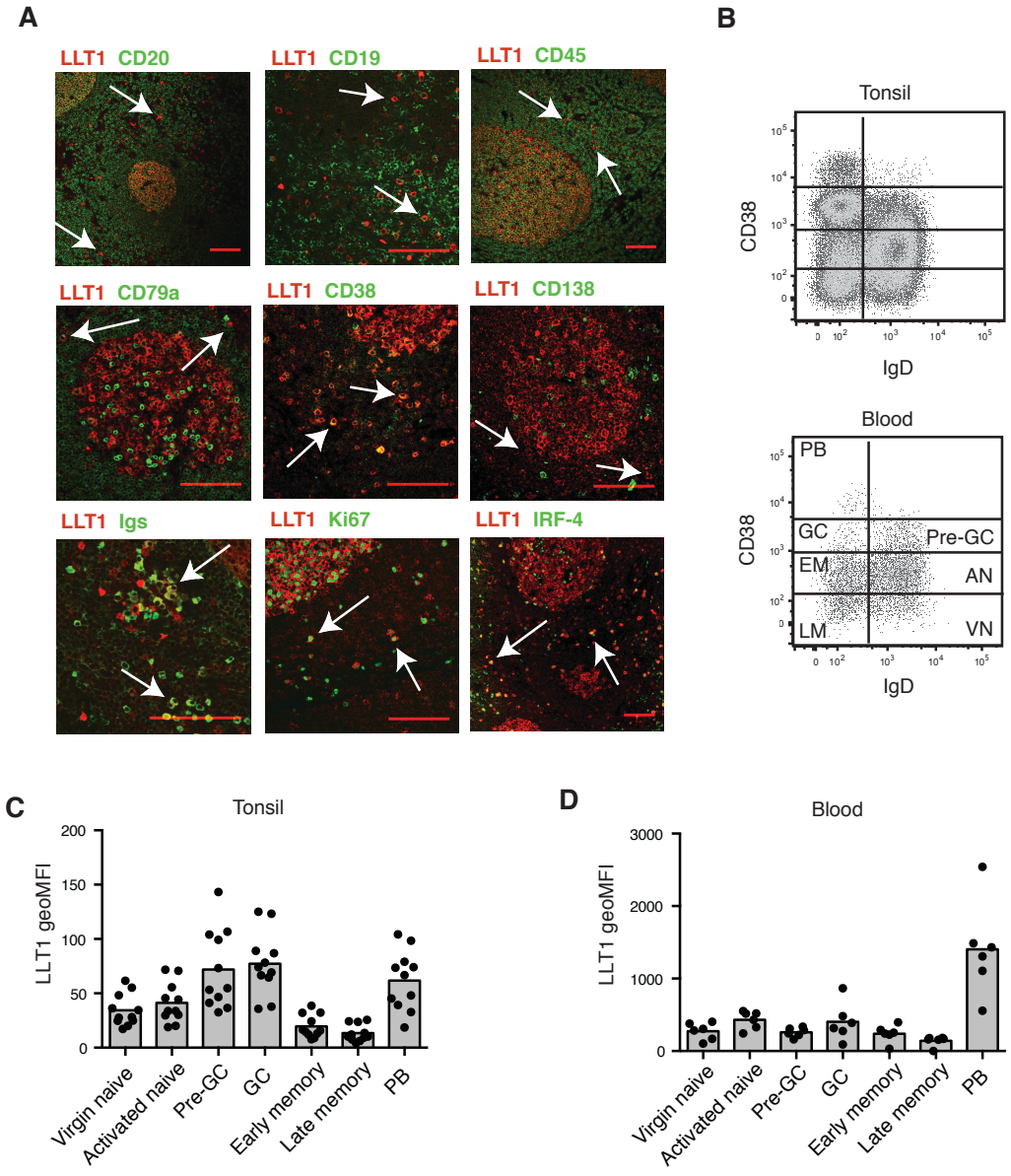


Figure 5-5. LLT1 is expressed on plasmablasts. (A) Costainings in FFPE human tonsillar tissue of LLT1 (goat polyclonal antibody AF3480) with different cellular markers revealed LLT1+ cells outside the germinal centres (pointed out with white arrows; scale bar = 100 µm) . They were negative for CD20 (x10) and CD138 (x20), low for CD19 (x20), CD45 (x10) and CD79a (x20) and mostly positive for CD38 (x20), Igs (20x), Ki67 (20x) and IRF-4 (10x). Representative plots of 3 independent experiments. (B) LLT1 expression was analysed in seven different B cell subsets using flow cytomery, both in tonsillar tissue and blood: Virgin naïve (VN), activated naïve (AN), Pre-germinal centre (Pre-GC), germinal centre (GC), early memory (EM), late memory (LM) and plasmablasts (PB). LLT1 geoMFI was measured in the different B cell populations (2H7 clone) in samples from tonsils (C; n=10) and blood (D, n=3) .

Ki67$^+$, IRF-4$^+$), although there remained a number of LLT1+ cells that did not fit this phenotype and still need to be identified. To further explore this possibility, I measured levels of LLT1 in different B cell subsets from both human tonsils and blood using flow cytometry.

In secondary lymphoid organs as well as in PBMCs, expression of CD38 and IgD has been used to identify different subsets of B cells, giving rise to what is known as the Bm1-Bm5 classification (Pascual et al. 1994, Frazer et al. 1997, Liu & Arpin 1997). Seven B cell subpopulations can then be distinguished: virgin naïve, activated naïve, pre-GC, GC, early memory, late memory and plasmablasts. The prevalence of each subset varies according to tissue, as illustrated in Figure 5-5B, where the seven B cell subpopulations were identified in samples from tonsils and PBMCs.

LLT1 expression levels were measured on each subset by flow cytometric analysis. In tonsillar tissue, pre and GC B cells as well as plasmablasts were the subgroups with higher expression of LLT1 (Figure 5-5C), thus matching the results obtained through immunofluorescence. The seven B cell subsets were further characterised using flow cytometry, and the expression of both surface markers (CD86, CD10, CD69, Fas, CD83, CD27, CXCR4 and CXCR5) as well as intracellular factors (BCL-6, BCL-2, IRF-4 and BLIMP-1) was analysed (Appendix 4).

Within B cells derived from PBMCs, plasmablasts stood out as the subset with the highest LLT1 levels of expression (Figure 5-5D). LLT1 geoMFI in plasmablasts from PBMCs was much greater than that seen on their tonsillar

counterparts. GC B cells were not particularly positive for LLT1 in the context of PBMCs. However, it must be considered that GC B cells are very rare in circulation. Similarly, as observed in Figure 5-5B, plasmablasts are also not an abundant subset in circulation. It has been described that their frequency increases one week after vaccination (Wrammert et al. 2008; Mei et al. 2009). Therefore, I next studied LLT1 in plasmablasts from vaccinated individuals.

5.4.6 LLT1 is expressed on plasmablasts from vaccinated individuals

Frequencies of different B cell subsets were measured in PBMCs from healthy individuals (Figure 5-6A). I confirmed that GC B cells and PB were scarce in circulation, whereas activated naïve B cells accounted for about half of the total B cell numbers. Considering my interest in PB and the fact that this population expands after vaccination, I decided to monitor the percentage of PB in samples from individuals who had received the Hepatitis B Virus (HBV) vaccine. A pre-vaccine sample was collected, and the individuals were followed up to 4 weeks post-vaccination. Figure 5-6B shows that the highest percentage of PB was achieved at week 1 post-vaccination, as had previously been reported (Wrammert et al. 2008; Mei et al. 2009). Therefore, I quantified LLT1 expression levels on the seven B cell subsets in samples from 1 week post-vaccinated individuals and confirmed that PB were the B cell subset with highest expression of LLT1 (Figure 5-6C). Their relative expression was compared to that of total B cells and, although variable, PB presented, on average, a 3-fold higher expression of LLT1 (Figure 5-6D). As observed in a representative FACS plot stain (Figure 5-6E), the whole PB population was

positive for LLT1 expression, confirming this C-type lectin as a phenotypical feature of PB. To confirm that these results were not HBV specific, I decided to complement this analysis with B cells from flu vaccinated individuals. Figure 5-6F shows the percentage of LLT1 expressing cells in vaccinated individuals from both HBV and flu one week after vaccination. In both cases, PB were the B cell subpopulation with a higher proportion of LLT1 expressing cells, thus confirming LLT1 expression as a generic characteristic of this B cell subset.

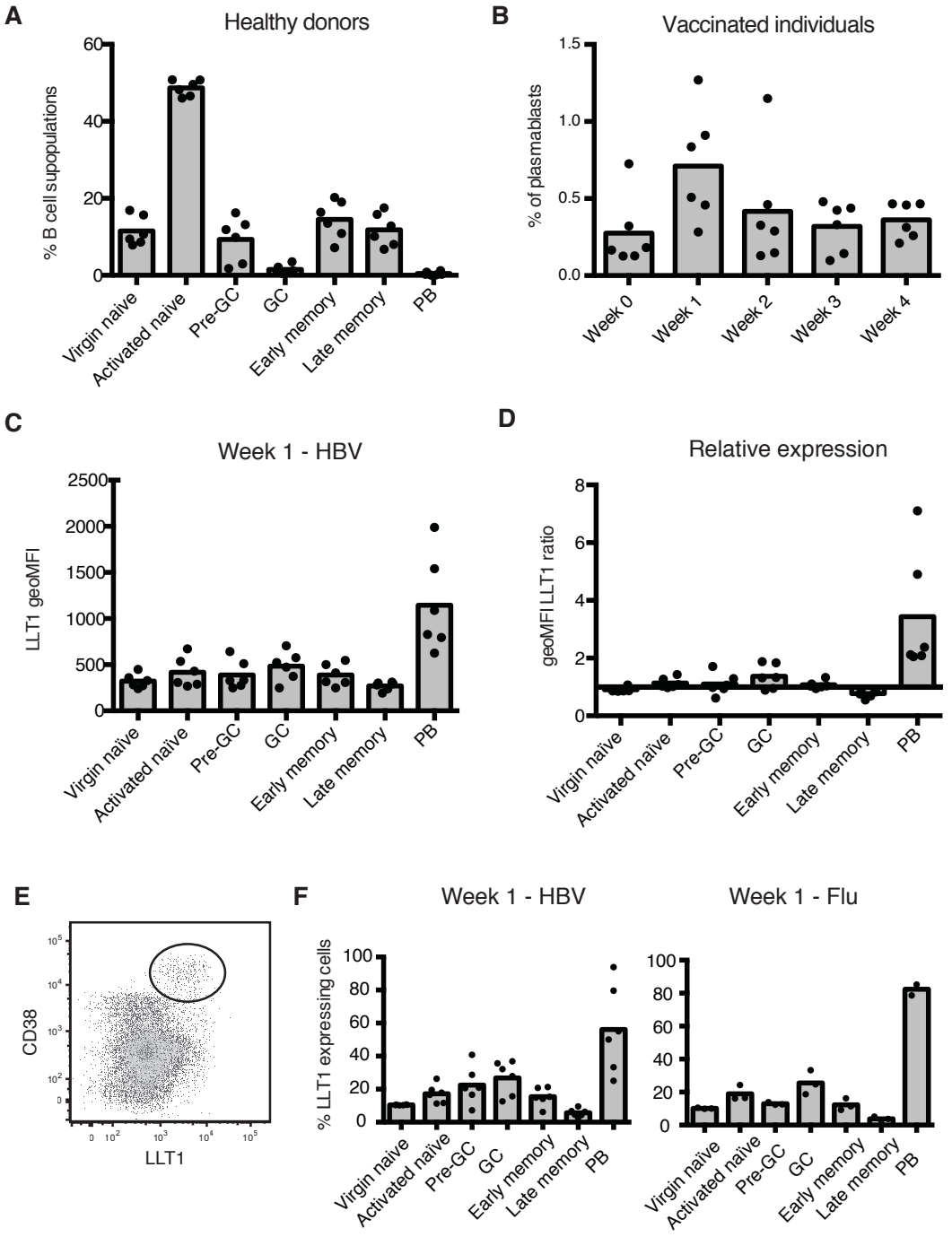


Figure 5-6. LLT1 on circulating B cells from vaccinated individuals (A) shows the percentage of different B cell populations present in PBMCs from heatlhy donors (n=6). (B) shows the percentage of plasmablasts in Hepatitis B (HBV) pre and post-vaccinated individuals (n=6). (C) Levels of LLT1 expression were measured by FACS in the different B cell subsets in B cells from one week HBV post-vaccinated individuals (n=6). (D) shows relative expression of LLT1 to the bulk of B cells one week post-HBV vaccination (n=6). (E) Representative FACS plot of the LLT1 positive plasmablast population one week post-flu vaccination. (F) Percentage of LLT1 expressing cells in the different B cells subsets one week post-HBV (n=6) and flu vaccination (n=3).

5.4.7 LLT1 is not expressed on plasma cells

Having confirmed the expression of LLT1 in plasmablasts, I wondered whether this particular B cell subset maintained LLT1 expression in different developmental stages, including the terminally differentiated one of plasma cells. In order to assess this, CD27+ memory B cells were purified from PBMCs and differentiated *in vitro* into plasma cells, following a 3-step and 10-day culture described in Jourdan *et al.* (Jourdan et al. 2009).

Figure 5-7A shows the CD19+ CD27+ B cell population selected for differentiation. Plasmablasts on day 4 (D4 PB) and day 7 (D7 PB) were identified using a CD38 and CD20 based gating strategy. Day 10 plasma cells (D10 PC) were determined through CD20 and CD138 expression. Four different B cell subsets were tested for LLT1 expression during the 10 day differentiation process; these are CD27+ memory B cells (Day 0), D4 PB, D7 PB and D10 PC and they are highlighted in Figure 5-7B.

Figure 5-7C shows representative FACS plots of LLT1 expression versus CD38 (Day 0, Day 4, Day 7) or CD138 (Day 10). Resting CD27+ memory B cells expressed very low levels of LLT1, whereas these were highly increased by day 4. LLT1 expression was seen on all $CD38^{high}$ cells at day 4. Furthermore, other B cell subsets with lower levels of CD38 were also positive for this C-type lectin. These correspond to B cells at different stages of activation. By day 7, the proportion of B cells expressing high levels of CD38 increased, relating to a greater degree of activation. However, the levels of LLT1 expression, both in the bulk of B cells and on D7 PB had largely

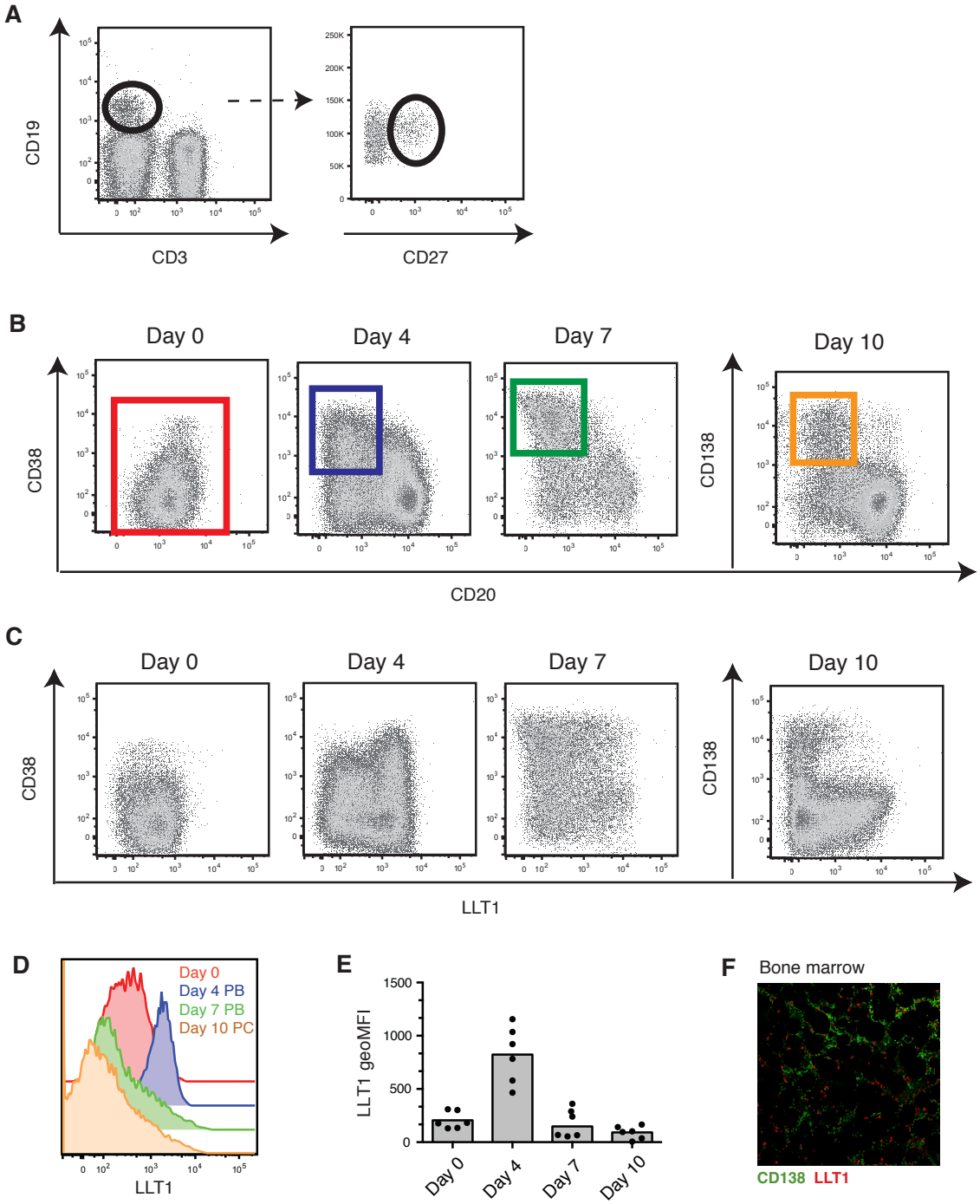


Figure 5-7. LLT1 is expressed on early plasmablasts but not on plasma cells. (A) B cells were negatively selected from PBMCs and then positively selected for CD27. CD27+ B cells were differentiated *in vitro* into plasma cells. (B) shows the stages in which levels of LLT1 were assessed: Day 0 (CD27+ Memory B cells, Red), Day 4 (D4 Plasmablasts, Blue), Day 7 (D7 Plasmablasts, Green) and Day 10 (D10 Plasma cells, Orange). (C) Representative FACS plots of LLT1 expression versus CD38/CD138 in the four analysed stages of plasma cell differentiation. (D) Representative histogram and (E) geoMFI values of LLT1 expression levels of CD27+ B cells on Day 0, Plamablasts on Day 4 and 7 and Plasma cells on Day 10 (n=6). Three independent experiments. (F). Immunofluorescent staining of FFPE bone marrow tissue with anti-LLT1 (goat polyclonal) and CD138. Representative image of n=3.

decreased (Figure 5-7C). This was also true for D10 PC. The vast majority of CD138+ cells did not express LLT1. However, there were abundant CD138- cells still positive for LLT1, probably corresponding to activated B cells or early PB. Figure 5-7D shows a representative histogram of LLT1 expression in CD27+ memory B cells (Day 0), D4 PB, D7 PB and D10 PC. It can be clearly seen that D4 PB presented high levels of LLT1, which was quickly downregulated in further stages of differentiation. LLT1 geoMFI values for these four distinct populations are presented in Figure 5-7E. D4 PB emerged as the subset with strongest LLT1 staining and expression of this C-type lectin went back to basal levels on D7 PB and D10 PC. Taken together, the results shown in Figure 5-5, 5-6 and 5-7 demonstrate that LLT1 is highly expressed on early PB.

With the aim of confirming the absence of LLT1 in terminally differentiated plasma cells, I performed immunofluorescent staining of bone marrow sections with LLT1 and CD138. The presence of abundant LLT1+ cells was obvious, but they were negative for CD138 (Figure 5-7F). As has been reported in the literature (Zhou et al. 2001), it is likely that these LLT1 expressing cells are osteoclasts and osteoblasts.

Given access to bone-marrow samples, I took the opportunity to assess expression levels of LLT1 on the early developmental stages of B cells; thus, I was able to assess LLT1 expression throughout the whole life of a B cell (Figure 5-8). I concluded that LLT1 is only expressed in the pre-GC, GC and early PB stages.

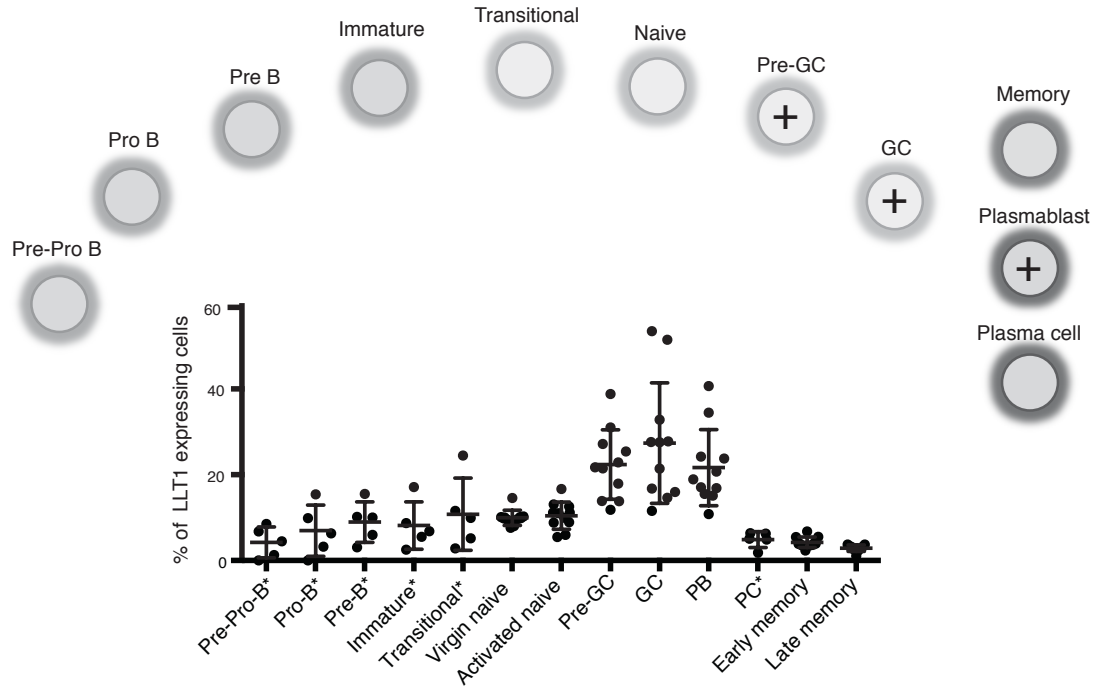


Figure 5-8. LLT1 is expressed in the stages of pre-GC, GC B cells and plasmablasts. LLT1 levels were analysed by FACS (2H7 clone) in different stages of B cell differentiation, using samples from bone marrow (*) and tonsils. Pre-Pro B (CD10+ CD19- CD34+ IgM-), Pro-B (CD10+ CD19+ CD20- CD34+ IgM-), Pre-B (CD19+ CD20+ CD34-IgM -), Immature (CD10+ CD19+ CD20+ IgM+), Transitional (CD19+ CD20+ IgM++), Virgin naïve (CD19+ IgD+ CD38-), Activated naïve (CD19+ CD38+ IgD+), Pre-GC (CD19+, CD38++, IgD+), GC (CD19+ CD38 ++ IgD-), PB (CD19low, CD38+++, IgD-), PC (CD19low CD138+ IgD-), Early memory (CD19+ CD38+ IgD-) and Late memory (CD19+ CD38- IgD-). LLT1 was not expressed on B cell precursors or transitional B cells, nor in tonsillar naïve B cells. However, LLT1 was highly expressed in pre-GC and GC B cells from tonsils. Its levels remained high in plasmablasts but were quickly downregulated in memory B cells. Terminally differenatiated plasma cells did not express LLT1. (Bone marrow n=5; Tonsils n=10).

5.4.8 Regulation of LLT1 expression

The upregulation of LLT1 on B cells following TLR9, BCR and CD40 stimulation has been shown before (Rosen et al. 2008). I wanted to confirm these findings using the novel 2H7 anti-LLT1 antibody as well as to explore the effect of different stimuli (e.g. cytokines) present in the GC environment on the levels of LLT1 expression on B cells.

The percentage of LLT1-expressing B cells was assessed by flow cytometry at different time points after CpG oligonucleotide stimulation (Figure 5-9A). The upregulation of LLT1 on purified B cells from PBMCs reached its maximum 48 hours post-stimulation and then decreased progressively. Figure 5-9B shows a dose-dependent effect of CpG in the upregulation of LLT1 on B cells. This upregulation could be prevented by using the MyD88 inhibitor Pepinh-MYD and this blocking effect was also dose-dependent (Figure 5-9C). Upregulation of LLT1 on B cells 48h post-CpG stimulation could be prevented by the addition of Brefeldin A (Figure 5-9D), suggesting that protein transport between the endoplasmatic reticulum and the Golgi apparatus is required to bring LLT1 on the cell surface.

Recently, the idea that TLR agonists can be used as adjuvants and contribute to the vaccine-induced GC responses is being widely explored (Rookhuizen & DeFranco 2014). After showing that the TLR9 agonist CpG was capable of LLT1 upregulation, I questioned whether other human TLR agonists could have similar effects. After 48h stimulation, B cells stimulated with TLR3 agonist Poly(I:C) were the ones that presented higher levels of LLT1 (Figure

5-9E). All the other TLR agonists tested caused lower responses than CpG, if any.

The GC reaction is a complex process that involves a wide range of cytokines secreted by different cell types such as T cells, B cells, FDCs and TBMs. To analyse the individual effects of cytokines present in the GC environment, I stimulated primary B cells with IL-4, IL-10, IL-21, PGE_2, IL-15 and BAFF. I could not detect changes in LLT1 expression levels on B cells 48h post-stimulation (Figure 5-9F).

Considering that the capture of antigen by B cells through their BCRs is the crucial event in the GC reaction, I assessed the consequences of BCR stimulation on PBMC-derived B cells over time. There was a progressive increase of LLT1 surface levels on B cells, with its expression reaching a peak by day 5 (Figure 5-9G). CD40 stimulation, another essential player within the GC, also resulted in enhanced expression of LLT1 on primary B cells (Figure 5-9H). However, upregulation of LLT1 in this context was quicker, having started to decrease by day 5.

Overall, the results show that LLT1 is upregulated on B cells with CpG, poly(I:C), BCR and CD40 stimulation.

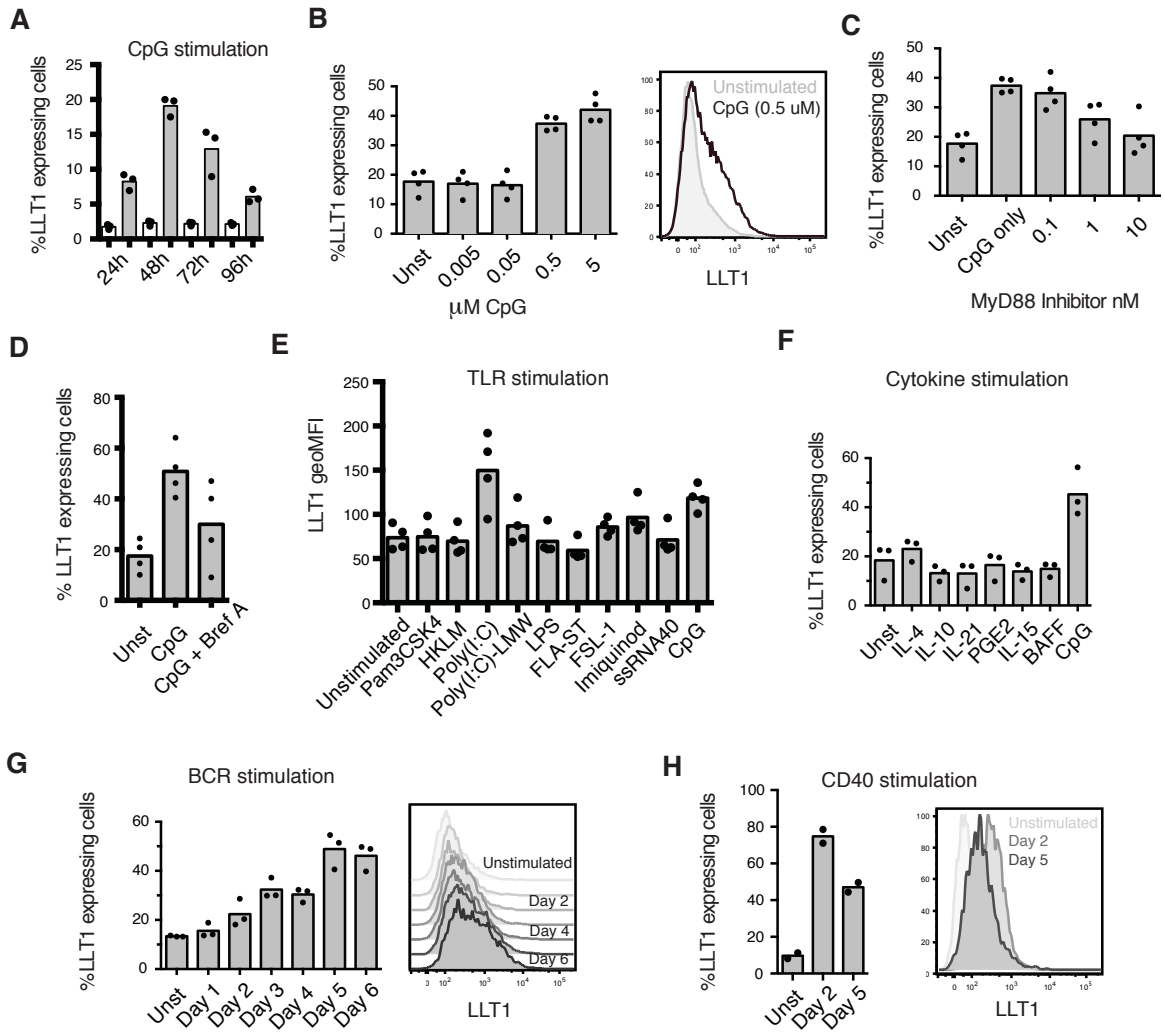


Figure 5-9. LLT1 was upregulated with CpG, Poly(I:C), BCR and CD40 stimulation. (A) Purified B cells from PBMCs were stimulated with TLR agonist CpG and the percentage of LLT1+ cells was measured at different time points (n=3). (B) Increasing concentrations of CpG were added to purified primary B cells for 48h, which resulted in a dose-dependent increase in the percentage of LLT1-expressing cells (2H7 clone) (n=4). (C) The effect was blockable with an MyD88 inhibitor, Pepinh-MYD, and it was also dose-dependent (n=4). (D) LLT1 upregulation could also be prevented by the addition of Brefeldin A (Bref A) (n=4). (E) The effects on LLT1 expression of different human TLR agonists were tested on purified B cells, being CpG and Poly(I:C) the main drivers of LLT1 upregulation (n=4). (F) Stimulation with diffierent cytokines (50ng/ml for 48h) did not alter expression levels of LLT1 on B cells (n=3). (G) BCR stimulation resulted in upregulation of LLT1 on B cells (n=3). (H) LLT1 was also upregulated on B cells upon CD40 stimulation (n=2). Representative graph of at least two independent experiments.

5.4.9 LLT1 expression is linked to B cell proliferation

I have shown LLT1 expression on GC B cells (Figure 5-1), B cell lymphomas (Figure 5-3) and plasmablasts (Figure 5-5, 5-6 and 5-7). One of their common features, which distinguish them from other B cell stages and subsets, is their highly proliferative state. Therefore, I decided to analyse whether there was an association between proliferation and LLT1 expression levels. I induced B cell proliferation using CpG and measured LLT1 geoMFI on the different rounds of B cell proliferation, which were identified through CTV stain. I could observe how LLT1 expression increased during the first rounds of B cell proliferation and then reached a plateau (Figure 5-10A). This upregulation pattern was similar to that seen with CD69 (Figure 5-10B) and differed from CD38 (Figure 5-10C) and HLA-DR (Figure 5-10D). Therefore, the data suggested a link between LLT1 expression and B cell proliferation.

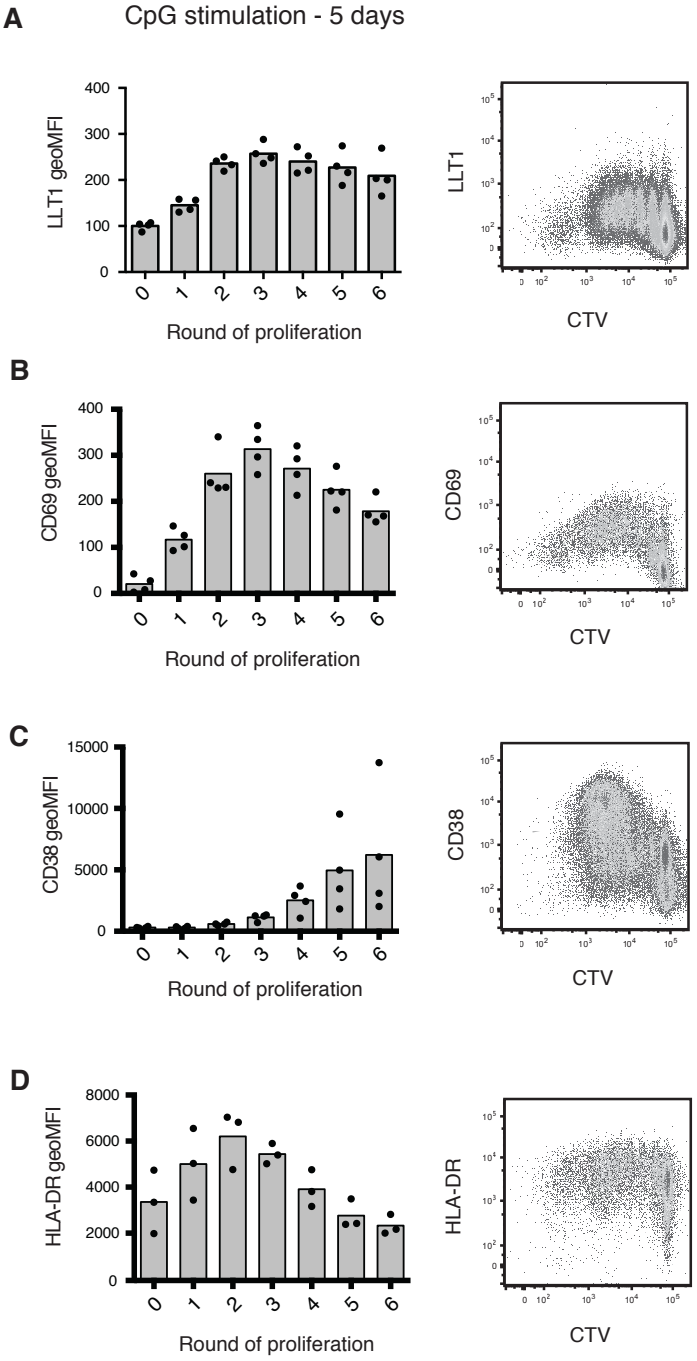


Figure 5-10. CpG-induced proliferation of purified B cells upregulates LLT1. Proliferation of purified B cells from PBMCs was induced with CpG oligonucleotides and levels of LLT1 were assessed by flow cytometry after 5 days. CpG stimulation resulted in upregulation of LLT1 expression (A), as well as CD69 (B), CD38 (C) and HLA-DR (D). (n=4). Representative FACS plots of three independent experiments.

5.5 Discussion

In this chapter, I reported the expression and regulation of LLT1 on B cells, and I focused on the GC environment.

The GC can be divided into two microanatomically distinct regions, the DZ and the LZ. Competition for antigen and Tfh cell help occur within the LZ, while SHM and proliferation is restricted to the DZ (Victora & Nussenzweig 2012). Although LLT1 expression was observed on all GC B cells (Figure 5-1), it was marginally higher on DZ B cells (Figure 5-2); however, an explanation for this remains to be elucidated.

High rates of proliferation and mutation are the main features of GC B cells. Slight deregulation of these processes can have highly detrimental effects, such as neoplasia. I have described expression of LLT1 in abundant GC-derived malignancies (Figure 5-3), although the presence of this C-type lectin was not necessary nor sufficient. Nonetheless, LLT1 could be of potential aid for the clinical diagnosis of B cell lymphomas, in particular non-Hodgkin's lymphomas, which represent 4-5% of all cancers diagnosed. Treatment selection relies on accurate diagnosis, staging of the disease, and identification of adverse prognostic factors. Expression of BCL-6, CD10 and IRF-4 are used in immunohistochemical stains to separate DLBCLs into GC and non–GC subtypes (England 2015). However, although IHC is widely used, it is not always reliable, in particular when identifying follicular lymphomas with atypical phenotypes. LLT1, therefore, provides a potential new marker for the clinical investigation of lymphomas, and warrants larger

prognostic studies to provide more data on the independent significance of positive or negative stains.

LLT1 expression was not restricted just to the GC, as LLT1+ cells were detected outside of the GC. Many of these cells expressed markers associated with a plasmablast phenotype ($CD45^{low}$, $CD20^{-}$, $CD19^{low}$, $CD79\alpha^{low}$, Ig^{+}, IRF-4^{+}, $CD38^{+}$, $Ki67^{+}$, $CD138^{-}$), although this does not exclude other cell types (Figure 5-4 and 5-5). The presence of Ig+ LLT1- cells within GCs could be indicative of both plasma cells or memory B cells that have re-entered the GC (Bende et al. 2007), although this requires further investigation.

Following Jourdan and colleagues *in vitro* model system for the generation of plasmablasts and plasma cells, LLT1 expression was confirmed on early (day 4) plasmablasts, and reduction as the cultures progressed towards terminally differentiated plasma cells at day 10 (Jourdan et al. 2009). However, whether LLT1 expression on plasmablasts *in vivo* is a mark of recent exit from the GC or is independently upregulated was not addressed in this study. The fact that LLT1 was specifically confined to the GC, with the adjacent B cells being all negative for this C-type lectin, together with early plasmablasts expressing it, but not plasma cells or memory B cells, suggests a very tight regulation of LLT1 and, therefore, an important role in the context of the GC reaction.

I described how key interactions occurring in the GC environment have an impact on high expression levels of LLT1 on B cells (ie. BCR and CD40) (Figure 5-9). I have also explored the consequences of TLR stimulation and

found that some human TLR agonist (ie. Poly(I:C), CpG) are capable of enhancing levels of this C-type lectin. TLR stimulation has emerged as a very promising possibility for vaccine adjuvants. Although several studies suggested that TLR agonists were able to drive an extrafollicular antibody response, producing moderate affinity antibodies, more recent work has highlighted the potential of TLR in enhancing GC responses. This involves the generation of high-affinity, class-switched antibodies as well as long-lived plasma cells (Rookhuizen et al. 2014). Particularly, the use of a TLR9 agonist in mice to boost antibody responses resulted in increased numbers of Tfh and GC B cells, as well as in a loss of follicular Treg cells. Overall, the presence of such adjuvant resulted in enhanced class-switch, affinity maturation and memory (Rookhuizen et al. 2014). However, the potential use of TLR agonists as vaccine adjuvants, as well as a possible role for LLT1 in this process requires further investigation.

It was noted that LLT1 was frequently associated with dividing cell populations: lymphomas, plasmablasts and GC B cells (in particular DZ B cells). Furthermore, I observed that *in vitro* LLT1 expression was highest in cells that had undergone a certain number of divisions after CpG stimulation then reaching a plateau (Figure 5-10), similar to the observation by Zhou *et al.* that OCIL mRNA expression was at its highest during the osteoblast proliferative phase of bone marrow cultures (Zhou et al. 2001). In contrast, LLT1 was absent from plasma cells and both early and late memory B cells, all of which are non-dividing cell types. Intriguingly, this suggests a possible link between proliferation and LLT1 expression; however, I have as yet been

unable to find any functional role for LLT1 during proliferation. On the other hand, the level of LLT1 expression may act as a surface marker of B cells with high affinity BCRs. GC B cells with high affinity BCRs are able to more efficiently present antigen to Tfh cells and consequently undergo a greater number of divisions (up to 6) (Gitlin et al. 2014). Thus, it is tempting to speculate that LLT1 may act in a similar manner as CD45RO, a phosphatase involved in cell signalling, which correlates with highly activated and mutated human GC B cells (Jackson et al. 2007). Nonetheless, this hypothesis warrants further investigation.

5.6 Summary

- LLT1 is expressed on GC B cells, early plasmablasts and B cell lymphomas
- LLT1 is upregulated with CpG, Poly(I:C), BCR and CD40 stimulation

6 The function of LLT1 on B cells

6.1 Introduction

In order to address the functionality of LLT1, it is important to understand the potential interactions with its ligand, CD161. The CLRs LLT1 and CD161 are genetically linked physiological binding partners, located adjacent to one another within the NKC (Iizuka et al. 2003; Aldemir et al. 2005; Rosen et al. 2005; Vogler et al. 2011); they bind, however, with a very low affinity (K_d of 48μM) (Kamishikiryo et al. 2011). Structurally, LLT1 shares the greatest homology with the other C-type lectins AICL and CD69 (Boles et al. 1999). Recently, studies regarding the crystal structure of LLT1 have been published (Skalova et al. 2015, Kita et al. 2015). Very little is known about LLT1 compared to its binding partner, CD161, which has been relatively well characterised, delineating a family of innate-like T-lymphocytes and NK cells (Fergusson et al. 2014).

Within the host immune response, studies exploring the role of LLT1 and CD161 have focused on NK and T cell function (Exley et al. 1998; Aldemir et al. 2005; Rosen et al. 2005; Rosen et al. 2008; Fergusson et al. 2014). Cross-linking of CD161 reduces NK cell cytotoxicity and cytokine production, leading to the suggestion that LLT1 could play a role, similarly to MHC Class I, in self-tolerance (Chen et al. 2015). Indeed, expression of LLT1 on a number of human B cell lymphoma cell lines (Rosen et al. 2008; Germain et al. 2010; Germain et al. 2015) and a glioblastoma line (Roth et al. 2007) has been

shown to prevent killing by NK cells. A role for LLT1 has also been described in the context of bone metabolism, inhibiting osteoblast differentiation (Nakamura et al. 2007), as well as osteoclast differentiation and function (Zhou et al; 2001; Hu et al. 2004). These studies suggest that interactions between LLT1-CD161 can result in bidirectional signalling and have functional consequences for both cells involved.

The study of signalling through LLT1 has been limited (Bambard et al. 2010), as well as the functional consequences of cross-linking it, which results in IFN-γ production by NK-derived cell lines (Mathew et al. 2004; Bambard et al. 2010). I wanted to analyse the signalling and function of LLT1 in GC B cells. Several C-type lectins have been shown to play a role in the modulation of BCR responses, these being CD22, CD72 and CD23 (Nitschke & Tsubata 2004; Reljii et al. 1997). Recently, the novel technique of phosphoflow has become available for the study of diverse phosphorylation patterns of BCR-associated signalling (Kheirallah et al. 2015; Polikowsky et al. 2015). Different studies have analysed BCR signalling in various B cell subsets and B cell lymphomas (Toapanta et al. 2012; Blix et al. 2012) and some have focused on the particularities of GC B cells (Polikowsky et al. 2015). Previous studies have shown that the BCR signal transduction in GC B cells is short-circuited, with most proliferating GC B cells lacking active BCR signalling (Khalil et al. 2012.; Bannard & Cyster 2012). This suggests that negative regulation of BCR signalling might play a role in the selection and cell fate determination within the GC reaction.

6.2 Aims

At this point, I had characterised the distribution and regulation of LLT1 in the GC environment. My next aim was to elucidate the function of LLT1 on B cells, within this particular context. The work performed in this chapter allowed the following questions to be addressed:

- Where is CD161, the ligand for LLT1, expressed within the GC environment?
- What signalling pathways are triggered through LLT1?
- What is the function of LLT1 on GC B cells?

6.3 Materials and Methods

Specific materials and methods for this chapter are detailed below. All other methods and reagents are described in Chapter 2.

6.3.1 Tissues

Tonsils for immunoflurorescent staining of Figure 6-1 and 6-2 were obtained following routine tonsillectomy from the Human Tissue Resource Centre, Barts and The London NHS Trust, Queen Mary School of Medicine and Dentistry. Sample collection and procedures were approved by the hospital Ethics Committee (REC/98/11/27 Guys and St. Thomas' NHS Trust and REC 05/Q0703/198 Barts and the London NHS Trust).

6.3.2 Real-time quantitative polymerase chain reaction (qPCR)

The following primers were used (Eurofins MWG Operon):

CD161-Forward 5'-AAATGCAGTGTGGACATTCAA-3'

CD161-Reverse 5'-CTCGGAGTTGCTGCCAATA-3'

CXCR4-Forward 5'- GGTGGTCTATGTTGGCGTCT-3'

CXCR4-Reverse 5'-ACTGACGTTGGCAAAGATGA-3'

6.3.3 Phosphoflow experiments

Anti-LLT1 antibody 2H7, recombinant CD161 protein (rCD161, R&D Systems) or IgG1 Fc Control (R&D Systems) were bound to a 96-well Enzyme Linked Immuno-Sorbent Assay (ELISA) plate (Greiner bio-one) overnight, washed three times with PBS the next morning and blocked with R10 for 2h at 37°C 5% CO_2.

Assays were performed either with whole PBMCs, with purified B cells or with Naïve, GC, Memory and PB FACS-sorted populations from tonsils, using MoFlo^{TM} XDP (Beckman Coulter). PMA and ionomycin (Cell Stimulation Cocktail, 500X, eBioscience), anti-BCR (goat anti-human IgM/G/A F(ab')$_2$ fragments, Jackson ImmunoResearch) or 300 cells (1:1 ratio) were used for stimulation. 2 x 10^5 cells were plated per well in a U-bottom 96-well plate and kept at 37°C 5% CO_2.

After stimulation, cells were fixed with BD Cytofix™ fixation buffer for 10 min at 37°C 5% CO_2 and permeabilised with BD Perm Buffer III for 30 min at 4°C.

Cells were then stained using pERK-PE, pIRF-7-AF488, pStat1-AF647, pStat3-AF488, pZap70-PE (BD Biosciences) for 20 min at RT.

6.3.4 Doublet formation

The blocking capabilities of the following anti-CD161 antibody clones were assessed (1μg/ml): 191B8 (Miltenyi Biotec), IMG14F1F11 (Abcam), B199.2 (AbD Serotec), Rabbit polyclonal (Novus Biologicals), Goat polyclonal (Santa Cruz Biotechnology) and HP-3G10 (BioLegend).

6.3.5 B cell activation assay

6.3.5.1 B cells from PBMCs

rCD161 (R&D Systems) or IgG1 Fc Control (R&D Systems) were bound to a 96-well ELISA plate (Greiner bio-one) overnight, washed three times with PBS the next morning and blocked with R10 for 2h at 37°C 5% CO_2. 2 x 10^5 purified B cells from PBMCs (see *5.3.3 B cell purification*) were added and incubated for 5 days at 37°C 5% CO_2, after which LIVE/DEAD® Fixable Near-IR Dead Cell Stain Kit (Life technologies) staining was performed, together with extracellular staining of the CD69, CD38, CD83 and CD86 (see Table 2.1) markers. Alternatively, intracellular staining of the apoptotic marker Annexin V was performed (Miltenyi Biotec, 1:20 dilution) at RT for 15 min in Annexin V binding buffer (Miltenyi Biotec). Levels of Activated-Caspase-3 were also measured (1:5 dilution, Table 2.1).

6.3.5.2 B cells from tonsils

Anti-LLT1 antibody 2H7, rCD161 protein (R&D Systems) or IgG1 Fc Control (R&D Systems) were bound to a 96-well ELISA plate (Greiner bio-one) overnight, washed three times with PBS the next morning and blocked with R10 for 2h at 37°C 5% CO_2. 2 x 10^5 purified B cells from tonsils (*5.3.3 B cell purification*) were added and incubated overnight at 37°C 5% CO_2. GC B cells were gated (IgD^-CD38^{mid}) and levels of CD83 and CXCR4 (1:200 dilution) receptors measured by flow cytometry.

6.3.6 Blocking experiments

For functional assays with tonsillar B cells, ~3mm tonsillar pieces were incubated in a solution of RPMI 1640 containing collagenase D (1 mg/ml; Boehringer Mannheim) and DNase I (0.1 mg/ml, Sigma Aldrich) and shaken for at least 1h at 37°C. The reaction was stopped by adding 0.5M EDTA (Sigma Aldrich). Cells were washed twice with RPMI and cultured at 5 x 10^6 cells/ml in 500 µl in a 48-well plate (Corning) with combinations of CpG (0.5µM, Invivogen), anti-CD40 (5µg/ml, Macbeth) + IL-4 (50ng/ml, PreproTech), anti-CD161 at 1µg/ml (clone 191.B8, Miltenyi Biotec) and IgG2A isotype control (R&D Systems). Cells were incubated for 7 days at 37°C 5% CO_2 and the percentage of live B cells was assessed using the LIVE/DEAD® Fixable Near-IR Dead Cell Stain Kit (Life technologies), together with intracellular staining of Ki67 and/or extracellular staining of CD19, CD83, and CD38 markers. Alternatively, a CTV stain was performed before plating the

cells (see *5.3.6 Proliferation assay*) and the percentage of proliferating cells measured.

6.3.7 CD161+ cell depletion

Tonsillar cells were stained with CD161-PE (Miltenyi Biotec) and depleted from the sample by FACS-sorting, using MoFlo^{TM} XDP (Beckman Coulter). After CpG (0.5µM, Invivogen) or anti-CD40 (5µg/ml, Macbeth) + IL-4 stimulation (50ng/ml, PreproTech), levels of CD38 and CD83, respectively, were measured in live CD19+ cells.

6.3.8 Data acquisition and analysis

For analysis of the CD161 immunofluoresecent staining, images were acquired on an Olympus Fluoview FV1000 microscope (Olympus) and analyzed using Fiji (ImageJ, National Institute of Health, USA). The Leica TCS-SP2 AOBS confocal laser scanning microscope was used for the CD161 immunofluorescence and the images were captured and processed with Leica Confocal, LCS Lite software, and Image-J.

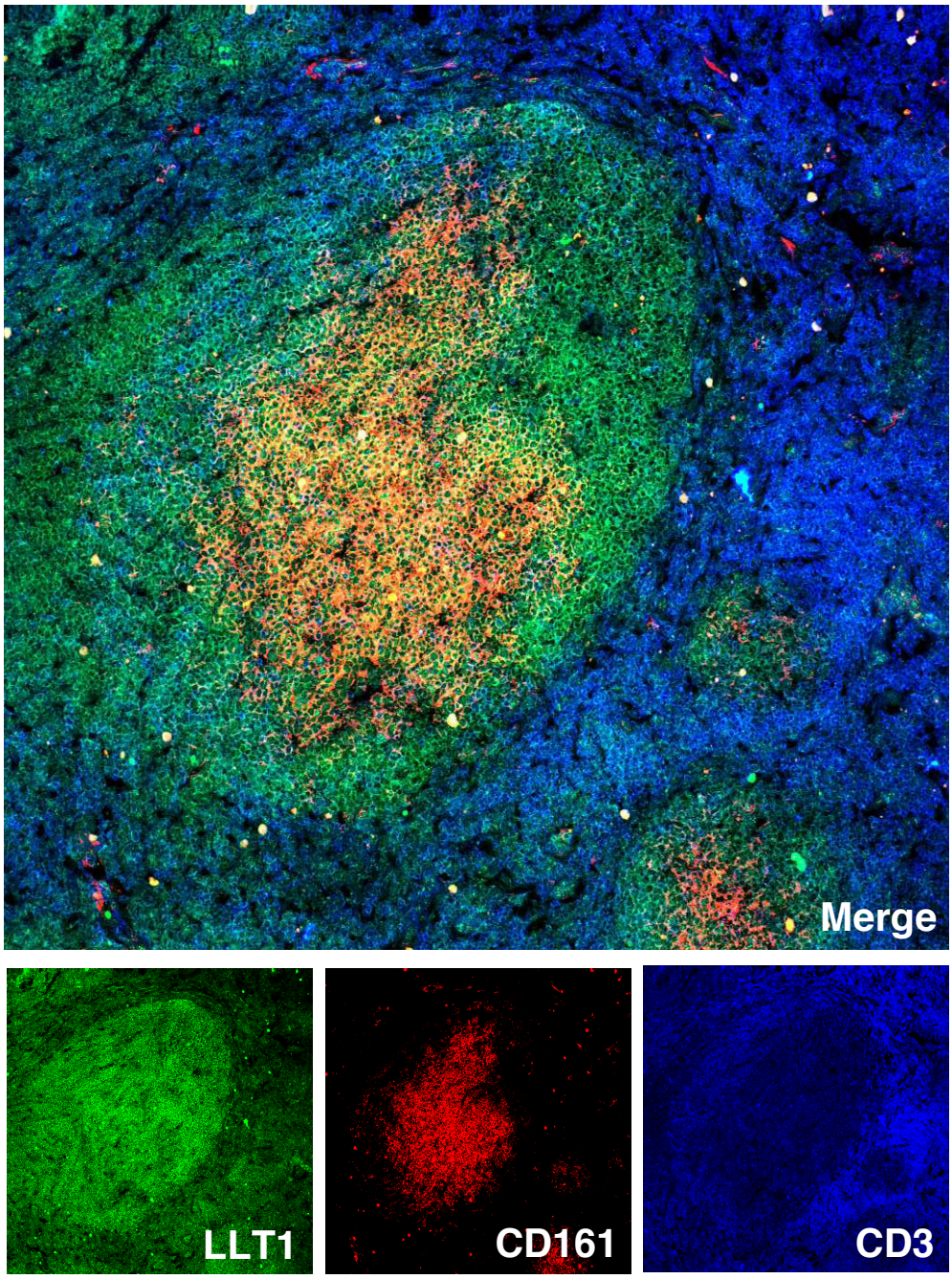
6.4 Results

6.4.1 CD161 is expressed on FDCs

At this point, I had described the distribution and regulation of LLT1 on GC B cells. B cells within the GC undergo a range of different processes that are

triggered through interactions with different GC-resident cell types. In order to assess the function of LLT1 in this particular context, I next explored the expression of its ligand, CD161, in the GC environment. Unexpectedly, immunofluorescent staining of frozen human tonsils revealed the expression of CD161 within a pattern similar to the one of FDCs (Figure 6-1A). This striking finding was confirmed by performing non-fluorescent immunostaining in FFPE human tonsillar sections (Figure 6-1B). Costaining of CD161 and a FDC marker (CNA.42 clone) showed a strong overlap, thus confirming the presence of CD161 on these stromal cells (Figure 6-1C). Costaining of Peanut agglutinin (PNA), LLT1 and CD161 showed interaction between LLT1 on GC B cells and CD161 expressed in a FDC pattern within the GC (Figure 6-1D). Finally, we confirmed the immunofluorescent staining of CD161 by using different CD161 antibody clones. Figure 6-1E shows stainings with three new anti-CD161 antibodies together with the FDC marker, all of them presenting a great degree of overlap and allowing us to conclude that FDCs strongly express the C-type lectin CD161.

A



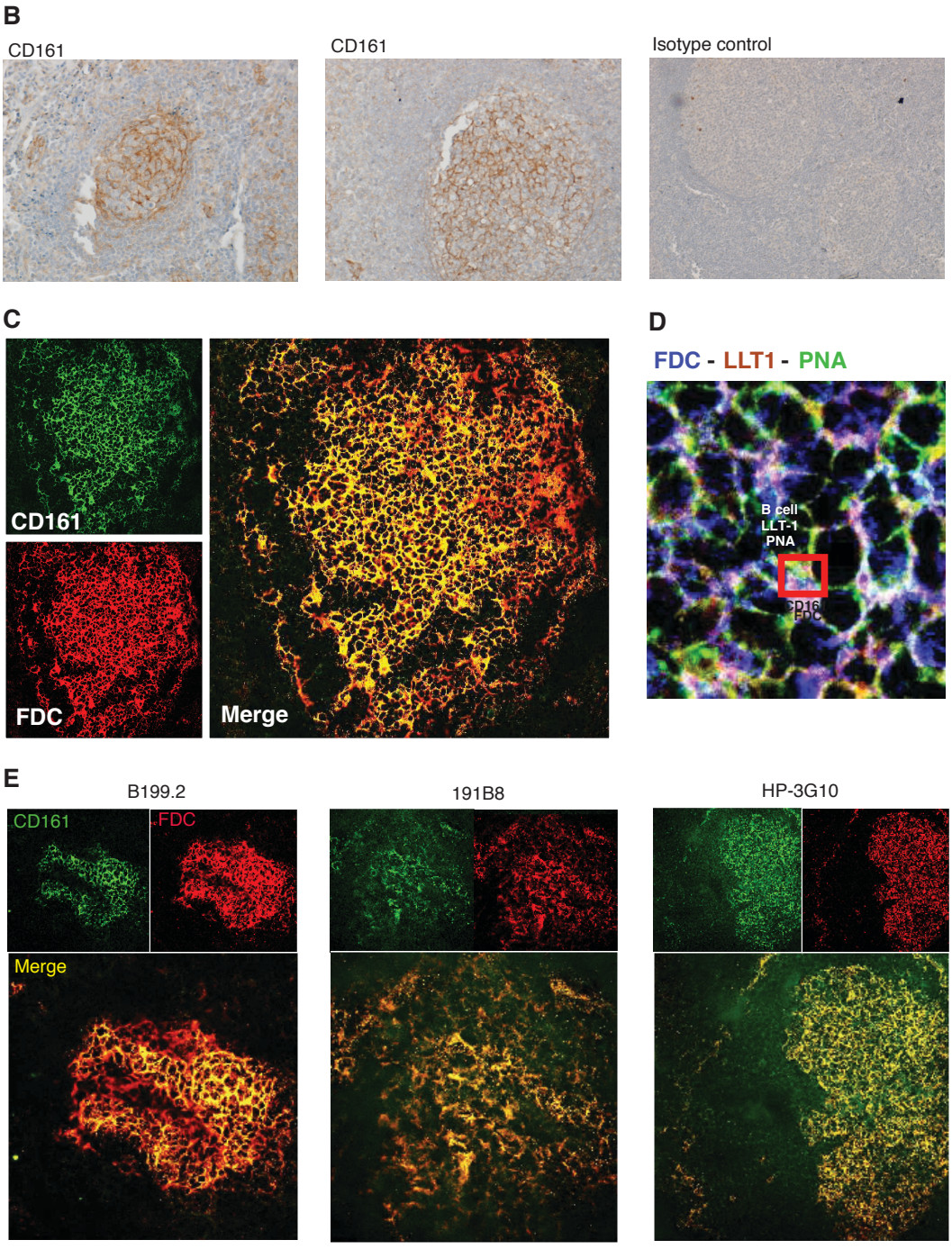


Figure 6-1. CD161 is expressed on FDCs. (A) Costaining of LLT1, CD161 and CD3 in human frozen tonsillar tissue sections. Image representative of six secondary follicles. (B) Staining with anti-CD161 antibody (brown; B199.2 clone) of FFPE human tonsillar tissue (CD161 20x, Isotype control 10x) revealed an expression pattern similar to the one of FDCs. Representative images of one out of 3 experiments are shown. (C) Immunofluorescent staining of frozen human tonsils with an FDC marker (clone CNA.42) and CD161 (clone IMG14F1F11) showed complete overlap between these two markers. (D) Triple FDC, LLT1 and PNA stain of a frozen tonsillar human section. Interaction between FDCs and double positive LLT1-PNA GC B cells can be observed (red square). Representative image of six different follicles. (E) Immunofluorescent staining of frozen human tonsils with the FDC marker and different anti-CD161 antibody clones (191B8, B199.2 and HP-3G10) confirmed expression of CD161 on FDCs.

6.4.2 CD161 is expressed on a subset of tonsillar T cells

CD161 expression has been described on both NK cells and T cells. Therefore, an obvious candidate cell type with the potential to interact with GC B cells are the Tfh cells. Flow cytometric analysis of tonsillar T cells revealed a loss of CD161 expression as the Tfh cells progressed to full GC phenotype, as defined by CXCR5 expression (Ma et al. 2012) (Figure 6-2A). This was confirmed at the mRNA level in sorted tonsillar T cells. Although a small fraction (<10%) of CXCR5++ Tfh cells did express CD161, they were not observed within any of the GC assessed by immunofluorescent microscopy (Figure 6-2B). Similarly, within the PBMC, circulating Tfh, defined simply as CXCR5+ (Breitfeld et al. 2000) also had lower frequencies of CD161+ cells compared to the CXCR5- fraction (Figure 6-2C).

Finally, CD161 expression was assessed on tonsillar macrophages (including TBM), define by CD68 expression. Flow cytometric analysis of this population showed that TBM did not express CD161 (Figure 6-2D).

These results showed the presence of CD161 in the GC environment, mainly on FDCs but also on a subset of T follicular cells, thus providing a feasible interaction between these two C-type lectins in this particular context.

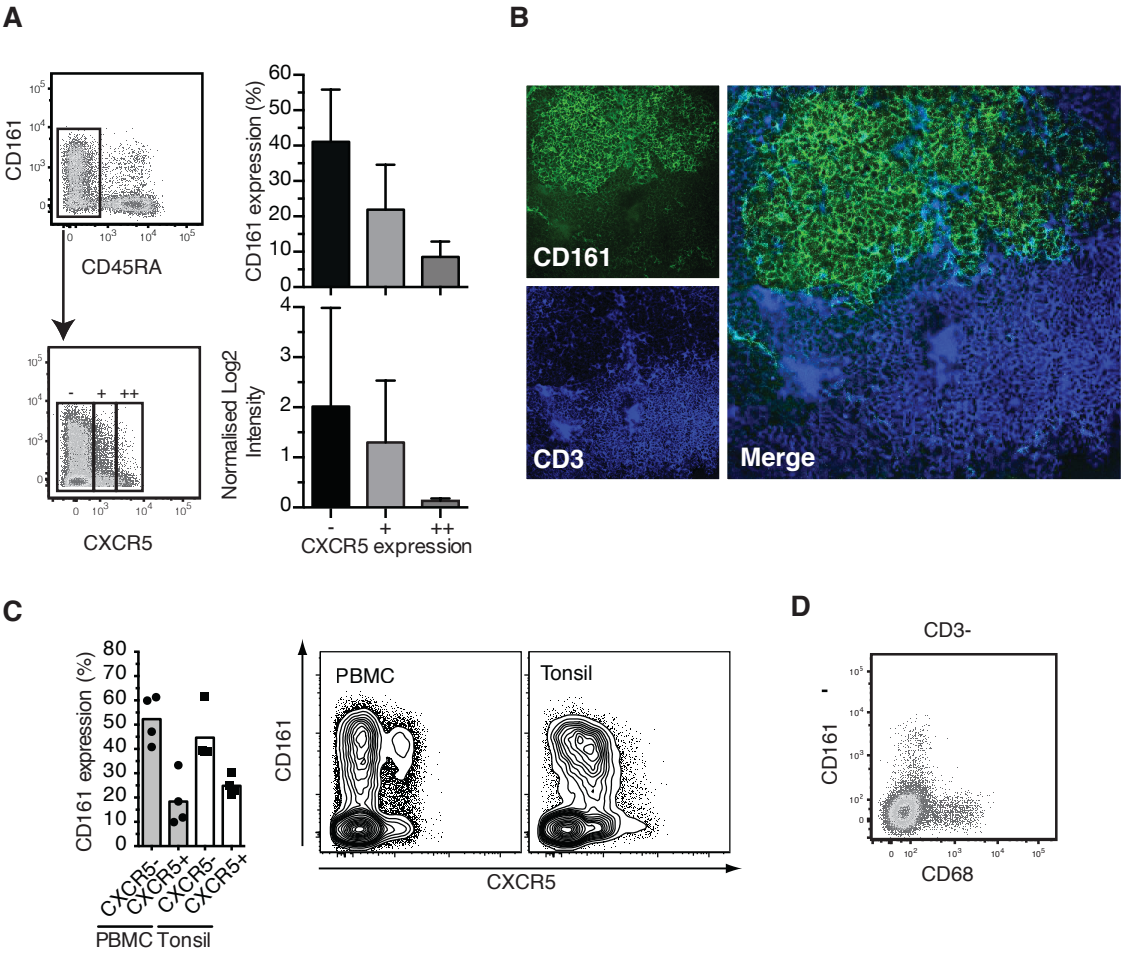


Figure 6-2. CD161 is expressed on a subset of tonsillar T cells. (A) CD161 expression negatively correlated with CXCR5 expression on CD45RA- T cells (CD3+ CD4+) assessed by FACS (n=5, 3 independent experiments) and qPCR (n=3, two independent experiments). (B) Costaining of CD161 and CD3, showing the absence of double positive cells within the germinal centre. (C) CD161 expression was lower on CXCR5+ CD4+T cells from both tonsils and PBMC than their CXCR5- counterparts, suggesting lower expression is not due to the local microenvironment (n=4). (E) CD68 internal staining showed that CD161 was not expressed on tonsillar macrophages (which includes the TBM population). Representative FACS plot (n=4).

6.4.3 LLT1 cross-linking on B cells does not involve ERK signalling

The literature regarding LLT1 signalling is scarce. Bambard *et al.* showed that ligation of LLT1 on NK92 cells with CD161 employed the ERK signalling pathway (Bambard et al. 2010). I wanted to assess whether this particular pathway was also used in LLT1 expressing B cells. I decided to analyse levels of phosphorylated ERK (pERK) using flow cyometry in an approach known as phosphoflow. This particular methodology has been recently used for studies involving B cell signalling (Topanta et al. 2012), and particularly in the GC context (Khalil et al. 2012; Polikowsy et al. 2015). I was able to show phosphorylation of ERK in PBMCs after PMA stimulation (Figure 6-3A). Initial upregulation of pERK was very quick, and it started to decrease 30 min post-stimulation. Levels of pERK could also be accurately measured on Raji cells after BCR stimulation, and the effect was dose-dependent (Figure 6-3B). Having set up the methodology, I tested whether phosphorylation of ERK could be induced through LLT1, either using plate-bound anti-LLT1 2H7 mAb or rCD161 protein. None of them were able to increase levels of pERK, neither on their own nor in conjunction with BCR stimulation (Figure 6-3C). Therefore, using a phosphoflow approach, I could not detect ERK phosphorylation after LLT1 ligation.

I next decided to examine different signalling pathways cross-linking LLT1 with rCD161 (IRF-7, Stat1, Zap70 and Stat3). However, I could not detect any changes in phosphorylation in any of the examined pathways, within the conditions tested (Figure 6-3D).

Finally, I incubated sorted tonsillar naïve, GC, memory B cells and PB with untransfected or CD161-transfected 300 cells. In this new setup, I was also unable to detect any changes in pERK levels (Figure 6-3E).

Overall, the data suggest that LLT1 does not trigger the pERK signalling pathway when cross-linked on B cells.

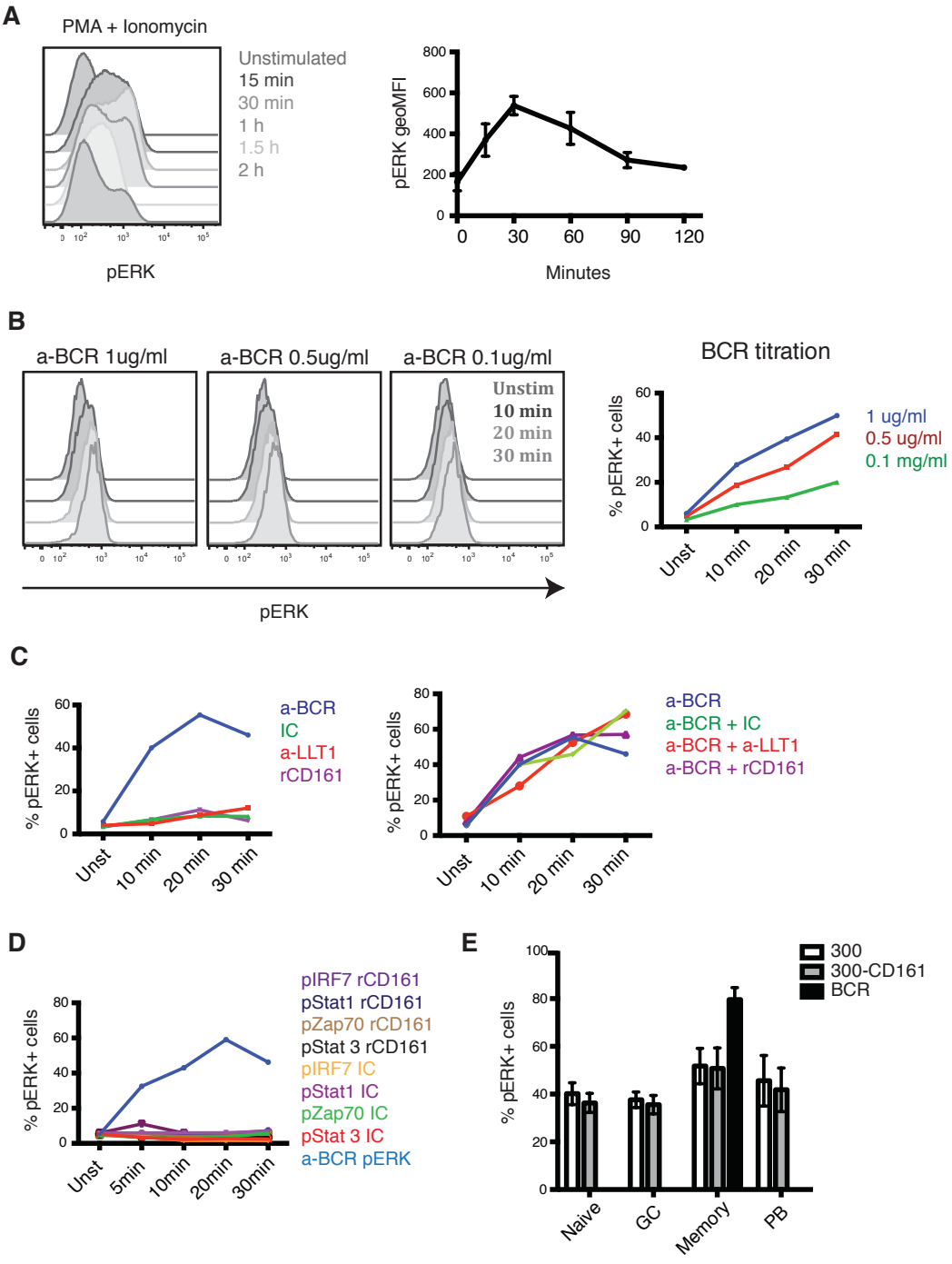


Figure 6-3. pERK signalling through LLT1 could not be detected using phosphoflow. (A) PMA stimulation of PBMCs resulted in increased levels of pERK (n=2). (B) BCR stimulation increased intracellular expression of pERK in Raji cells in a dose-dependent manner. Representative plots of two independent experiments. (C) BCR stimulation, but not the 2H7 anti-LLT1 antibody or rCD161, resulted in an increased expression of pERK on Raji cells. Neither the 2H7 antibody or the rCD161 protein altered pERK expression levels when combined with BCR stimulation. Representative plot of three independent experiments. (D) The presence of rCD161 did not alter levels of pIRF-7, pStat1, pZap70 or pStat3. Representative plot of two independent experiments. (E) LLT1 stimulation (20 min) did not enhance intracellular levels of phosphorylated ERK on any tonsillar B cell subsets; Naïve, Germinal centre (GC) , Memory and Plasmablasts (PB). (n=4). Two independent experiments.

6.4.4 Blocking LLT1-CD161 interaction reduces B cell survival and proliferation

In order to study the functional consequences of LLT1-CD161 interaction, I thought it would be useful to assess the blocking capabilities of different anti-CD161 antibodies. I performed the aggregate assay formation with transfected 300-LLT1 and 300-CD161 cells (see *3.3.2 Doublet formation*) and found two clones, the 191B8 and the HP-3G10, able to block aggregation (Figure 6-4A). They were further titrated and the 191B8 clone showed a greater effect at the lowest concentration tested (1 μg/ml). All the following blocking experiments were performed using this particular clone at 1 μg/ml.

I wanted to explore the consequences of blocking LLT1-CD161 interaction in the context of human GC B cells. In order to do so, I digested fresh tonsillar tissue with collagenase D and DNase I (see *6.3.6 Blocking experiments*) to ensure that the resulting cell suspension contained all the different cell types present, including the stromal ones such as FDCs. Tonsillar cells were incubated for 7 days on their own or with CpG or anti-CD40 + IL-4, stimuli known to promote B cell survival and proliferation and which are relevant within GC responses (Pauly et al. 2002). The effects of adding anti-CD161 antibody were tested in all three conditions. Both the addition of CpG and CD40 + IL-4 increased the percentage of live B cells seven days post-stimulation (Figure 6-4B). Interestingly, in both the unstimulated and stimulated samples, the presence of anti-CD161 reduced the proportion of surviving B cells, compared to the isotype control. Therefore, preventing LLT1-CD161 interaction had detrimental effects for B cell survival.

I next repeated the same experiment, this time assessing levels of B cell proliferation by intracellular staining of the nuclear antigen Ki67. The percentage of Ki67 expressing cells was lower in the samples containing anti-CD161, either when CpG or anti-CD40 + IL-4 stimuli were used (Figure 6-4C). The same procedure was performed, this time including a CTV stain to monitor cell proliferation. According to the Ki67 staining, the addition of anti-CD161 blocked B cell proliferation (Figure 6-4D) and this effect was dose-dependent (Figure 6-4E). These results suggest that blocking LLT1-CD161 interaction impairs B cell proliferation. As a control, I tested whether the presence of anti-CD161 on its own had any impact on B cell survival and found the percentage of live B cells was the same as in the unstimulated or isotype control samples (Appendix 5).

Overall, the data suggest that preventing LLT1-CD161 interaction reduces B cell survival and proliferation[3].

[3] These results were much more subtle, if detectable, when frozen tonsillar samples were used instead of fresh.

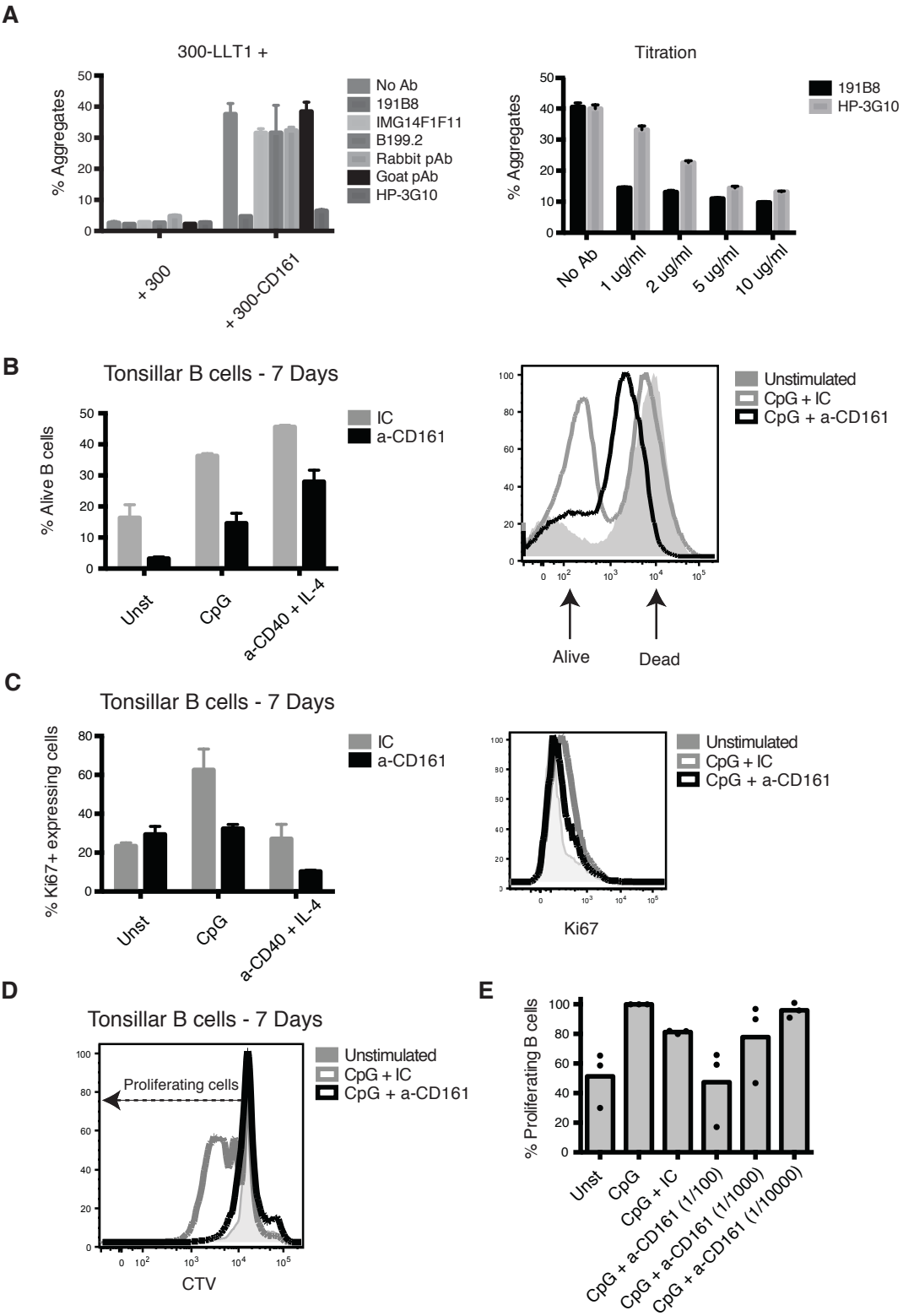
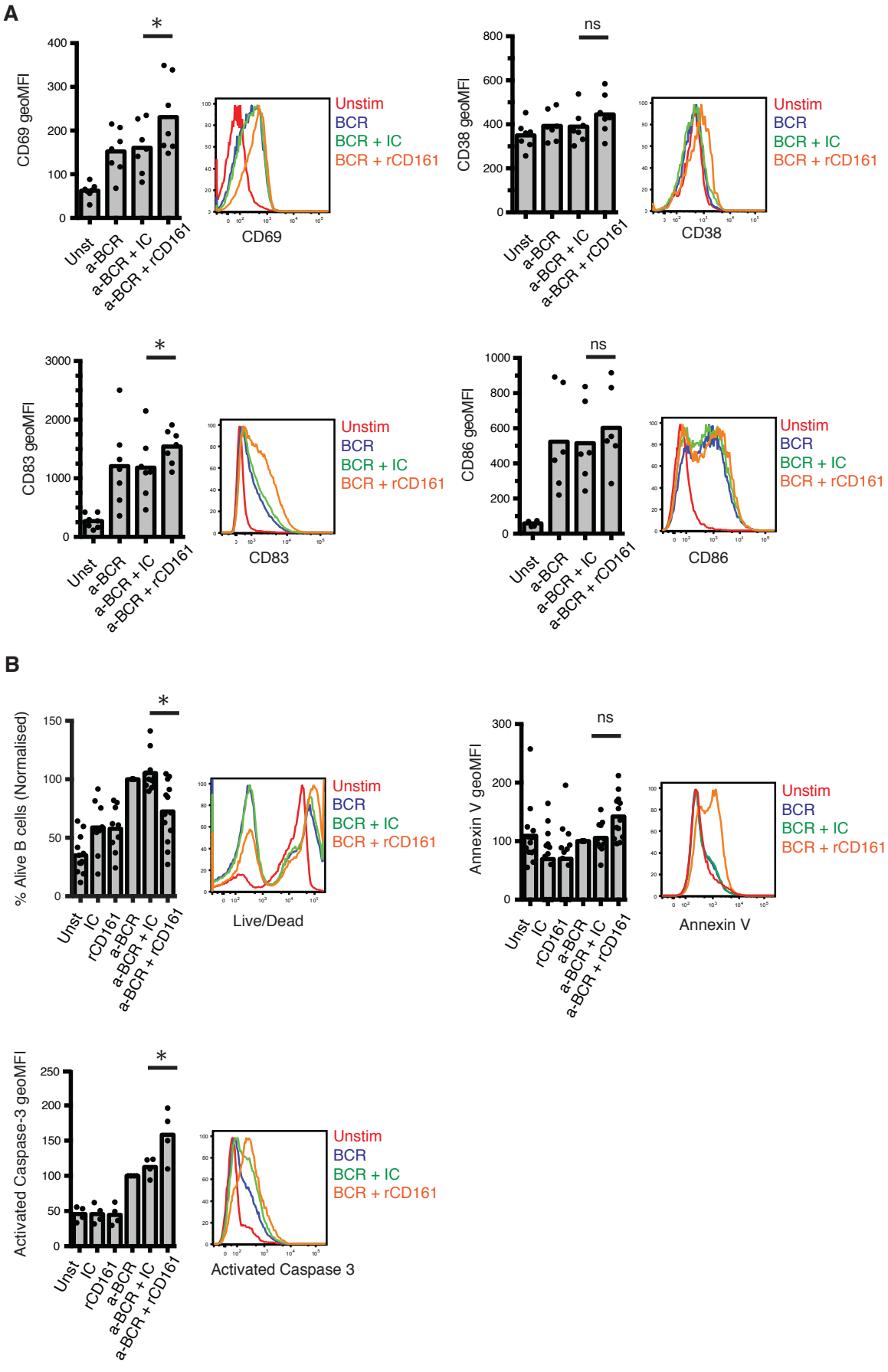


Figure 6-4. Blocking CD161-LLT1 interaction reduces B cell survival and proliferation. (A) CD161-LLT1 interaction could be blocked using two different clones of anti-CD161 antibodies (n=3). (B) The percentage of alive B cells after CpG stimulation for seven days decreased in the presence of anti-CD161 (n=4; two independent experiments). The presence of anti-CD161 decreased B cell proliferation after seven days, measured through the percentage of Ki67 expressing cells (C) or proliferating cells using a CTV stain (D) (n=4; two independent experiments). (E) shows the normalised percentage of proliferating B cells with different concentrations of anti-CD161, suggesting a dose-dependent effect (n=3).

6.4.5 LLT1 cross-linking promotes B cell activation and drives B cells towards a LZ phenotype

I have demonstrated the presence of the receptor-ligand pair LLT1 and CD161 in the GC environment, on B cells and FDCs respectively. Interactions between these two cell types are complex, involving a wide range of molecules (El Shikh MEM et al. 2010). Binding of the BCR to antigen presented by the FDC and CD40 to CD40L are crucial for the B cells' progression to receive Tfh cell help and go on to re-entre the DZ or exit the GC as plasmablasts or memory B cells (Crotty 2011; Meyer-Hermann et al. 2012; Victora et al. 2012; De Silva & Klein 2015).

As B cell - FDC interactions involve many different ligands and receptors, I started by exploring the role of LLT1 in isolated B cells. Initially, I investigated LLT1 signalling in primary B cells, inducing LLT1 expression through stimulation with anti-BCR, as previously described, ± rCD161 or a control protein (IC). The optimal concentrations for both BCR and rCD161 stimulation were titrated (Appendix 6) and the final concentrations used were 1µg/ml in both cases. Five days after stimulation, B cell expression of the activation markers CD69, CD38, CD83 and CD86 were measured by flow cytometry. Triggering of LLT1 on B cells through rCD161, in conjunction with BCR stimulation, resulted in enhanced B cell activation, with significantly higher increases in CD69 and CD83 seen in the presence of rCD161 compared to the controls (Figure 6-5A). Increases in CD38 and CD86 did not reach significance.


A
CD69 geoMFI
*
Unst
a-BCR
a-BCR + IC
a-BCR + rCD161
CD69
Unstim
BCR
BCR + IC
BCR + rCD161
CD38 geoMFI
ns
CD38
CD83 geoMFI
CD83
CD86 geoMFI
CD86
B
% Alive B cells (Normalised)
Unst
IC
rCD161
a-BCR
a-BCR + IC
a-BCR + rCD161
Live/Dead
Annexin V geoMFI
Annexin V
Activated Caspase-3 geoMFI
Activated Caspase 3

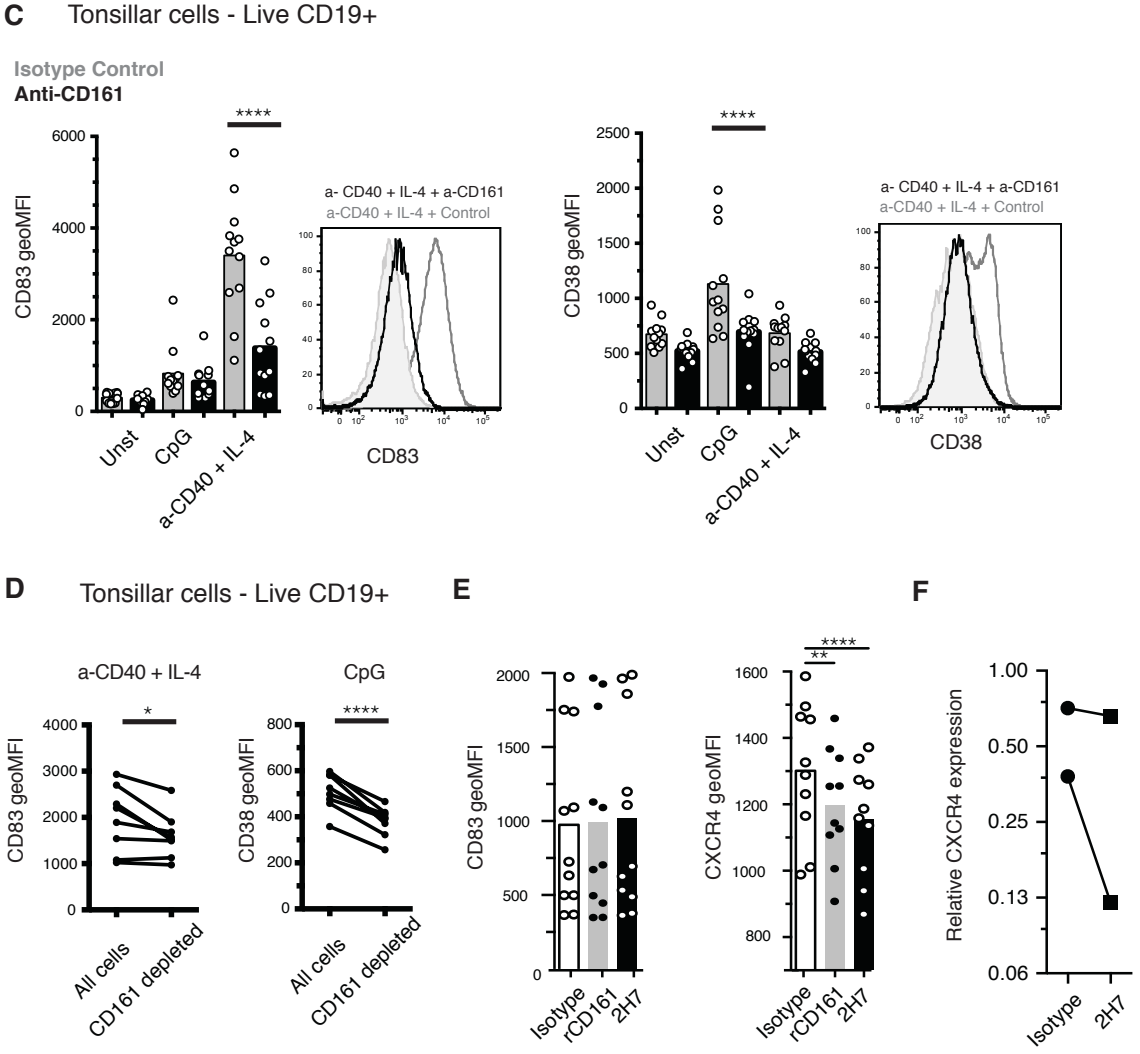


Figure 6-5. LLT1 promotes B cell activation and drives B cells towards a LZ phenotype. (A) Costimulation of purified B cells from PBMCs with anti-BCR and rCD161 resulted in higher levels of CD69, CD38 and CD83, but not CD86, than the isotype control (n=7), measured by flow cytometry. Data from three independent experiments; *<0.05. (B) Costimulation of purified B cells from PBMCs with anti-BCR and rCD161 resulted in a decrease in cell survival, compared to BCR stimulation only (n=9). This increased cell death correlated with higher levels of Annexin V (n=13) and activated caspase-3 (n=4) expression. Data from four (Cell survival and Annexin V) and three (Activated caspase-3) independent experiments.**<0.01 (C) Tonsillar cells were cultured for 3 days with CpG or anti-CD40 + IL-4. The blocking effects of anti-CD161 (191.B8) or Isotype Control (IC) were assessed by measuring the markers of B cell activation CD83 and CD38. Blocking LLT1-CD161 interaction resulted in a decreased expression of CD83 and CD38 on B cells (n=12; ****<0.0001 unpaired t-test). Data pulled together from four independent experiments. (D) Depletion of CD161+ cells from tonsillar cells resulted in decreased expression of CD83 (anti-CD40 + IL-4 stimulation) and CD38 (CpG stimulation) on B cells after 3 days (n=8; *<0.05, ****<0.0001 unpaired t-test). Data from two independent experiments. (E) Overnight (ON) stimulation of tonsillar B cells with rCD161 or 2H7 anti-LLT1 antibody did not change the expression of CD83 on GC B cells (n=11) but did reduce expression of CXCR4 (n=10, **<0.01, ****<0.0001). Data from three independent experiments (F) Repeated experiments on sorted DZ B cells revealed a down-regulation of CXCR4 mRNA. All statistics were analysed by two-way ANOVA using a multiple comparisons test unless otherwise specified.

I next analysed whether this same stimulation had any impact on B cell survival. The presence of rCD161 together with BCR stimulation resulted in decreased B cell survival (Figure 6-5B). Such results did not fit with my previous data, in which preventing LLT1-CD161 interaction also resulted in reduced B cell survival (Figure 6-4B). Considering that the stimulation provided activated the B cells to a great extent, I wondered whether the impaired survival could be due to Activation-induced cell death (AICD). To explore this possibility, I measured levels of Annexin V and Activated Caspase-3 and found that their expression was increased in the presence of rCD161 together with anti-BCR. However, the increment in Annexin V did not reach significance.

Overall, these results suggest that LLT1 stimulation through CD161 leads to B cell activation and this might cause AICD. As both proteins are highly glycosylated and have a weak binding strength (K_d of 48μM, Kamishykiryo et al. 2011), I wondered whether binding of naturally expressed LLT1 and CD161 would reveal stronger signalling. To analyse this, I cultured tonsillar cells for 3 days with either CpG or anti-CD40 + IL-4 and assessed their activation state by flow cytometry on day 3. The effect of LLT1 signalling was measured through the use of blocking antibodies to CD161 (Figure 6-4A). Stimulation of B cells with anti-CD40 + IL-4 resulted in a striking upregulation of CD83 on day 3, which could be prevented by adding anti-CD161 antibody (Figure 6-5C). The same effect could be observed with the CpG stimulated sample, although it was much less prominent. In contrast, levels of CD38 expression were highly increased upon CpG stimulation. Once again, this

effect could be prevented when the anti-CD161 antibody was used. These changes in CD83 and CD38 were B cell specific, as they could not be observed in the CD19- population (data not shown). The effect of the anti-CD161 blocking antibody on CD38 upregulation was assesed over time and using different stimuli (CpG, anti-CD40 + IL-4, anti-BCR and anti-CD40 + IL-4 + anit-BCR) (Appendix 7). In all cases, blocking LLT1-CD161 reduced B cell activation.

I repeated the experiments depleting the CD161-expressing cells and obtaining the same results (Figure 6-5D). Notice, however, how the decrease in both CD83 and CD38 expression were less prominent than with just blocking the specific LLT1-CD161 interaction, suggesting an important role for other receptors/ligands present in CD161+ cells or that the purity of the depletion was not 100%.

Finally, I explored the functional consequences of LLT1 cross-linking on GC B cells. The presence of rCD161 or the anti-LLT1 antibody (2H7) did not have an impact on CD83 expression levels, however, LLT1 cross-linking resulted in a reduction of CXCR4 (Figure 6-5E)[4]. Cross-linking of LLT1 not only had an effect on CXCR4 at a protein level but also at the mRNA, measured by qPCR (Figure 6-5F).

These findings suggest that LLT1 is involved in the transition of DZ B cells to the LZ, contributing to enhanced levels of CD83 expression while reducing

[4] This was also analysed on sorted light and dark zone B cells, where the effect of LLT1 cross-linking was most strongly seen in dark zone B cells. Under these circumstances, DZ B cells upregulated CD83 as well as downregulating CXCR4. However, these results could not be reproduced later on.

expression of the chemokine receptor CXCR4, a key feature of DZ B cells. Overall, these data support the idea that triggering LLT1 on B cells causes activation and drives DZ B cells towards a LZ phenotype.

6.5 Discussion

To better understand what function LLT1 might have within the context of the GC, I investigated potential sites of interaction by seeking the expression of its ligand, CD161. Lanier *et al.* originally identified the expression of CD161 on both CD4+ and CD8+ T cells, with a higher surface density on the latter (Lanier et al. 1994; Takahashi et al. 2006). More recently, CD161 expression has also been demonstrated on NK cells, CD4−CD8− double negative (DN) TCRαβ+ and TCRγδ+ T cells (Maggi et al. 2010; Fergusson et al. 2014). Further analysis identified two CD161+CD8+ populations, with intermediate or high CD161 expression levels (Takahashi et al. 2006; Billerbeck et al. 2010; Fergusson et al. 2014).

Given the close association of CD161 expression and T cells, CD161 expression was investigated on Tfh cells ($CXCR5^{mid/high}$). However, CD161 expression negatively correlated with CXCR5 expression, at both protein and mRNA levels (Figure 6-2). A potential explanation for this may lie in the transcription factor BCL-6. This master transcription factor drives maturation of T and B cells towards a full GC phenotype. As BCL-6 expression increases it suppresses other lineage-associated transcription factors, such as RORγT – a transcription factor associated with CD161 expression (Maggi et al. 2010;

Ivanov et al. 2006; Cosmi et al. 2008; Yu et al. 2009). Thus, it is plausible that BCL-6 inhibits the expression of CD161 through the suppression of RORγT. It is also possible that LLT1 is involved in modulating the initial interaction pre-Tfh ($CXCR5^{low}$) and the recently activated B cell in the T-B cell border within secondary follicles. The consequences of such interaction should be assessed in further studies.

Unexpectedly, CD161 was observed on FDCs (Figure 6-1). This was particularly surprising as it is uncommon for NK cell receptors to be expressed on non-haematopoietic cells, although relevant examples exist, e.g. KACL on keratinocytes (Spreu et al. 2010) and LLT1 on osteoblasts (Zhou et al. 2001).

Blocking LLT1-CD161 interaction decreased the percentage of live dividing B cells (Figure 6-4), suggesting a role for LLT1 in B cell survival and proliferation. It must be acknowledged that the increased percentage of live B cells could be a consequence of enhanced B cell division. Therefore, cross-linking of LLT1 on GC B cells would increase their chances of proliferation. In this particular environment, highly proliferative states are seen in DZ B cells as well as in recently exited plasmablasts. Thus, LLT1 arises as a potential modulator for B cell fate within the GC context and its exact role will require further investigation.

B cells compete, via their BCR, for antigen presented on the surface of FDCs. In addition, FDCs express a number of receptors that provide B cells with co-stimulatory signals required for subsequent progression within the GC (Gaspal et al. 2006; El Shikh et al. 2009; Wu et al. 2009; Kretschmer et al. 2007; Uhde

et al. 2013; Tew et al. 2001). In the context of other stimuli such as cross-linking of the BCR, LLT1 promoted the activation of B cells, as seen through increased expression of markers such as CD69, CD38 and CD83 (Figure 6-5A).

In addition to its role in defining the different transitional stages of B cells within the GC, as discussed below, CD83 is of particular interest because of its regulatory capacity. Studies using transgenic mice overexpressing CD83 have shown reduced B cell proliferation, Ig production and responsiveness to immunisation (Kretschmer et al. 2007; Uhde et al. 2013). Furthermore, CD83 signalling has been shown to directly interfere with BCR signalling (Kretschmer et al. 2007; Uhde et al. 2013). This may prevent overstimulation by the increased potency of Ag presented on FDCs (El Shikh et al. 2010; Tew et al. 2001; Aydar et al. 2005; Wu et al. 2007). An alternative function for CD83 is the promotion of MHC class II and CD86 expression required for subsequent Tfh cell interactions (Tze et al. 2011). Thus, LLT1's influence on CD83 expression may be important in preventing weakly binding BCRs from proceeding within the GC reaction, and/or preventing B cells with very high affinity BCRs from over-activation, while concurrently promoting Tfh cell interactions.

The role of particular lectins in the modulation of BCR responses has been explored before. For instance, CD22 and CD72 have been shown to down-modulate BCR-mediated signals (Nitschke et al. 2004). Furthermore, the C-type lectin CD23, the low affinity receptor for IgE, is also relevant in the

context of B cell responses (Reljii et al. 1997), as it acts as a ligand for CD21 within the BCR complex. Interestingly, CD23 has been found highly expressed in a proportion of FDCs. Thus, the data presented here is consistent with a contribution of C-type lectins to B cell responses through FDC-B cell interactions. This is particularly meaningful, as CLRs, once believed to be essentially involved in innate immunity, have now been shown to play a prominent role in the GC reaction, a hallmark of adaptive immunity.

To my knowledge, one sole paper describing the signalling pathway employed by LLT1 has been published (Bambard et al. 2010). Bambard and colleagues ligated LLT1 on NK92 cells using fixed, transfected K562-CD161 cells and reported ERK phosphorylation through western blot analysis. I was not able to detect changes in pERK in B cells stimulated with rCD161 using a phosphoflow approach. The different levels of LLT1 and CD161 expression on the cell types tested, the distinct nature of the cells examined, as well as the presence of other receptors and the methodology used could potentially explain such differences. Further investigation is required to elucidate the signalling pathway of LLT1, which might contribute to a better understanding of its function in different contexts.

In addition to physical separation, light and dark zone B cells have distinct gene expression profiles that reflect the underlying processes being undertaken (Victora et al. 2012; McHeyzer-Williams et al. 2015). The light and dark zones can be identified by the predominant expression of CD83 (LZ) and CXCR4 (DZ) (Victora & Nussenzweig 2012; Victora et al. 2010; Allen et al. 2004; Caron et al. 2009). Using multi-photon laser microscopy and transgenic

mice that expressed photoactivatable green fluorescent protein, Victora *et al.* tracked the movement of B cells between the zones and demonstrated that entry into the DZ was determined by Tfh cell contact; this was recently extended by Gitlin *et al.* (Victora et al. 2010; Gitlin et al. 2014). Bannard *et al.* observed that the physical separation of cells into the DZ was dispensable for B cells to proceed through the GC reaction, as $CXCR4^{-/-}$ B cells were still able to transit into a centroblast phenotype and acquire mutations, albeit at a lower level compared to their wild type (w/t) counterparts. However, CXCR4 expression was required for efficient participation in the GC reaction, as $CXCR4^{-/-}$ cells were outcompeted by w/t B cells (Bannard et al. 2013).

Here, cross-linking of LLT1 alone resulted in a reduction in both surface expression of CXCR4 and at mRNA level (Figure 6-5E and 6-5F). Given the importance of CXCR4 in the migration of B cells into the DZ, and together with the previously shown upregulation of CD83, this suggests that LLT1 could play an important role in orienting B cells within the LZ. Overall, these results fit with the recently described transitional states of successful B cell clones (McHeyzer-Williams et al. 2015). According to the study performed by McHeyzer-Williams *et al.*, DZ resident stage 1 B cells ($CD83^{-}$ $Pol\eta^{-}$) migrate to the LZ, transitioning to stage 2 and upregulating CD83. As I also found a link between LLT1 cross-linking and proliferation, it is tempting to speculate that together with promoting a LZ phenotype, LLT1 would play a role in keeping B cells dividing. However, whether that is in the form of plasmablasts that have exited the GC after being selected in the LZ or in re-entering the DZ for further rounds of proliferation and mutation remains unknown.

The data presented here suggests a critical role for innate components of human immunological responses such as LLT1 and CD161 in the GC, a core element within adaptive immunity. I propose that LLT1-CD161 interaction plays a key role in the GC reaction, activating GC B cells, promoting the DZ to LZ switch, facilitating Tfh interaction, and, thus, selection of high affinity B cell clones.

Although GCs were first characterised more than 125 years ago, the concrete details of how the GC reaction is orchestrated are still unknown. A deep understanding of how it functions and the interplay between all the cell types involved will be very useful for effective vaccine design and targeted production of high-affinity antibodies. It will also provide invaluable input on how reactive self-antibodies are generated as well as the mechanisms underlying malignant transformation, thus helping the prevention of autoimmunity and cancer.

6.6 Summary

- CD161 is expressed on FDCs and on a subset of T follicular cells
- LLT1 cross-linking on B cells does not involve the ERK signalling pathway
- LLT1 cross-linking is associated with B cell activation, proliferation and survival, as well as with promoting phenotypes associated with the DZ to LZ transition

7 Discussion

This thesis set out to explore the distribution, regulation and function of LLT1. Most of the results described in this thesis have already been discussed in their respective chapters. This final chapter will be used to summarise the main findings, to explain how they fit and contribute to the current knowledge, particularly within the concepts of immune-privilege and the GC reaction, as well as to acknowledge the limitations of the work and possible future directions.

7.1 The original aims of the thesis

The main aims of this thesis, together with its main related findings are summarised below:

1. *Identify, characterise and optimise the tools necessary for the study of LLT1*

   Two novel anti-LLT1 mAbs have been studied. The 7G7 clone can effectively be used for immunohistological staining of LLT1 on GCs. The 2H7 clone can also be used for its immunohistological staining, as well as for extracellular FACS staining. Furthermore, it is a valuable tool for functional studies, as it is capable of cross-linking LLT1, as well as blocking CD161-LLT1 interactions.

2. *Describe the distribution of LLT1 in healthy human tissue and how it may be altered in the context of disease*

LLT1 is expressed in various human healthy tissues, and its expression is particularly strong in immune-privileged sites. Furthermore, it is upregulated in the liver under inflammatory conditions. Within PBMCs, it is expressed on B cells and monocytes. LLT1 is highly expressed on GC B cells, early plasmablasts and most GC-derived B cell lymphomas (Table 7.1).

3. *Investigate the regulatory mechanisms that determine the levels of LLT1 expression on B cells*

LLT1 is upregulated on B cells with CpG, Poly(I:C), BCR and CD40 stimulation, and its expression is associated with proliferation.

4. *Explore the distribution of CD161 in the context of LLT1 and investigate the function of LLT1 in the GC*

LLT1 inhibits NK cell degranulation. In the GC environment, CD161 is expressed on FDCs and on a subset of T follicular cells. LLT1 cross-linking is associated with B cell activation, proliferation and survival, as well as with promoting phenotypes associated with the DZ to LZ transition.

	Cell type	Potential sites for interaction	Potential function
CD161 expression	T cells NK cells **FDCs cells**		**NK cell inhibition** T cell inhibition/activation
LLT1 expression	Osteoblast PBMCs (Table 1.1) **GC B cells** **Early Plasmablasts** **B cell lymphomas** RSV-infected lung epithelia RA joints **Inflamed liver** **Brain, placenta, testes**	Bone Lymph nodes **Inflamed tissues** **Germinal centres** **Immune-privileged sites**	NK IFN-γ production Osteoclast inhibition **B cell activation** **DZ to LZ transition**

Table 7.1. CD161 and LLT1 expression and function. Cell types expressing the C-type lectins CD161 and LLT1 are specified, as well as potential sites for their interaction and functions as described in the published literature. The work performed in this project is highlighted (bold).

7.2 Tools

7.2.1 Anti-LLT1 antibodies

Due to a limited availability of tools, the published literature regarding the distribution, regulation and function of LLT1 has been scarce and presents inconsistencies. Here, I present various antibodies and transfected cell lines that will contribute importantly to the study of LLT1.

One of the main discrepancies arising from previous studies regards LLT1 expression on PBMCs (Table 1.1). I have shown that efficient binding of different anti-LLT1 antibodies can be technique-dependent (Chapter 3) and can rely on the specific status of the cells examined, such as activation or glycosylation (Figure 3-8). Moreover, in the case of IHC, the results show how the processing of the sample (eg. fixation, antigen retrieval) may impact the effectiveness of the staining. This includes alteration of the native conformation of the protein, as well as masking/unmasking of particular epitopes.

Overall, despite describing and validating some new tools for the study of LLT1, further characterisation is required to fully understand how different anti-LLT1 antibodies recognise this C-type lectin and whether other Clec2D spliced variants are also recognised.

7.2.2 Anti-CD161 antibodies

I explored the blocking capabilities of distinct anti-CD161 antibodies and decided to use the 191B8 clone for the functional experiments (Figure 6-4). However, the potential cross-linking effects of this particular clone were not assessed in this study. Therefore, although it is unlikely that the effects seen due to the anti-CD161 are a product of its ligation on FDCs and/or T cells (the ligand LLT1 is already present), this possibility cannot conclusively be ruled out.

7.2.3 LLT1 ELISA

Amongst the different Clec2D spliced variants, two are soluble (Germain et al. 2010): soluble LLT1 and soluble variant 4 (see *1.4.2 Human LLT1*). The potential role of soluble LLT1 was not addressed in this study. One of the key techniques for the analysis of soluble proteins is the ELISA. The work required to set up and optimise an ELISA for the detection of LLT1 has been started but is still, however, in its early stages.

7.3 LLT1 Function

7.3.1 Cross-talk

I found LLT1 and CD161 to be expressed in different subgroups of lymphocytes as well as monocytes (Figure 4-1) and stromal cells (Figure 6-1). I also described expression of LLT1 in various human healthy tissues and particularly in immune-privileged sites (Figure 4-3 and Table 4-1). It is tempting to speculate that this pair of C-type lectins is involved in the cross-talk between distinct LLT1 and CD161 expressing immune cell types, such as B cells and T cells or monocytes and NK cells. The closely related pair of C-type lectins NKp80-AICL follows this same pattern: they are expressed on NK cells and monocytes, respectively, and playing a role in reciprocal cell activation (Welte et al. 2006). The other well-described human C-type lectin pair is NKp65-KACL, which is expressed mainly on NK cells and keratinocytes, respectively (Spreu et al. 2007). Thus, this particular pair illustrates a very different case, as it is involved in the immune surveillance of

a specific tissue (ie. skin). This framework could also apply to LLT1 and CD161, both in terms of B cell – FDC interaction and of NK cells and immune-privileged sites, although these hypotheses require further investigation.

7.3.2 Activation

Studies regarding the function of LLT1 in cells that express this C-type lectin are very limited. Cross-linking of LLT1 on primary NK cells as well as in NK cell-derived cell lines (YT and NK92) resulted in increased IFN-γ production, with no alteration of their cytotoxic capacity (Mathew et al. 2004; Bambard et al. 2010). Although I could not detect LLT1 on primary NK cells, it is possible that the particular conditions in which the cells were kept resulted in these differences.

Interestingly, I characterised LLT1's involvement in B cell activation (Figure 6-5). Therefore, the data available suggest that LLT1 may promote activation of immune cells, which is supported by the lack of an ITIM motif in its cytoplasmic domain (Boles et al. 1999).

7.3.3 Immune-privilege

I showed high expression of LLT1 in immune-privileged sites (Figure 4-3 and Figure 4-4). It is believed that immune-privilege is the result of an evolutionary process that confers special immune tolerance to certain structures (Hong and Van Kaer 1999). Organs such as the eye, the brain or the placenta present the exceptional capacity of preventing classical inflammatory

responses that could be highly detrimental or even fatal. This singular immune status is linked to low expression levels of MHC class I molecules, which subsequently leads to increased susceptibility to being killed by NK cells.

I have shown that the presence of LLT1 results in decreased NK cell function (Figure 4-6), as other studies have done (Aldemir et al. 2005; Rosen et al. 2005; Roth et al. 2007; Rosen et al. 2008; Mathew et al. 2014). Therefore, LLT1 could play a prominent role in keeping NK cells under control in immune-privileged sites, thus preventing damage of low-expressing MHC class I tissues. This hypothesis matches with the role described for the mouse version of LLT1, mClr-b. However, the distribution of mClr-b differs substantially from its human homolog, as it is believed to be expressed almost ubiquitously, similarly to MHC class I molecules (Zhang et al. 2012).

7.3.4 The GC Model

I described high expression of LLT1 on GC-associated B cells, early plasmablasts and GC-derived lymphomas. LLT1 expression was readily induced via BCR, CD40 and CpG stimulation on B cells. Unexpectedly, I found high expression of the LLT1 ligand, CD161, on FDCs. Triggering of LLT1 supported B cell activation, CD83 upregulation and CXCR4 downregulation, consistent with a role in driving transition from a dark to a light zone phenotype. The model outlined in Figure 7.1 summarises my findings.

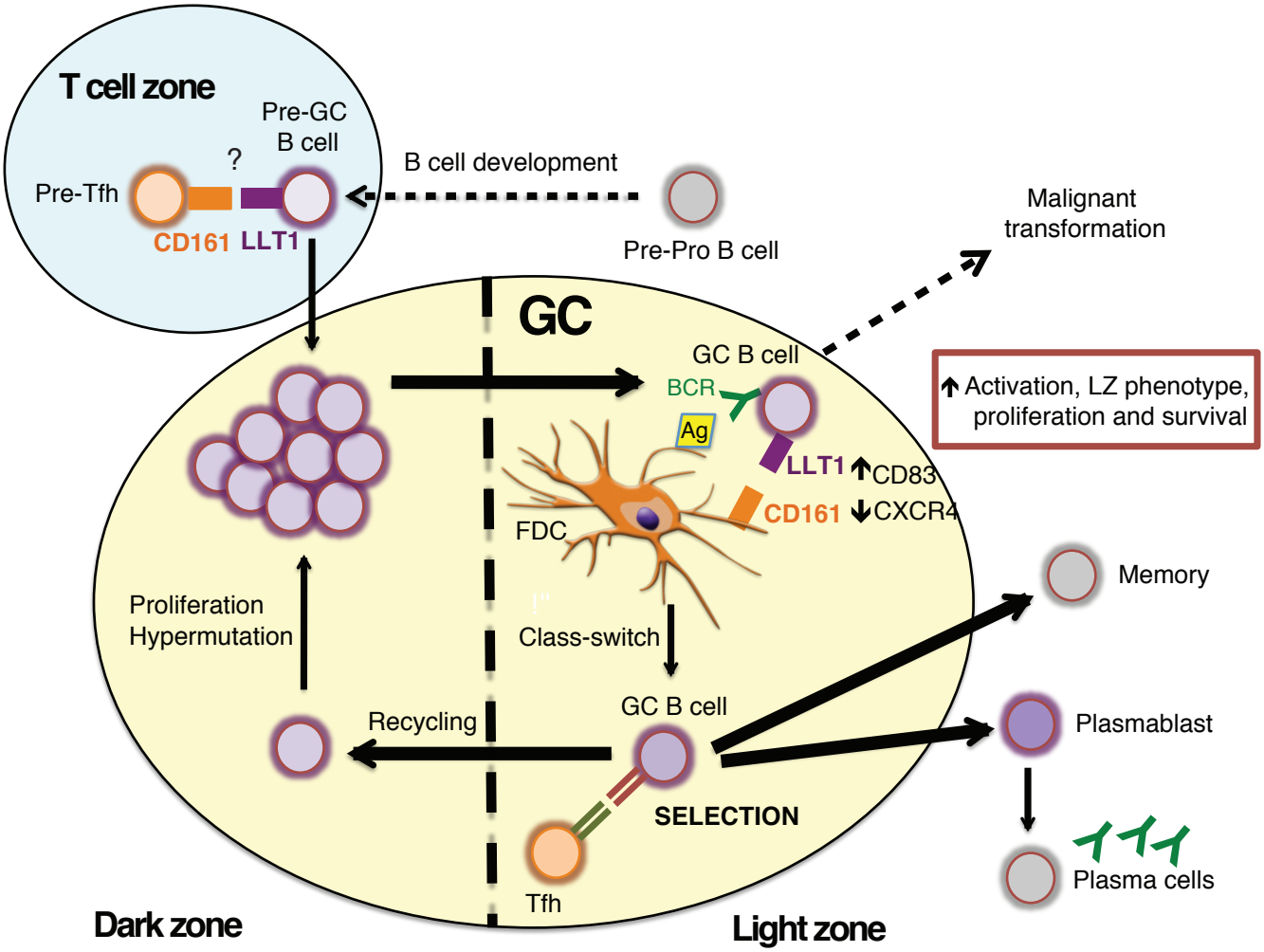


Figure 7-1. The role of LLT1 in GC. LLT1 is not expressed on early stages of B cell differentiation, until reaching the pre-GC state. In the T-B cell border, pre-GC B cells interact with pre-Tfh cells, which express lower CXCR5 levels than their Tfh cell counterparts and, accordingly, higher levels of CD161. The ones with highest affinity enter the GC reaction, proliferating and mutating their BCRs in the DZ. They then migrate to the LZ, where they capture antigen from FDCs while being stimulated by CD161. These interactions result in increased B cell activation, proliferation and survival; B cells will upregulate CD83 and downregulate CXCR4, switching into a full LZ phenotype and preparing for optimal Tfh interaction and, therefore, selection. High affinity clones will either exit the GC as memory B cells or plasmablasts, or re-enter the DZ for iterative rounds of proliferation and mutation to fine-tune their BCRs.

7.4 Limitations and Future directions

During the course of this work, I have encountered several limitations, which are detailed below. This thesis has also raised a number of questions, which are also summarised in this section, together with possible means to answer them.

7.4.1 LLT1 distribution

The availability of tissue arrays for LLT1 staining was a good tool for initial studies aiming to broadly characterise LLT1 distribution. However, the limited amount of tissue sample, the difficulty of performing a tissue-dependent optimisation and the fact that the assessment of LLT1 expression was qualitative made it difficult to reach definitive conclusions. It would be ideal to examine and optimise tissues individually, as well as to quantify levels of LLT1 mRNA in a wide variety of them, a process started by Boles *et al*. (Boles et al. 1999).

7.4.2 Immune-privilege and inflammation

I have shown expression of LLT1 in immune-privileged sites. To assess whether LLT1 protects from NK cell killing in this particular setting, LLT1-expressing neuronal or placental-derived cell lines could be used as target cells. Levels of NK cell degranulation (ie. CD107a) or cytokine production (e.g. IFN-γ) could be assessed and compared with those produced when LLT1-CD161 interaction is blocked, for example, using the 2H7 clone.

The same experiment could be performed to assess whether LLT1 inhibitis NK/MAIT cell function when interacting with inflamed hepatocytes. Huh7 or HHL12 cells could be treated with Poly(I:C) to upregulate LLT1 (Figure 4-7) and NK killing assays, with and without blocking antibodies, performed. MAIT cells could be stained intracellularly for cytokines such as IFN-γ, IL-17 (Ussher JE et al. 2014; Dusseaux et al. 2011) or perforin and granzymes (Kurioka et al. 2015), as correlates of function.

7.4.3 Signalling through LLT1

I could not detect ERK signalling through LLT1, as previously described (Bambard et al. 2010). Further studies will be necessary to elucidate the potential role of LLT1 in modulating BCR signalling. Different techniques such as western blot and phosphoflow could be tested, targeting several proteins involved in the BCR signalling pathway. Calcium mobilisation assays could also be performed. Studies such as the one describing how the drug Rituximab inhibits BCR signalling could be a good starting point (Kheirallah et al. 2015). Alternatively, a microarray analysis could be performed to extensively analyse the pathways triggered by LLT1 cross-linking.

7.4.4 Pre-Tfh – pre-GC B cell interaction

I described a negative correlation between expression levels of CXCR5 on tonsillar T cells and CD161 (Figure 6-2), as well as upregulation of LLT1 on B cells upon activation (Figure 6-5). Therefore, it would be interesting to study

the impact of CD161+ pre-Tfh cells with recently activated LLT1+ B cells in the B-T cell border within secondary follicles. Levels of typical Tfh phenotypical markers could be measured, such as CXCR5, ICOS, PD-1 (Crotty et al. 2003; McAdam et al. 2001; Tafuri et al. 2001; Haynes et al. 2007), alongside the transcription factor BCL-6 (Johnston et al. 2009; Yu et al. 2009) or the cytokines IL-4 and IL-21 (Howard et al. 1982; Peschel et al. 1987; Parrish-novak et al. 2000). On the B cell side, levels of chemokine receptors such as CXCR4 and CXCR5 could be measured (Allen et al. 2004), as well as BCL-6 (Ci et al. 2009; Phan & Dalla-favera 2004; Ranuncolo et al. 2007), AID (Durandi et al. 2003), CD83 or Polη (McHeyzer-Williams et al. 2015). Such experiments would permit us to analyse whether CD161-LLT1 interaction contributes to the maturation of pre-Tfh and pre-GC B cells to Tfh and GC B cells, respectively.

7.4.5 LLT1 function within the GC

The results presented in this thesis show that LLT1 cross-linking is associated with B cell activation, proliferation and survival, as well as with the promotion of phenotypes associated with the DZ to LZ transition (Figure 6-4, 6-5 and 6-6). To further characterise it, a transcriptional microarray analysis could be performed in LLT1-expressing GC B cells cross-linked with rCD161, the 2H7 mAb or 300-CD161 cells. This would help to elucidate the functional consequences of CD161-LLT1 interaction on B cells. Furthermore, levels of AID and Polη could be measured by FACS or qPCR to see whether LLT1 is involved in BCR diversification of GC B cells.

7.4.6 CD161 function within the GC

It would be of great interest to explore the consequences of LLT1-CD161 ligation on CD161-expressing cells in the GC context (ie. FDCs or follicular T cells). CD161-expressing T cells could be FACS-sorted and stimulated with a cross-linking anti-CD161 antibody, 300-LLT1 cells or sorted GC B cells. Different phenotypical and functional markers (see *7.4.4 Pre-Tfh – pre-GC B cell interaction)* could be measured though FACS, qPCR or a microarray transcriptional analysis performed. It would be interesting to study whether CD161 has any effect on T follicular cell proliferation, as I could not detect any CD4+ Ki67+ cells in tonsils (Appendix 8) and subsets of CD8+ $CD161^{high}$ T cells unable to proliferate have been described (Takahashi et al. 2006).

Work with FDCs proved to be challenging. These stromal cells are large and fragile, difficult to isolate, stain and culture. I encountered several technical limitations when trying to analyse them using flow cyometry or FACS-sorting. This was due to abundant non-specific binding despite blocking of Fc receptors, poor staining with the CNA.42 clone and scarcity of single cells due to their close interactions with other cell types (e.g. B cells). If such technical limitations could be overcome, FDCs could be FACS-sorted and directly stimulated with a cross-linking anti-CD161 antibody, 300-LLT1 cells or GC B cells. Alternatively, the same blocking experiments could be performed and levels of IL-6 or CXCL13 could be measured by intracellular FACS staining or ELISA (Wu et al. 2009; Estes et al. 2004). CXCL13 is mainly produced by FDCs and attracts CXCR5+ cells (Ansel et al. 2000). IL-6 can be produced by various cell types including FDCs, and its role in GC development, antibody

production and receptor editing has been described (Kopf et al. 1998; Yan et al. 2012). Ultimately, a microarray transcriptional analysis could also be performed.

7.4.7 LLT1 in plasmablasts

I characterised high levels of LLT1 expression on early plasmablasts (Figure 5-5, 5-6 and 5-7). I showed a slight increase in cell survival when plasma cells were differentiated *in vitro* from memory B cells (Appendix 9). It would be interesting to explore LLT1 functionality on this cell type, particularly, whether it plays a role in antibody production or the class switching of antibodies, which could be studied using ELISA. Furthermore, BCR sequencing could bring some insight into possible correlations between the number of acquired mutations and LLT1 expression.

7.4.8 Mouse work

Finally, and once there is a better understanding of the similarities and differences between the mouse and human systems, it would be particularly revealing to perform studies *in vivo*.

The presence of Clr-b on mouse B cells has not been explored in detail. Nonetheless, the fact that a positive signal could be detected after staining 300 cells (derived from murine pre-B cells) with anti-LLT1 antibodies (Figure 3-1) suggests a certain degree of cross-reactivity, and thus potential

expression of Clr-b in murine B cells. It would be of particular interest to look at GC murine B cells.

Clr-b$^{-/-}$ mice exist[5] (Kartsogiannis et al. 2008) and their phenotypic abnormalities are limited to bone, with these animals suffering from osteopenia. However, despite their overall healthy appearance, these mice were never immunologically challenged. If the homology between both systems is high enough, *Clr-b*$^{-/-}$ mice could become an invaluable tool for the study of human GC responses. They would facilitate the process of vaccine design and help us to understand and target the generation of autoantibodies and malignant transformation. If Clr-b is expressed on murine GC B cells, and if an antibody capable of recognising it and blocking interaction with its receptor Nkrp1B/D is available, it would be of great interest to block such interaction and study the consequences in GC responses. GC formation, GC development, proliferation and mutation of B cells, as well as antibody production and class-switching could be assessed.

Conditional knock-outs would also be a very useful tool. Once the GC is formed and functional, it would be interesting to study dynamics and movements of GC B cells depending on the presence or absence of LLT1. One could also monitor and time their interactions with other cell types present, such as FDCs or Tfh. Ultimately, the generation of high affinity plasma cells and memory B cells could be measured.

[5] Although we did not have access to them.

Alternatively, GC centres could be generated *in vitro* and the consequences of blocking LLT1-CD161 interactions could be analysed using blocking antibodies. Although it is still technically challenging, the generation of *ex vivo* engineered three-dimensional organoids mimicking GCs has been reported (Sukumar et al. 2011; Purwada et al. 2015).

Following this, a therapeutic role for anti-LLT1 antibodies could be tested. These could act in a similar way to Rituximab, a mAb against CD20, which destroys B cells and is therefore useful for the treatment of different diseases characterised by excessive, overactive or dysfunctional B cells, such as different B cell lymphomas, RA or systemic lupus erythematosus (Maloney et al. 2015; Pescovitz 2006; Gashi et al. 2014; Beckwith & Lightstone 2014).

7.5 Summary and implications

This work focuses on the genetically linked C-type lectin-like receptor pair LLT1 and CD161, the tools for their study and their role in immune responses. These molecules are tightly regulated and can modify lymphocyte behaviour – but their functional impact, particularly in critical tissues, had not been fully explored. Here, I demonstrate the central role that they play in the GC reaction and a potential regulatory function in immune-privileged and inflamed tissues.

I identified the presence of both LLT1 and its ligand CD161 in the GC, predominantly on GC B cells and FDCs, respectively (Table 7.1). I defined the main factors involved in LLT1 regulation and its expression on GC B cells

both through normal development and in cancer. Most importantly, at a functional level, I showed that LLT1 contributes to B cell activation and promotes the switch from a DZ B cell phenotype to a LZ B cell phenotype, thus potentially enabling the essential process of selection of high affinity B cell clones. These results show the significance of this molecular pair, which is associated with innate lymphocyte populations at a critical point in the adaptive immune response.

This study provides a new set of tools for research on human LLT1/CD161, interventional studies, and for the elucidation of crucial aspects of human GC biology. The main outcome of the GC reaction is the selection of clones expressing high affinity BCRs that are essential for effective vaccine design as well as development of autoantibodies. Moreover, as GCs show high rates of proliferation and mutation, they become hot spots for the development of B cell lymphomas. This study is therefore broadly relevant to the immunological field as it characterises fundamental aspects of the human GC reaction, with implications for host defence, innate and adaptive immunity, inflammation and cancer.

8 References

Aldemir H. et al., 2005. Cutting edge: lectin-like transcript 1 is a ligand for the CD161 receptor. *J Immunol*, 175(12), pp.7791–5.

Alexander C.M., et al., 2011. T regulatory cells participate in the control of germinal centre reactions. *Immunology*, 133(4), pp.452–68.

Alizadeh, A.A. et al., 2000. Distinct types of diffuse large B-cell lymphoma identified by gene expression profiling. *Nature*. 3;403(679), pp.503-11.

Allen, C.D. et al., 2004. Germinal center dark and light zone organization is mediated by CXCR4 and CXCR5. *Nat Immunol* 5(9), pp.943–952.

Allen, C.D & Okada, T., 2007. Imaging of germinal center selection events during affinity maturation. *Science* 315(5811), pp.528–532.

Allen, C.D.C., Okada, T. & Cyster, J.G., 2007. Germinal-center organization and cellular dynamics. *Immunity*, 27(2), pp.190–202.

Allman, D. & Pillai, S., 2008. Peripheral B cell subsets. *Curr Opin Immunol*, 20(2), pp.149–57.

Ansel, K.M. et al., 2000. A chemokine-driven positive feedback loop organizes lymphoid follicles. *Nature* 406(6793), pp.309–314.

Bambard, N.D., Mathew, S.O. & Mathew, P. a, 2010. LLT1-mediated activation of IFN-gamma production in human natural killer cells involves ERK signalling pathway. *Scand J Immunol*, 71(3), pp.210–9.

Bannard, O. et al., 2013. Germinal center centroblasts transition to a centrocyte phenotype according to a timed program and depend on the dark zone for effective selection. *Immunity*, 39(5), pp.912–24.

Barker C. F. & Billingham RE, 1977. Immunologically privileged sites. *Adv. Immunol.* 25, pp.1-54.

Basso, K. & Dalla-Favera, R., 2015. Germinal centres and B cell lymphomagenesis. *Nat Rev Immunol*, 15(3), pp.172–184.

Batista, F.D. & Harwood, N.E., 2009. The who, how and where of antigen presentation to B cells. *Nat Rev Immunol*, 9(1), pp.15–27.

Baumjohann, D., Okada, T. & Ansel, K.M., 2011. Cutting Edge: Distinct waves of BCL6 expression during T follicular helper cell development. *J Immunol* 187(5), pp.2089–92.

Béguelin, W. et al., 2013. EZH2 Is Required for Germinal Center Formation and Somatic EZH2 Mutations Promote Lymphoid Transformation. *Cancer Cell*, 23(5), pp.677–692.

Von Behring, E. & Kitasato, S., 1890. Ueber das zutandekommen der diphtherie-immunitat und der tetanus-immunitat bei thieren. *Deutsche Medizinsche Wochenschrift*, 16, pp.1113–1114.

Baumann I. et al., 2002. Impaired uptake of apoptotic cells into tingible body macrophages in germinal centers of patients with systemic lupus erythematosus. *Arthritis Rheum.* 46(1), pp.191-201.

Bende R.J. et al., 2007. Germinal centers in human lymph nodes contain reactivated memory B cells. *J Exp Med.* 204(11), pp.2655-65.

Bernard, O. & Hozumi, N., 1978. Sequences of Mouse Immunoglobulin Light Chain Genes before and after Somatic Changes. *Cell* 15(4), pp.1133–1144.

Biassoni, R. et al., 2005. Molecular and functional characterization of NKG2D, NKp80, and NKG2C triggering NK cell receptors in rhesus and cynomolgus macaques : Monitoring of NK Cell Function during Simian HIV Infection 1. *J Immunol*. 174(9), pp.5695-705.

Blink, E.J. et al., 2005. Early appearance of germinal center-derived memory B cells and plasma cells in blood after primary immunization. *J Exp Med*, 201(4), pp.545–54.

Boles, K.S. et al., 1999. Cloning of a new lectin-like receptor expressed on human NK cells. *Immunogenetics*, 50(1-2), pp.1–7.

Brooks, S.A., 2004. Appropriate glycosylation of recombinant proteins for human use: implications of choice of expression system. *Mol Biotech* 28(3), pp.241-55.

Bruton, O. C. 1952. Agammaglobulinemia. *Pediatrics.* 6, 722–728.

Bubeník, J., 2005. MHC Class I Downregulation , Tumour Escape from Immune Surveillance and Design of Therapeutic Strategies. *Folia Biol* 51(1): pp.1–2.

Burnet, F.M., 1959. The Clonal Selection Theory of Acquired Immunity. *Vanderbilt Univ. Press*.

Caganova, M. et al., 2013. Germinal center dysregulation by histone methyltransferase EZH2 promotes lymphomagenesis. *J Clin Invest*, 123(12), pp.5009–22.

Cambi, A. & Figdor, C.G., 2003. Dual function of C-type lectin-like receptors in the immune system. *Curr Opin Cell Biol*, 15(5), pp.539–546.

Cambi, A., Koopman, M. & Figdor, C.G., 2005. How C-type lectins detect pathogens. *Cellular microbiology*, 7(4), pp.481–8.

Carlyle, J.R. et al., 2008. Evolution of the Ly49 and Nkrp1 recognition systems. *Semin Immunol*, 20(6), pp.321–30.

Carlyle, J.R. et al., 2004. Missing self-recognition of Ocil/Clr-b by inhibitory NKR-P1 natural killer cell receptors. *Proc Natl Acad Sci U S A*, 101(10), pp.3527–32.

Carlyle, J.R. et al., 2006. Molecular and genetic basis for strain-dependent NK1.1 alloreactivity of mouse NK cells. *J Immunol*, 176(12), pp.7511–7524.

Caron, G. et al., 2009. CXCR4 expression functionally discriminates centroblasts versus centrocytes within human germinal center B cells. *J Immunol,* 182(12), pp.7595–602.

Carsetti, R., 2004. Peripheral development of B cells in mouse and man. *Immunol Rev*, 197, pp.179–191.

Cattoretti, B.G. et al., 1995. BCL-6 protein is expressed in germinal-center B cells. *Blood*, 86(1), pp.45-53

Cattoretti, G. et al., 2005. Deregulated BCL6 expression recapitulates the pathogenesis of human diffuse large B cell lymphomas in mice. *Cancer cell*, 7(5), pp.445–55.

Chalan, P. et al., 2015. Expression of Lectin-Like Transcript 1, the Ligand for CD161, in Rheumatoid Arthritis. *Plos One*, 10(7), e0132436.

Chambers, W.H. et al., 1989. Monoclonal antibody to a triggering structure expressed on rat natural killer cells and adherent lymphokine-activated killer cells. *J Exp Med*, 169(4), pp.1373–1389.

Chan, T.D. et al., 2012. Elimination of germinal-center-derived self-reactive B cells is governed by the location and concentration of self-antigen. *Immunity*, 37(5), pp.893–904.

Christmas, P., 2010. Toll-Like Receptors: Sensors that Detect Infection. *Nature Education*, 3(9), p.85.

Ci, W. et al., 2009. The BCL6 transcriptional program features repression of multiple oncogenes in primary B cells and is deregulated in DLBCL. *Blood*, 113(22), pp.5536–5549.

Claman, H. N., Chaperon, E. A. & Triplett, R.F., 1966. Thymus-marrow cell combinations. Synergism in antibody production. *Proc. Soc. Exp. Biol. Med*, 122, pp.1167–1171.

Clark, E.A. & Ledbettert, J.A., 1986. Activation of human B cells mediated through two distinct cell surface differentiation antigens , Bp35 and Bp5O. *Proc Natl Acad Sci U S A* 83(12), pp.4494–4498.

Clayton R.F. et al., 2005. Liver cell lines for the study of hepatocyte functions and immunological response. *Liver Int.* 25(2), pp.389-402.

Crotty, S., 2015. A brief history of T cell help to B cells. *Nature Reviews Immunology*, 15(3), pp.185–189.

Crotty, S. et al., 2003. SAP is required for generating long-term humoral immunity. *Nature*, 421(6920), pp.282–7.

Cummings RD, Varki A, Esko JD, Freeze HH, Stanley P, Bertozzi CR, GW Hart. 2009. *Essentials of Glycobiology* 2nd edition, New York: old Spring Harbor Laboratory Press.

Cyster JG, et al. 2000. Follicular stromal cells and lymphocyte homing to follicles. *Immunol Rev.* 176, pp.181-93.

Cyster, J.G., 2010. B cell follicles and antigen encounters of the third kind. *Nat Immunol*, 11(11), pp.989–96.

Daigneault, M. et al., 2010. The identification of markers of macrophage differentiation in PMA-stimulated THP-1 cells and monocyte-derived macrophages. *PloS one*, 5(1), p.e8668.

Dalla-favera, R. et al., 1982. Human c-myc onc gene is located on the region of chromosome 8 that is trnslocated in Burkitt lymphoma cells. *Proc Natl Acad Sci U S A* 79(24), pp.7824–7827.

Dave SS. et al., 2006. Molecular Diagnosis of Burkitt's Lymphoma. *N Engl J Med*, 354(23), pp.2431–2442.

Davidson, A., She, R. & Livneh, A., 1987. The role of somatic mutation of immunoglobulin genes in autoimmunity. *Annu Rev Immunol*, 5: pp.85–108.

Dennehy, K.M., Klimosch, S.N. & Steinle, A., 2011. Cutting edge: NKp80 uses an atypical hemi-ITAM to trigger NK cytotoxicity. *J Immunol*, 186(2), pp.657–661.

Drickamer, K., 1999. C-type lectin-like domains. *Curr Opin Struct Biol*, 9(5), pp.585–90.

Durandy, A., 2003. Activation-induced cytidine deaminase: a dual role in class-switch recombination and somatic hypermutation. *Eur J Immunol*, 33(8), pp.2069–73.

Early, P. et al., 1980. An Immunoglobulin Heavy Chain Variable Region Gene Is Generated from Three Segments of DNA : VH , D and JH. *Cell,* 19(4), pp.981–992.

Edelman, G.M., 1959. Dissociation of gamma-globulin. *J. Am. Chem. Soc*, 81, pp.3155–3156.

Eisen H.N. and Siskind G.W. 1964/ Variations in affinities of antibodies during the immune response. *Biochem*. 3, pp.996-1008.

Ehrlich, P., 1908. Nobel Lecture. *Nobel lectures, Physiology or Medicine*.

Eichler, W. et al., 2001. Differentially induced expression of C-type lectins in activated lymphocytes. *Journal of cellular biochemistry. Supplement*, Suppl 36, pp.201–8.

Exley M., 1998. CD161 (NKR-P1A) costimulation of CD1d-dependent activation of human T cells expressing invariant Vα24JαQ T cell receptor α chains. *J Exp Med*, 188(5),pp.867-876.

Ferguson, T.A., Thomas, S. & Ferguson, T.A., A vision of cell death : insights into immune privilege. *Immunol Rev*, 156, pp.167–185.

Fergusson, J.R. et al., 2014. CD161 Defines a Transcriptional and Functional Phenotype across Distinct Human T Cell Lineages Article CD161 Defines a Transcriptional and Functional Phenotype across Distinct Human T Cell Lineages. *Cell Rep*, 9(3)pp.1075–1088.

Fine, J.H. et al., 2010. Chemotherapy-induced genotoxic stress promotes sensitivity to natural killer cell cytotoxicity by enabling missing-self recognition. *Cancer research*, 70(18), pp.7102–13.

Flügel, A. *et al*. 2001. Neuronal MCP-1 expression in response to remote nerve injury. *J. Cereb. Blood Flow Metab.* 21,pp.60–76

Forrester, J. V et al., 2008. Immune privilege or privileged immunity? *Mucosal Immunol*, 1(5), pp.372–81.

Fowler, C.B. et al., 2011. Antigen retrieval causes protein unfolding: evidence for a linear epitope model of recovered immunoreactivity. *The journal of histochemistry and cytochemistry : official journal of the Histochemistry Society*, 59(4), pp.366–81.

Fraenkel-Conrat H, Brandon B, Olcott H. 1947 The reaction of formaldehyde with proteins. IV Participation of idole groups Gramicidin. *J Biol Chem*, 168,pp.99–118

Frazer J.K. et al., 1997. Identification and cloning of genes expressed by human tonsillar B lymphocyte subsets. *Ann N Y Acad Sci.* 815, pp.316-8.

Frungieri M.B. et al., 2002. Number, distribution pattern, and identification of macrophages in the testes of infertile men. *Fertil Steril.* 78(2), pp.298-306.

Galea, I., Bechmann, I. & Perry, V.H., 2007. What is immune privilege (not)? *Trends Immunol*, 28(1), pp.12–8.

Garrido, C. et al., 2012. MHC class I molecules act as tumor suppressor genes regulating the cell cycle gene expression, invasion and intrinsic tumorigenicity of melanoma cells. *Carcinogenesis,* 33(3):687-93.

Gay, B.D. et al., 1993. Receptor Editing : An Approach by Autoreactive B Cells to Escape Tolerance. *J Exp Med*, 177, pp.999-1008.

Germain, C. et al., 2010. Characterization of alternatively spliced transcript variants of CLEC2D gene. *J Biol Chem*, 285(46), pp.36207–15.

Germain, C. et al., 2011. Induction of lectin-like transcript 1 (LLT1) protein cell surface expression by pathogens and interferon-γ contributes to modulate immune responses. *J Biol Chem,* 286(44), pp.37964–75.

Germain C. et al., 2015. Lectin-like transcript 1 is a marker of germinal center-derived B-cell non-Hodgkin ' s lymphomas dampening natural killer cell functions. *OncoImmunol,*4(8)e1026503.

Giorda, R. et al., 1990. NKR-P1, a signal transduction molecule on natural killer cells. *Science,* 249(4974), pp.1298–300.

Glick, B., Chang, T. S. & Jaap, R. G. 1956. The bursa of fabricius and antibody production. *Poultry Science* 35**,** pp.224–225.

Good, R. A. & Varco, R. 1955. L. A clinical and experimental study of agammaglobulinemia. *Lancet* 75, **pp.**245–271.

Guan, J. et al., 1985. Glycosylation Allows Cell-Surface Transport of an Anchored Secretory Protein. *Cell*, 42(2), pp.489-96.

Guilbert, B. & Dighiero, G., 1982. Naturally occurring antibodies against nince common antigens in human sera. *J Immunol,* 128(6), pp.2779-87.

Gupta, G.S., 2012. Animal Lectins: Form, Function and Clinical Applications. 2012, Springer.

Hamann, J. et al., 1997. AICL: A new activation-induced antigen encoded by the human NK gene complex. *Immunogenetics*, 45(5), pp.295–300.

Hansen, T.H. & Bouvier, M., 2009. MHC class I antigen presentation: learning from viral evasion strategies. *Nat Rev Immunol*, 9(7), pp.503–13.

Hao, J. et al., 2010. Central nervous system (CNS)-resident natural killer cells suppress Th17 responses and CNS autoimmune pathology. *J Exp Med*, 207(9), pp.1907–21.

Hao, L., Klein, J. & Nei, M., 2006. Heterogeneous but conserved natural killer receptor gene complexes in four major orders of mammals. *Proc Natl Acad Sci U S A*, 103(9), pp.3192–7.

Hatzi, K. & Melnick, A., 2014. Breaking bad in the germinal center: how deregulation of BCL6 contributes to lymphomagenesis. *Trends Mol Med*, 20(6), pp.343–52.

Haynes, N.M. et al., 2007. Role of CXCR5 and CCR7 in Follicular Th Cell Positioning and Appearance of a Programmed Cell Death Gene-1High Germinal Center-Associated Subpopulation. *J Immunol*, 179(8), pp.5099–5108.

Hedger, M.P., 2012. Chapter Immune Privilege of the Testis: Meaning, Mechanisms, and Manifestations. Infection, Immune Homesotasis and Immune Privilege. J. Stein-Streilein, 2012 edition Springer. , pp.31–53.

Hedger, M.P., 1997. Testicular leukocytes : what are they doing ? *Rev Reprod*, 2(1), pp.38–47.

Hicklin, D.J., Marincola, F.M. & Ferrone, S., 1999. HLA class I antigen downregulation in human cancers : T-cell immunotherapy revives an old story. *Mol Med Today*, 5(4), pp.178-86.

Hilschmann, B.Y.N. & Craig, L.C., 1966. Amino acid sequence studies with Bence-Jonce proteins. *Proc Natl Acad Scie U S A* , 53(6), pp.1403–1409.

Hogerkorp, C.-M. & Borrebaeck, C. a. K., 2006. The Human CD77- B Cell Population Represents a Heterogeneous Subset of Cells Comprising Centroblasts, Centrocytes, and Plasmablasts, Prompting Phenotypical Revision. *J Immunol*, 177(7), pp.4341–4349.

Hong S & Van Kaer L. 1999. Immune privilege: keeping an eye on natural killer T cells. *J Exp Med*. 190, pp.1197–1200.

Howard M, Paul WE., 1982. Interleukins for B lymphocytes. *Lymphokine Res.* 1(1):1–4.

Hozumi, N. & Tonegawa, S., 1976. Evidence for somatic rearrangement of immunoglobulin genes coding for variable and constant regions. *Proc Natl Acad Sci U S A*, 73(10), pp.3628–3632.

Hsu, H.-C. et al., 2008. Interleukin 17-producing T helper cells and interleukin 17 orchestrate autoreactive germinal center development in autoimmune BXD2 mice. *Nat Immunol*, 9(2), pp.166–75.

Hu, Y.S. et al., 2004. Isolation of a human homolog of osteoclast inhibitory lectin that inhibits the formation and function of osteoclasts. *J Bone Miner Res,* 19(1), pp.89–99.

Huard, B. & Früh, K., 2000. A role for MHC class I down-regulation in NK cell lysis of herpes virus-infected cells. *Eur J Immunol*, 30(2), pp.509–515.

Huarte, E. et al., 2008. PILAR is a novel modulator of human T-cell expansion. *Blood*, 112(4), pp.1259–1268.

The Human Protein Atlas (2008) [Online]. Available from: http://www.proteinatlas.org [Accessed March 2013]

Iwakoshi NN, et al., 2003. Plasma cell differentiation and the unfolded protein response intersect at the transcription factor XBP-1. *Nat Immunol*.4(4), pp.321-9.

Iizuka, K. et al., 2003. Genetically linked C-type lectin-related ligands for the NKRP1 family of natural killer cell receptors. *Nat Immunol*, 4(8), pp.801–7.

Jackson S.M. et al., 2007. CD45RO enriches for activated, highly mutated human germinal center B cells. *Blood.* 110(12), pp.3917-25.

Jacob, B.J. & Kelsoe, G., 1992. In Situ Studies of the Primary Immune Response to (4-hydroxy-3-nitrophenyl)acetyl. II. A Common Clonal Origin for Periarteriolar Lymphoid Sheath-associated Foci and Germinal Centers. *J Exp Med*, 176(3), pp.679-687.

Jerne N.K..1951.A study of avidity based on rabbit skin responses to diphtheria toxin-antitoxin mixtures. *Acta Pathol. Microbiol. Scand. Suppl.* 87, pp.1–183

Johnston, R.J. et al., 2009. Bcl-6 and Blimp-1 are reciprocal and antagonistic regulators of T follicular helper cell differentiation. *Science*, 325(5943), pp.1006-10.

Kallies, A. et al., 2004. Plasma cell ontogeny defined by quantitative changes in blimp-1 expression. *J Exp Med*, 200(8), pp.967–77.

Kamishikiryo, J. et al., 2011. Molecular basis for LLT1 protein recognition by human CD161 protein (NKRP1A/KLRB1). *J Biol Chem*, 286(27), pp.23823–30.

Kanellopoulos-Langevin C. et al., 2003. Tolerance of the fetus by the maternal immune system: role of inflammatory mediators at the feto-maternal interface. *Reprod Biol Endocrinol.* 1:121

Kärre, K. et al., 1986. Selective rejection of H-2-deficient lymphoma variants suggests alternative immune defence strategy. *Nature*, 319(6055), pp.675–678.

Kartsogiannis, V. et al., 2008. Osteoclast inhibitory lectin, an immune cell product that is required for normal bone physiology in vivo. *J Biol Chem*, 283(45), pp.30850–60.

Kaufman, J. et al., 1999. The chicken B locus is a minimal essential major histocompatibility complex. *Nature*, 401(6756), pp.923–925.

Kelley, J., Walter, L. & Trowsdale, J., 2005. Comparative genomics of natural killer cell receptor gene clusters. *PLoS Genetics*, 1(2), pp.0129–0139.

Kerfoot, S.M. et al., 2011. Germinal center B cell and T follicular helper cell development initiates in the interfollicular zone. *Immunity*, 34(6), pp.947–60.

Kim CH. et al., 2001. Subspecialization of CXCR5+ T Cells : B Helper Activity Is Focused in a Germinal Center-localised Subset of CXCR5+ T Cells. *J Exp Med,* 193(12), pp.1373-81.

Kita, S. et al., 2015. Crystal structure of extracellular domain of human lectin-like transcript 1 (LLT1), the ligand for natural killer receptor-P1A. *Eur J Immunol*, 45(6), pp.1605-13.

Klein, U. et al., 2006. Transcription factor IRF4 controls plasma cell differentiation and class-switch recombination. *Nat Immunol*, 7(7), pp.773–82.

Klein, U.L.F. et al., 2003. Gene Expression Dynamics during Germinal Center Transit in B Cells. *Ann N Y Acad Sci* , 987 pp.166–172.

Klimosch, S.N. et al., 2013. Genetically coupled receptor-ligand pair NKp80-AICL enables autonomous control of human NK cell responses. *Blood*, 122(14), pp.2380–2389.

Kohler G & Milstein C. et al., 1975. Continuous cultures of fused cells secreting antibody of predefined specificity. *J Immunol.* 174(5), pp.2453-5.

Konig, R., Ashwell, G. & Hanover, J.A., 1988. Glycosylation of CD4. Tunicamycin inhibits surface expression. *J Biol Chem*, 263(19), pp.9502–9507.

Kreja, L. et al., 2008. Mechanical regulation of osteoclastic genes in human osteoblasts. *Biochem Biophys Res Commun*, 368(3), pp.582–7.

Kridel, R., Sehn, L.H. & Gascoyne, R.D., 2012. Pathogenesis of follicular lymphoma. *J Clin Invest*, 122(10), pp.3424-31.

Krutzik S.R. et al., 2005. TLR activation triggers the rapid differentiation of monocytes into macrophages and dendritic cells. *Nat Med*. 11(6), pp.653-60

Küppers, R., 2005. Mechanisms of B-cell lymphoma pathogenesis. *Nat Rev Cancer*, 5(4), pp.251–62.

Kuttruff, S. et al., 2009. NKp80 defines and stimulates a reactive subset of CD8 T cells. *Blood*, 113(2), pp.358–69.

Landsteiner, K. & Chase, M. W. 1942. Experiments on transfer of cutaneous sensitivity to simple compounds. *P. Soc. Exp. Biol. Med.* 49, pp. 688–690.

Lanier LL et al., 1994. Human NKR-P1A. A disulphide-linked homodimer of the C-type lectin superfamily expressed by a subset of NK and T lymphocytes. *J Immunol,* 153(6), pp,2417-28.

Li, Y. et al., 2013. Structure of NKp65 bound to its keratinocyte ligand reveals basis for genetically linked recognition in natural killer gene complex. *Proc Natl Acad Sci U S A*, 110(28), pp.11505-10.

Lin, K. et al., 2002. Blimp-1-Dependent Repression of Pax-5 Is Required for Differentiation of B Cells to Immunoglobulin M-Secreting Plasma Cells. *Mol Cell Biol*, 22(13), pp.4771–4780.

Liu YJ et al., 1989. Mechanism of antigen-driven selection in germinal centres. *Nature.* 342,pp.929-30.

Liu YJ & Bancherau J., 1997. Regulation of B-cell commitment to plasma cells or to memory B cells. *Semin Immunol.* 9, pp.235-240.

Liu YJ & Arpin C.,1997. Germinal center development. *Immunol Rev.* 15, pp.111-126.

Linterman, M. a et al., 2011. Foxp3+ follicular regulatory T cells control the germinal center response. *Nat Med*, 17(8), pp.975–982.

Lisowska, E., 2002. Cellular and Molecular Life Sciences The role of glycosylation in protein antigenic properties. *Cell Mol Life Scie*, 59(3) pp.445–455.

Lohr, J.G. et al., 2012. Discovery and prioritization of somatic mutations in diffuse large B-cell lymphoma (DLBCL) by whole-exome sequencing. *Proc Natl Acad Sci U S A*, 109(10), pp.3879–84.

Louveau, A. et al., 2015. Structural and functional features of central nervous system lymphatic vessels. *Nature*, 523(7560), pp. 337-41.

Luther, S.A. et al., 2000. Coexpression of the chemokines ELC and SLC by T zone stromal cells and deletion of the ELC gene in the plt/plt mouse. *Proc Natl Acad Sci U S A*, 97(23), pp.12694-9.

Lysenko, O. et al., 2013. BACL is a novel brain-associated, non-NKC-encoded mammalian C-type lectin-like receptor of the CLEC2 family. *PloS one*, 8(6), p.e65345.

Ma, C.S. et al., 2012. The origins, function, and regulation of T follicular helper cells. *J Exp Med*, 209(7), pp.1241–53.

Ma, D., 2002. ER transport signals and trafficking of potassium channels and receptors. *Curr Opin Neurobiol*, 12(3), pp.287–292.

MacLennan, I.C., 1994. Germinal centers. *Annu Rev Immunol*, 12, pp.117–39.

MacLennan IC. et al., 2003. Extrafollicular antibody responses. *Immunol Rev*, 194, pp.8–18.

Maggi, L. et al., 2010. CD161 is a marker of all human IL-17-producing T-cell subsets and is induced by RORC. *Eur J Immunol*, 40(8), pp.2174–81.

Maloney DG, Smith B, Appelbaum FR. 1996.The anti-tumor effect of monoclonal anti-CD20 antibody (mAb) therapy includes direct anti-

proliferative activity and induction of apoptosis in CD20 positive non-Hodgkin's lymphoma (NHL) cell lines. *Blood*, 88 (Suppl 1), pp.637. 18

Manis JP, Tian M, Alt FW. 2002. Mechanism and control of class-switch recombination. *Trends Immunol*. 23(1), pp.31-9.

Martin, E. et al., 2009. Stepwise development of MAIT cells in mouse and human. *PLoS biology*, 7(3), p.e54.

Mathew, P., 2004. The LLT1 receptor induces IFN-γ production by human natural killer cells. *Mol Immunol*, 40(16), pp.1157–1163.

Mathew P et al. 2014. Lectin-like transcript-1 (LLT1) and exosomal PCNA inhibit NK cell effector function against prostate cancer cells (TUM2P.892). *J Immunol.* 192 (Suppl 1)71.16

Matsuki, H. et al., 2003. Monoclonal Antibodies with Defined Recognition Sequences in the Stem Region of CD44 : Detection of Differential Glycosylation of CD44 between Tumor and Stromal Cells in Tissue. *Cancer Res,* 63(23):8278-83.

Matter, K. & Balda, M.S., 2003. Holey barrier: claudins and the regulation of brain endothelial permeability. *J Cell Biol,* 161(3), pp.459–60.

Matzinger, P., 1994. Tolerance, danger, and the extended family. *Annu Rev Immunol,* 12pp.991–1045.

Mavilio, D. et al., 2005. Identification of NKG2A and NKp80 as specific natural killer cell markers in rhesus and pigtailed monkeys. *Blood*, 106(5), pp.1718–1725.

Mcadam, A.J. et al., 2001. ICOS is critical for CD40-mediated antibody class switching. *Nature*, *409(6816)pp102-5.*

Mcheyzer-williams, M.G, Nossal, G.J., 1988. Clonal analysis of autoantibody-producing cell precursos in the preimmune B cell repertoire'. *J Immunol*, 141(12), pp.4118-23.

Medawar P. B. 1948. Immunity to homologous grafted skin; the fate of skin homografts transplanted to the brain, to subcutaneous tissue, and to the anterior chamber of the eye. *Br. J. Exp. Pathol.* 29 pp.58–69

Medawar P. B. 1961. Immunological tolerance. *Nature* 189 pp.14–17

Mesci A, et al, 2006. NKR-P1 Biology: from prototype to missing self. *Immunol Res*, 35(1-2)pp.13–26.

Medzhitov, R. 1998. innate immune recognition and control of adaptive immune respones. *Semin Immunol*, 10(5), pp.351-53.

Minton, K., 2015. B cell memory: A second chance for antibodies. *Nat Rev Immunol*, 15(3), p.131.

Mirosavljevic, D. et al., 2003. T-cells mediate an inhibitory effect of interleukin-4 on osteoclastogenesis. *J Bone Miner Res,* 18(6), pp.984–93.

Mitchell, B.Y.G.F. & Miller, 1968. Cell to cell interaction in the immune response. II. The source of hemolysin-forming cells in irradiated mice given bone marrow and thymus or thoracic duct lymphocytes. *J Exp Med*, 3, pp.821–837.

Montoto, S. & Fitzgibbon, J., 2011. Transformation of indolent B-cell lymphomas. *J Clin Oncol,* 29(14), pp.1827–34.

Murphy, K., 2011. *Janeway's Immunobiology* 8th ed., Garland Science. New York.

Nakamura, A. et al., 2007. Osteoclast inhibitory lectin (OCIL) inhibits osteoblast differentiation and function in vitro. *Bone*, 40(2), pp.305–15.

Nakayama, Y. et al., 2006. A limited number of genes are involved in the differentiation of germinal center B cells. *J Cell Biochem,* 99(5), pp.1308–25.

Le Naour, F. et al., 2001. Profiling changes in gene expression during differentiation and maturation of monocyte-derived dendritic cells using both oligonucleotide microarrays and proteomics. *J Biol Chem*, 276(21), pp.17920–17931.

Ngo, B.V.N. et al., 1999. Lymphotoxin α/β and Tumor Necrosis Factors Are Required for Stromal Cell Expression of Homing Chemokines in B and T Cell Areas of the Spleen. *J Exp Med*, 189(2)pp403-412.

Nickel, W. & Seedorf, M., 2008. Unconventional mechanisms of protein transport to the cell surface of eukaryotic cells. *Annu Rev Cell Dev Biol*, 24, pp.287–308.

Nierop, K. Van & Groot, C. De, 2002. Human follicular dendritic cells : function, origin and development. *Semin Imunol*, 14(02), pp.251–257.

Nieuwenhuis, P. & Opstelten, D., 1984. Functional Anatomy of Germinal Centers. *Am J Anat*, 170(3)pp.421–435.

Nutt, S.L. et al., 2015. The generation of antibody-secreting plasma cells. *Nature reviews. Immunology*, 15(3), pp.160–171.

Nutt, S.L. & Tarlinton, D.M., 2011. Germinal center B and follicular helper T cells: siblings, cousins or just good friends? *Nat Immunol*, 131(6), pp.472–477.

Onizuka T., 1995. BCL-6 Gene Product, a 92- to 98-kD Nuclear Phosphoprotein, Is Highly Expressed in Germinal Center B Cells and Their Neoplastic Counterparts. *Blood*, 86(1), pp.28–37.

Osmond, D. G. & Nossal, G.J., 1974. Differentiation of lymphocytes in mouse bone marrow. II. Kinetics of maturation and renewal of antiglobulin-binding cells studied by double labeling. *Cell Immunol*, 13, pp.132–145.

Park, E.K. et al., 2007. Optimized THP-1 differentiation is required for the detection of responses to weak stimuli. *Inflamm Res*, 56(1), pp.45–50.

Parrish-novak, J. et al., 2000. Interleukin 21 and its receptor are involved in NK cell expansion and regulation of lymphocyte function. *Nature*, 408(6808)pp.57–63.

Pascual et al., 1994. Analysis of somatic mutation in five B cell subsets of human tonsil. *J Exp Med*. 180(1)pp.329-39.

Pasqualucci, L. et al., 2003. Plenary paper Mutations of the BCL6 proto-oncogene disrupt its negative autoregulation in diffuse large B-cell lymphoma. *Blood*, 101(8), pp.2914–2923.

Pernis, B.Y.B. et al., 1965. Cellular localization of immunoglobulins with different allotypic specificities in rabbit lymphoid tissues. *J Exp Med,* 122(5)pp.853-876.

Peschel, C. et al., 1987. Role of B cell stimulatory factor 1/interleukin 4 in clonal proliferation of B cells. *J Immunol,* 139,pp.3338-3347.

Petsko G. et al., 2009. Protein structure and function. Folding of Glycoproteins: toward Understanding the Biophysics of the Glycosylation Code. *Curr Opin Struct Biol.* 19(5)pp.524-33.

Phan, R.T. & Dalla-favera, R., 2004. The BCL6 proto-oncogene suppresses p53 expression in germinal-centre B cells. *Nature*, 432(7017), pp.635–639.

Pineda, B. et al., 2008. The Asn19Lys substitution in the osteoclast inhibitory lectin (OCIL) gene is associated with a reduction of bone mineral density in postmenopausal women. *Calcif Tissue Int*, 82(5), pp.348–53.

Plougastel, B., Dubbelde, C. & Yokoyama, W.M., 2001. Cloning of Clr , a new family of lectin-like genes localized between mouse Nkrp1a and Cd69. *Immunogenetics*, 53(3), pp.209–214.

Pollanen P & Niemi M., 1987. Immunohistochemical identification of macrophages, lymphoid cells and HLA antigens in the human testis. *Int J Androl.* 10(1)37-42.

Porter, B.Y.R.R., 1956. The Hydrolysis of Rabbit y-Globulin and Antibodies with Crystalline Papain. *Biochem J*, 73(1948), pp.119–127.

Pozo, D. et al., 2013. CD161 (Human NKR-P1A) Signaling in NK Cells Involves the Activation of Acid Sphingomyelinase 1. *J Immunol*, 176(4)pp2397-2406.

Quan, J. et al., 2009. Cloning and analysis of rat osteoclast inhibitory lectin gene promoter*J Cell Biochem*, 106(4), pp.599–607.

Radbruch, A. et al., 2006. Competence and competition: the challenge of becoming a long-lived plasma cell. *Nat Rev Immunol*, 6(10), pp.741–50.

Rahim, M.M. a et al., 2015. The mouse NKR-P1B:Clr-b recognition system is a negative regulator of innate immune responses. *Blood*, 125(14), pp.2217–27.

Rajoriya, N. et al., 2014. Gamma Delta T-lymphocytes in Hepatitis C and Chronic Liver Disease. *Front Immunol*, 26(5), p.400.

Ranuncolo, S.M. et al., 2007. Bcl-6 mediates the germinal center B cell phenotype and lymphomagenesis through transcriptional repression of the DNA-damage sensor ATR. *Nat Immunol*, 8(7), pp.705–14.

Rasheed, A.-U. et al., 2006. Follicular B helper T cell activity is confined to CXCR5(hi)ICOS(hi) CD4 T cells and is independent of CD57 expression. *Eur J Immunol*, 36(7), pp.1892–903.

Recny, M.A. et al., 1992. N-Glycosylation Is Required for Human CD2 Immunoadhesion Functions. *Biol Chem* , 267(31*)*pp.22428–22435.

Reimold AM, et al., 1996. Transcription factor B cell lineage-specific activator protein regulates the gene for human X-box binding protein 1. *J Exp Med*. 183:pp393–401.

Rodda, L.B. et al., 2015. Phenotypic and Morphological Properties of Germinal Center Dark Zone Cxcl12-Expressing Reticular Cells. *J Immunol*. 195(10):4781-91.

Rogers, S.L. et al., 2005. Characterisation of the chicken C-type lectin-like receptors B-NK and B-lec suggests that the NK compled and the MHC share a common ancestral region. *J Immunol.* 174(6)3475-83.

Roitt IM, et al.., 1969. The cellular basis of immunological responses. *Lancet* 1969; 2: 367–371.

Rosen DB. et al., 2005. Cutting edge: lectin-like transcript 1 is a ligand for the inhibitory human NKR-P1A receptor.*J Immunol*. 175(12), pp.7796-9.

Rosen, D.B. et al., 2008. Functional consequences of interactions between human NKR-P1A and its ligand LLT1 expressed on activated dendritic cells and B cells. *J Immunol.* 180(10), pp.6508–17.

Roth, P. et al., 2007. Malignant glioma cells counteract antitumor immune responses through expression of lectin-like transcript-1. *Cancer research*, 67(8), pp.3540–4.

Rudd, P.M., 2001. Glycosylation and the Immune System. *Science*, 291(5512), pp.2370–2376.

Ryan, J.C. & Seaman, W.E., 1997. Divergent functions of lectin-like receptors on NK cells. *Immunol Rev*, 155(1), pp.79–89.

Ryser, J., Vassalli, P. & Alerts, E., 1974. Mouse Bone Marrow Lymphocytes and Their Differentiation. *J Immunol.* 113(3),pp719-28.

Sancho, D. & Reis e Sousa, C., 2012. Signaling by myeloid C-type lectin receptors in immunity and homeostasis. *Annu Rev Immunol*, 30, pp.491–529.

Satkunanathan, S. et al., 2014. Respiratory syncytial virus infection, TLR3 ligands, and proinflammatory cytokines induce CD161 ligand LLT1 expression on the respiratory epithelium. *J Virol* 88(5), pp.2366–73.

Schatz, D.G. & Oettinger, M.A., 1989. The V (D) J Recombination Activating Gene , RAG-1. *Cell*, 59(6), pp.1035–48.

Schmitz, R. et al., 2012. Burkitt lymphoma pathogenesis and therapeutic targets from structural and functional genomics. *Nature*, 490(7418), pp.116–20.

Schröder J. et al., 1980. Monoclonal antibodies: a new tool for research and immunodiagnostics. *Med Biol.* 58(3),pp140-8.

Schwickert, T. a et al., 2009. Germinal center reutilization by newly activated B cells. *J Exp Med*, 206(13), pp.2907–14.

Schwickert, T. a et al., 2007. In vivo imaging of germinal centres reveals a dynamic open structure. *Nature*, 446(7131), pp.83–7.

Sciammas, R. et al., 2006. Graded expression of interferon regulatory factor-4 coordinates isotype switching with plasma cell differentiation. *Immunity*, 25(2), pp.225–36.

Shaffer, A.L. et al., 2002. Blimp-1 Orchestrates Plasma Cell Differentiation by Extinguishing the Mature B Cell Gene Expression Program. *Immunity*, 17(1),pp.51–62.

El Shikh, M.E.M. et al., 2010. Activation of B cells by antigens on follicular dendritic cells. *Trends Immunol*, 31(6), pp.205–11.

El Shikh, M.E.M. et al., 2009. T-independent antibody responses to T-dependent antigens: a novel follicular dendritic cell-dependent activity. *J Immunol*, 182(6), pp.3482–91.

Shlomchik, M.J., 2012. Germinal center selection and the development of memory B and plasma cells. *Immunol Rev*, 247(1),pp.52–63.

Shulman, Z. et al., 2014. Dynamic signaling by T follicular helper cells during germinal center B cell selection. *Science*, 345(6200),pp1058-62.

Shulman, Z. et al., 2013. T follicular helper cell dynamics in germinal centers. *Science*, 341(6146), pp.673–7.

Skazal AK, Kosko MH, Tew JG, 1988. A novel in vivo follicular dendritic cell-dependent iccosome-mediated mechanism for delivery of antigen to antigen-processing cells. *J Immunol,* 140(2):pp341-53.

De Silva, N.S. & Klein, U., 2015. Dynamics of B cells in germinal centres. *Nat Rev Immunol*, 15(3),pp.137-48.

Skálová, T. et al., 2015. Four crystal structures of human LLT1, a ligand of human NKR-P1, in varied glycosylation and oligomerization states. *Acta Crystallographica Section D Biological Crystallography*, 71(3), pp.578–591.

Smith J.P., et al., 1998. Tingible body macrophages in regulation of germinal center reactions. *Dev Immunol.* 6(3-4):pp.285-94.

Souroujon, M. et al., 1988. Preferential autoantibody reactivity of the preimmune B cell repertoire in normal mice. *J Immunol.* 140(12)4173-9.

Spreu, J. et al., 2007. CLEC2A: a novel, alternatively spliced and skin-associated member of the NKC-encoded AICL-CD69-LLT1 family. *Immunogenetics*, 59(12), pp.903–12.

Spreu, J. et al., 2010. Interaction of C-type lectin-like receptors NKp65 and KACL facilitates dedicated immune recognition of human keratinocytes. *Proc Natl Acad Sci U S A,* 107(11), pp.5100–5.

Srikrishna, G. & Freeze, H.H., 2009. Endogenous Damage-Associated Molecular Pattern Molecules at the Crossroads of Inflammation and Cancer. *Neoplasia*, 11(7), pp.615–628.

Stevenson FK. et al., 2001. The occurrence and significance of V gene mutations in B cell-derived human malignancy. *Adv Cancer Res*, 83:pp,81-116.

Sukumar S. et al., 2011. In vitro germinal centers. Patent US 8003385 B2.

Sungalee, S. et al., 2014. Germinal center reentries of BCL2-overexpressing B cells drive follicular lymphoma progression. *J Clin Invest*, 124(12), pp.5337–5351.

Suto, Y. et al., 1997.The human natural killer gene complex (NKC) is located on chromosome 12p13.1-p13.2. *Immunogenetics*, 46(2),pp.159–162.

Tafuri, A. et al., 2001. ICOS is essential for effective T-helper-cell responses. *Nature*, 409(6816),pp.105–109.

Takahashi, T., Dejbakhsh-Jones, S. & Strober, S., 2005. Expression of CD161 (NKR-P1A) Defines Subsets of Human CD4 and CD8 T Cells with Different Functional Activities. *J Immunol*, 176(1), pp.211–216.

Taub, R., 1982. Translocation of the c-myc gene into the immunoglobulin heavy chain locus in human Burkitt lymphoma and murine plasmacytoma cells. *Proc Natl Acad Scie U S A* 79(24), pp.7837–7841.

Taylor, J.J., Pape, K. a & Jenkins, M.K., 2012. A germinal center-independent pathway generates unswitched memory B cells early in the primary response. *J Exp Med*, 209(3), pp.597–606.

Thai TH. Et al., 2007. Regulation of the germinal center response by microRNA-155. *Science.* 316(5824):604-8.

Tiegs, B.S.L., Russell, D.M. & Nemazee, D., 1993. Receptor Editing in Self-reactive Bone Marrow B Cells, *J Exp Med*, 177(4),pp.1009-20.

Tiffts, C.J., Proia, R.L. & Camerini-otero, R.D., 1992. The Folding and Cell Surface Expression of CD4 Requires Glycosylation. *J Biol Chem*, 267(5) pp.3268–3273.

Tran, J. et al., 2010. Altering the specificity of NK:target cell interactions by genetic manipulation of NK receptor expression on primary mouse NK cells. *Vaccine*, 28(22), pp.3767–72.

Turner, C.A., Mack, D.H. & Davis, M.M., 1994. Blimp-l , a Novel Zinc Finger-Containing Protein That Can Drive the Maturation of B Lymphocytes into Immunoglobulin-Secreting Cells. *Cell*, 77(2), pp.297–306.

Uhde M. et al., 2013. Differntial regulation of marginal zone and follicular B cell responses by CD83. *Int Immunol.* 25(9).pp.507-20.

Uhlen, M. et al., 2015. Tissue-based map of the human proteome. *Science*, 347(6220), pp.1260419–1260419.

Varki, A., 1993. Biological roles of oligosaccharides : all of the theories are correct. *Glicobiology*, 3(2), pp.97–130.

Victora, G.D. et al., 2010. Germinal center dynamics revealed by multiphoton microscopy with a photoactivatable fluorescent reporter. *Cell*, 143(4), pp.592–605.

Victora, G.D. et al., 2012. Identification of human germinal center light and dark zone cells and their relationship to human B-cell lymphomas. *Blood*, 120(11), pp.2240–2248.

Victora, G.D. & Nussenzweig, M.C., 2012. Germinal centers. *Annu Rev Immunol*, 30, pp.429–57.

Viertlboeck, B.C. et al., 2008. Chicken C-type lectin-like receptor B-NK, expressed on NK and T cell subsets, binds to a ligand on activated splenocytes. *Mol Immunol* 45(5), pp.1398–404.

Vitale, M. et al., 2001. Identification of NKp80 , a novel triggering molecule expressed by human NK cells. *Eur J Immunol*, 31(1), pp.233–242.

Vogler, I. & Steinle, A., 2011. Vis-à-vis in the NKC: genetically linked natural killer cell receptor/ligand pairs in the natural killer gene complex (NKC). *J Innate Immun*, 3(3), pp.227–35.

Voigt, S. et al., 2007. Cytomegalovirus evasion of innate immunity by subversion of the NKR-P1B:Clr-b missing-self axis. *Immunity*, 26(5), pp.617–27.

Wabl, M. & Steinbergt, C., 1982. A theory of allelic and isotypic exclusion for immunoglobulin genes, *Proc Natl Acad Sci U S A,* 79(22), pp.6976–6978.

Weigert, M. G., Cesari, I. M., Yonkovich, S. J. & Cohn, M., 1970. Variability in the lambda light chain sequences of mouse antibody. *Nature*, 228, pp.1045–1047.

Weis, W.I., Taylor, M.E. & Drickamer, K., 1998. The C-type lectin superfamily in the immune system. *Immunol Rev*, 163(1), pp.19–34.

Weller R.O., Engelhardt B., Phillips M.J., 1996. Lymphocyte targeting of the central nervous system: a review of afferent and efferent CNS-immune pathways. *Brain Pathol.* 6(3):pp.275-88.

Welte, S. et al., 2006. Mutual activation of natural killer cells and monocytes mediated by NKp80-AICL interaction. *Nat Immunol*, 7(12), pp.1334–42.

Wenkel, H., Streilein, J.W. & Young, M.J., 2000. Systemic Immune Deviation in the Brain That Does Not Depend on the Integrity of the Blood-Brain Barrier. *J Immunol*, 164(10), pp.5125–5131.

Wijdenes J. et al., 1996. A plasmocyte selective monoclonal antibody (B-B4) recognizes syndecan-1. *Br J Haematol.* 94:pp.318-323.

Williams, K.J.N. et al., 2012. Poxvirus infection-associated downregulation of C-type lectin-related-b prevents NK cell inhibition by NK receptor protein-1B. *J Immunol,* 188(10), pp.4980–91.

Xu, H. et al., 2003. Requirements for passage of T lymphocytes across non-inflamed retinal microvessels. *J Neuroimmunol*, 142(1-2), pp.47–57.

Xu, H. et al., 2005. Differentiation to the CCR2+ Inflammatory Phenotype In Vivo Is a Constitutive, Time-Limited Property of Blood Monocytes and Is Independent of Local Inflammatory Mediators. *J Immunol*, 175(10), pp.6915–6923.

Xu S. et al., 2012. The RNase III enzyme Dicer is essential for germinal center B-cell formation. *Blood.* 119(3)767-76.

Yang, T. et al., 2006. CD161B:ClrB interactions mediate activation of enhanced lysis of tumor target cells following NK cell:DC co-culture. *Immunol Res*, 36(1-3), pp.43–50.

Yates, S.F. et al., 2007. Induction of Regulatory T Cells and Dominant Tolerance by Dendritic Cells Incapable of Full Activation. *J Immunol*, 179(2), pp.967–976.

Yokoyama, W.M. et al., 1990. Chromosomal location of the Ly-49 (A1, YE1/48) multigene family. Genetic association with the NK 1.1 antigen. *J Immunol*, 145(7), pp.2353–2358.

Yokoyama W.M. et al., 1991. cDNA cloning of mouse NKR-P1 and genetic linkage with LY-49. Identification of a natural killer cell gene complex on mouse chromosome 6. *J Immunol*, 147(9) pp.3229–3236.

Yokoyama, M., 1993. Recognition structures on natural killer cells. *Curr opin Immunol*, 5(1),pp67-73.

Yokoyama, W.M. & Plougastel, B.F.M., 2003. Immune functions encoded by the natural killer gene complex. *Nat Rev Immunol*, 3(4), pp.304–16.

Yu, D. et al., 2009. The transcriptional repressor Bcl-6 directs T follicular helper cell lineage commitment. *Immunity*, 31(3), pp.457–68.

Zelensky, A.N. & Gready, J.E., 2005. The C-type lectin-like domain superfamily. *FEBS J*, 272(24), pp.6179–6217.

Zhang J, et al., 1988. Is rapid proliferation in B centroblasts linked to somatic mutation in memory B cell clones? *Immunol Lett.* 18(4):297-9

Zhang, Q. et al., 2012. Mouse Nkrp1-Clr Gene Cluster Sequence and Expression Analyses Reveal Conservation of Tissue-Specific MHC-Independent Immunosurveillance. *PloS one*, 7(12), p.e50561.

Zhang, Y. et al., 2013. Germinal center B cells govern their own fate via antibody feedback. *J Exp Med*, 210(3), pp.457–464.

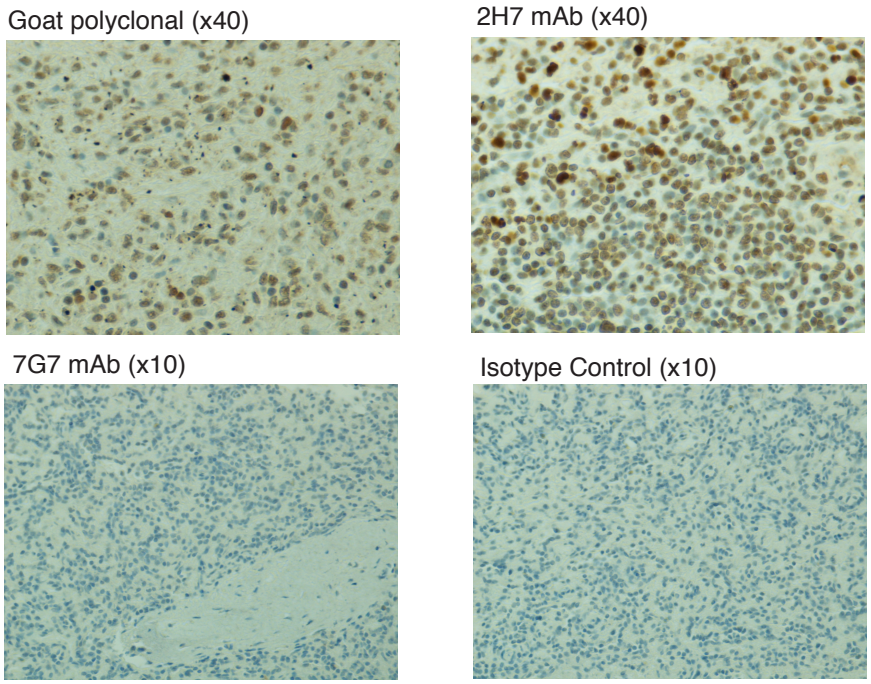
Zhou, H. et al., 2001. A novel osteoblast-derived C-type lectin that inhibits osteoclast formation. *J Biol Chem*, 276(18), pp.14916–23.

Zhou, H. et al., 2002. Osteoclast inhibitory lectin, a family of new osteoclast inhibitors. *J Biol Chem y*, 277(50), pp.48808–15.

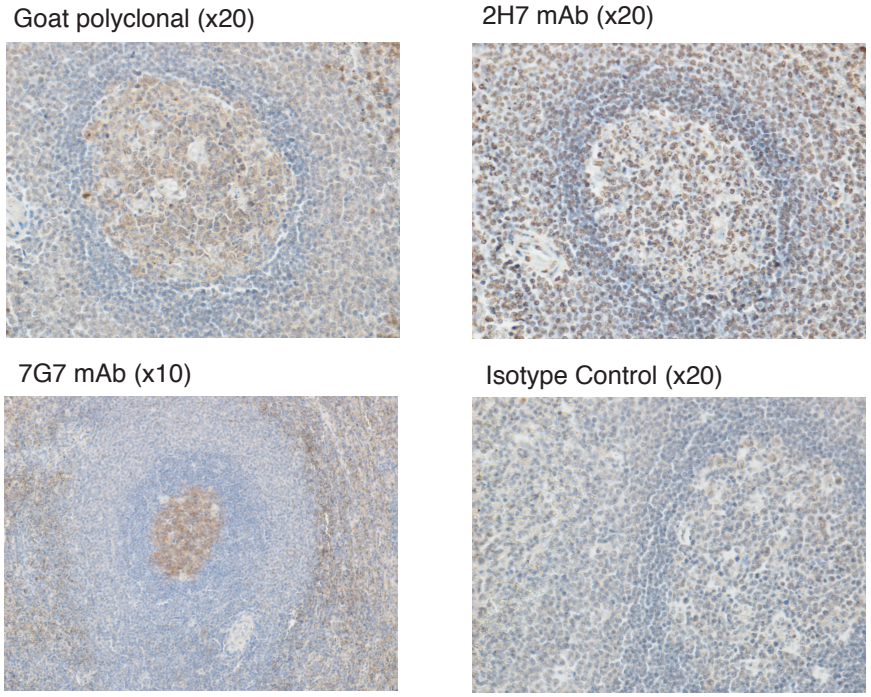
Zhou, Y. et al., 2010. Oral tolerance to food-induced systemic anaphylaxis mediated by the C-type lectin SIGNR1. *Nat Med*, 16(10), pp.1128–33.

9 Appendix

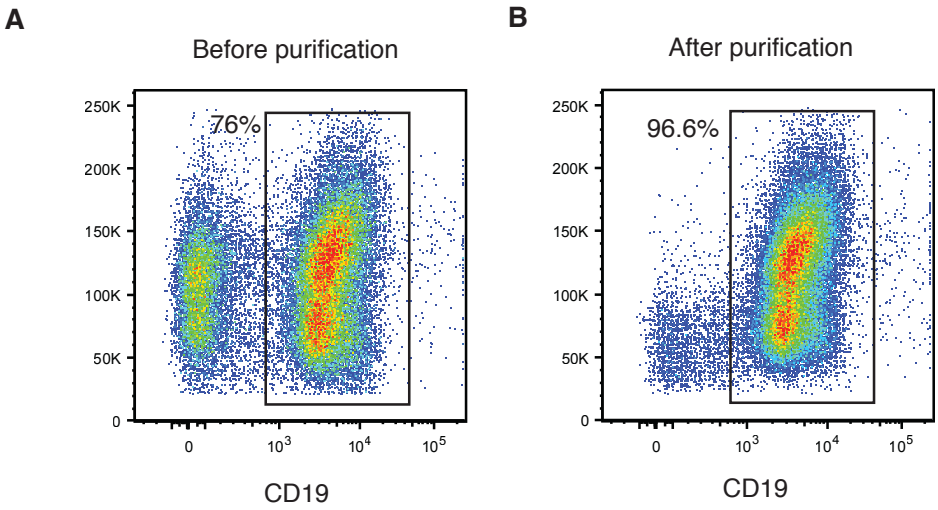
A **Spleen** (Tissue array, AMS Biotechnology)



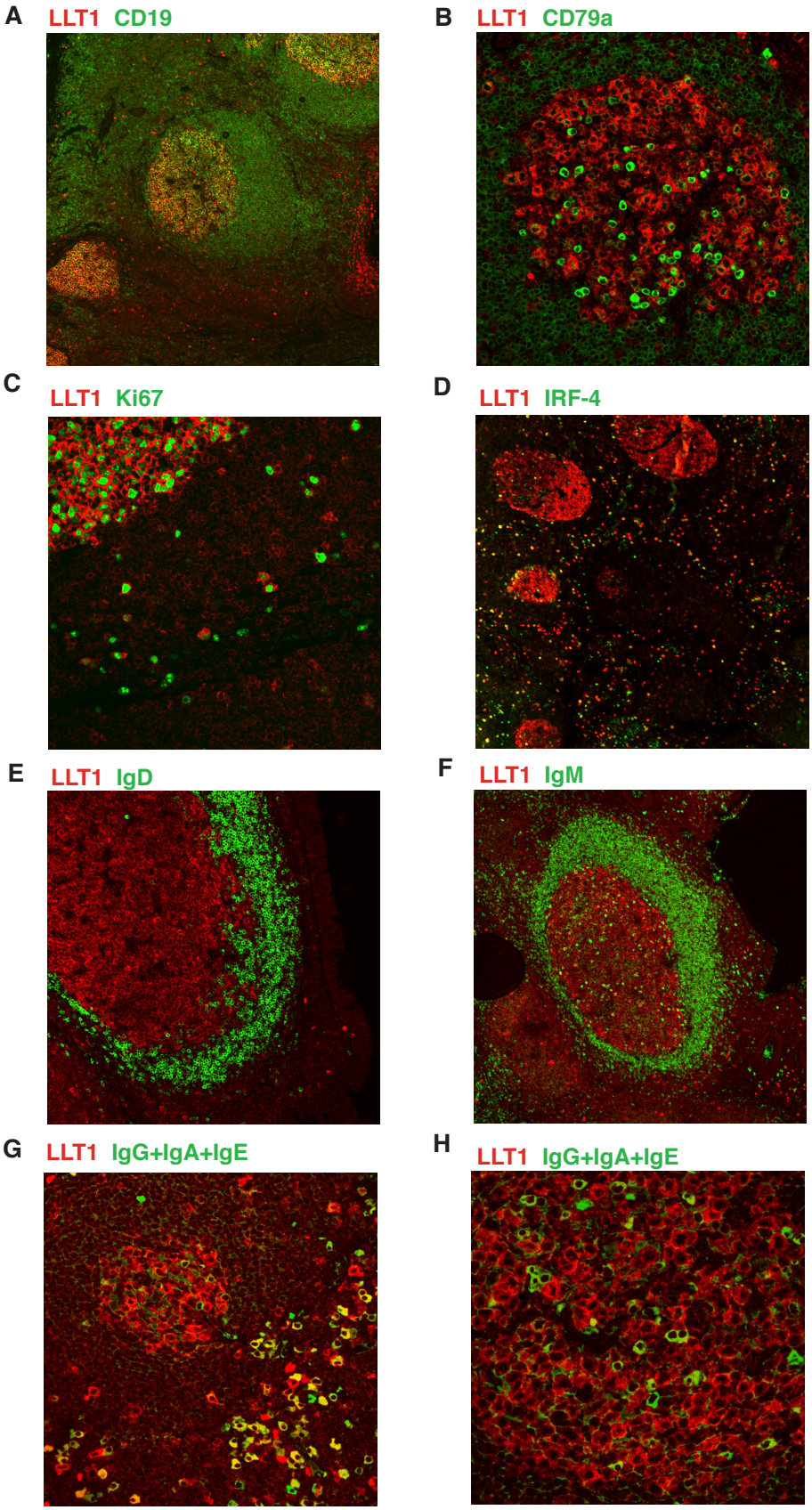
B **Spleen** (Proteogenix)



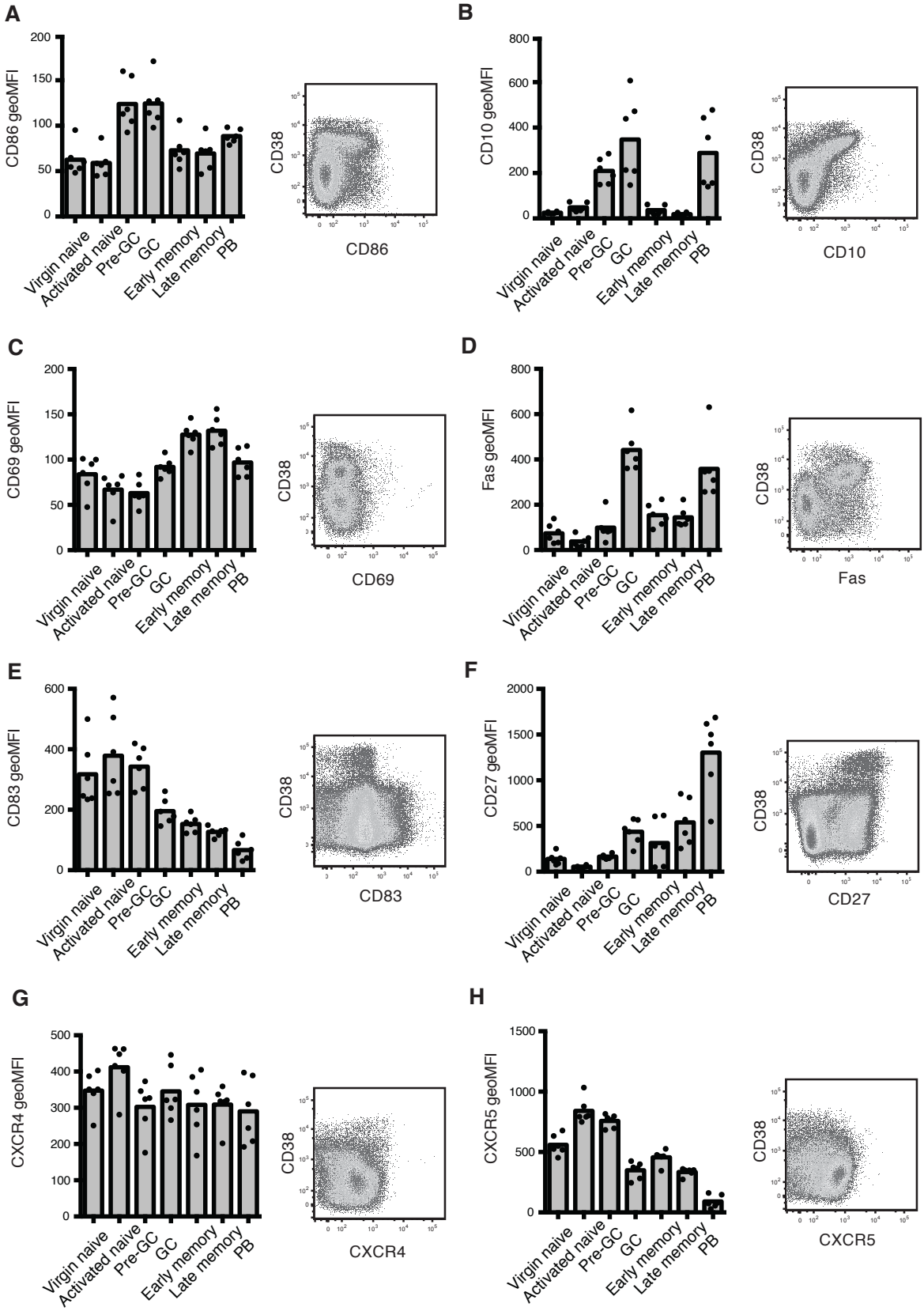
Appendix 1. Impact of sample processing on LLT1 antibody recogiition. Spleen samples from AMS Biotechnology (A) and Proteogenix (B) were stained using the goat polyclonal antibody (1:100), the 2H7 and 7G7 mAbs (1:500) and the respective isotype controls. n=3. Representative stains of three independent experiments.

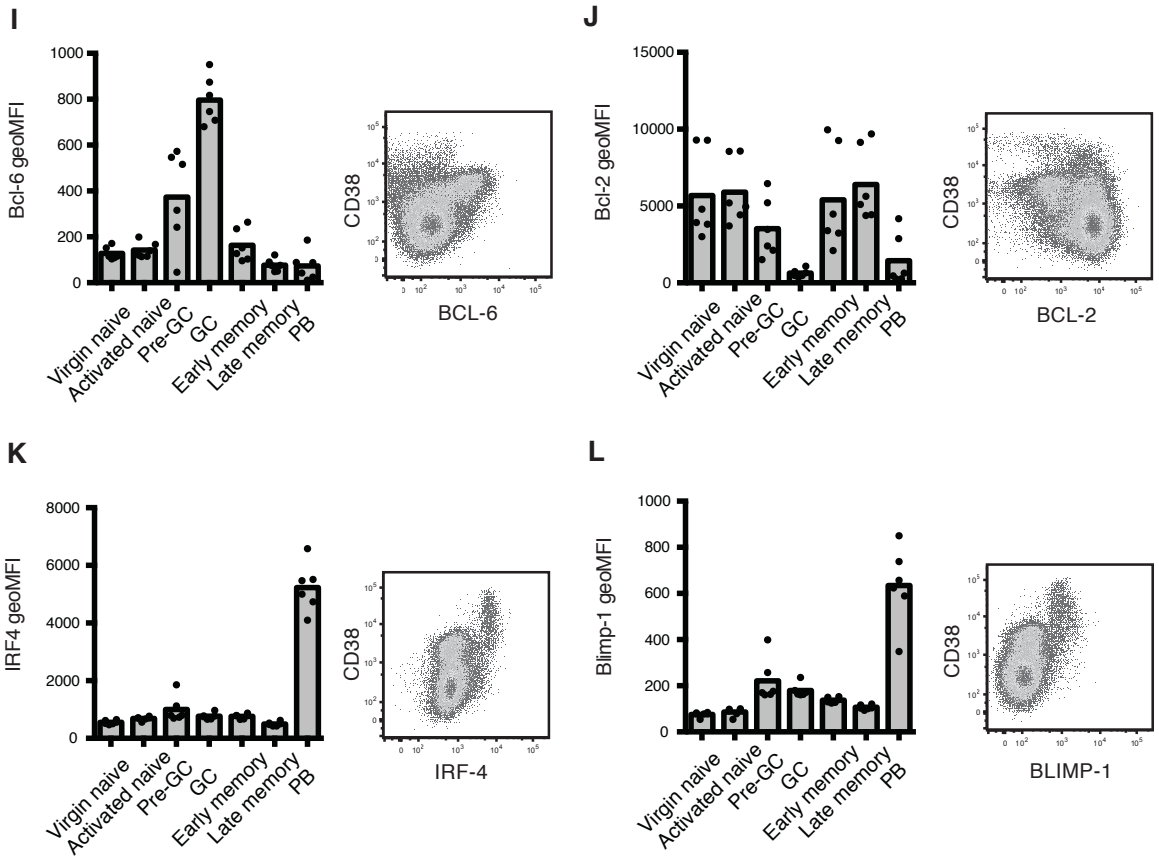


Appendix 2. Quality control of the B cell purification process. Tonsillar B cells were purified from a tonsillar cell suspension using the EasySep™ Human B Cell Enrichment Kit.(A) Shows a representative FACS plot gated on alive lymphocytes before the purification process and (B) shows the enrichment of B cells in the sample (96.6% of B cells). Representative plots of 10 independent experiments.

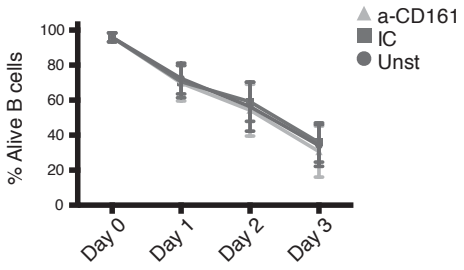


Appendix 3. Immunofluorescent costaining of LLT1 with different markers. Immunofluorescent stainings were performed in FFPE sections of human tonsils. LLT1 was costained with CD19 (x10) (A), CD79a (x40) (B), Ki67 (x40) (C), IRF-4 (X10) (D), IgD (x20) (E), IgM (x20) (F) and a combination of IgG, IgA and IgE (x40), allowing to see double positives outside the GC (E) but not inside (F). Representative images of three independent experiments.

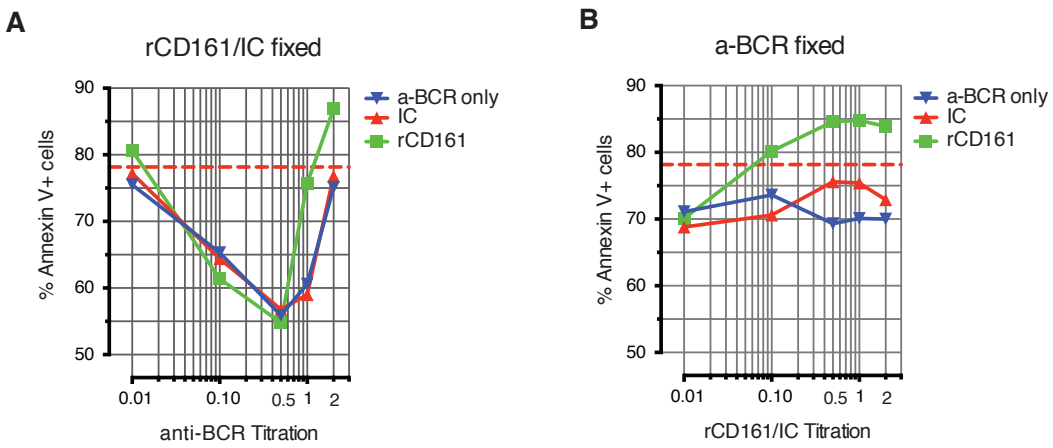

A
CD86 geoMFI
200
150
100
50
0
Virgin naive
Activated naive
Pre-GC
GC
Early memory
Late memory
PB
CD38
CD86
B
CD10 geoMFI
800
600
400
200
0
CD38
CD10
C
CD69 geoMFI
CD38
CD69
D
Fas geoMFI
CD38
Fas
E
CD83 geoMFI
CD38
CD83
F
CD27 geoMFI
2000
1500
1000
500
0
CD38
CD27
G
CXCR4 geoMFI
500
400
300
200
100
0
CD38
CXCR4
H
CXCR5 geoMFI
1500
1000
500
0
CD38
CXCR5



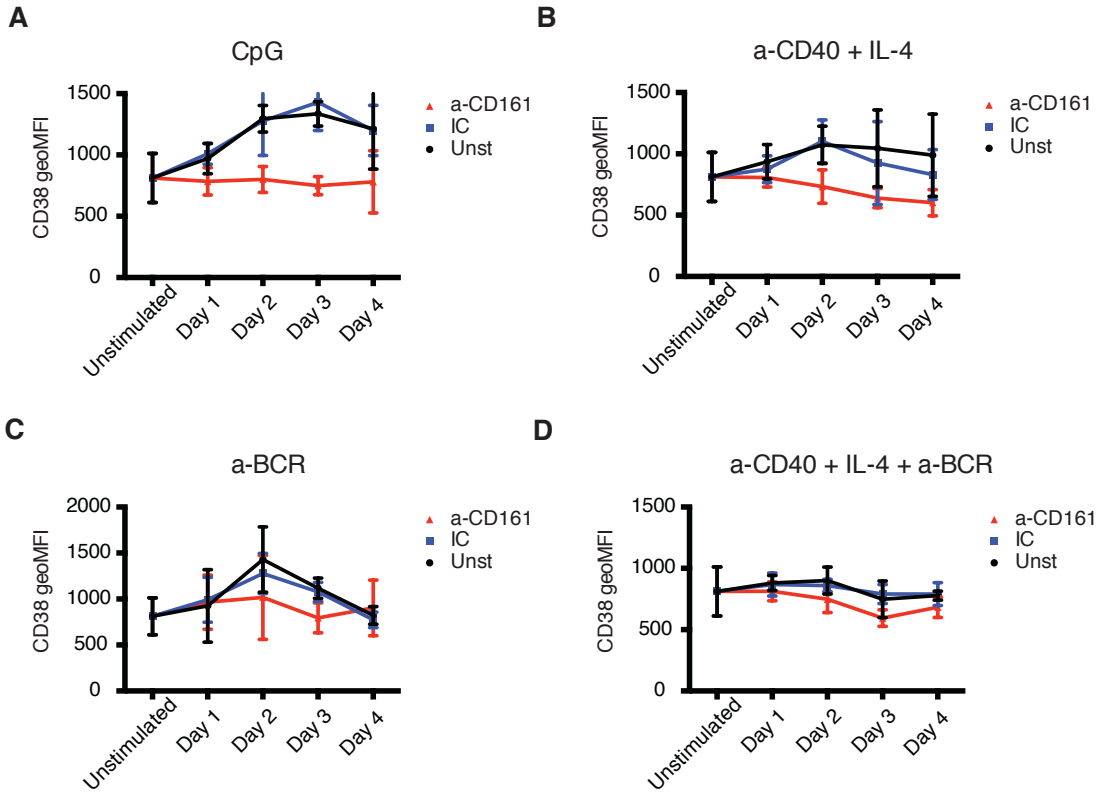
Appendix 4. Phenotyping of tonsillar B cells. Tonsillar B cells were divided into seven different subsets (see Figure 5-5) and geoMFI expression of the surface markers CD86 (A), CD10 (B), CD69 (C), Fas (D), CD83 (E), CD27 (F), CXCR4 (G), CXCR5 (H) and the intracellular factors BCL-6 (I), BCL-2 (J), IRF-4 (K) and BLIMP-1 (L) were measured by flow cytometry (n=6). Two independent experiments.



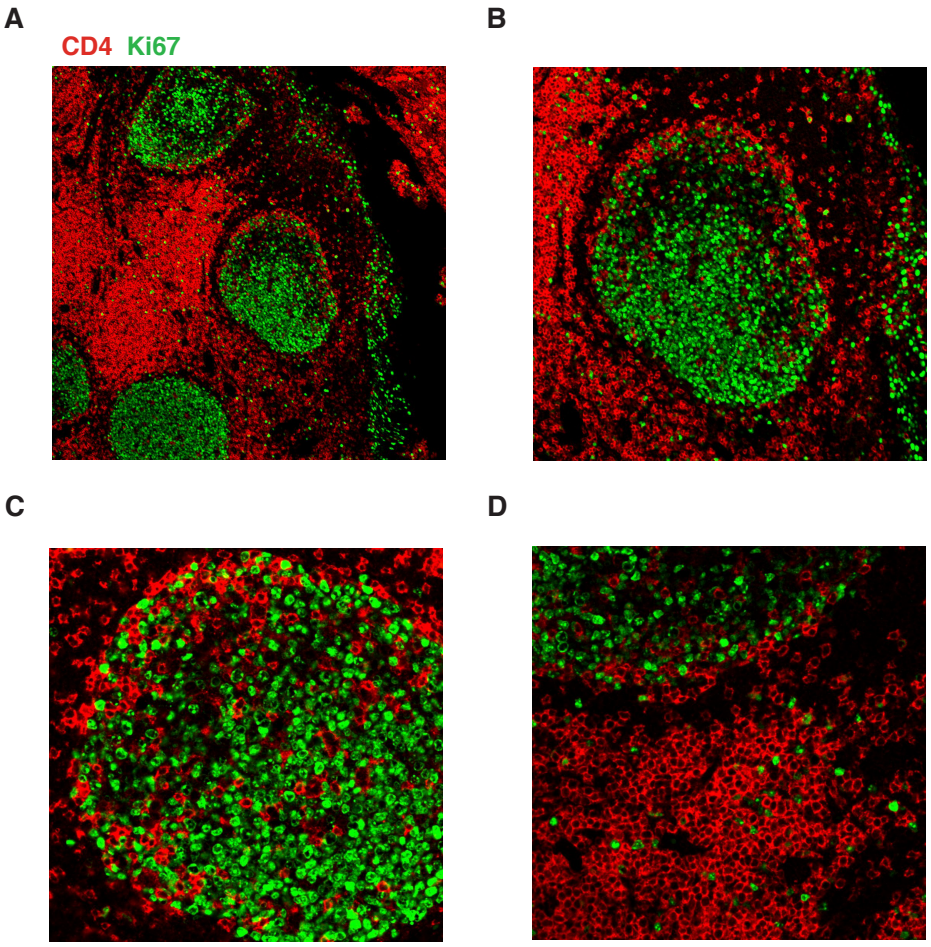
Appendix 5. Controls for the functional experiments. The anti-CD161 on its own had no effect on B cell survival (n=4).



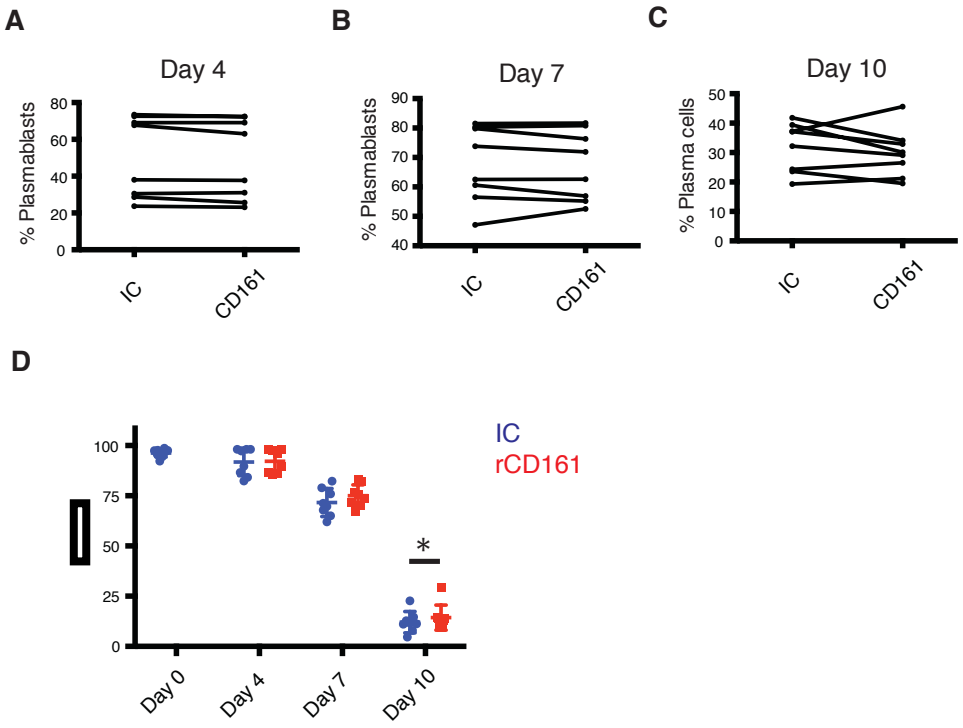
Appendix 6. Titration of anti-BCR and and rCD161. Purified B cells from PBMCs were incubated for 5 days with (A) a fixed concentration of rCD161 or isotype control (IC) (1µg/ml) and increasing concentrations of anti-BCR or (B) a fixed concentration of anti-BCR (1µg/ml) and increasing concentrations of rCD161. Percentage of Annexin V expressing cells were measured by flow cytometry. The dashed red line shows maximum levels of Annexin V positive cells when only anti-BCR stimulation was used. Representative plots of two independent experiments (n=2).



Appendix 7. CD38 time-course. Tonsillar cells were stimulated with CpG (A), anti-CD40 + IL-4 (B), anti-BCR (C) or anti-CD40 + IL-4 + anti-BCR (D) in the presenece of anti-CD161 or isotype control (IC). Alive CD19+ cells were gated and levels of CD38 measured by flow cytometry (n=4).



Appendix 8. Tonsillar T cells do not express Ki67. Immunofluorescent staining of FFPE human tonsillar sections with CD4 (red) and Ki67 (green) revealed no double positives. A (10x), B (20x), C and D (40x). n=4. Two independent experiments.



Appendix 9. **rCD161 stimulation does not alter plasma cell differentiation**. LLT1 stimulation through rCD161 did not alter the percentage of plasmablasts differentiated on Day 4 (A) and Day 7 (B), neither the one of plasma cells on Day 10 (C), compared to the isotype conotrl (IC). On Day 10, the percentage of surviving cells was significantly higher on the LLT1 stimulated sample (D). (n=8; two-way ANOVA using a Bonferroni multiple comparisons test, *p<0.05;). Two independent experiments.

LLT1 and CD161 Expression in Human Germinal Centers Promotes B Cell Activation and CXCR4 Downregulation

Alba Llibre,* Constantino López-Macías,[†,1] Teresa Marafioti,[‡,1] Hema Mehta,* Amy Partridge,* Carina Kanzig,* Felice Rivellese,[§] Jacob D. Galson,[¶] Lucy J. Walker,[‖] Paul Milne,[‖] Rodney E. Phillips,* Dominic F. Kelly,[¶] Gordon J. Freeman,[#] Mohey Eldin ~~M.~~ El Shikh,[§] Paul Klenerman,*[,**,2] and Christian B. Willberg*[,**,2]

Germinal centers (GCs) are microanatomical structures critical for the development of high-affinity Abs and B cell memory. They are organized into two zones, light and dark, with coordinated roles, controlled by local signaling. The innate lectin-like transcript 1 (LLT1) is known to be expressed on B cells, but its functional role in the GC reaction has not been explored. In this study, we report high expression of LLT1 on GC-associated B cells, early plasmablasts, and GC-derived lymphomas. LLT1 expression was readily induced via BCR, CD40, and CpG stimulation on B cells. Unexpectedly, we found high expression of the LLT1 ligand, CD161, on follicular dendritic cells. Triggering of LLT1 supported B cell activation, CD83 upregulation, and CXCR4 downregulation. Overall, these data suggest that LLT1–CD161 interactions play a novel and important role in B cell maturation within the GC in humans.
***The Journal of Immunology*, 2016, 196: 000–000.**

The germinal center (GC) reaction is critical for long-lasting protection against pathogens. GCs are the anatomical sites within secondary lymphoid organs where B cells proliferate and mutate their BCRs to be selected according to their affinity for Ag. Two distinct areas with different functions can be identified within the GC; these are the dark zone (DZ) and the light zone (LZ). In the former, B cells proliferate and hypermutate their BCRs to generate Ab variation, whereas the quality of these BCRs is assessed in the latter, ultimately leading to selection of high-affinity B cell clones (1, 2). DZ B cells are characterized by being $CD83^{low}CXCR4^{high}$, whereas LZ B cells are $CD83^{high}CXCR4^{low}$ (3). B cells that have successfully competed for Ag develop into clones and exit the GC expressing high-affinity Abs and long-lived memory. Thus, this process is crucial to vaccinology. At the same time, however, as a site of mutation and proliferation, aberrant reactions can lead to the development of B cell lymphomas and autoimmunity. Understanding the mechanisms that drive this process has significant implications in health care.

C-type lectin-like receptors (CLRs) are encoded in the NK gene complex (NKC) and can be expressed in a wide range of human cell types, including NK cells. They are particularly relevant in the context of innate immune responses. The CLRs lectin-like transcript 1 (LLT1) and CD161 are genetically linked physiological binding partners, located adjacent to one another within the NKC (4–7). Structurally, LLT1 shares the greatest homology with the other C-type lectins activation-induced C-type lectin and CD69 (8). Within murine models, LLT1 shows a similar expression pattern to MHC class I (9, 10), whereas in humans it is limited to activated lymphocytes and monocytes (8, 11–13) and recently on respiratory syncytial virus–infected primary human bronchial epithelial cells (14), although the published literature presents some inconsistencies. In contrast, the expression of LLT1's

COPYRIGHT DISTRIBUTION PROHIBITED

*Peter Medawar Building for Pathogen Research, University of Oxford, Oxford OX1 3SY, United Kindgom; [†]Medical Research Unit on Immunochemistry, Specialties Hospital, National Medical Centre "Siglo XXI," Mexican Institute for Social Security, 06720 Mexico City, Mexico; [‡]Department of Histopathology, University College London, London WC1E 6JJ, United Kingdom; [§]Centre for Experimental Medicine and Rheumatology, William Harvey Research Institute, Barts and the London School of Medicine and Dentistry, Queen Mary University of London, London ~~E1 2AT,~~ United Kingdom; [¶]Oxford Vaccine Group, Department of Paediatrics, National Institute for Health Research, Oxford Biomedical Research Centre, University of Oxford, Oxford OX3 7LJ, United Kingdom; [‖]Newcastle University, Newcastle upon Tyne NE1 7RU, United Kingdom; [#]Department of Medical Oncology, Dana-Farber Cancer Institute, Harvard Medical School, Boston, MA 02215; and **Oxford National Institute for Health Research Biomedical Research Centre, Oxford OX3 9DU, United Kingdom

[1]C.L.-M. and T.M. contributed equally to this work.

[2]P.K. and C.B.W. contributed equally to this work as cosenior authors.

ORCIDs: 0000-0003-3315-9424 (C.K.); 0000-0003-4916-800X (J.D.G.); 0000-0001-5299-9344 (C.B.W.).

Received for publication November 23, 2015. Accepted for publication January 3, 2016.

This work was supported by grants from the University College London Hospitals/University College London National Institute for Health Research Comprehensive Biomedical Research Centre (to T.M.), the National Institute for Health Research Biomedical Research Centre, Oxford (to C.B.W. and P.K.), National Institutes of Health/National Institute of Allergy and Infectious Diseases U19 Bio-Defense Program (National Institutes of Health/National Institute of Allergy and Infectious Diseases Grant 1U19AI082630-01) (to C.B.W.), and by Wellcome Trust Senior Fellowship WT091663MA (to P.K.) and Obra Social La Caixa (to A.L.).

A.L., C.B.W., C.L.-M., M.E.~~M.~~E.S., and P.K. designed, performed, and analyzed experiments, and wrote the manuscript; R.E.P. provided overall guidance; J.D.G. and D.F.K. provided the vaccine samples; L.J.W. and P.M. provided the bone marrow samples; G.J.F. provided the anti-LLT1 Abs and the 300 cell lines; all of the remaining authors contributed to specific experiments; and P.K. designed experiments and provided overall guidance.

Address correspondence and reprint requests to Dr. Christian B. Willberg or Dr. Mohey Eldin ~~M.~~ El Shikh, Peter Medawar Building for Pathogen Research, University of Oxford, South Parks Road, Oxford OX1 3SY, U.K. (C.B.W.) or ~~William Harvey Research Institute, Queen Mary University of London, 2nd Floor John Vane Science Centre, Charterhouse Square,~~ London EC1M 6BQ, U.K. (M.E.~~M.~~E.S.). E-mail addresses: chris.willberg@ndm.ox.ac.uk (C.B.W.) or m.elshikh@qmul.ac.uk (M.E.~~M.~~E.S.)

The online version of this article contains supplemental material.

Abbreviations used in this article: CLR, C-type lectin-like receptor; CTV, CellTrace Violet; DZ, dark zone; FDC, follicular dendritic cell; GC, germinal center; IRF, IFN regulatory factor; LLT1, lectin-like transcript 1; LZ, light zone; NKC, NK gene complex; PNA, peanut agglutinin; Tfh, T follicular helper.

This is an open-access article distributed under the terms of the CC-BY 3.0 Unported license.

Copyright © 2016 The Authors 0022-1767/16

binding partner, CD161, has been relatively well characterized, delineating a family of innate-like T lymphocytes and NK cells (15). Functional studies have described inhibitory and activating roles for both molecules (6, 7, 15–23). These studies suggest that interactions between LLT1 and CD161 can result in bidirectional signaling and have functional consequences for both cells involved.

In this study, we show the high expression of LLT1 on human GC B cells and GC-derived B cell lymphomas, extending previous studies (6, 8, 11–13, 17). We also show that LLT1 expression remains on early plasmablasts, but is absent from memory B cells and plasma cells. The LLT1 ligand, CD161, was found, unexpectedly, on follicular dendritic cells (FDCs). Finally, triggering of LLT1 promoted the upregulation of CD83 on B cell and drives DZ B cells toward a LZ phenotype through the downregulation of CXCR4. Previously, LLT1 and CD161 were considered part of innate immune responses. The present study ~~demonstrates, to our knowledge for the first time,~~ a functional role for an innate receptor pairing at the heart of a critical adaptive immune process, the GC reaction in humans.

Materials and Methods

Tissues, cells, and cell lines

Human tonsillar tissue was obtained following routine tonsillectomy from the files of the Department of Cellular Pathology (University College London Hospital, London, U.K.); Human Tissue Resource Centre, Barts and the London National Health Service Trust, Queen Mary School of Medicine and Dentistry; and from the Ear, Nose, and Throat Department, John Radcliffe Hospital, Oxford, U.K. Normal tonsillar tissue sections were obtained from ProteoGenix (Schiltigheim, France). Tonsil-derived single cells were collected by mechanical disruption of tonsil samples or collagenase D (1 mg/ml; Boehringer Mannheim) and DNase I (0.1 mg/ml; Sigma-Aldrich, Dorset, U.K.) digestion, as stated. The lymphoma samples analyzed were in the form of 0.6- to 1-mm core tissue arrays.

PBMCs obtained from the National Blood Transfusion Service (National Health Service Blood and Transplant) were isolated on a Lymphoprep gradient (Axis-Shield, Dundee, U.K.).

Bulk B cells were isolated by negative selections from PBMCs or tonsils by magnetic isolation (Stemcell Technologies, Cambridge, U.K.) following manufacturer's protocols.

300.19-hCLEC2D cells were created by transfection of 300.19 with a vector expressing human CD161/CLEC2D cDNA and maintained under selection.

Vaccine samples were obtained from the Oxford Vaccine Group, Churchill Hospital (Oxford, U.K.) following HBV vaccinations.

Bone marrow samples were obtained from routine hip joint operations (Newcastle University, Newcastle upon Tyne, U.K.). Samples were filtered (40 mm), washed with PBS, homogenized, isolated on a Lymphoprep gradient (Axis-Shield) and aliquoted in FCS plus 10% DMSO (Sigma-Aldrich) and stored in liquid nitrogen until required.

For sorted cells, DZ B cells were FACS sorted using a MoFlo XDP (Beckman Coulter, High Wycombe, U.K.) from purified B cells and defined as singlets, alive, $CD38^{mid}IgD^{-}CXCR4^{high}CD83^{low}$ cells.

Informed consent was obtained from all subjects.

In vitro differentiation of plasma cells

Memory B cells were differentiated in vitro into plasmablasts and plasma cells, following the protocol described in Jourdan et al. (24). Briefly, $CD27^{+}$ Memory B cells were first purified as bulk B cells by negative selection from PBMCs by magnetic isolation followed by positive selection for $CD27^{+}$ cells (Stemcell Technologies) following the manufacturer's protocol. The cells were then seeded at 1.5×10^5 cells/ml and cultured for 4 d in the presence of CpG oligodeoxynucleotide 2006 (10 μg/ml; Invitrogen, Paisley, U.K.), soluble human his-rCD40L (50 ng/ml; R&D Systems, Abingdon, U.K.) and anti–poly-his (5 μg/ml; R&D Systems), IL-2 (20 U/ml; R&D Systems), IL-10 (50 ng/ml; Miltenyi Biotec, Surrey, U.K.), and IL-15 (10 ng/ml; Miltenyi Biotec). At day 4 of culture, the cells were washed and cultured at 2.5×10^5 cells/ml with IL-2 (20 U/ml; Miltenyi Biotec), IL-10 (50 ng/ml), IL-15 (10 ng/ml; PeproTech, London, U.K.), and IL-6 (50 ng/ml; Miltenyi Biotec). At day 7 of culture, cells were washed and seeded with IL-ɒ (50 ng/ml; PeproTech), IL-15 (10 ng/ml; PeproTech), and IFN-α (500 U/ml; R&D Systems) for 3 d.

Flow cytometry

FACS staining was external unless otherwise specified. Cells were stained with a Live/Dead fixable near-IR dead cell stain kit, for 633 or 635 nm excitation (Invitrogen). For internal staining, cells were fixed with 2% formaldehyde (Sigma-Aldrich) and permeabilized with ~~IX~~ permeabilization buffer (eBioscience, Hatfield, U.K.). The following Abs were used for flow cytometric analysis: anti–CD4-PerCp-Cy5.5 (RPA-T4), anti–CD19-Pacific Blue (HIB19), anti–CD38-PerCP-Cy5.5 (HIT2), anti–IgD-FITC (IA6-2), anti–CXCR5-Pacific Blue (J252D4), anti–CD27-PE-Cy7 (M-T271), anti–CD34-FITC (561), anti–CD68-allophycocyanin (Y1/82A), anti–CD83-BV421 (HB15e), anti–ICOS-allophycocyanin (C398.4A) (BioLegend, London, U.K.), anti–CD20-Pacific Orange (HI47, Life Technologies, Paisley, U.K.), anti–CD138-allophycocyanin (B-A38, Beckman Coulter), anti–CD10-PE-Cy7 (HI10a), anti–CD45-RA-FITC (T6D11), anti–CD161-PE (191B8), anti–IgM-allophycocyanin (PJ2-22H3), anti–CXCR4-allophycocyanin (12G5, Miltenyi Biotec), anti–CD3-FITC (ICHT1, R&D Systems), anti–LLT1-PE (402659, R&D Systems), anti–IgG isotype control-PE, IgG1 and IG2A isotype controls (R&D Systems), and anti–mouse IgG-PE (R&D Systems).

Novel mouse anti-human CLEC2D (LLT1) mAbs were generated, including clones 359.7G7 (mIgG1) and 359.2H7 (mIgG2al). All purified Abs are dialyzed against PBS, are low in endotoxin (<2 endotoxin units/mg), and are filtered sterile.

Immunohistochemistry

Tissue deparaffinization was performed using Histo-Clear (National Diagnostics, Hull, U.K.) and ethanol (Sigma-Aldrich; 100, 90, and 70%). Heat-mediated Ag retrieval was achieved using Dako target retrieval solution (Dako, Ely, U.K.). Endogenous peroxidase activity was blocked using 3% H_2O_2 (5 min × 2; Alfa Aesar, Heysham, U.K.) and 0.1% sodium azide (15 min; Sigma-Aldrich) in water. Nonspecific binding was blocked with 0.5% blocking reagent (PerkinElmer, Beaconsfield, U.K.) in PBS.

Cy5/fluorescein stains were amplified using amplification reagents (PerkinElmer) diluted in tyramide amplification buffer (12 ml 500 mM Tris, 18 ml H_2O, 20 mg imidazole [Sigma-Aldrich], 1 μl H_2O_2). Residual peroxidase activity was blocked by incubating the slides in 3% H_2O_2 and then 0.1% sodium azide in water. Slides were mounted with ProLong Gold antifade reagent with DAPI (Invitrogen).

A goat polyclonal anti-LLT1 Ab (AF3480, R&D Systems) and a novel mouse mAb (7G7) were used for immunohistological staining, as well as CD3 (clone LN10, Leica Microsystems, Cambridge, U.K.) and PAX-5 (clone 24, BD Biosciences, Oxford, U.K.).

Anti-CD161 (B199.2, AbD Serotec, Kidlington, U.K.; 1:100), IgG1, or IgG2A isotype controls (R&D Systems) were also used and incubated overnight at 4˚C and then incubated with anti-goat/mouse polymer (Vector Laboratories, Peterborough, U.K.) HRP conjugated (Vector Laboratories), followed by ImmPACT diaminobenzidine peroxidase substrate (Vector Laboratories). The section was covered with hematoxylin (Vector Laboratories) and washed.

In addition to these stains, the following Abs were used for fluorescence immunohistochemistry: anti-LLT1 goat polyclonal (AF3480, R&D Systems, 1:200), anti-CD68 (1:200, clone PG-M1), anti-FDC (1:100, clone CNA.42), anti-CD19 (1:500, clone LE-CD19), anti-CD20cy (1:1000, clone L26), anti-CD3 (1:200, clone F7.2.38), anti-CD79α (1:200, clone JCB117), anti-CD45 (1:1000, clone 2B11 plus PD7/26), anti-IgG (1:1000, rabbit), anti-IgM (1:1000), anti-CD38 (1:200, clone At13/5), anti-CD138 (1:100, clone MI15), anti-Ki67 (1:200, clone MIB-1), and anti–IFN regulatory factor (IRF) 4 (1:200, clone MUM1) (Dako); anti–cathepsin G (1:1000), anti-IgD (1:200), anti-IgA (1:300) (Leica Biosystems, Newcastle upon Tyne, U.K.); anti-IgE (rabbit, Abcam, Cambridge, U.K.), and normal goat IgG and mouse IgG1/IgG2A isotype controls (R&D Systems). Abs were mouse derived unless otherwise specified.

For the FDC and CD161 costaining in frozen tonsils, four different anti-CD161 Abs were used: 191B8 (Miltenyi Biotec), IMG141F1F1 (Abcam), B199.2 (AbD Serotec), and HP-3G10 (BioLegend). Ten-micrometer-thick frozen tonsillar sections were labeled with 10 μg/ml goat anti-LLT1 (R&D Systems, AF3480-SP), mouse anti-CD161 (Abcam, ab23624), and rabbit anti-CD3 (Dako, A0452), followed by 10 μg/ml donkey anti–goat-Alexa Fluor 488, donkey anti–mouse-Alexa Fluor 594, and donkey anti–rabbit-Alexa Fluor 647 (Jackson ImmunoResearch, Suffolk, U.K.), respectively, and peanut agglutinin (PNA; Vector Laboratories, Peterborough, U.K.).

FINAL DISTRIBUTION PROHIBITED

B cell activation

Isolated B cells were stimulated with oligodeoxynucleotide 2006 (CpG, InvivoGen, Wiltshire, U.K.) for 48 h. TLR signaling inhibition studies used the MyD88 inhibitory peptide Pepinh-MYD at the given concentration (InvivoGen). B cell stimulations were achieved using goat anti-human IgM/G/A F(ab′)$_2$ (Jackson ImmunoResearch) fragments at 1 μg/ml, anti-CD40 (clone S2C6, Macbeth) at 5 μg/ml, or with IL-4 (PeproTech), IL-10, IL-21 (Miltenyi Biotec), PGE_2 (Sigma-Aldrich), IL-15 (Miltenyi Biotec), and BAFF (Miltenyi Biotec) (all at 50 ng/ml). Proliferations assays were performed using a CellTrace Violet (CTV) cell proliferation kit (Life Technologies).

The CD161 blocking assay included 2×10^6 B cells/ml in 500 μl in a 48-well plate (Corning, ~~U.K.~~) with combinations of CpG (5 μM), anti-CD40 (5 μg/ml) plus IL-4 (50 ng/ml), anti-CD161 at 1 μg/ml (clone 191.B8, Miltenyi Biotec), and IgG2A isotype control (R&D Systems).

For LLT1 crosslinking, recombinant CD161 (R&D Systems) or IgG1 isotype control (R&D Systems) were bound to a 96-well ELISA plate (Greiner Bio-One, Stonehouse, U.K.) overnight prior to the addition of B cells and BCR stimulus as described above.

Proliferation assay

Proliferation assays were performed using a CTV cell proliferation kit (Life Technologies). Purified B cells were stained with 2.5 μM CTV for 10 min at room temperature, following the manufacturer's instructions. Cells were then counted and 2×10^5 B cells were plated per well in a U-bottom 96-well plate with CpG (0.5 μg/ml) for 5 d.

CD161 depletion

Tonsillar cells were stained with CD161-PE (Miltenyi Biotec) and depleted from the sample by FACS sorting using a MoFlo (Beckman Coulter). After CpG (0.5 μM, InvivoGen) or anti-CD40 (5μg/ml, Macbeth) plus IL-4 stimulation (50 ng/ml, PeproTech), levels of CD38 and CD83, respectively, were measured in alive CD19$^+$ cells.

Real-time PCR

For real time RT-PCR, amplification was assessed using molecular probes 32 (for CD161) and 60 (for GAPDH) from the Universal ProbeLibrary set, human (Roche, Welwyn Garden City, U.K.) on a LightCycler 480 (Roche). The following primers were used: CD161, forward, 5′-AAATGCAGTGTGGACATTCAA-3′, reverse, 5′-CTCGGAGTTGCTGCCAATA-3′ (Eurofins MWG Operon, Ebersberg, Germany); GADPH, forward, 5′-AGCCACATCGCTCAGACAC-3′, reverse, 5′-GCCCAATACGACCAAATCC-3′; CXCR4, forward, 5′- GGTGGTCTATGTTGGCGTCT-3′, reverse, 5′-ACTGACGTTGGCAAAGATGA-3′ (Eurofins MWG Operon, Germany).

Data acquisition and analysis

FACS analysis was performed on Miltenyi Biotec MACSQuant cytometer and analyzed with FlowJo version 9.6.2 software (Tree Star, Ashland, OR). Graphs and statistical analysis were performed using GraphPad Prism version 6.0a (GraphPad Software, San Diego, CA).

For analysis of immunohistochemical staining, images were acquired on a DSS1 Coolscope slide scanner (Nikon, Kingston upon Thames, U.K.).

For immunofluorescent microscopy, images were acquired on an Olympus Fluoview FV1000 microscope (Olympus, Southend-on-Sea, U.K.) and analyzed using Fiji (ImageJ, National Institutes of Health, Bethesda, MD). The Leica TCS-SP2 AOBS confocal laser-scanning microscope was used for the CD161 immunofluorescence, and the images were captured and processed with Leica confocal software (LCS Lite) and ImageJ.

Results

LLT1 is highly expressed on GC B cells

LLT1 expression was observed within normal human tonsils and predominantly expressed within GCs (Fig. 1A). This was demonstrated by immunohistological staining using two independent Abs: a commercial goat polyclonal anti-LLT1 Ab, and a novel anti-LLT1 Ab (clone 7G7, see *Materials and Methods*, Supplemental Fig 1A, 1B). Furthermore, this was not restricted to tonsillar tissue, as GCs within spleen, lymph nodes, and Peyer's patches were also LLT1$^+$ (Supplemental Fig. 1C–F).

LLT1 expression within GC cells was restricted to PAX-5$^+$ cells, B cells (Fig. 1B). Intra-GC T cells (Fig. 1B), tingible body macrophages, neutrophils, and FDCs within secondary follicles were all negative for LLT1 (data not shown). However, within the interfollicular areas, LLT1 expression was seen on a small proportion of CD3$^+$ T cells (Fig. 1B, *inset*). Furthermore, LLT1 expression on GC B cells was confirmed by costaining for CD20 (Fig. 1C), Ki67 (Fig. 1D), and CD38 (Fig. 1E). FACS analysis, using a second novel anti-LLT1 Ab (clone 2H7), also confirmed LLT1 on GC B cells, defined as CD38^{mid}IgD$^-$, as previously described (25–27) (Fig. 1F).

LLT1 expression was not homogeneous throughout the GC. A clear difference in LLT1 staining intensity could be seen by immunohistology. Cross-sectional analysis through the GC revealed increased LLT1 levels within the DZ compared with the LZ (defined by the presence of CD3$^+$ cells, stained green, Fig. 1G). Moreover, FACS analysis confirmed higher LLT1 expression on DZ B cells (CD83^{low}CXCR4^{high}) compared with LZ B cells (CD83^{high}CXCR4^{low}) (Fig. 1H).

LLT1 is expressed on plasmablasts but not memory B cells

B cells exit the GC upon differentiation into plasma or memory B cells. Whether LLT1 expression is maintained in these GC B cell derivatives is not known; therefore, we sought to track LLT1 expression through these stages. Plasmablasts were identified by costaining tonsillar sections with LLT1 plus CD19, CD20, CD38, CD45, CD79α, CD138, IRF4 (MUM-1), and Igs (Fig. 2A). LLT1$^+$ cells coexpressed these markers in a pattern suggestive of a plasmablast phenotype (CD45^{low}, CD20$^-$, CD19^{low}, CD79α$^{-/low}$, pan Ig$^+$, MUM-1$^{+/-}$, CD38$^+$, Ki67$^{+/-}$, CD138$^-$), although there remained a number of LLT1$^+$ cells that did not fit this phenotype and remain to be identified.

FACS analysis, using the Bm1–Bm5 classification based on CD38 and IgD markers (Fig. 2B), revealed that LLT1 expression was restricted to GC B cells, pre-GC B cells, and plasmablasts within tonsillar-derived cells (Fig. 2C) and plasmablasts within PBMCs (Fig. 2D) (25, 26, 28). The IgD$^+$CD38^{low} compartment, comprising both naive and transitional B cells, were mainly negative for LLT1 (Fig. 2C, 2D) (29). As plasmablast frequencies are normally low in circulation, we also confirmed LLT1 expression on plasmablasts in individuals 1 wk postvaccination, where plasmablasts are readily detectable (30, 31) (Fig. 2E). LLT1 expression, however, was not detected on plasma cells or memory B cells (Fig. 2A–C).

To confirm that LLT1 is downregulated as plasmablasts mature into plasma cells, we differentiated CD27$^+$ memory B cells into plasmablasts and then plasma cells in vitro, as described by Jourdan et al. (24). LLT1 expression was measured by FACS analysis at days 0 (memory B cells), 4 (early plasmablasts), 7 (late plasmabalsts), and 10 (plasma cells) (Fig. 2F). Day 0 resting CD27$^+$ memory B cells expressed very low levels of LLT1, but LLT1 was highly upregulated at day 4 on early plasmablasts, but downregulated at further stages of differentiation (Fig. 2G). Additionally, we confirmed the absence of LLT1 on plasma cells in vivo by FACS and immunohistological staining of long-lived, bone marrow–resident CD138$^+$ cells from bone marrow samples (data not shown).

Given access to bone marrow samples, we took the opportunity to assess expression levels of LLT1 on the early developmental stages of B cells; thus, we were able to assess LLT1 expression throughout the whole life of a B cell (Supplemental Fig. 2).

Regulation of LLT1 expression on memory B cells

Next we questioned how LLT1 was regulated within B cells. Previous work has shown LLT1 can be upregulated following TLR9, BCR, and CD40 stimulation (21). We confirmed CpG-

© AAI DISTRIBUTION PROHIBITED

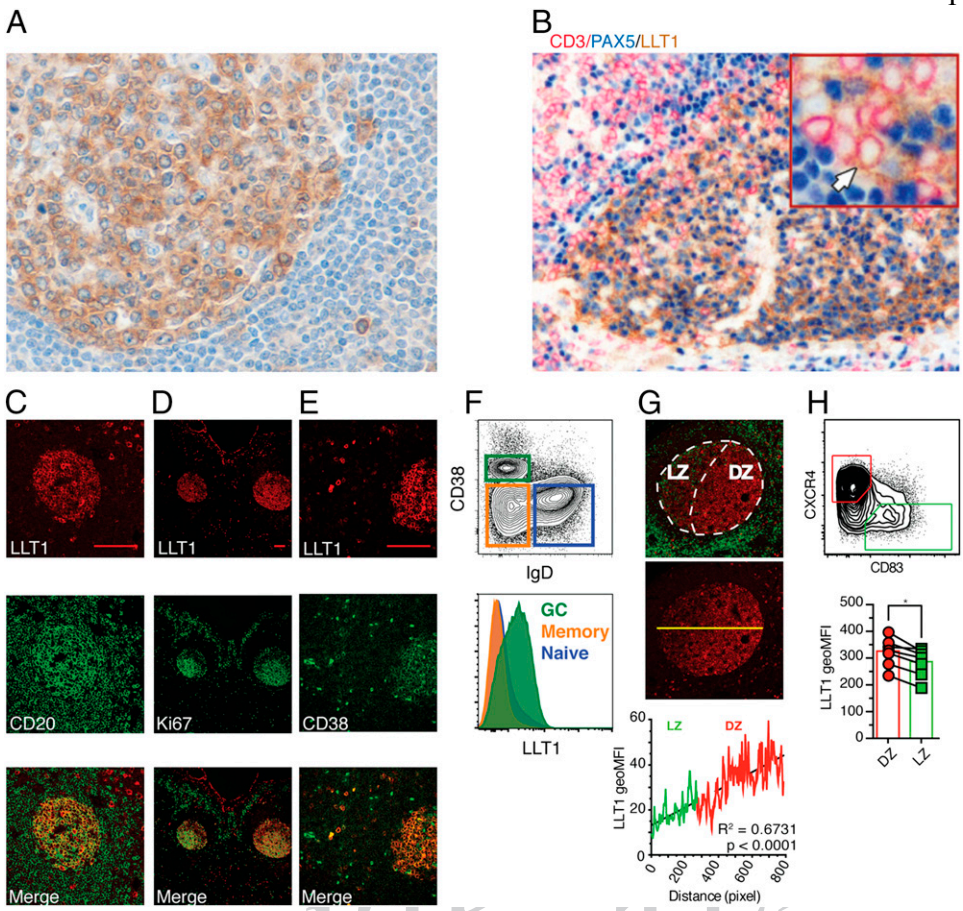


FIGURE 1. LLT1 is expressed on GC B cells. (**A**) Expression of LLT1 (brown), using the 7G7, was assessed in formalin-fixed, paraffin-embedded human tonsillar tissue sections (original magnification ×40) (representative of five sections). (**B**) Triple staining for LLT1 (membrane and cytosol brown), CD3 (membrane pink), and PAX-5 (nuclear blue) showed LLT1 (goat-polyclonal, brown) strongly associated with PAX-5 and only rarely with CD3 (arrow in *inset*) (original magnification ×20, *inset* ×60). Costaining of LLT1 (goat-polyclonal) with CD20 (**C**), Ki67 (**D**), and CD38 (**E**) (scale bar, 100 μm, representative of three sections). (**F**) FACS analysis of LLT1 expression on naive (blue), memory (orange), and GC (green) B cells (representative plot of five independent experiments). (**G**) Cross-sectional analysis through a region (yellow band) of a GC (green indicates CD3, red indicates LLT1; representative of three independent experiments). Geometric mean fluorescence intensity (geoMFI) of LLT1 expression within the defined yellow region plotted against pixel count; the LZ (green) and DZ (red) regions are highlighted. (**H**) FACS analysis of LLT1 (2H7 clone) on LZ and DZ, CXCR4 and CD83, respectively (*$p <$ 0.05, nonparametric paired *t* test).

induced expression (Fig. 3A) and extended this to show that this mechanism is MyD88-dependent, as the presence of the MyD88 inhibitor, Pepinh-MYD, blocked upregulation (Fig. 3B). In addition to CpG, we explored the kinetics of both BCR and CD40 stimulation to induced LLT1 expression. BCR signaling in isolated PBMC-derived memory B cells induced a maximum expression after 5 d (Fig. 3C), whereas CD40 stimulation induced LLT1 expression within 2 d (Fig. 3D). Furthermore, B cell activation is associated with a broad range of cytokines; therefore, we assessed the ability of IL-4, IL-10, IL-21, PGE_2, IL-15, and BAFF to upregulate LLT1. None of the cytokines tested was able to induce LLT1 expression (Fig. 3E) (32–35).

Interestingly, LLT1 expression was associated with early rounds of proliferation after CpG stimulation, increasing with each division until the third, were it plateaued (Fig. 3F). This is consistent with the observation of high LLT1 expression within DZ B cells (Fig. 1G, 1H), plasmablasts (Fig. 2), and B cell lymphomas (see Fig. 6).

CD161 is expressed on FDCs and on a subset of tonsillar T cells

Before we addressed the function of LLT1, we looked for the expression of the LLT1 ligand, CD161, within the context of the GC. CD161 expression has been described on both NK cells and T cells. Therefore, T follicular helper (Tfh) cells were an obvious candidate cell type, with a potential to interact with GC B cells. Flow cytometric analysis of tonsillar T cells revealed a loss of CD161 expression as the Tfh cells progressed to full GC phenotype, as defined by CXCR5 expression (36) (Fig. 4A, *top right panel*). This was confirmed at the mRNA level in sorted tonsillar T cells (Fig. 4A, *bottom right panel*). Although a small fraction (<10%) of $CXCR5^{high}$ Tfh cells expressed CD161, they were not observed within any of the GCs assessed by immunofluorescence microscopy (Fig. 4B, Supplemental Fig. 3). Similarly, within the PBMCs, circulating Tfh cells (defined simply as $CXCR5^{mid}$) (37) also had lower frequencies of $CD161^{+}$ cells compared with the $CXCR5^{-}$ fraction (Supplemental Fig. 3).

Next, CD161 expression was assessed on tonsillar macrophages (including tingible body macrophages), defined by CD68 expression; however, no expression was observed (Supplemental Fig. 3).

Unexpectedly, immunofluorescence staining of human tonsils revealed the expression of CD161 on FDCs (Fig. 4C). Costaining of CD161 and a FDC marker (CNA.42 clone) showed a strong overlap, with a typical stain pattern associated with FDCs. This striking finding was confirmed by histological staining and was not specific to just one clone of anti-CD161 Ab (Supplemental

FIRST PROOFS

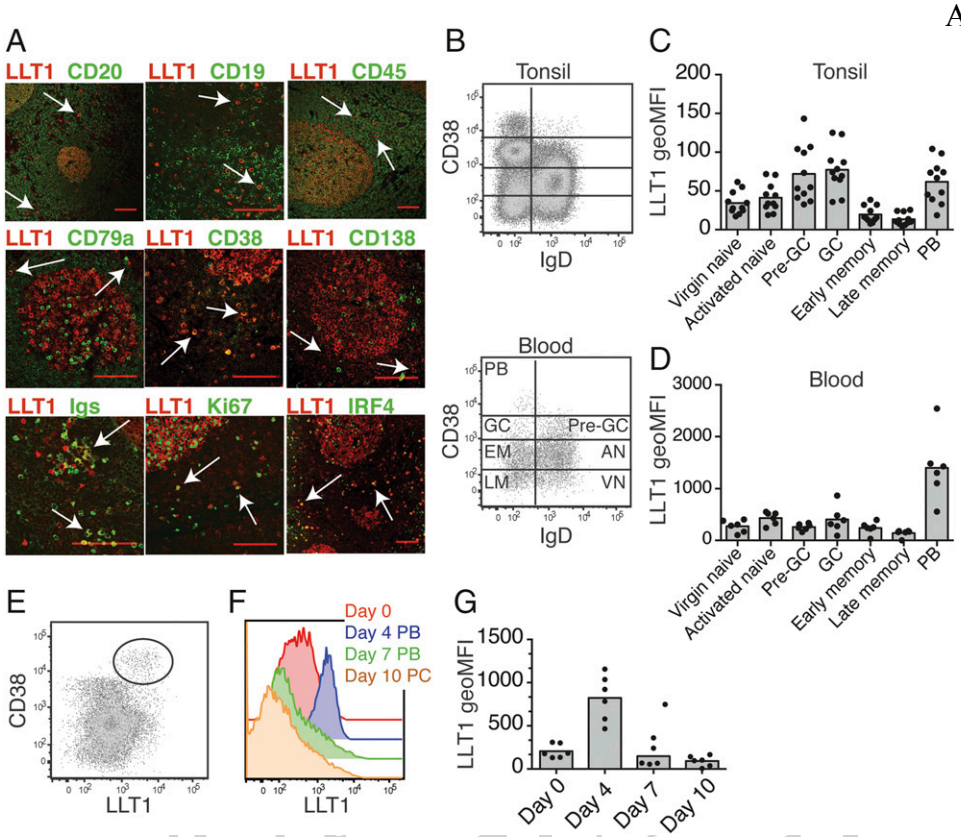


FIGURE 2. LLT1 is expressed on early plasmablasts. (**A**) Costainings in formalin-fixed, paraffin-embedded human tonsillar tissue of LLT1 with CD20 (original magnification ×10), CD19 (original magnification ×20), CD45 (original magnification ×10), CD79a (original magnification ×20), CD38 (original magnification ×20), CD138 (original magnification ×20), Igs (original magnification ×20), Ki67 (original magnification ×20), and IRF4 (original magnification ×10). White arrows indicate double-positive cells (scale bars, 100 μm), representative of three independent sections. (**B**) Seven different B cell subsets identified by IgD and CD38 expression in tonsillar tissue (*top*) and PMBCs (*bottom*): virgin naive (VN), activated naive (AN), pre-GC, early memory (EM), late memory (LM), and plasmablasts (PB) are shown. Geometric mean fluorescence intensity (geoMFI) of LLT1 was measured in the subsets: tonsils (**C**, $n = 10$) and blood (**D**, $n = 3$). (**E**) Expression of LLT1 in the plasmablast subset in an example vaccinated individual 1 wk post-immunization, representative of eight similar individuals. (**F** and **G**) LLT1 expression in in vitro–generated plasmablasts analyzed on day 0, day 4 plasmablasts (PB), day 7 PB, and day 10 plasma cells (PC). (F) Representative FACS plot of time course. (G) Graphed data pooled from three independent experiments (total $n = 6$).

DISTRIBUTED PROHIBITED

Fig. 3). Costaining of PNA, LLT1, and CD161 showed interaction between LLT1 on GC B cells and CD161, expressed in a FDC pattern, within the GC (Fig. 4D).

LLT1 promotes B cell activation and downregulation of CXCR4 in GC B cells

Interactions between FDCs and B cells are complex, involving a wide range of receptors (38). Binding of BCRs to Ags, presented by the FDC, and of CD40 to CD40L delivers crucial signals required for B cells to progress to the next stage of the GC reaction and interact with Tfh cells, and subsequently go on to re-enter the DZ (10, 39–41).

As B cell–FDC interactions involve many different ligands and receptors, we explored the role of LLT1 in isolated B cells. Initially, we investigated LLT1 signaling in primary B cells, inducing LLT1 expression through stimulation with anti-BCR, as described above, with and without rCD161 protein or a control protein (IC). After 5 d of stimulation, B cell expression of CD83 and CD38 was measured by flow cytometry. Triggering of LLT1 on B cells through rCD161 resulted in increased B cell activation. Significantly higher increases in CD83 and CD38 were seen on B cells in the presence of rCD161 compared with the controls (Fig. 5A).

As both proteins are highly glycosylated and have a weak binding strength (K_d of 48 μM), we addressed whether binding of naturally expressed LLT1–CD161 would reveal stronger signaling (42). To analyze this, we cultured tonsillar cells, which included both B cells and CD161$^+$ cells, for 3 d with either anti-CD40 plus IL-4 or CpG and assessed their activation state by flow cytometry on day 3. The effect of LLT1 signaling was measured through the use of blocking Abs to CD161 (Fig. 5B, *left panel*). Stimulation of B cells with anti-CD40 plus IL-4 resulted in a striking upregulation of CD83 on day 3, which was significantly inhibited by the addition of the anti-CD161 Ab. This was not observed with the CpG-stimulated sample. In contrast, levels of CD38 expression were highly increased upon CpG stimulation. Once again, the addition of the anti-CD161 blocking Ab significantly reduced CD38 upregulation (Fig. 5B, *right panel*). Furthermore, depletion of CD161$^+$ cells from the cellular cultures, prior to stimulation with either anti-CD40 plus IL-4 or CpG, also resulted in a significant decrease in CD83 and CD38 expression, respectively (Fig. 5C, *left panel* for anti-CD40 plus IL-4 stimulation and *right panel* for CpG stimulation).

Finally, we explored the functional consequences of LLT1 triggering on GC B cells. The presence of rCD161 or the crosslinking anti-LLT1 Ab (2H7) did not have an impact on CD83 expression levels (Fig. 5D), CD38, or survival (Supplemental Fig. 4); however, LLT1 signaling resulted in a significant reduction of CXCR4 (Fig. 5E). This was also analyzed on sorted DZ B cells, where the effect of LLT1 crosslinking resulted in the downregulation of CXCR4 at mRNA level (Fig. 5F).

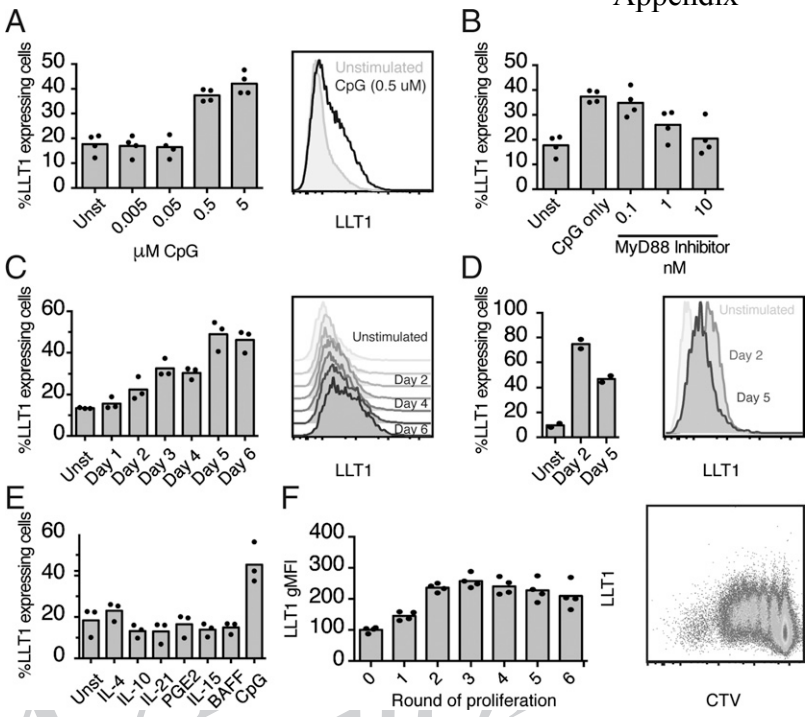


FIGURE 3. LLT1 is upregulated with CpG, anti-BCR, and anti-CD40 stimulation. (**A**) Purified B cells from PBMCs were stimulated with increasing concentrations of TLR9 agonist CpG for 48 h, which resulted in a dose-dependent increase in the percentage of LLT1-expressing B cells (2H7 clone). (**B**) The effect was blockable with MyD88 inhibitor, Pepinh-MYD, and it was also dose-dependent. (**C**) BCR stimulation resulted in upregulation of LLT1 on B cells. (**D**) LLT1 was also upregulated on B cells upon CD40 stimulation. (**E**) Stimulation with different cytokines (50 ng/ml for 48 h) did not alter expression levels of LLT1 on B cells. (**F**) B cell proliferation, measured by CTV dilution, after 5 d with CpG stimulation (0.5 μM). LLT1 increased in successive rounds of proliferation and reached a plateau. Representative plots of three independent experiments are shown.

These findings suggest that LLT1 is involved in the transition of DZ B cells to the LZ through the downregulation of CXCR4, while contributing to enhanced levels of CD83 expression.

LLT1 is expressed in human B cell lymphomas

As a site of mutation and proliferation, many B cell lymphomas are derived from the GC. Therefore, having established LLT1 expression on GC B cells in vivo under normal conditions, we next examined whether such linked expression was maintained in the context of neoplasia. We assessed LLT1 expression in five B cell lymphoma cell lines. FL18, KHM2, L421, and SUDHL6 were positive for LLT1, whereas Burkitt's lymphoma–derived Namalwa cells where negative (data not shown). Using a commercially available LLT1 Ab (goat polyclonal, see *Materials and Methods*),

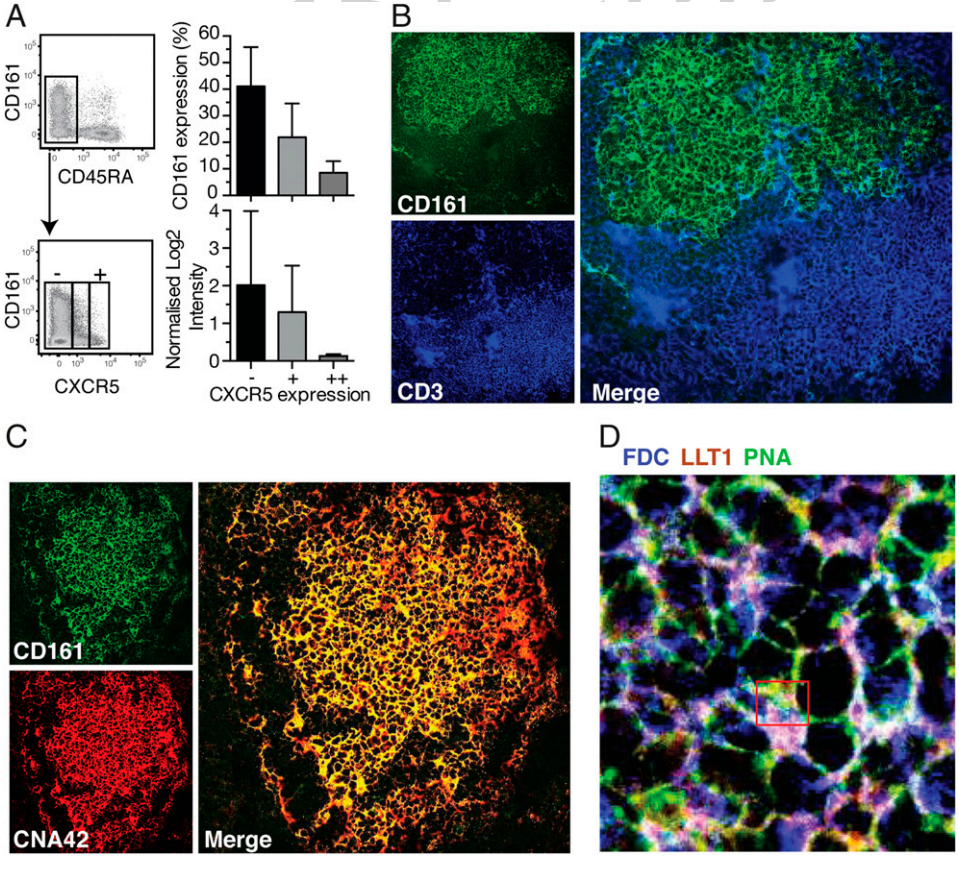


FIGURE 4. CD161 is expressed on FDCs and on a subset of tonsillar T cells. (**A**) CD161 expression negatively correlated with CXCR5 expression on CD45RA$^-$ T cells (CD3$^+$ CD4+) assessed by FACS (n = 5, three independent experiments) and real-time PCR (n = 3, two independent experiments). (**B**) Costaining of CD161 and CD3, showing no double-positives within the GC. (**C**) Immunofluorescence staining of frozen human tonsils with an FDC marker (clone CNA.42) and CD161 (clone IMG14F1F11) showed complete overlap between these two markers. (**D**) Triple FDC, LLT1, and PNA stain of a frozen tonsillar human section. Interaction between FDCs and double-positive LLT1-PNA GC B cells can be observed (red square). Representative image of six different follicles.

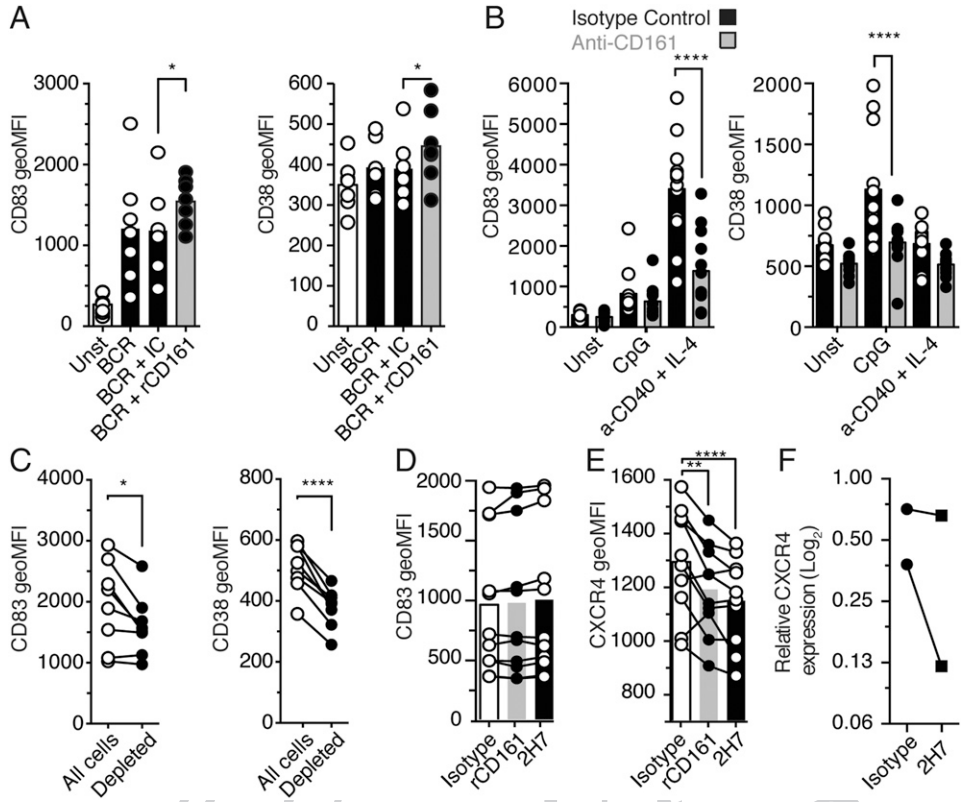


FIGURE 5. LLT1 promotes B cell activation. (**A**) Purified B cells from PBMCs were stimulated with anti-BCRs only or with anti-BCRs with and without rCD161 or IC. Geometric mean fluorescence intensities (GeoMFI) of CD83 and CD38 were measured by flow cytometry. B cell stimulation with rCD161 resulted in enhanced levels of CD83 and CD38; data were pooled from three independent experiments ($n = 7$, $^{**}p < 0.01$). (**B**) Tonsillar cells were cultured for 3 d with CpG or anti-CD40 plus IL-4. Blocking LLT1–CD161 interaction resulted in a decreased expression of CD83 and CD38 on B cells; data were pooled from four independent experiments ($n = 12$, $^{****}p < 0.0001$). (**C**) Depletion of $CD161^+$ cells from tonsillar cells resulted in decreased expression of CD83 (anti-CD40 plus IL-4 stimulation) and CD38 (CpG stimulation) on B cells after 3 d; data were pooled from two independent experiments ($n = 8$; $^{*}p < 0.05$, $^{****}p < 0.0001$, paired t test). (**D**) Overnight stimulation of tonsillar B cells with rCD161 or 2H7 anti-LLT1 Ab did not change the expression of CD83 on GC B cells ($n = 5$). (**E**) However, a decrease in CXCR4 expression levels was observed GC B cells ($n = 10$; $^{**}p < 0.01$, $^{****}p < 0.0001$). (**F**) Repeated experiments on sorted DZ B cells revealed a downregulation of CXCR4 mRNA. All statistics were two-way ANOVA using a Bonferroni multiple comparisons test, unless stated otherwise.

DISTRIBUTED
PROHIBITED

LLT1 expression was evaluated in a series of lymphomas (Fig. 6A–E). LLT1 was absent on non-GC –derived lymphomas, such as B-ALL and plasma cell neoplasms. In contrast, LLT1 expression was seen on most Burkitt lymphomas (14 of 19, 73.68%), follicular lymphomas (48 of 95, 51%), and also on Hodgkin lymphomas (7 of 16, 44%). Subdivision of the follicular lymphomas revealed the highest association of LLT1 on atypical phenotypes that have been previously described: $Bcl\text{-}2^-$ (59%) and $Bcl\text{-}2^-$ and $CD10^-$ (62%) (Fig. 6F, *lower left panel*) (43). Interestingly, LLT1 expression was seen on lymphocyte-predominant Hodgkin lymphomas and not classical Hodgkin lymphomas (Fig. 6F, *lower right panel*). Our data suggest that LLT1 is maintained during malignant transformation in some GC-derived lymphomas and may be a useful additional diagnostic marker.

Discussion

GC were first characterized >125 years ago. In recent years, our understanding of how these dynamic and complex reactions are orchestrated has advanced rapidly. In this study, we report the expression and function of the innate receptor pairing, LLT1 and CD161, within the GC reaction in humans.

A GC can be divided into two microanatomically distinct regions, the LZ and the DZ. Competition for Ag and Tfh cell help occurs within the LZ, whereas somatic hypermutation and proliferation are restricted to the DZ (reviewed in Ref. 40).

Although LLT1 expression was marginally higher on DZ cells, it was observed on all GC B cells in all lymphoid tissues tested. LLT1 expression was not, however, restricted just to GC B cells, as $LLT1^+$ cells were detected outside of the GC. Many of these cells expressed markers associated with a plasmablast phenotype ($CD45^{low}$, $CD20^-$, $CD19^{low}$, $CD79\alpha^{low}$, Ig^+, IRF^+, $CD38^+$, $Ki67^+$, $CD138^-$), although this does not exclude other cell types. In vitro differentiation of memory B cells into plasmablasts and then plasma cells demonstrated that LLT1 expression was lost as cultures progressed toward terminally differentiated plasma cells at day 10 (24). This was also confirmed on staining bone marrow–derived plasma cells. It appears that LLT1 expression on plasmablasts in vivo is a marker of recent exit from the GC, although whether it can also be independently upregulated remains to be addressed.

It was noted that LLT1 was frequently associated with dividing cell populations both in vivo and in vitro. Zhou et al. (23) also observed that OCIL (LLT1) mRNA expression was at its highest during the osteoblast proliferative phase of bone marrow cultures. In contrast, we observed that LLT1 was absent from plasma cells and both early and late memory B cells, which are nondividing cells. This suggests a link between proliferation and LLT1 expression, although we have not as yet been able to find any

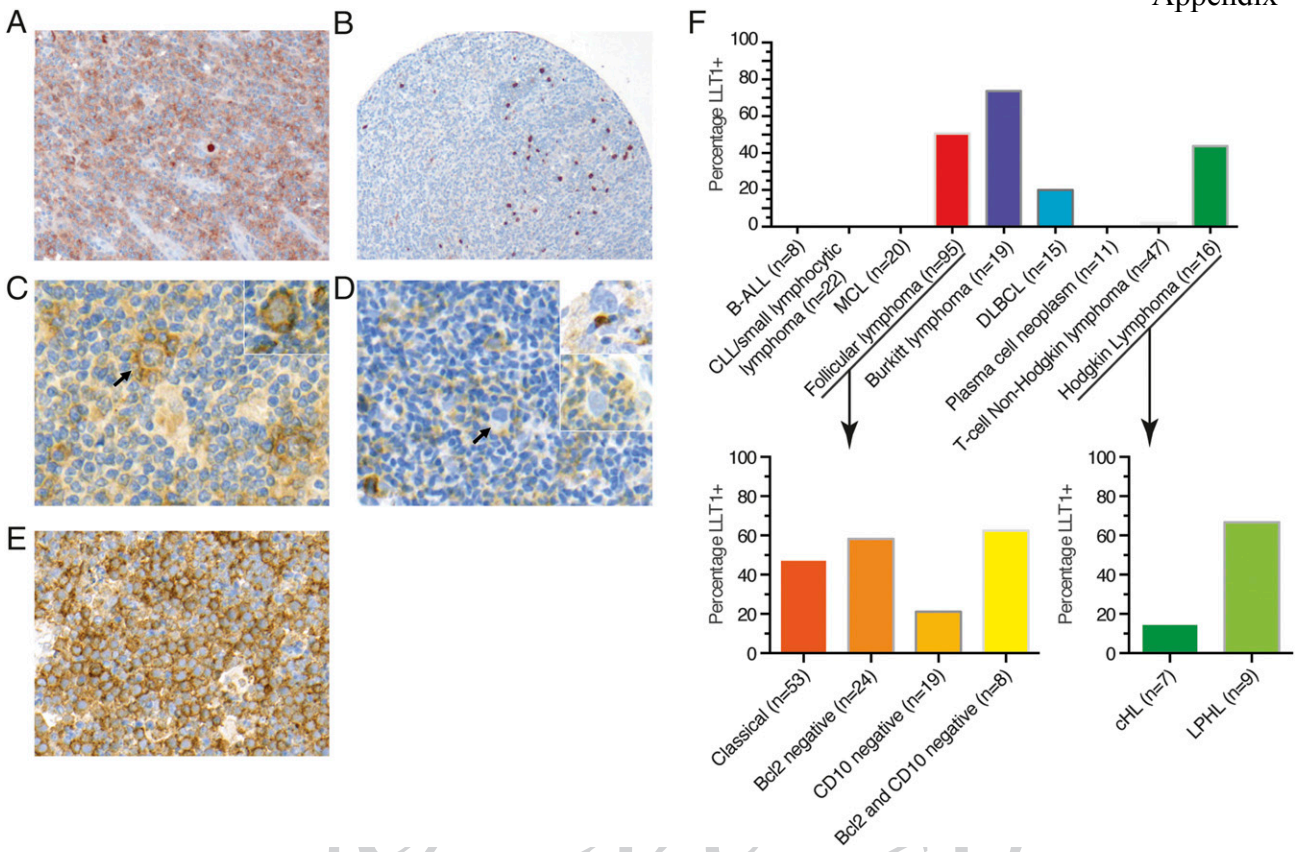


FIGURE 6. LLT1 is expressed in human B cell lymphomas. (**A**–**E**) Representative stainings of LLT1 (membrane and cytosol brown) as assessed (polyclonal Ab AF3480) in formalin-fixed, paraffin-embedded tissue sections of follicular lymphoma samples ~~(A and B)~~, lymphocyte-predominant Hodgkin lymphoma [(C) original magnification ×40; arrow and *inset* highlighting LLT1^{+} staining], classical Hodgkin lymphoma [(D) original magnification ×40; arrow and *inset* highlighting LLT1$^{+/-}$ staining], and Burkitt lymphoma [(E) original magnification ×40]. (**F**) The percentage of LLT1^{+} lymphomas was assessed by immunohistochemistry in different B cell non-Hodgkin lymphomas, T cell non-Hodgkin lymphomas, and Hodgkin lymphomas. cHL, classical Hodgkin lymphoma; LPHL, lymphocyte-predominant Hodgkin lymphoma.

functional involvement of LLT1 during proliferation (data not shown). However, LLT1 might be a useful marker for the identification of GC B cells with high-affinity BCRs, as B cells with high-affinity BCRs are able to more efficiently present Ag to Tfh cells and consequently undergo more rounds of division (44).

To better understand the function of LLT1 within the context of the GC, we investigated potential sites of interactions by seeking the expression of its ligand, CD161. Lanier et al. (45) originally identified the expression of CD161 on both CD4^{+} and CD8^{+} T cells, which has been broadened to include innate lymphocyte subsets (15, 46–49). However, murine homologs of CD161, NKR-P1B and NKR-P1D, are not fully analogous, as they differ both in expression profiles and function (reviewed in Ref. 50).

Unexpectedly, CD161 was observed on FDCs. This was particularly surprising, as it is uncommon for NK cell receptors to be expressed on nonhematopoietic cells, although relevant examples exist, for example, KACL on keratinocytes (51) and LLT1 on osteoblasts (23).

Given the close association of CD161 expression and T cells, CD161 expression was also investigated on Tfh cells (CXCR5$^{mid/high}$). However, CD161 expression negatively correlated with CXCR5 expression, at both the protein and mRNA levels. A potential explanation for this may lie in the transcription factor Bcl-6. This master transcription factor drives maturation of T and B cells toward a full GC phenotype. As Bcl-6 expression increases it suppresses other lineage-associated transcription factors, such as retinoic acid–related orphan receptor γT, a transcription factor associated with CD161 expression (46, 52–54). Thus, it is plausible that Bcl-6 inhibits the expression of CD161 through the suppression of retinoic acid–related orphan receptor γT.

The LZ and DZ can be identified by the higher expression of either CD83 or CXCR4, respectively (1, 3, 55–57). Movement between the zones is fundamental for efficient participation within the GC reaction (3, 44, 58). Entry into the DZ requires Tfh interactions and the expression of CXCR4, although CXCR4$^{-/-}$ B cells are still able to transit into a centroblast phenotype and acquire mutations, albeit at a lower level compared with their wild-type counterparts (3, 44, 58). Migration back to the LZ is associated with lower CXCR4 expression, but the underlying mechanisms have not been identified. In this study, crosslinking of LLT1 alone resulted in a reduction in the expression of CXCR4 in DZ B cells. Therefore, these data suggest that LLT1 triggering occurs within the LZ.

Once within the LZ, B cells interact with FDCs and Tfh cells and receive a number of costimulatory signals (59–62). A key receptor in these interactions expressed by the B cells is CD83 (63–65). Triggering of LLT1 alone did not alter the expression of CD83 GC B cells. However, in the context of BCR or CD40 signaling, LLT1 triggering promoted CD83 expression. This suggests that LLT1 may also help enhance B cell interactions with both FDCs and Tfh cells. Combined with the downregulation of CXCR4, these data suggest that LLT1 triggering helps drive B cells through the different GC transitional states within the LZ (57).

LLT1's high expression within the GC, and its association with proliferating cells, suggests its use as a potential aid for the clinical diagnosis of B cell lymphomas, in particular non–Hodgkin

lymphomas, which represent 4–5% of all cancers diagnosed (66). Treatment selection relies on accurate diagnosis, staging of the disease, and identification of adverse prognostic factors. Expressions of Bcl-6, CD10, and IRF4 are used in immunohistochemical stains to separate diffuse large B cell lymphomas into GC and non-GC subtypes (67, 68). However, although immunohistochemistry is widely used, it is not always reliable, in particular when identifying follicular lymphomas with atypical phenotypes. LLT1, therefore, provides a potential new marker for the clinical investigation of lymphomas, and it warrants larger prognostic studies to provide more data on the independent significance of positive or negative stains.

LLT1 and CD161 are both CLRs encoded within the NKC, located adjacent to one another (4–7, 51, 69). Expression of other NKC proteins within the GC is limited to CD69 on both B cell and Tfh cells; however, a function for CD69 within the GC has not been described. The role of particular lectins in the modulation of BCR responses has been explored before. For instance, CD22 and CD72 have been shown to downmodulate BCR-mediated signals (70). Furthermore, the C-type lectin CD23, the low-affinity receptor for IgE, is also relevant in the context of B cell responses (71), as it acts as a ligand for CD21 within the BCR complex. Interestingly, CD23 has been found highly expressed in a proportion of FDCs. Thus, the data presented in this study are consistent with a contribution of C-type lectins to B cell responses through FDC–B cell interactions. This is particularly meaningful, as CLRs, once thought to be essentially involved in innate immunity, have now been shown to play a prominent role in the GC reaction, a hallmark of adaptive immunity.

The data presented in the present study suggest a role for innate components of the human immune system, such as LLT1 and CD161, in the GC reaction. Our data suggest that LLT1 triggering may play a key role in the GC reaction promoting B cell activation and downregulating CXCR4, thus helping to promote an LZ phenotype and facilitating both FDC and Tfh interactions.

Acknowledgments

We thank the patients and staff at the Department of Cellular Pathology at the University College London Hospital (London, U.K.), the Ear, Nose, and Throat Department at John Radcliffe Hospital (Oxford, U.K.), and the Barts and the London School of Medicine and Dentistry (London, U.K.). We also thank Prof. Lynn Dustin, Dr. Tal Arnon, Dr. Matthew Collin, Dr. Joannah Fergusson, and Dr. Ayako Kurioka for comments and critical reading of this manuscript.

Disclosures

The authors have no financial conflicts of interest.

References

1. Victora, G. D., D. Dominguez-Sola, A. B. Holmes, S. Deroubaix, R. Dalla-Favera, and M. C. Nussenzweig. 2012. Identification of human germinal center light and dark zone cells and their relationship to human B-cell lymphomas. *Blood* 120: 2240–2248.
2. Nieuwenhuis, P., and D. Opstelten. 1984. Functional anatomy of germinal centers. *Am. J. Anat.* 170: 421–435.
3. Victora, G. D., T. A. Schwickert, D. R. Fooksman, A. O. Kamphorst, M. Meyer-Hermann, M. L. Dustin, and M. C. Nussenzweig. 2010. Germinal center dynamics revealed by multiphoton microscopy with a photoactivatable fluorescent reporter. *Cell* 143: 592–605.
4. Iizuka, K., O. V. Naidenko, B. F. M. Plougastel, D. H. Fremont, and W. M. Yokoyama. 2003. Genetically linked C-type lectin-related ligands for the NKRP1 family of natural killer cell receptors. *Nat. Immunol.* 4: 801–807.
5. Vogler, I., and A. Steinle. 2011. Vis-à-vis in the NKC: genetically linked natural killer cell receptor/ligand pairs in the natural killer gene complex (NKC). *J. Innate Immun.* 3: 227–235.
6. Rosen, D. B., J. Bettadapura, M. Alsharifi, P. A. Mathew, H. S. Warren, and L. L. Lanier. 2005. Cutting edge: lectin-like transcript-1 is a ligand for the inhibitory human NKR-P1A receptor. *J. Immunol.* 175: 7796–7799.
7. Aldemir, H., V. Prod'homme, M.-J. Dumaurier, C. Retiere, G. Poupon, J. Cazareth, F. Bihl, and V. M. Braud. 2005. Cutting edge: lectin-like transcript 1 is a ligand for the CD161 receptor. *J. Immunol.* 175: 7791–7795.
8. Boles, K. S., R. Barten, P. R. Kumaresan, J. Trowsdale, and P. A. Mathew. 1999. Cloning of a new lectin-like receptor expressed on human NK cells. *Immunogenetics* 50: 1–7.
9. Plougastel, B., C. Dubbelde, and W. M. Yokoyama. 2001. Cloning of *Clr*, a new family of lectin-like genes localized between mouse *Nkrp1a* and *Cd69*. *Immunogenetics* 53: 209–214.
10. Meyer-Hermann, M., E. Mohr, N. Pelletier, Y. Zhang, G. D. Victora, and K.-M. Toellner. 2012. A theory of germinal center B cell selection, division, and exit. *Cell Reports* 2: 162–174.
11. Eichler, W., P. Ruschpler, M. Wobus, and K. Drössler. 2001. Differentially induced expression of C-type lectins in activated lymphocytes. *J. Cell. Biochem. Suppl.* 2001(Suppl. 36): 201–208.
12. Mathew, P. A., S. S. Chuang, S. V. Vaidya, P. R. Kumaresan, K. S. Boles, and H. T. Pham. 2004. The LLT1 receptor induces IFN-γ production by human natural killer cells. *Mol. Immunol.* 40: 1157–1163.
13. Germain, C., A. Meier, T. Jensen, P. Knapnougel, G. Poupon, A. Lazzari, A. Neisig, K. Håkansson, T. Dong, N. Wagtmann, et al. 2011. Induction of lectin-like transcript 1 (LLT1) protein cell surface expression by pathogens and interferon-γ contributes to modulate immune responses. *J. Biol. Chem.* 286: 37964–37975.
14. Satkunanathan, S., N. Kumar, M. Bajorek, M. A. Purbhoo, and F. J. Culley. 2014. Respiratory syncytial virus infection, TLR3 ligands, and proinflammatory cytokines induce CD161 ligand LLT1 expression on the respiratory epithelium. *J. Virol.* 88: 2366–2373.
15. Fergusson, J. R., K. E. Smith, V. M. Fleming, N. Rajoriya, E. W. Newell, R. Simmons, E. Marchi, S. Björkander, Y.-H. Kang, L. Swadling, et al. 2014. CD161 defines a transcriptional and functional phenotype across distinct human T cell lineages. *Cell Reports* 9: 1075–1088.
16. Germain, C., F. Bihl, S. Zahn, G. Poupon, M.-J. Dumaurier, H. H. Rampanarivo, S. B. Padkjær, P. Spee, and V. M. Braud. 2010. Characterization of alternatively spliced transcript variants of CLEC2D gene. *J. Biol. Chem.* 285: 36207–36215.
17. Germain, C., T. Guillaudeux, E. D. Galsgaard, C. Hervouet, N. Tekaya, A.-S. Gallouet, J. Fassy, F. Bihl, G. Poupon, A. Lazzari, et al. 2015. Lectin-like transcript 1 is a marker of germinal center-derived B-cell non-Hodgkin's lymphomas dampening natural killer cell functions. *OncoImmunology* 4: e1026503.
18. Hu, Y. S., H. Zhou, D. Myers, J. M. W. Quinn, G. J. Atkins, C. Ly, C. Gange, V. Kartsogiannis, J. Elliott, P. Kostakis, et al. 2004. Isolation of a human homolog of osteoclast inhibitory lectin that inhibits the formation and function of osteoclasts. *J. Bone Miner. Res.* 19: 89–99.
19. Exley, M., S. Porcelli, M. Furman, J. Garcia, and S. Balk. 1998. CD161 (NKR-P1A) costimulation of CD1d-dependent activation of human T cells expressing invariant Vα24JαQ T cell receptor α chains. *J. Exp. Med.* 188: 867–876.
20. Nakamura, A., C. Ly, M. Cipetić, N. A. Sims, J. Vieusseux, V. Kartsogiannis, S. Bouralexis, H. Saleh, H. Zhou, J. T. Price, et al. 2007. Osteoclast inhibitory lectin (OCIL) inhibits osteoblast differentiation and function in vitro. *Bone* 40: 305–315.
21. Rosen, D. B., W. Cao, D. T. Avery, S. G. Tangye, Y.-J. Liu, J. P. Houchins, and L. L. Lanier. 2008. Functional consequences of interactions between human NKR-P1A and its ligand LLT1 expressed on activated dendritic cells and B cells. *J. Immunol.* 180: 6508–6517.
22. Roth, P., M. Mittelbronn, W. Wick, R. Meyermann, M. Tatagiba, and M. Weller. 2007. Malignant glioma cells counteract antitumor immune responses through expression of lectin-like transcript-1. *Cancer Res.* 67: 3540–3544.
23. Zhou, H., V. Kartsogiannis, Y. S. Hu, J. Elliott, J. M. Quinn, W. J. McKinstry, M. T. Gillespie, and K. W. Ng. 2001. A novel osteoblast-derived C-type lectin that inhibits osteoclast formation. *J. Biol. Chem.* 276: 14916–14923.
24. Jourdan, M., A. Caraux, J. De Vos, G. Fiol, M. Larroque, C. Cognot, C. Bret, C. Duperray, D. Hose, and B. Klein. 2009. An in vitro model of differentiation of memory B cells into plasmablasts and plasma cells including detailed phenotypic and molecular characterization. *Blood* 114: 5173–5181.
25. Pascual, V., Y. J. Liu, A. Magalski, O. de Bouteiller, J. Banchereau, and J. D. Capra. 1994. Analysis of somatic mutation in five B cell subsets of human tonsil. *J. Exp. Med.* 180: 329–339.
26. Frazer, J. K., J. LeGros, O. de Bouteiller, Y.-J. Liu, J. Banchereau, V. Pascual, and J. D. Capra. 1997. Identification and cloning of genes expressed by human tonsillar B lymphocyte subsets. *Ann. N. Y. Acad. Sci.* 815: 316–318.
27. Lebecque, S., O. de Bouteiller, C. Arpin, J. Banchereau, and Y. J. Liu. 1997. Germinal center founder cells display propensity for apoptosis before onset of somatic mutation. *J. Exp. Med.* 185: 563–571.
28. Liu, Y.-J., and C. Arpin. 1997. Germinal center development. *Immunol. Rev.* 156: 111–126.
29. Sims, G. P., R. Ettinger, Y. Shirota, C. H. Yarboro, G. G. Illei, and P. E. Lipsky. 2005. Identification and characterization of circulating human transitional B cells. *Blood* 105: 4390–4398.
30. Wrammert, J., K. Smith, J. Miller, W. A. Langley, K. Kokko, C. Larsen, N. Y. Zheng, I. Mays, L. Garman, C. Helms, et al. 2008. Rapid cloning of high-affinity human monoclonal antibodies against influenza virus. *Nature* 453: 667–671.
31. Mei, H. E., T. Yoshida, W. Sime, F. Hiepe, K. Thiele, R. A. Manz, A. Radbruch, and T. Dörner. 2009. Blood-borne human plasma cells in steady state are derived from mucosal immune responses. *Blood* 113: 2461–2469.
32. Toellner, K. M., D. Scheel-Toellner, R. Sprenger, M. Duchrow, L. H. Trümper, M. Ernst, H. D. Flad, and J. Gerdes. 1995. The human germinal centre cells,

COPYRIGHT DISTRIBUTION PROHIBITED

follicular dendritic cells and germinal centre T cells produce B cell-stimulating cytokines. *Cytokine* 7: 344–354.
33. Zotos, D., J. M. Coquet, Y. Zhang, A. Light, K. D'Costa, A. Kallies, L. M. Corcoran, D. I. Godfrey, K.-M. Toellner, M. J. Smyth, et al. 2010. IL-21 regulates germinal center B cell differentiation and proliferation through a B cell-intrinsic mechanism. *J. Exp. Med.* 207: 365–378.
34. Linterman, M. A., L. Beaton, D. Yu, R. R. Ramiscal, M. Srivastava, J. J. Hogan, N. K. Verma, M. J. Smyth, R. J. Rigby, and C. G. Vinuesa. 2010. IL-21 acts directly on B cells to regulate Bcl-6 expression and germinal center responses. *J. Exp. Med.* 207: 353–363.
35. Magari, M., Y. Nishikawa, Y. Fujii, Y. Nishio, K. Watanabe, M. Fujiwara, N. Kanayama, and H. Ohmori. 2011. IL-21-dependent B cell death driven by prostaglandin E_2, a product secreted from follicular dendritic cells. *J. Immunol.* 187: 4210–4218.
36. Ma, C. S., E. K. Deenick, M. Batten, and S. G. Tangye. 2012. The origins, function, and regulation of T follicular helper cells. *J. Exp. Med.* 209: 1241–1253.
37. Breitfeld, D., L. Ohl, E. Kremmer, J. Ellwart, F. Sallusto, M. Lipp, and R. Förster. 2000. Follicular B helper T cells express CXC chemokine receptor 5, localize to B cell follicles, and support immunoglobulin production. *J. Exp. Med.* 192: 1545–1552.
38. El Shikh, M. E. M., R. M. El Sayed, S. Sukumar, A. K. Szakal, and J. G. Tew. 2010. Activation of B cells by antigens on follicular dendritic cells. *Trends Immunol.* 31: 205–211.
39. Crotty, S. 2011. Follicular helper CD4 T cells (TFH). *Annu. Rev. Immunol.* 29: 621–663.
40. Victora, G. D., and M. C. Nussenzweig. 2012. Germinal centers. *Annu. Rev. Immunol.* 30: 429–457.
41. De Silva, N. S., and U. Klein. 2015. Dynamics of B cells in germinal centres. *Nat. Rev. Immunol.* 15: 137–148.
42. Kamishikiryo, J., H. Fukuhara, Y. Okabe, K. Kuroki, and K. Maenaka. 2011. Molecular basis for LLT1 protein recognition by human CD161 protein (NKRP1A/KLRB1). *J. Biol. Chem.* 286: 23823–23830.
43. Marafioti, T., C. Copie-Bergman, M. Calaminici, J. C. Paterson, V. H. Shende, H. Liu, M. Baia, A. D. Ramsay, C. Agostinelli, J. Brière, et al. 2013. Another look at follicular lymphoma: immunophenotypic and molecular analyses identify distinct follicular lymphoma subgroups. *Histopathology* 62: 860–875.
44. Gitlin, A. D., Z. Shulman, and M. C. Nussenzweig. 2014. Clonal selection in the germinal centre by regulated proliferation and hypermutation. *Nature* 509: 637–640.
45. Lanier, L. L., C. Chang, and J. H. Phillips. 1994. Human NKR-P1A. A disulfide-linked homodimer of the C-type lectin superfamily expressed by a subset of NK and T lymphocytes. *J. Immunol.* 153: 2417–2428.
46. Maggi, L., V. Santarlasci, M. Capone, A. Peired, F. Frosali, S. Q. Crome, V. Querci, M. Fambrini, F. Liotta, M. K. Levings, et al. 2010. CD161 is a marker of all human IL-17-producing T-cell subsets and is induced by RORC. *Eur. J. Immunol.* 40: 2174–2181.
47. Takahashi, T., S. Dejbakhsh-Jones, and S. Strober. 2006. Expression of CD161 (NKR-P1A) defines subsets of human CD4 and CD8 T cells with different functional activities. *J. Immunol.* 176: 211–216.
48. Billerbeck, E., Y.-H. Kang, L. Walker, H. Lockstone, S. Grafmueller, V. Fleming, J. Flint, C. B. Willberg, B. Bengsch, B. Seigel, et al. 2010. Analysis of CD161 expression on human $CD8^+$ T cells defines a distinct functional subset with tissue-homing properties. *Proc. Natl. Acad. Sci. USA* 107: 3006–3011.
49. Kang, Y.-H., B. Seigel, B. Bengsch, V. M. Fleming, E. Billerbeck, R. Simmons, L. Walker, C. B. Willberg, E. J. Barnes, A. Bhagwanani, et al. 2012. $CD161^+$ $CD4^+$ T cells are enriched in the liver during chronic hepatitis and associated with co-secretion of IL-22 and IFN-γ. *Front. Immunol.* 3: 346.
50. Fergusson, J. R., V. M. Fleming, and P. Klenerman. 2011. CD161-expressing human T cells. *Front. Immunol.* 2: 36.
51. Spreu, J., S. Kuttruff, V. Stejfova, K. M. Dennehy, B. Schittek, and A. Steinle. 2010. Interaction of C-type lectin-like receptors NKp65 and KACL facilitates dedicated immune recognition of human keratinocytes. *Proc. Natl. Acad. Sci. USA* 107: 5100–5105.
52. Ivanov, I. I., B. S. McKenzie, L. Zhou, C. E. Tadokoro, A. Lepelley, J. J. Lafaille, D. J. Cua, and D. R. Littman. 2006. The orphan nuclear receptor RORγt directs the differentiation program of proinflammatory IL-17^+ T helper cells. *Cell* 126: 1121–1133.
53. Cosmi, L., R. De Palma, V. Santarlasci, L. Maggi, M. Capone, F. Frosali, G. Rodolico, V. Querci, G. Abbate, R. Angeli, et al. 2008. Human interleukin 17-producing cells originate from a $CD161^+CD4^+$ T cell precursor. *J. Exp. Med.* 205: 1903–1916.
54. Yu, D., S. Rao, L. M. Tsai, S. K. Lee, Y. He, E. L. Sutcliffe, M. Srivastava, M. Linterman, L. Zheng, N. Simpson, et al. 2009. The transcriptional repressor Bcl-6 directs T follicular helper cell lineage commitment. *Immunity* 31: 457–468.
55. Allen, C. D. C., K. M. Ansel, C. Low, R. Lesley, H. Tamamura, N. Fujii, and J. G. Cyster. 2004. Germinal center dark and light zone organization is mediated by CXCR4 and CXCR5. *Nat. Immunol.* 5: 943–952.
56. Caron, G., S. Le Gallou, T. Lamy, K. Tarte, and T. Fest. 2009. CXCR4 expression functionally discriminates centroblasts versus centrocytes within human germinal center B cells. *J. Immunol.* 182: 7595–7602.
57. McHeyzer-Williams, L. J., P. J. Milpied, S. L. Okitsu, and M. G. McHeyzer-Williams. 2015. Class-switched memory B cells remodel BCRs within secondary germinal centers. *Nat. Immunol.* 16: 296–305.
58. Bannard, O., R. M. Horton, C. D. C. Allen, J. An, T. Nagasawa, and J. G. Cyster. 2013. Germinal center centroblasts transition to a centrocyte phenotype according to a timed program and depend on the dark zone for effective selection. *Immunity* 39: 912–924.
59. Qin, D., J. Wu, G. F. Burton, A. K. Szakal, and J. G. Tew. 1997. A role for CR2 in FDC-B cell interactions. *Adv. Exp. Med. Biol.* 417: 493–497.
60. Gaspal, F. M. C., F. M. McConnell, M.-Y. Kim, D. Gray, M. H. Kosco-Vilbois, C. R. Raykundalia, M. Botto, and P. J. L. Lane. 2006. The generation of thymus-independent germinal centers depends on CD40 but not on CD154, the T cell-derived CD40-ligand. *Eur. J. Immunol.* 36: 1665–1673.
61. El Shikh, M. E. M., R. M. El Sayed, A. K. Szakal, and J. G. Tew. 2009. T-independent antibody responses to T-dependent antigens: a novel follicular dendritic cell-dependent activity. *J. Immunol.* 182: 3482–3491.
62. Wu, Y., M. E. M. El Shikh, R. M. El Sayed, A. M. Best, A. K. Szakal, and J. G. Tew. 2009. IL-6 produced by immune complex-activated follicular dendritic cells promotes germinal center reactions, IgG responses and somatic hypermutation. *Int. Immunol.* 21: 745–756.
63. Breloer, M., B. Kretschmer, K. Lüthje, S. Ehrlich, U. Ritter, T. Bickert, C. Steeg, S. Fillatreau, K. Hoehlig, V. Lampropoulou, and B. Fleischer. 2007. CD83 is a regulator of murine B cell function in vivo. *Eur. J. Immunol.* 37: 634–648.
64. Kretschmer, B., K. Lüthje, A. H. Guse, S. Ehrlich, F. Koch-Nolte, F. Haag, B. Fleischer, and M. Breloer. 2007. CD83 modulates B cell function in vitro: increased IL-10 and reduced Ig secretion by CD83Tg B cells. *PLoS One* 2: e755.
65. Tze, L. E., K. Horikawa, H. Domaschenz, D. R. Howard, C. M. Roots, R. J. Rigby, D. A. Way, M. Ohmura-Hoshino, S. Ishido, C. E. Andoniou, et al. 2011. CD83 increases MHC II and CD86 on dendritic cells by opposing IL-10-driven MARCH1-mediated ubiquitination and degradation. *J. Exp. Med.* 208: 149–165.
66. Ansell, S. M. 2015. Non-Hodgkin lymphoma: diagnosis and treatment. *Mayo Clin. Proc.* 90: 1152–1163.
67. Rosenwald, A., G. Wright, W. C. Chan, J. M. Connors, E. Campo, R. I. Fisher, R. D. Gascoyne, H. K. Muller-Hermelink, E. B. Smeland, J. M. Giltnane, et al; Lymphoma/Leukemia Molecular Profiling Project. 2002. The use of molecular profiling to predict survival after chemotherapy for diffuse large-B-cell lymphoma. *N. Engl. J. Med.* 346: 1937–1947.
68. Hans, C. P., D. D. Weisenburger, T. C. Greiner, R. D. Gascoyne, J. Delabie, G. Ott, H. K. Müller-Hermelink, E. Campo, R. M. Braziel, E. S. Jaffe, et al. 2004. Confirmation of the molecular classification of diffuse large B-cell lymphoma by immunohistochemistry using a tissue microarray. *Blood* 103: 275–282.
69. Welte, S., S. Kuttruff, I. Waldhauer, and A. Steinle. 2006. Mutual activation of natural killer cells and monocytes mediated by NKp80-AICL interaction. *Nat. Immunol.* 7: 1334–1342.
70. Nitschke, L., and T. Tsubata. 2004. Molecular interactions regulate BCR signal inhibition by CD22 and CD72. *Trends Immunol.* 25: 543–550.
71. Reljić, R., G. Cosentino, and H. J. Gould. 1997. Function of CD23 in the response of human B cells to antigen. *Eur. J. Immunol.* 27: 572–575.

Appendix 10. Accepted publication at The Journal of Immunology.

The Journal of Immunology